Decisional Tools for Cost-effective Bioprocess Design for Cell Therapies and Patient-specific Drug Discovery Tools

An EngD Thesis submitted to

University College London

by

Michael Joseph Jenkins

Declaration

I, Michael Joseph Jenkins, confirm that the work presented in this thesis is my own. Where information has been derived from other sources, I confirm that this has been indicated in the thesis.

‘Mwenda mbio hujikwaa dole’

‘A person in a hurry stubs a toe’

- Swahili proverb

Abstract

A specific challenge to the translation of cell therapies and stem-cell derived products is the ability to develop and manufacture such products in a cost-effective, scalable and robust manner. To this end, this thesis investigates the creation and application of a set of computational tools designed to aid bioprocess design decisions for cell therapy and stem-cell derived research products.

The decision-support tools comprise advanced bioprocess economics models with databases tailored to cellular products. These are linked to Monte Carlo simulation for uncertainty analysis and techniques to identify optimal bioprocess designs that include brute-force search algorithms, an evolutionary algorithm, and multi-attribute decision making analysis. A trio of industrially-relevant case studies is presented within this thesis, along with an additional study included in the appendices of this work, in order to demonstrate the applicability of the decisional tools to bioprocess design for different cell therapies (allogeneic, human embryonic stem cell-derived retinal pigment epithelial (RPE) cells for macular degeneration, allogeneic CAR-T cells for oncology) and induced pluripotent stem cells (iPSCs) for drug discovery applications. Questions tackled included manual versus automated production, cost-effective inflection points of planar vs microcarrier-based bioprocess strategies, and the identification optimal process technologies for an allogeneic CAR-T cell therapy based on both qualitative and quantitative attributes. The analyses highlighted key bioprocess economic drivers and process bottlenecks. Furthermore, the Monte Carlo simulation technique was used in order to capture the effects of the inherent uncertainty associated with cell therapy bioprocessing on manufacturing costs and process throughputs. Future process improvements required to create financially feasible bioprocesses were also identified.

This thesis presents the application of a series of decisional tools to bioprocess design problems and demonstrates how they can facilitate informed decisions

regarding cost-effective process design in the cell therapy sector.

Acknowledgements

First and foremost, I would like to thank my supervisor, Professor Suzanne Farid, to whom I owe a debt of gratitude for presenting me with the opportunity to carry out this work. The influence of her astute guidance and support throughout the course of my EngD cannot be overstated.

The insight, patience, and generosity of the team at Pfizer made it an absolute joy to work them, particularly Sa Ho and Ron Fedechko. I wish Sa the happiest of retirements and I hope my path continues to cross with Ron in our future endeavours.

I would also like to thank everyone within the Department of Biochemical Engineering at UCL, especially Richard Allmendinger and Ana Sofia Simaria for their efforts in developing my programming skills. Des, Stefan, James, Ben, and Alex (and many others), thanks for being there to take the heat out of our research over a beer.

Gushing praise has never been a family trait. However, I'd like to thank my Mum and Dad for instilling me with a passion for learning and investigating; also for convincing me that I can do some decent work when I put my mind to it. Rob, thanks for being the most supportive of big brothers throughout life, but especially over the last few years. I wish to thank Abi, primarily for simply putting up with me, but also for her love, patience and support (especially in the final stages of writing this thesis).

I'd like to thank my former flatmate and bandmate James Stewart, who stuck with me to very nearly the end so deserves almost a full acknowledgemen. Finally, thanks to the members of Dulwich Lawn Tennis Club for offering a much needed sanctuary away from cell therapy bioprocessing.

Table of Contents

List of Tables

List of Figures

Abbreviations

ACFM	Automatic Cell Factory Manipulator
AMD	Age-related macular degeneration
AMR	Automated media removal
ATMP	Advanced therapy medicinal product
ATPS	Aqueous two-phase systems
CAR	Chimeric antigen receptor
CF	Planar culture flask
cGMP	current Good Manufacturing Practice
cGTP	current Good Tissue Practice
cL	multilayer planar vessel (e.g. HYPERStack)
CMO	Contract manufacturing organisation
COG	Cost of Goods
cT	compact multilayer planar vessel
CTS	CompacT SelecT
DC	Direct costs
DD-MC	Microcarrier-based, directed differentiation bioprocess
DD-PL	Planar-based, directed differentiation bioprocess
DSP	Downstream processing
EA	Evolutionary algorithm
EMA	European Medicines Agency
FACS	Fluorescent activated cell sorting
FBC	Fluidised bed centrifugation
FBS	Foetal bovine serum
FCI	Fixed capital investment
FDA	(USA) Food and Drug Administration
GA	Genetic algorithm

GF	Growth factor
GPV	Gas permeable vessel
GvHD	Graft versus Host Disease
hESC	Human embryonic stem cell
hiPSC	Human induced pluripotent stem cell
hPSC	Human pluripotent stem cell
HSC	Haematopoietic stem cell
HTA	Health technology assessment
HTA	High throughput screening
IDC	Indirect costs
INT	Integrated bioprocess platform
MACS	Magnetic activated cell sorting
MADM	Multi-attribute decision making
MCB	Master cell bank
MSC	Mesenchymal stem cell
NCE	Novel chemical entity
NICE	National Institute for Healthcare and Clinical Excellence
NPV	Net present value
PBP	Plate-based pharmacological analysis
PCA	Patch clamp analysis
PSC	pluripotent stem cell
QALY	Quality adjusted life years
RMA	(Japanese) Regenerative Medicine Act
RMB	Rocking motion bioreactor
RPC	Retinal pigment cell
RPE	Retinal pigment epithelium
RSA	risk sharing agreement

SD-MC	Microcarrier-based, spontaneous differentiation bioprocess
SD-PL	Planar-based, spontaneous differentiation bioprocess
SMF	Spinning membrane filtration
SUB	Single use bioreactor
TCR	T-cell receptor
TFF	Tangential flow filtration
TSP	Target selling price
XF	Xeno-free

Chapter 1: Scope and Background

1.1 Introduction

Cell therapies have opened fresh avenues in modern medicine that have the potential to revolutionise healthcare; they have applications in a range of medicinal fields, including treatment of stroke, age-related blindness (including macular degeneration), and a variety of cancers. If cell therapies are to achieve their full clinical and commercial potential, significant challenges must be overcome with regards to current abilities to produce therapies of the consistent quality to support their function at commercially relevant scales. Reimbursement pressures have resulted in an increased awareness of the importance of estimating and improving manufacturing costs for cell therapy products. The aim of this thesis is to create and apply decisional tools to help identify cost-effective process designs for cell therapies and stem cell-reived research products.

This chapter aims to provide an introduction to cell therapies and the key topics and challenges surrounding their development and manufacture. Decision-support tools and their applications to the field of bioprocessing are also introduced. Section 1.2 gives an overview of cell therapies, including different types of cell therapies along with the clinical and commercial applications of cell therapies and stem-cell derived products. Section 1.3 introduces product and process development in the context of cell therapies and gives an overview of the current risks and challenges to cell therapy translation and commercialisation. The concept of bioprocess economics and key parameters used to measure the cost of manufacturing a cell therapy and the success of cell therapy projects are introduced in Section 1.4. Section 1.5 outlines previous applications of decision-support tools to bioprocessing, and details how they are currently being applied within the cell therapy sector to improve bioprocess design

and aid effective decision-making during process development. Finally, the aims and organisation of this thesis is outlined in Section 1.6.

1.2 Introduction to cell therapies

Cell therapy is defined as the administration of live whole cells to a patient in order to treat a disease (American Society of Gene & Cell Therapy [no date]). Cell therapies can be categorised as minimally manipulated cells for homologous use (e.g. blood transfusions), and those which are considered as medicines by regulatory bodies, referred to as Advanced Therapy Medicinal Products (ATMPs) (Mount et al. 2015). ATMP is a broad term that encompasses gene therapy products, somatic cell therapy products, and tissue-engineered products. It is applied to cell therapies that utilise cells that have undergone substantial manipulation, or where cells are intended for non-homologous functions. Cell therapy products administered to human beings with the target of regenerating or replacing human tissue to restore normal function, or treating, preventing and diagnosing a disease through pharmacological, metabolic, or immunological mechanisms are also considered ATMPs (Mason and Dunnill 2008; Pla 2016).

The prevalence of cell therapies has increased rapidly in recent years. As of 2015, there were 1,342 active clinical trials investigating the use of cell-based therapies, and 9,700 open trials (including observational and duplicate trials (Heathman et al. 2015). This is in comparison to 1,750 open trials in 2013 (Abbasalizadeh and Baharvand 2013). Annual cell therapy revenues are currently in excess of US$1bn (Mason et al. 2012), and are forecasted to exceed US$10bn by 2021 (Bloomberg 2012).

Cell therapy applications are broad in range, from the treatment of stroke, to heart failure, age-related blindness (including macular degeneration), and a variety of

cancers. A summary of the target indications for which cell therapy clinical trials are currently being conducted is shown in Table 1.1.

The work presented in this thesis will focus on two main classes of cell therapy and related products, which are outlined below along with their applications: namely, human pluripotent stem cell (hPSC)-derived products (Section 1.2.1) and chimeric antigen receptor (CAR) T-cell therapies (Section 1.2.2). However, other cell therapy classifications exist including adult somatic cell products, derived from cells found naturally in adult humans (e.g. mesenchymal stem cells (MSCs), haematopoietic stem cells (HSCs) and skin stem cell products such as Apligraf®), and three-dimensional technologies for the replacement of tissues and organs (e.g. tissue scaffolds and structures and novel 'organoid' technologies).

Table 1.1 – Summary of indications under investigation for treatment by advanced cell therapies in clinical trials, and typical dose sizes required for treatment

	Indication	Dose size (nr of cells)	Source/ NCT number
hPSC-derived therapies	Macular Degeneration	$5x10^4$ – $2x10^5$	NCT01691261, NCT01344993
	Spinal Cord Injuries	10^6	
MSC-based therapies	Ischemic stroke	10^6/Kg	NCT01678534
	Crohn's disease	$2x10^6$ – $8x10^6$ per Kg	NCT00294112
	Osteogenesis imperfect	10^6 – $5x10^6$ per Kg	NCT00186914 (Horwitz et al. 2002)
	Myocardial Infarction	$0.5x10^6$ – $5x10^6$	NCT00114452 (Hare et al. 2009)
	Graft versus host disease	$2x10^6$ – $9x10^6$ per Kg	(Ringden et al. 2006; Prasad et al. 2011)
	Multiple sclerosis	~$2x10^6$ per Kg[8]	NCT00395200, NCT02587715
	Liver cirrhosis	10^6 – $3x10^6$ per Kg	NCT02705742, NCT02652351
	Systemic lupus erythematosus	10^6 – $5x10^6$	NCT02633163
	Ulcerative Colitis	$3x10^8$ - $7.5x10^8$	
	Rheumatoid arthritis	$2x10^7$	NCT02643823
	Cartilage defects	$2.5x10^6$ per cm^2	NCT01626677
	Parkinson's Disease	10^6 – 10^7 per Kg	NCT02611167
CAR-T cell therapies	Acute lymphoblastic leukemia (ALL)	$1.4x10^6$ – $1.2x10^7$per Kg	(Grupp et al. 2013) NCT02614066
	Chronic lymphocytic leukemia (CLL)	$1.5x10^5$ per Kg	(Porter et al. 2011)
	Lymphoma	$2x10^6$ – $2x10^7$ per Kg	NCT02348216, NCT01840566
	Glioma		NCT01454596
	Head and neck cancer	10^7 - 10^9	NCT01818323 (van Schalkwyk, Papa, Jeannon, Guerrero Urbano, et al. 2013)
	Neuroblastoma	$5x10^5$ – 10^7 per Kg	NCT02311621

	10^7 – $2x10^8$	NCT01822652
Metastatic pancreatic cancer	10^8 – $3x10^8$ per m^2	NCT01897415
Metastatic melanoma	10^9	NCT00910650
Prostate cancer	$3x10^7$ – $1x10^8$ per Kg	NCT01140373

Note: "NCT" numbers (i.e. NCTxxxxxxxx) provided are the ClinicalTrials.gov registry number for a given study. ClinicalTrials.gov is maintained by the United States FDA and National Institute of Health (NIH)

1.2.1 Human pluripotent stem cells and their clinical applications

Pluripotent stem cells (PSCs) have the capacity to differentiate into all mature cell types. This makes hPSCs, which consist of human embryonic stem cells (hESCs) and human induced pluripotent stem cells (hiPSCs), attractive candidates for use as cell therapies (Takahashi et al. 2007; Robinton and Daley 2012). hESCs are derived and isolated from the inner cell mass of the human blastocyst. hiPSCs are derived from somatic cell lines (usually blood or skin cells) by a process called reprogramming, which involves the forced expression of one or more of the Yamanaka factors to drive differentiated cells to a state of pluripotency.

hPSC-derived cell therapies currently under development consist primarily of retinal progenitor cells and pancreatic β-cells derived from hESCs (Idelson et al. 2009; Schulz et al. 2012; Sivertsson et al. 2012). Promising results have also been observed for cell therapies derived from hiPSCs, such as retinal pigment epithelial (RPE) cells for macular degeneration (Schwartz et al. 2012; Carr et al. 2013; Nazari et al. 2015) (Table 1.1). hPSC-derived cardiomyocytes are also being explored for their potential in the treatment of heart failure, although no product has yet been entered into clinical trials (Zweigerdt 2007; Masuda and Shimizu 2016; Tzatzalos et al. 2016).

1.2.2 Human pluripotent stem cell-derived products as clinical research tools

Beyond there applications as potential cell therapies, there is a more immediate use of a variety of cell lineages such as neurons, cardiomyocytes, and hepatocytes derived from hiPSCs as research and diagnostic tools (Brock et al. 2012). hPSCs

offer a unique platform by which to augment, and even redefine, current drug discovery and drug screening programmes by the provision of a human *in vitro* tool with which to perform efficacy and toxicity screens for novel chemical entities (NCEs) (Ebert and Svendsen 2010; Grskovic et al. 2011). hiPSCs in particular might provide a diagnostic tool capable of lowering the high late-phase failure rate of NCEs in clinical trials (Zeevi-Levin et al. 2012; Hochedlinger 2013). hiPSCs could also pave the way for personalised medicine through the medium of responder versus non-responder "trial in a dish" models (Kiskinis and Eggan 2010). Finally, hiPSCs could provide a valuable tool with which to carry out mechanistic modelling of disease pathogenesis for poorly understood disorders such as Alzheimer's or Parkinson's disease (Soldner et al. 2009; Nguyen et al. 2016; Táncos et al. 2016). Universal hPSCs for use as research tools are available as commercial products, and are currently marketed at $2000-$3000/vial (Rajamohan et al. 2013).

Current drug screening platforms, such as animal models, will continue to have an important role in the drug development pipeline. However, in some instances they prove to be of limited predictive value due to fundamental biochemical, physiological and genomic variations from humans. The cost of taking a new drug to market is currently estimated to be US$1.2bn - US$1.7bn (Ebert and Svendsen 2010; Kiskinis and Eggan 2010; Scott et al. 2013). This, when juxtaposed with an attrition rate that rises above 90%, has caused drug developers to display caution when committing candidate therapies to clinical trials (Zeevi-Levin et al. 2012; Engle and Vincent 2014; Hay et al. 2014).

Patient-specific hiPSC-derived cells offer an additional branch of pre-clinical drug development programs in order to assess safety of NCEs, where the degree of efficacy of observed within a patient may depend upon a specific geno- or phenotype (Ko and Gelb 2014). Furthermore, the ability of patient-specific hiPSC-derived cells to model genetic and epigenetic variations of a broad spectrum population may also

augment Phase I/II clinical trials via the demonstration of a drug's safety and efficacy within a target population in vitro (Engle and Vincent 2014). Thus, hiPSC-derived cells provide a platform upon which NCEs may be assayed for efficacy and toxicity which promises to be of better predictive value than current drug screening models. In this manner they offer a powerful medium via which the time, costs, and risks associated with committing a drug to clinical trials can be alleviated.

1.2.3 Chimeric antigen receptor T-cells and their clinical applications

CAR-T cell therapies are a form of adoptive T-cell transfer, which involves the isolation and infusion of T lymphocytes into a patient to treat diseases (Kalos and June 2013). Whilst adoptive T-cell transfer has been shown to be effective in the treatment of viral infections in transplant patients, CAR-T cells have emerged as a powerful tool in the field of oncology (Porter et al. 2011; Grupp et al. 2013). CAR-T cells represent the most advanced form of adoptive T-cell transfer, and are currently under investigation as a treatment for a range of cancers (Table 1.1). CAR-T cells are genetically modified in order to express recombinant antigen receptors that bind to tumour-specific antigens with unparalleled affinity (Levine 2015). In practice, this makes tumour cells 'visible' to a patient's immune system (Lipowska-Bhalla et al. 2012). Unprecedented success has been achieved in the treatment of late-stage cancers using CAR-T therapies, particularly leukemias, whereby complete remission has been observed in some patients (Brentjens et al. 2011; Kalos et al. 2011; Porter et al. 2011; Kochenderfer et al. 2012).

1.3 Product development of cell therapies

As with traditional pharmaceutical product development, the primary goal of cell therapy product development can be said to be to establish a bioprocess and product formulation to support the manufacture and delivery of a product whose critical quality attributes, which define its safety and efficacy, match those of the target product profile. In addition to this, the product must be delivered within the confines of

economic parameters that will determine its commercial success. Market size and share, reimbursement value, manufacturing costs and development costs must all be considered early on during product development to ensure the commercial success of a cell therapy.

Despite the allocation of considerable resources and efforts by a number of different companies operating in the cell therapy sector, at the time of writing, few cell therapy products have achieved a market license in Europe and the USA (Table 1.2). This is a reflection of the complexity of cell therapy development and translation.

Table 1.2 – Cell therapies approved for marketing in Europe and the USA[a]

Marketing area	Product	Description	Target Indication	Manufacturer
USA	Kymriah®	Autologous CAR-T cell therapy	Acute lymphoblastic leukemia (ALL)	Novartis
	Provenge®	Autologous immunotherapy	Graft versus host disease (GvHD	Dendreon Corporation
	Carticel®	Autologous cultured chondrocytes	Cartilage repair	Genzyme
	Gintuit®	Allogeneic keratinocytes	Ulcer and skin wound repair	Organogenesis
	Laviv®	Autologous fibroblasts	Cosmetic anti-ageing skin product	Fibrocell Technologies Inc.
Europe	Strimvelis®	Autologous immunotherapy	Severe combined immunodeficiency (SCID)	GSK
	Chrondocelect®	Autologous chondrocytes	Cartilage repair	TIGenix
	MACI®	Matrix-induced autologous chondrocyte implantation	Cartilage repair	Genzyme
	Spherox	Autologous chondrocyte spheroids	Cartilage repair	CO.DON AG
	Holocar®	Autologous limbal stem cells	Corneal injury repair	Chiesi Farmaceutici

[a]Minimally manipulated products such as blood products for homologous use have been excluded from this list

1.3.1 Clinical development pathway

The clinical development pathway of cell therapies, including clinical trials, is intended to provide the basis by which a cell therapy product can be proven to be consistently safe and efficacious across its target market.

Table 1.3 – Overview of current phased clinical trials; patient numbers, purpose and length of time

Trial Phase	Pre-clinical	I	II	III	IV (Post-market)
Number of patients	Lab & Animal testing	10-100	100-200	1,000+	N/A
Purpose	Assess safety and indication of efficacy	Demonstrate safety and dosage	Evaluate efficacy	Long-term safety and efficacy across broad sample	Monitor long-term side-effects
Time (nr of years)	1-5	1-2	1-3	1-5	Ongoing

Clinical development of new medicines, be they novel chemical entities (NCEs), or cell therapies is a costly and time-consuming process. The cost to develop a new medicine can exceed US$1bn (Kola and Landis 2004). Equally, the time to market for early cell therapy products ranged from 13 to 20 years (Dodson and Levine 2015). Indeed, the current platform consisting of phased clinical trials, outlined in Table 1.3, is a significant challenge to cell therapy developers, which consist predominantly of non-commercial entities (academia and charities) and SMEs, most of whom will lack the financial resources and capacity to navigate the required regulatory procedures (Maciulaitis et al. 2012). Lengthy post-approval testing and monitoring is also likely to be required for many ATMPs, particularly those involving the use of PSC-derived products or gene modification (Mount et al. 2015).

Worldwide, regulatory bodies are taking measures to curtail the time and cost associated with clinical development of cell therapies, particularly those which target severe conditions for which curative treatments are not currently available. Japan's Regenerative Medicine Act (RMA) enables a rapid (2-3 years) route to market for ATMPs (Fujita and Kawamoto 2016) with a conditional and time limited approval. Cell therapy products can obtain a time-limited market approval and reimbursement based on the results of a small scale (Phase I/II) clinical trial to establish safety and an indication of efficacy. Further data on long-term safety and efficacy collected during the initial marketing period (up to 7 years) can then be used to support an application for full market approval (Fujita and Kawamoto 2016). HeartSheet (Terumo, Tokyo, Japan), an autologous skeletal myoblast sheet, is the first product to gain market authorisation through the RMA regulatory route. Key differences between the regulatory pathways in the RMA and the current phased trials paradigm are highlighted in Figure 1.1.

The FDA's breakthrough therapy designation is designed to expedite drug development for therapies which demonstrate significant improvements on existing medicines for serious conditions. Breakthrough designation permits an accelerated development path, whereby a therapy maybe entered into a pivotal (Phase II/III equivalent) study following a successful Phase I trial (Sherman et al. 2013). To alleviate the development burden for novel therapies which target an unmet clinical need, the European Medicines Agency (EMA) have trialled staggered market approval, beginning with a restricted patient population whilst the risk-benefit balance of a product can be established (Eichler et al. 2012). Similar to Japan's RMA, the EMA adaptive pathways scheme will allow use of a therapy with restricted market access to supplement early-phase clinical trial development in order to pave the way for full market approval. 18 medicines were selected for use in an EMA pilot project to test the adaptive pathways scheme between 2014 and 2016 (EMA 2016).

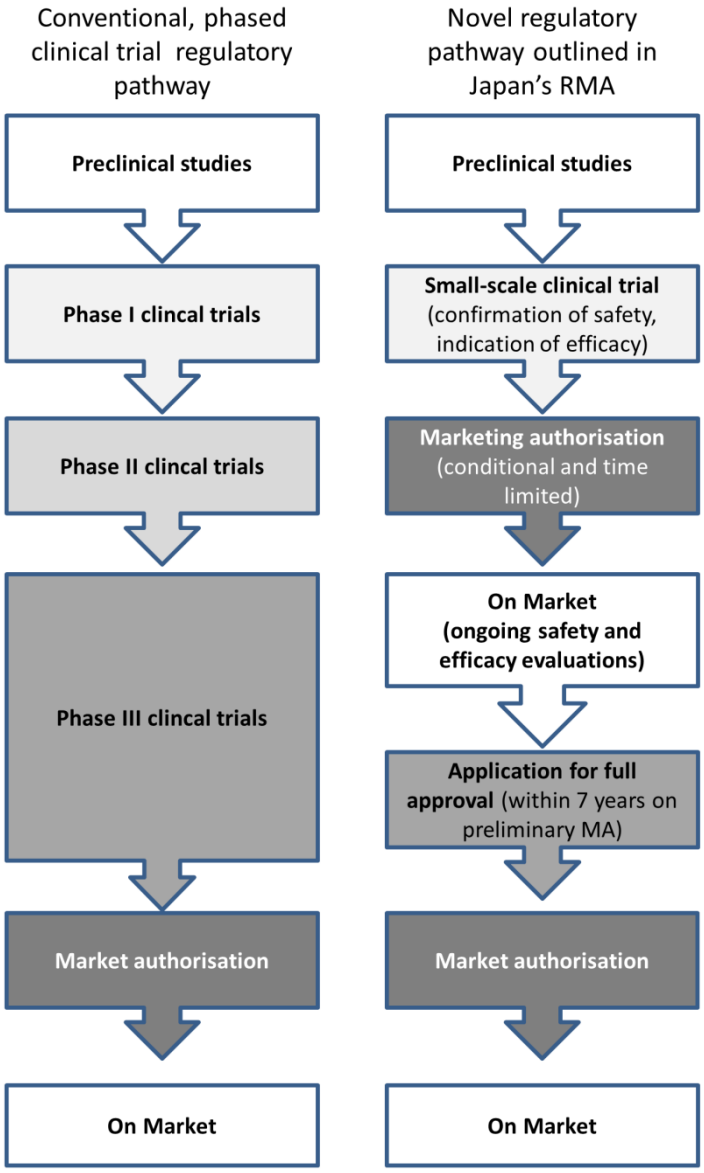

Figure 1.1 The novel regulatory pathway for translation of certain regenerative medicine products, as outlined in Japan's Regenerative Medicine Act (RMA). Figure adapted from Fujita and Kawamoto (Fujita and Kawamoto 2016).

All of the novel regulatory pathways above acknowledge a key caveat to drug (or in this instance, cell therapy) development; namely, that not all products granted these expedited market pathways will in fact fulfil the potential suggested by their pre-clinical and early clinical data. Therefore, updated approval pathways do not grant long-term, unrestricted market authorisation for ATMPs. Rather, they offer the opportunity to

monitor the safety and efficacy of ATMPs during a limited period of conditional approval, before a product may be submitted for full marketing authorisation.

A clearer route to market is beginning to emerge for ATMPs. This is a reflection of the acknowledgement of regulatory bodies that current, binary, regulatory pathways are unlikely to prove appropriate for novel therapies under development. Whilst this may be the case, it is still vital that developers of ATMP products identify critical quality attributes, and appropriate assays by which these can be measured, as early as possible following conception of a product. This will ensure that product quality can be assured prior to first-in-man trials, and lay the foundations for clinical translation.

1.3.2 Process development and manufacturing of cell therapies

Cell therapies are highly complex products. Thus, it is important to develop a robust manufacturing process that is conducive to the production of a safe and efficacious therapy. When examining process options for cell therapy manufacture, it is important to consider not only the operational performance but also the consequences on the economics, quality, regulatory compliance, safety, and flexibility. These key considerations are summarised in Table 1.4.

Guidelines and regulations concerning the production of cell therapies are known as current Good Manufacturing Practice (cGMP), and all aspects of a manufacturing process must be compliant with this set of regulations. Equally important to cell therapy production are current Good Tissue Practice (cGTP) guidelines, which govern the handling of tissue acquisition which acts as the starting material for cell therapy bioprocesses (Palau and Van Deusen 2016). The underlying concept of cGMP and cGTP regulation is to ensure reproducibility of product quality as a result of a comprehensively designed and robust bioprocess and tissue acquisition protocol (Römhild 2016).

In early phase clinical trials, risk of failure is high and developers of ATMPs have understandably strived to keep development costs low at this point of the translation cycle. It has been acknowledged that there has been a lack of investment with regards to developing a scalable and cost-effective manufacturing strategy, characterised by the 'fail quickly, fail cheaply' business model employed by many in the industry (Shaw et al. 2014; Mount et al. 2015). A key challenge in the development of ATMPs, and even in more established sectors such as antibody-based therapies, is the fact that product quality (including safety and efficacy) must be established by the end of Phase I trials. However, efforts to realise a scalable cost-effective process which can offer business sustainability, often occur far later than this (Farid et al. 2000; Shaw et al. 2014)

In the cell therapy industry, where there is significant heterogeneity in process design, even for products of the same nature, translation of these bench-top processes to standardised commercial manufacturing strategies has proven a significant challenge. One contributing factor to this is that, unlike traditional pharmaceutical products, it is challenging to characterise and prove the therapeutic equivalence of a population of cells (Caplan et al. 2016).

Delaying investment in process development may therefore cause substantial comparability-related risks for a product in the latter stages of the clinical translation cycle. Scale-up and adaptation of an early process design to one that will satisfy the demands of late-phase trials and commercial manufacturing may necessitate time-consuming and costly bridging studies before clinical development of a product can continue. Not only does this require significant financial resources, but it can add significantly to the time-to-market of a cell therapy product. This could be particularly damaging to the sustainability of both an ATMP as a commercial product, and to the organisation developing such a product.

Table 1.4 – Bioprocess development considerations for cell therapy products

Criteria	Example
Operational Performance	Expansion yields (harvest densities) Expansion folds Differentiation efficiencies Downstream process (DSP) yields Purity Resource utilization Scalability Lot processing time
Economic	Capital investment Cost of goods (materials, labour, quality control, indirect) Economies of scale - scale-up versus scale-out Fresh versus frozen product transportation and storage Process development costs Supply chain replenishment Product shelf-life Reimbursement value
Quality Control & Regulatory Compliance	cGMP and cGTP standards Process robustness and reproducibility Process validation, acceptable ranges of operation Product characterisation Quality, consistency and source of raw materials Automated versus manual processing
Safety	Contamination and containment Live human tissue handling Patient safety - side-effects, risk of tumour formation
Flexibility	Process changes Manufacturing demand changes Process bottlenecks Process scalability

The development of a scalable, robust, and cost-effective manufacturing process is a vital part of the development of a cell therapy, and should be considered as early as possible. Whilst the costs of cell therapy manufacture (and the price to the end user) are likely to remain high due to their complexity, market competition may eventually force reductions in selling prices (Caplan et al. 2016). The development of cost-effective manufacturing processes is therefore likely to be an important factor in determining a cell therapy's commercial success in such an environment. Optimisation of the manufacturing process, alongside consideration of manufacturing costs, early on during product development may help to reduce the time and cost associated with product development in the long-term, as well as increasing the likelihood of achieving a robust, scalable and cost-effective cell therapy bioprocess design (Shaw et al. 2014; Dodson and Levine 2015; Mount et al. 2015; Hassan et al. 2016).

1.3.3 Challenges constraining cell therapy commercialisation

Safety concerns

There are a variety of safety concerns associated with cell therapies. This is not to say that factors affecting the safety of cell therapies cannot be controlled and the risk to patients cannot be reduced to similar levels associated with biopharmaceutical products. However, risks are inevitable when the complexity of cell therapy products is fully considered. Unlike pharmaceutical drugs, which are naturally metabolised by the body, populations of therapeutic cells are likely to be incorporated into living tissue and survive in the body for an extended period of time (Caplan et al. 2016). Caution is required from a regulatory perspective in order to fully understand what effects cell therapies cause within the body, and the mechanisms by which these occur. Mount et al. (2015), define the three main safety concerns associated with cell therapies as tumorigenicity, immunogenicity and complications arising from the method of implantation of cells.

The risk of tumorigenecity in hPSC-derived therapies is high. This owes itself to the potential for teratoma formation as a result of the presence of undifferentiated cells (Brederlau et al. 2006). It is important that undifferentiated PSCs are removed from the process stream in order to mitigate such risks. Extensive assays have been developed in order to screen for the risk of tumorigenicity in PSC-derived products, which must be carefully monitored throughout the clinical development process (Kawamata et al. 2015)

Genetically engineered cell therapies, including CAR-T cells and iPSC-derived therapies, are also at risk of tumorigenicity (Herberts et al. 2011). However, improvements in viral vectors and scientific understanding related to genetic modifications of human cells have alleviated concerns related to insertional mutagenesis though the activation and suppression of genes (Mount et al. 2015)

Immunogenic responses are a risk in many allogeneic, or universal, cell therapies, where conditions such as graft versus host disease (GvHD) can result from cell therapy transplantation (Yang et al. 2015). Furthermore, CAR-T cell therapies, which harness the immune response to treat target indications, have been shown to cause immunogenic reactions within the body. Silencing of genes that induce the expression of T-cell receptors (TCRs) can prevent alloreactivity of transplants that is associated with the use of allogeneic CAR-T cell therapies (Valton et al. 2015).

Generally, PSC-derived and many MSC-based therapies are not thought to be at great risk of immunogenicity, although this is likely to depend on dose size, repetition of doses and site of administration (Li et al. 2004; Drukker et al. 2006; Nasef et al. 2008; Mount et al. 2015). Immunogenicity may not be a risk to patients if cells are administered to an immune-privileged site. This is thought to be the case with therapies which target age-related macular degeneration (AMD) and retinal pigment cell (RPC)-related disorders (Carr et al. 2013; Nazari et al. 2015). However, ocular immune privilege is not absolute, and its mechanims are not fully understood (Zhou

and Caspi 2010 – article 1); researchers should be therefore be cautious in assuming ocular immune privlege when considered human trials for cell therapies.

Tissue-engineered products, consisting of complex three dimensional structures, will likely require complex surgical procedures in order to implant a therapy into patients (Fabre et al. 2016; Feric and Radisic 2016). As with all surgical procedures, the risk-to-benefit ratio in this instance must be carefully weighed up by the medical practitioner responsible for a patient.

Reimbursement

Cell therapies are expensive to manufacture (Simaria et al. 2014; Hassan et al. 2015; Weil et al. 2017), and expensive to develop (Want et al. 2012; Mount et al. 2015; Caplan et al. 2016; Hassan et al. 2016). Whilst factors such as market competition, increased potency, and economies of scale associated with commercial manufacture of cell therapies will affect the cost of manufacturing, cell therapies are likely to command a high price tag in order to generate profits for their companies (Caplan et al. 2016). A balance between what manufacturers consider a fair price, and what healthcare providers are willing to, or can afford to, pay for ATMPs must be reached in order for successful cell therapy commercialisation.

There are a variety of factors that affect the reimbursement value of a cell therapy. Health Technology Assessments (HTAs) are employed to assess the cost-benefit ratio of new medicines. In the United Kingdom, the National Institute for Health Care and Excellence (NICE) has explicit cost-effectiveness controls in place that determine whether or not new medicines a for use by the National Health Service (NHS). NICE uses quality-adjusted life-years (QALYs) to assess the impacts of a treatment on the quality and longevity of a patient's life (Mahalatchimy 2016). Currently a cost of £30,000 is set as the upper benchmark per QALY for novel treatments.

Most HTA bodies, particularly across Europe, use the comparative clinical efficacy of a novel therapy against current comparators to assess its value (Jørgensen and Kefalas 2015). Therefore cell therapies are most likely to achieve their target selling price if they target indications with unmet clinical needs (Mount et al. 2015). This could include conditions for which no treatment exists (e.g. dry age-related macular degeneration (AMD) or where palliative care is available but no curative treatment is currently available (e.g. certain cancers and diabetes).

The clinical data to provide head-to-head comparisons that shape HTAs can be difficult to obtain for cell therapies, due to some of the clinical development challenges discussed in Section 1.3.1 and a shortage of access to patients. In order to combat uncertainty over the comparative performance of expensive ATMPs, pricing of such products is increasingly built on risk-sharing agreements (RSAs). RSAs allow a reduction in the reimbursement value received by a cell therapy manufacturer if the performance of a therapy does not meet expectations (Jorgenson and Kefalas 2015).

Walker & Johnson (Walker and Johnson 2016) predict that the QALY system would allow a price of ~US$120,000 – US$240,000 for a CAR-T cell therapy that would induce long-term remission in a patient for 5-10 years. However, a recent NICE report judged that CAR-T medications could be worth up to US$649,000 assuming patients gain 10 QALYs compared to current standard of care treatments (Hettle et al. 2017).

In Japan, both HeartSheet (Terumo), and Prochymal (JCR Pharmaceuticals Co., Hyogo, Japan) for the treatment of heart failure and GvHD respectively, have been priced between US$100,000 and US$150,000 dollars. Furthermore, Glybera, a gene therapy for the treatment of lipoprotein lipase deficiency was recently priced at US$1.4 million in Germany; the highest price medicine in existence for a rare disease (Yla-Herttuala 2015). Equally, Kymirah (Novartis, Switzerland) and Yescart (Gilead, CA, USA) have been priced at US$475,000 and US$373,000 respectively in the USA. These values indicate that healthcare providers and insurers are willing to pay the

high prices associated with cell and gene therapies providing they can offer unrivalled patient benefits. However, as more ATMPs that target the same indication reach the market, innovations that allow for either more efficient production of a therapy or incremental therapeutic benefits are likely to be required to drive down the cost-benefit ratio versus comparator products, rather than the novelty of the therapy itself (Mount et al. 2015; Caplan et al. 2016)

Capability and capacity for large scale production of cell therapies

Dose sizes reported for cell therapy products currently range from 5 x 10^4 cells for indications such as macular degeneration to 10^9 cells for some cancers and treatment of conditions such as myocardial infarction and liver disease (Mason and Dunnill 2009; van Schalkwyk, Papa, Jeannon, Urbano, et al. 2013; Simaria et al. 2014).

Reproducible and robust cell therapy bioprocesses are required to secure a sustainable commercial future for cell therapies. Traditional, planar tissue-culture technologies such as T-flasks (both single and multi-layer) may struggle to satisfy this global demand for cell therapies, particularly those which require large dose sizes (Want et al. 2012; Simaria et al. 2014). Platforms that rely on manual operation also increase the risk of batch failure due to human error or a lack of reproducibility. Several novel platforms that offer scale-up solutions for cell therapy manufacturing have recently been developed. These include automated planar bioreactors for adherent cell culture (Collignon 2012), microcarrier-based culture of adherent cells in single-used bioreactors (Bardy et al. 2012), rocking motion bioreactors for single-cell suspension cultures (GE Healthcare [no date]), and gas permeable vessels for suspension culture of cells at high densities (Vera et al. 2010).

Further to issues related to scale-up of human cell culture, there has not been a great deal of focus on harvest strategies following large scale culture of therapeutic cells (Chen et al. 2013). Translation of bench scale cell therapy culture unit operations to

commercial bioprocesses will be dependent on the consideration of how to detach, or collect cells from culture vessels and to reduce the media volume in advance of any DSP operations in a timely manner.

The success of many cell therapies is also dependent on the enrichment, or purification of therapeutic cells at high yields, so as to reduce the burden on USP operations such as cell culture, or differentiation stages of the bioprocesses. The development of efficient, scalable and cost-effective purification processes is one the major challenges facing the commercialisation and licensing of many hPSC-derived cell therapies (Weil and Veraitch 2013).

Any operation involving the transfer of cells from one piece of manufacturing equipment to another, where cells are exposed to the open environment, necessitates the need for expensive cleanrooms and risks contamination of process materials. Considerable emphasis has been placed on the need for contained processing of cell therapy products, which will ease the burden of cleanroom costs as well as alleviating the risks associated with 'open' manufacturing. Process platforms offering the potential for automated and contained bioprocessing include the CompacT SelecT (Sartorius Stedim, Gottingen, Germany), integrated process platforms such as the Prodigy (Miltenyi, Bergisch, Germany) and Cocoon (Octane, Ontario, Canada).

Current approaches to the manufacture of cell therapies and technological innovations to aid cell therapy bioprocessing are reviewed in detail in Chapter 2.

1.4 Cell Therapy Bioprocess Economics

Owing to growing reimbursement pressures associated with novel therapies, it is important to not only accurately estimate manufacturing costs for stem cell and cell therapy products, but also identify methods by which these can be reduced. This section discusses factors that influence two key cost metrics; fixed capital investment (FCI) and cost of goods (COG).

1.4.1 Capital investment

FCI represents the cost to build a manufacturing facility ready for start-up. It includes the cost of the building with the fixed (non-disposable) equipment, piping, instrumentation and utilities installed. Estimates of facility costs are often made using factorial estimates. These are well-established for traditional stainless steel biopharmaceutical facilities using the Lang Factor method (Lang 1948), which involves multiplying the total equipment purchase cost by the "Lang Factor". At present, there are no published studies that have determined an appropriate factorial method for cell therapy manufacturing facilities. The Lang Factor is usually derived based on the analysis of costs of previous projects; as yet very few FCI benchmarks have been published for stem cell manufacturing facilities. Investment costs for stem cell facilities will also be influenced by the degree of open versus closed processing and the consequences on the cleanroom classification required and whether automated or manual process techniques are employed. Stem cell bioprocessing is also dependent on disposable or single-use process platforms such as T-flasks, CellStacks and single-use bioreactors (SUBs). To this end, a Lang Factor method adapted for disposable-based biopharmaceutical facilities has previously been used to approximate the FCI associated with stem cell manufacturing (Pollock et al. 2013). Ongoing work at University College London is focused on developing a Lang Factor-style method which more accurately describes the FCI required for a cell therapy manufacturing facility.

1.4.2 Cost of goods

COG represents the cost to manufacture a cell therapy product and comprises direct (e.g. materials) and indirect (e.g. maintenance) costs. Direct costs are a function of utilisation and vary according to the scale and demand of a given bioprocess. Indirect costs include costs that are independent of resource utilisation and include

expenditures such as facility overheads and depreciation that are often estimated in proportion to the FCI.

Economies of scale are a relevant factor affecting COG for all bioprocesses, including those designed for the manufacture of cell therapy products, as demand and lot size are varied as well as dose for cell therapies and required cell population sizes for cells as drug screening tools. Outputs of COG calculations are usually expressed as COG per cell population for screening tools or COG per dose for therapeutic applications.

1.4.3 Process economic drivers

In order to achieve cost-effective bioprocesses for the manufacture of cell therapies, efforts need to focus on increasing the overall productivity and/or decreasing the overall production costs. Hence, critical process economic drivers for cell therapy processes can include an array of different parameters such as expansion and differentiation yields, target cell recovery during purification, and the cost of resources such as media and labour. Chapter 2 seeks to give an overview of advances made with regards to the performance of key unit operations in cell therapy bioprocesses, and the platforms that might support commercial-scale production of cell therapy products.

1.4.4 Project valuation

Decisions pertaining to bioprocess design will inevitably impact upon bioprocess economic metrics such as COG and FCI. These metrics can be used to feed into project valuation models in order to compare different projects proposed to solve a similar problem. One measure of the value of a project is the discounted cash flow, which is used to calculate a project's net present value (NPV) (Novais et al. 2001). Whilst many factors contribute to decisions regarding the feasibility and potential value of a project, those with a greater NPV are generally seen as a favourable proposition.

1.5 Decision-support tools and bioprocess modelling

In any bioprocess, it is important to determine a cost-effective, robust manufacturing process early on during product development. Changes to a manufacturing process once a product has entered clinical trials can result in the need for bridging studies, affecting both the monetary cost of product development and the time taken to get a product to market (Farid et al. 2000).

Decision-support software capable of the evaluation of different bioprocess strategies and designs can greatly improve the design of cost-effective, robust bioprocesses. Furthermore, *in silico* assessments of the operational and economic feasibility of bioprocess designs allow effective decisions to be made with regards to bioprocess design prior to committing a product to clinical trials. This can save cell therapy manufacturers both time and money during product development.

1.5.1 Applications of decisional tools

To date, much of the research into process simulation models and decisional tools in the biotechnology arena has been associated with the biopharmaceutical protein sector. Process simulation can be applied to a variety of bioprocessing scenarios. Thus far, applications have varied from equipment selection for a manufacturing process designed to produce material for clinical trials (Suzanne S. Farid et al. 2005), to evaluation of full-scale manufacturing flowsheets (Lim et al. 2006), and the appraisal of potential post-validation changes to bioprocesses (Chhatre et al. 2007). The identification of key process economic drivers associated with different bioprocesses may also highlight areas where process optimisation efforts should be focused for maximum effect (Farid 2009).

Decisional tools investigating process feasibility are able to select optimal processes based not only on throughput but also based on multiple criteria (including operational

and environmental process attributes) (Suzanne S. Farid et al. 2005; Pollock et al. 2013).

Uncertainty is inherent within the field of bioprocessing. Contamination risks, variability in process yields and equipment failure can all impact on manufacturing costs associated with a cell therapy. Stochastic modelling, such as Monte Carlo simulations, of bioprocesses has allowed evaluation of biopharmaceutical production processes under manufacturing uncertainty (Suzanne S. Farid et al. 2005; Lim et al. 2006; Stonier et al. 2012; Pollock et al. 2013). Stochastic modelling produces a significantly larger amount of data than deterministic modelling as thousands of simulations must be evaluated in order to gauge the risks associated with a given solution to a bioprocess design problem (Stonier 2013).

Decisional tools have been shown to be of great value in the biopharmaceutical industry; aside from the more general applications mentioned above, exploration of topical process design scenarios via individual case studies have highlighted how they can be used to contibute to the the bioprocess industry.

Decisional tools have been used to illustrate bioprocesses can be designed to cope with ongoing technological advances (in both processing equipment and in molecular biotechnology resulting in increased target product titers) (Farid 2001; Novais et al. 2001; Stonier et al. 2012; Pollock et al. 2013). Decisional tools provided detailed COG analyses where potentially hidden costs of ancillary tasks (e.g. buffer and media preparation and storage) and their impact on overall manufacturing costs were considered for the first time (Farid 2009). The importance of this was demonstrated by Sinclair and Monge (2002) who provided a detailed study of the effect of the use of disposable technologies for buffer preparation and storage on overall COG.

Early examples of decisional tools within the bioprocessing sector focused on how the use of disposable processing equipment might impact upon manufacturing COG

and FCI (Farid et al. 2000; Novais et al. 2001; Sinclair and Monge 2002). In the case of Farid (2000) and Novais et al. (2001), NPV calculations were provided in order to demonstrate the feasibilty of disposable based bioprocesses within the biopharmaceutical sector.

Further applications of decisional tools have seeen them applied to DSP or purificaiton design problems as a result of advances in biotechnology associated with mAb expression systems, which saw achievable cell culture titers for therapeutic antibodies increase drastically (Stoner et al. 2012). The identification of DSP production bottlenecks that would liklely result from increased cell culture yields was one area where decisional tools were able to demonstrate their applicability to industrial process design problems. Furthermore, decisional tools have been shown to be adept platofrms for the exploration of purification strategies and column sizing that could help alleviate such issues whilst taking into account the impact of such strategies on manufacturing COG (Stonier et al. 2012; Allmendinger et al. 2016). The Stonier et al. (2012) study also highlighted the manner in which decisional tools could be used to highlight issues and solutions that go beyond those which may perhaps be considered intuitive to bioprocess experts; buffer storage limitations were shown to be a limiting factor in the potentially capacity of legacy bioprocess facilities. Stonier et al. (2012) demonstrated that the development of purificaiton platforms resulting in a reduction of buffer consumption may be a potential solution to this problem.

Pollock et al. (2013) demonstrate the value of decisional tools in assessing the economic viability of novel technologies. Traditional fed-batch cell culture strategies were compared to first-generation and emermging pefusion culture platofrms; next generation perfusion cell culture platofrms were shown to be singificantly more cost-effective than fed-batch methods. This case study shows how decisional tools can be used to explore the use of new technologies and their effect on manufacturing COG in silico in order to demonstrate their feasilibility.

Taking the examples above, it is evident that decisional tools have a place in aiding cost-effective bioprocess design, but can also be used to explore future proofing strategeis of legacy facilities by exploring the use of novel manufacturing strategies and technologies *in silico* in order to evaluate their impact on facility design, manufacturing cost of goods and a variety of resource requirements (Farid et al 2000; Stonier et al. 2012).

1.5.2 Decision-support tools and their applications in the cell therapy sector

As a relatively nascent field, the cell therapy sector is challenged by a lack of consensus as to the optimal bioprocess strategy and design for many products. Cell therapy products are likely to experience manufacturing cost of goods that are larger than those associated with conventional pharma products (Prescott 2011). As such, prudent and swift bioprocess design is required in this sector. As has been shown by their application to bioprocessing of biopharmaceutical products, decisional tools can help promote effective decision-making with regards to cell therapy bioprocessing.

At the time of writing, a small, but growing collection of studies investigating the applicability of decision-support tools to cell therapy bioprocessing is in existence. Commercially available flowsheeting software packages have been employed to cost stem cell process designs at fixed scales (Darkins and Mandenius 2013). Simaria et al. (2014) and Hassan et al. (2015) present the development and application of decisional tools that integrate models for mass balancing, equipment sizing, and bioprocess economics with optimization algorithms for allogeneic MSC production. The tools were used to predict the most cost-effective upstream and downstream technologies for commercial MSC manufacture across a range of different scales and doses. The analyses presented in these works illustrate how such tools can be used to determine the scale at which planar technologies cease to be cost-effective in contrast to microcarrier-based SUBs, when downstream processing bottlenecks occur, as well as future required performance capabilities of promising technologies

to close existing technology gaps and meet COG targets. Project valuation tools have been developed to assess the impact of process changes throughout the clinical development pathway of an allogeneic hMSC therapy (Hassan et al. 2016). Furthermore, the studies above summarise the key factors that influence COG values for stem cell products; these include process efficiencies, technology choices and the resources required and unit costs based upon these choices (Simaria et al. 2014; Hassan et al. 2015; Hassan et al. 2016). It can therefore be said that the application of decisional tools in the cell therapy sector thus far has been not only to demonstrate the optimal process technology choices from a cost-perspective in a given scenario; but also to demonstrate limitations in existing technologies for cell and gene therapy bioprocesses in order to highlight the need for scalable, cost-effective technologies (Simaria et al. 2014; Hassan et al. 2015; Hassan et al. 2016; Weil et al. 2017). Use of decisional tools for such scenario analyses and gap analyses may eventually help shape TPPs for future process platforms in order that they allow manufactruing within a target COG threshold.

1.5.3 Limitation and Decisional Tools

The evidence and research reviewed up to this point in this section demonstrates the value of decisional tools; indeed this thesis aims to further demonstrate the applicabiltiy of such tools to the cell therapy sector (this is expanded in Section 1.6).

Whilst there is a strong case to be made for the use of decisional tools within the biorpcoess industry, there are certain challenges and limitations to their use. One such limitation is the fact that decisional tools require a great deal of time and effort to produce, which may discourage their use in indutrial settings. General purpose software, which can be used for many different types of process are challegning to develop may help with this. A commercially available software, BioSolve (BioPharm Services, Buckinghamshire, UK) is available for bopharmaceutical process design, and can be tailored to individual processes to a certain extent. However many

bioprocesses particiularly those for cell and gene therapy prodcuts require specific processes that general use software may struggle to capture in a necessary amount of detail. The devleopment of decisional tools therefore requires considerable time and effort in order that an appropriate level of proess specific detail be captured. This is evident in case studies of decisional tools published for cell and gene therapies to date, whereby process designs for MSCs have been explored (Simaria et al. 2014; Hassan et al. 2015; Hassan et al 2016). General purpose tools, may fail to accurately capture all resources required as part of a bioprocess, thus limiting the value of the tool itself.

A further limitation of decisional tools in the bioprocess sector is the fact that, whilst uncertainty can be accounted for using methods such as the Monte Carlo simulaiton method, they do rely on *in silico* analysis; translation of the findings of a tool into practice is not always a trivial act. For example, bioprocess design choices have sometimes been based upon company know-how and experience in th mAb sector (Pollock et al. 2013). The qualitative aspects of receptiveness to, and effort required to make, process design changes that a decisonal tool may suggest are cost-effective are somewhat harder to accurately quantify using decisional tools.

Finally, whilst rigour has undoubtedly been at the heart of research into decisional tools to date, it is impossible to be 100% accurate in the estimation of resource requirements. Generally a 10% margin of error is taken as read when analysing the results of decisional tools, which can sometimes make it difficut to distinguish between closely matched solutions to process design problems (Farid 2002).

Despite their limitations, decisional tools have played a prominent and positive role in helping to shape bioprocess design considerations in the biophmarmaceuitacal sector to date. Furthermore, they are beginning to emerge asa powerful platform upon which to analyse and evaluate cell and gene therapy manufactruing strategeis and

process design. As outlined in Section 1.6, this thesis aims to further explore their applicability in this sector.

1.6 Thesis aims and objectives

This chapter has sought to provide an overview of cell therapies and highlight key issues related to their development and manufacturing. Furthermore, the applications of process simulation and decisional tools to the field of cell therapy and the broader bioprocess sector have been detailed.

A literature review has revealed that at present there are few existing studies, or tools, which allow the evaluation of bioprocess designs and manufacturing strategies for cell therapies. Those that do exist focus on adult cell types, such as MSCs (Simaria et al. 2014; Hassan et al. 2015; Hassan et al. 2016). No such studies were found to exist for hPSC-derived cell therapies, or those which involve *ex vivo* genetic modification, such as CAR-T cell therapies.

The aim of this thesis was to investigate the applicability of decisional tools, which capture both technical and business perspectives of cell therapy manufacturing, to advanced cell therapy bioprocess design. It is hypothesised that this approach is likely to facilitate informed decision-making with regards to bioprocess design during the early phases of product development. To this end, a series of case studies was carried out, whereby decisional tools developed as part of this thesis were used to analyse bioprocess design for three independent cell therapy or stem-cell derived products. The remainder of this thesis is therefore formed of chapters which seek to investigate the applicability of decisional tools to the cell therapy industry.

Chapter 2 examines current and future trends in cell therapy bioprocesses, and their applicability to large-scale commercial cell therapy production. An overview of cell therapy bioprocesses, and the unit operations contained therein, is provided. Analysis and appraisal of currently available bioprocess platforms is carried out, and this was

used as a basis to determine selection of technologies to be included in the decisional tools described in subsequent chapters.

In Chapter 3, the materials and methods by which the work in this thesis was carried out are detailed. The core framework, or architecture, of the decisional tools developed is presented. Following this, the process models developed to capture different unit operations and bioprocess economic attributes of a given bioprocess are described. Finally, the computational methods by which optimal bioprocess designs and manufacturing strategies were identified are outlined, along with computational techniques used to deal with uncertainty in bioprocessing.

In Chapter 4, a case study is presented whereby a decisional tool is applied to the production of patient-specific induced pluripotent stem cells, to provide a platform for drug screens probing the potential for stratified pain medication. A brute-force search algorithm was applied in order to provide a bioprocess economic comparison of automated vs. manual bioprocess platforms. The Monte Carlo simulation technique was applied in order to provide evaluation of bioprocess techniques under uncertainty. The processing of patient-specific hiPSC-derived cell lines for drug screening purposes (Chapter 4) was investigated because, at the time the work was carried out, this was perceived as a more immediate, tangible application of hiPSCs than cell therapies.

Analysis of an hPSC-derived cell therapy bioprocess is provided in a case study detailed in Chapter 5. Different bioprocess strategies, including directed vs. spontaneous differentiation and microcarrier-based vs. planar-based cell culture, are evaluated for the production of a hESC-derived cell therapy. The evolutionary algorithm developed in order to identify the most cost-effective process flowsheet for each manufacturing strategy is the first of its kind to be applied to cell therapy process design. Stochastic modelling techniques were used to incorporate manufacturing uncertainties into the analysis. Finally, different business models with regards to the

production and distribution of a cell therapy product are explored from a quantitative and qualitative viewpoint. A decisional tool to evaluate different bioproess strategies for hESC-derived cell therapies was developed in order to build upon the work dscribed in Chapter 4, so as to demontrate the applicability of the approaches detailed in this thesis to allogeneic hPSC cell therapies. The type of cell therapy used to explore this approach, a patch of hESC-derived RPE cells for the treatment of age-related macular degeneration, was an approach that had resulted in early success in first-in-man trials. This was therefore selected as the focus of the work in Chapter 5.

Chapter 6 describes the application of a decisional tool to bioprocess design for an allogeneic CAR-T cell therapy. Different process flowsheets were evaluated from a bioprocess economic perspective. Sensitivity analyses were used to highlight key process economic drivers, and scenario analyses were used to highlight how future process improvements might impact upon COG as a percentage of target selling price. Multi-attribute decision making (MADM) analysis is used in order to highlight the benefits of accounting for operational, as well as financial, attributes in the evaluation of different bioprocess designs. In Chapter 6, the development and application of a decisional tool to investigate bioprocess economics associated with allogeneic CAR T-cell production was conducted in order to prove the applicability of such methods to the wider cell and gene thearpy industry. Whereas previous sections (Chapters 4 & 5) focus on hPSC-derived cells for a variety of applications, Chapter 6 focuses on a gene therapy approach in order to demonstrate the versatility of decisional tools in the cell and gene therapy space.

Chapter 7 provides a summary of the contributions of this work to the field and details proposals for future work. Appendix A presents a manuscript that describes an integrated experimental and economic approach to bioprocess design. This manuscript was co-authored with colleagues in the Department of Biochemical Engineering and has been submitted for publication in a peer-reviewed journal.

Academic papers published by the author through the course of this work are attached in Appendix B. Finally, Appendix C is used to highlight the importance of process validation, and how this might be achieved for a cell therapy bioprocess.

Chapter 2: Cell therapy bioprocessing

Cell therapy bioprocesses are complex procedures. They often involve multiple unit operations and significant variations can be observed between the bioprocesses used to produce different types of cell therapies (e.g. allogeneic vs autologous and somatic cell types vs hPSCs).

This chapter provides an overview of cell therapy bioprocesses, and the technologies that are used to support them. Section 2.1 outlines the typical differences in the manufacture of different types of cell therapies; autologous and allogeneic cell therapy production is discussed, as is the production of somatic cell and pluripotent stem cell therapies. Sections 2.2 through 2.5 discuss key unit operations associated with cell therapy production including cell culture (Section 2.2), differentiation (Section 2.3), genetic modification (Section 2.4), and downstream processing operations (Section 2.5). In these sections current techniques and technologies are introduced and evaluated based on currently available literature. Novel techniques and future trends are also introduced. Section 2.6 outlines current efforts aimed at the creation of contained bioprocess platforms. Finally, manufacturing and distribution strategies are discussed in Section 2.7.

2.1 Bioprocess flowsheet variations for different types of cell therapies

Significant differences occur between commercial production techniques for different classifications of cell therapies. This section aims to introduce the strategies used to scale production for commercial purposes for both autologous and allogeneic cell therapies. Additionally, typical process flowsheets and the unit operations contained therein are introduced for both adult cell therapies (MSCs and CAR-T cell therapies) and hPSC-derived therapies. Key differences in the processes used to produce the above therapies are also detailed.

2.1.1. Autologous vs. allogeneic cell therapy bioprocess flowsheets

Autologous cell therapies

Autologous, or patient-specific, cell therapies are derived from a patient's own biopsy. Cells are then processed according to the specific demands of the therapy, and returned to the patient, either surgically, or via an infusion. Autologous cell therapies can negate the risk of immunological responses as the therapeutic material is derived from the patient. However, there have been instances of immune responses to CAR-T cell therapies where a patient's cells have undergone significant modification as part of the production process (Tey 2014). Due to the fact that the patient's own cells must be processed, autologous cell therapies are unsuitable for use as 'off-the-shelf', emergency products.

Allogeneic cell therapies

Allogeneic, or universal, cell therapies rely on a single source of cells to treat many patients. Cells are collected from a donor sample to create a master cell bank (MCB). The MCB is then used as the source to create cell populations that are processed according to the demands of the specific therapy. The final cell populations are then used to treat multiple patients. Allogeneic therapies are more adept at satisfying 'off-the-shelf' supply models, where emergency treatment might be required. Allogeneic therapies increase the risk of eliciting an immune response within a patient, and immunosuppressive therapies are sometimes administered in combination with allogeneic products.

Scale-up vs scale-out approaches

Allogeneic bioprocess design can be approached using a scale-up methodology. This is a manufacturing approach analogous to that of the pharmaceutical industry, whereby many doses are produced per manufacturing lot. This approach allows economies of scale to be achieved that are beyond those of the scale-out approach

required of autologous cell therapy manufacture (Mason and Dunnill 2009). Due to the fact that many doses can be produced within the same manufacturing lot, allogeneic processes are not limited in the same capacity that autologous processes are; they are generally less labour-intensive and result in reduced capital investment per dose than autologous therapies. However, this is also dependent on the choice of technology and bioprocess strategy (see Sections 2.2 – 2.7).

Some therapies, such as allogeneic CAR-T cell therapies may require a hybrid approach, whereby a bioprocess may be scaled-up to a certain point, before it is scaled out. This is due to limitations on the number of doses that can be produced from each donor sample. Allogeneic therapies benefit from having a fixed process schedule; there is a guaranteed supply of raw material for the production process coming from a working cell bank. This is in contrast to autologous cell therapies, for which process scheduling can be complex in instances where production can only begin once a patient's material is received at a manufacturing facility. Furthermore, donor-to-donor variability adds an additional layer of complexity to autologous process design and scheduling – although occasionally, pre-screening of a patient's cells can help to predict their performance within a bioprocess.

Patient samples must be strictly segregated for autologous therapies to avoid cross-contamination. Therefore, autologous cell therapies necessitate that a scale-out, rather than a scale-up approach to bioprocess design be adopted, whereby the manufacturing scale, or lot size, is kept constant and replicated for each patient (Figure 2.1). From a manufacturing perspective, autologous treatment results in a one lot = one patient treatment. Autologous cell therapy bioprocesses are more labour-intensive compared to allogeneic manufacturing strategies; they require the same process to be carried out multiple times at a relatively small scale. Furthermore, this can increase the capital investment required, particularly in instances where complex, automated platforms are used within a bioprocess. Unless a piece of machinery is

designed to handle multiple patient samples in a segregated manner, each patient sample being processed at any given time requires a separate piece of equipment. The need for multiple pieces of fixed equipment can be alleviated somewhat by scheduling a bioprocess to maximise equipment utilisation. There are now a number of specialist pieces of equipment that aim to provide an automated, contained platform for autologous cell therapies; these are discussed in Section 2.6.

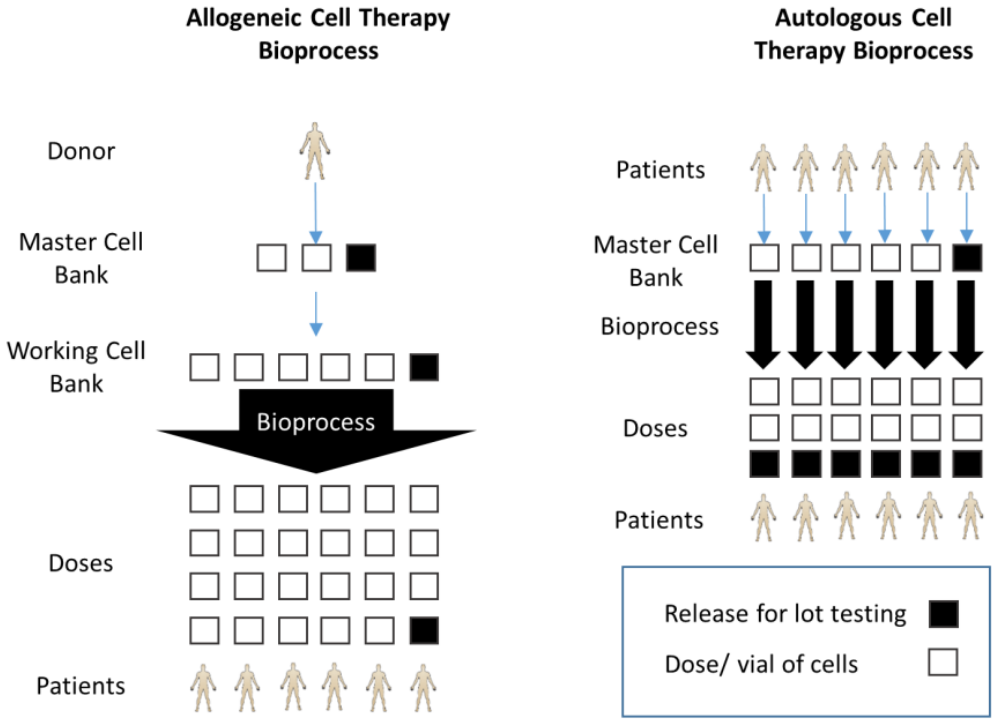

Figure 2.1 (adapted from Brandenberger et al. (2011)) A comparison of the scaling strategies used for **a)** an allogeneic cell therapy bioprocess, which is scaled using a 'scale-up' approach so that one lot can produce doses for multiple patients, and **b)** an autologous cell therapy bioprocess, which is scaled using a 'scale-out' approach, whereby the bioprocess is replicated for each patient equating to a one lot = one dose manufacturing paradigm

2.1.2 Adult cell therapy bioprocesses vs pluripotent stem cell-derived bioprocesses

Typical bioprocess flowsheets for MSC-based cell therapies (adult stem cell), CAR-T cell therapies (adult cell) and pluripotent stem cell-derived therapies are shown in Figure 2.2. Whilst all cell therapy bioprocesses share common unit operations, such as expansion (or cell culture), different types of cell therapies demand that specific unit operations and manipulations be included in a bioprocess.

Unit operations common to all cell therapy bioprocesses

All cell therapy bioprocesses require certain unit operations that are common to every type of cell therapy (see Figure 2.2). These include tissue acquisition, cell culture, harvest, and formulation stages. Tissue acquisition involves the collection of a biopsy from a donor or patient in order to provide the starting material for a bioprocess. Cell culture is the expansion of a cell population to a clinically relevant size. Harvest strategies involve separation of cells from cell anchorage materials and media used in culture-based unit operations. Formulation stages involve the manipulation of a cell therapy product into its final form, suitable for administration to patients.

Unlike PSC-derived, or CAR-T cell therapy manufacturing, bioprocesses by which MSC-based therapies are produced do not contain any unit operations that are specific to the type of cell therapy being produced. However, tissue acquisition for cell line creation is seen as a key phase in MSC bioprocesses as it presents a potential source of process variation. This is particularly true for autologous therapy processes, where different MSC lines often display variable expansion capabilities, in terms of both achievable lot sizes and growth kinetics (Lo Surdo and Bauer 2012).

Additionally, MSCs are cultured at relatively low densities compared to hPSCs and T-cells. Juxtaposed against lot sizes which may lie in the order of trillions of cells (Rowley et al. 2012), this can result in cell culture volumes comparable to those

observed in biopharmaceutical bioprocesses. Technologies to support the large lot sizes required for MSC therapies are discussed in Section 2.2. Large cell culture volumes place a subsequent burden on the harvest and concentration unit operations, which must be carried out within a short time-frame so as to maintain cell viability and potency (Veraitch et al. 2008). Current technologies available for harvest and concentration of cell populations are detailed in Section 2.5.

CAR-T cell bioprocess-specific unit operations

Figure 2.2b shows a typical CAR-T cell therapy bioprocess flowsheet. T-cells are collected by leukapheresis. This is the process by which whole blood is removed from a patient's body and separated into constituent parts. The required material for a cell therapy is removed and the remainder is returned to the donor. Further unit operations must be carried out prior to T-cell culture within a CAR-T cell bioprocess. T-cells are activated, or stimulated in order to amplify their immune response to tumour cells. This is done by exposing T-cells to antigens and costimulatory molecules. In the past, dendritic cells and B-cells have been used for T-cell activation (Levine 2015). Either anti-CD3/ anti-CD28 paramagnetic beads, gels, or nanomatrix beads are most commonly for products currently under development. This is due to both variations in the activation of T-cells exposed to DCs and B-cells and the additional complexity of handling additional cell types within a bioprocess. Transduction, whereby recombinant CAR genes are delivered to the T-cells in order to be expressed, must also be carried out. This is the process by which a T-cell is modified to express the CAR protein on which its potency relies. Allogeneic CAR-T cell therapy bioprocesses include an additional unit operation compared to their autologous counterparts (Figure 2.2b). This unit operation facilitates the genetic knockout of a surface protein believed to cause graft versus host disease (Yang et al. 2015). There are several methods to achieve this, including viral transduction, electroporation and transduction of genes using novel mechanical membrane disruption technology (Singh et al. 2013;

Vannucci et al. 2013; Sharei et al. 2015). Genetic modification of cells for cell therapy is discussed in Section 2.4. Some allogeneic bioprocesses include a preparatory cell culture stage prior to gene knockout in order to boost viable T-cell numbers.

Allogeneic CAR-T cell therapy bioprocesses include a purification step in order to remove cells where genetic modifications to knockout T-cell receptors that cause GvHD have failed. This can be performed using affinity-based cell purification techniques (Valton et al. 2015) which are discussed in Section 2.5.

Pluripotent stem cell-derived therapy bioprocess-specific unit operations

Figure 2.2c shows a typical process flowsheet for PSC-derived therapies. PSC-derived therapy bioprocesses contain an additional, inherent degree of complexity compared to adult stem cell therapy bioprocesses. This is partially due to the differentiation unit operation that PSC-derived cell therapies necessitate. Differentiation is a culture-based process by which pluripotent stem cells are driven towards a specialised progenitor lineage required for a specific cell therapy. The differentiation unit operation is discussed in Section 2.3. Human embryonic stem cell lines are derived from the inner cell mass of developing embryos. A working cell bank can be created directly from this source material. Induced pluripotent stem cell lines must be created through the process of cellular reprogramming.

Reprogramming is the process by which an (adult) somatic cell is induced to become a pluripotent stem cell. iPSC lines have been via the use of a number of different vectors, details of which can be found in Section 2.4. Unit operations involved in the creation of hiPSC lines are shown in the box in Figure 2.2c marked ‘cell line creation for hiPSC bioprocesses’. For autologous iPSC-derived cell therapies, tissue acquisition and cellular reprogramming must be carried for each individual patient in order to create a master cell bank (this can then be used for repeat doses if necessary). For allogeneic iPSC-derived therapies, cellular reprogramming only

needs to be carried out on an individual donor's material in order to create a universal iPSC line from which a master cell bank can be generated. A major advantage of iPSCs is that they can be used to create autologous, non-immunogenic therapies. However, allogeneic iPSC therapies are rare due to the cost and difficulty of cellular reprogramming, and concerns over their immunogenicity when used for allogeneic therapies are perhaps why no clinical trials currently involve allogeneic iPSC therapies.

Certain DSP operations, such as cell harvesting following PSC expansion and purification, are not always essential to PSC therapy bioprocesses. The need for harvesting between culture-based operations can be negated in some integrated bioprocess strategies (discussed in section 2.6). Furthermore, culture conditions used in certain differentiation protocols promote only the proliferation and survival of target cell types, resulting in a very pure population of viable cells following removal of the culture media. This can negate the need for affinity-based purification methods such as MACS or FACS, which are used when hPSC therapies do require purification unit operations.

Having introduced the overall bioprocess flowsheets for three key variants of cell therapy, the subsequent sections provide further detail on key unit operations. General information is given where possible. In instances where information that is specific to a certain type of cell therapy is discussed, this is stated clearly within the text.

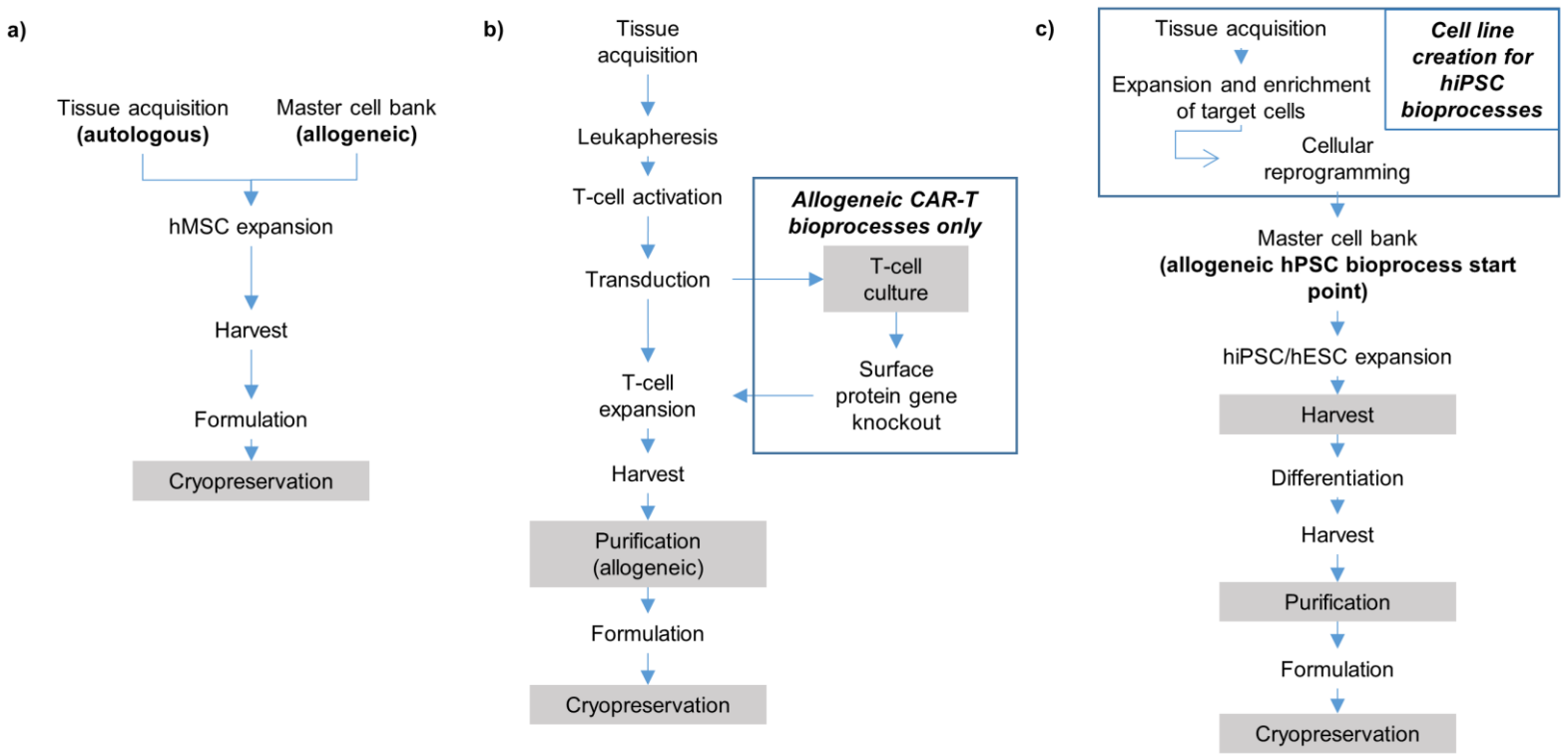

Figure 2.2 A comparison of typical bioprocess flowsheets for **a)** an MSC-based cell therapy, **b)** a CAR-T cell therapy and **c)** an hPSC-based therapy. Specific operations required for allogeneic CAR-T cell therapy manufacture are shown in the boxed section of panel **b)**. Upstream unit operations required for hiPSC bioprocesses are shown in the boxed section at the top of panel **c)**. Unit operations which are occasionally not required, depending on the bioprocess strategy employed, are depicted by shaded boxes

2.2. Culture strategies for cell therapies

2.2.1 Planar culture systems for therapeutic cell culture

MSCs and hPSCs can be grown as adherent colonies, anchored to tissue culture plastic, feeder layers, or synthetic substrates in vessels such as T-flasks. CAR-T cells are cultured in suspension; traditionally this has been done in T-flasks or static cell culture bags.

One concern associated with the use of traditional culture platforms, such as T-flasks for the growth of cells in monolayers is the lack of capabiltiy for appropriate environmental monitoring on control. Temperature and dissolved oxygen concentrations vary greatly across incubators, which are often used to house tissue-culture plastic based vessels during cell growth. Furthermore, real-time monitoring of cell cultures is not feasible in such platforms and environmental homogeneity in terms of temperature, pH and nutrient distribution, even within the same vessel, cannot be ensured.

Traditional, planar hPSC culture platforms relied heavily on the use of xenogeneic growth substrates and non-human feeder layers, which risk contamination of hPSC-derived products. Furthermore, feeder layers differentially secrete signalling factors, resulting in poorly defined culture conditions that are unsuitable for empirical study of hPSC expansion (Eiselleova et al. 2008). The development of anchorage materials comprising of a mixture of synthetic and/or recombinant biological motifs have allowed hPSC culture to progress away from the use of feeder layers (Villa-Diaz et al. 2013). MSCs are anchorage-dependent cells and can be characterised by their natural adherence to standard tissue culture plastics (Panchalingam et al. 2015). Conventional MSC and T-cell culture is reliant on serum-based media. Foetal bovine serum (FBS), is inappropriate for GMP-based manufacturing owing to the risk of both pathogen transmission and immune reaction in patients that is inherent in its use and

its lot-to-lot variability (Spees et al. 2004; Bernardo et al. 2007). The development of xeno-free, defined media is crucial to the robust bioprocessing of cell therapies (Abbasalizadeh and Baharvand 2013). Optimisation of media composition has seen the release of commercially available, serum-free media for the culture of both T-cells and MSCs (Gottipamula et al. 2013; Smith et al. 2015). The simplicity of defined media may reduce costs associated with cell expansion materials by 30-60% (Wang et al. 2013).

The labour-intensive nature of T-flasks limits their throughput and applicability to larger scale processes (Placzek et al. 2009; Want et al. 2012). This is particularly true of MSC-based and allogeneic CAR-T cell therapies, where lot sizes are likely to be in the order of billions or trillions of cells. Systems that stack multiple culture chambers above one another vertically have enabled greater cell yields than traditional 2-D culture methods at lower factory floor footprints (Rowley et al. 2012). The Cell Factory (ThermoFisher Scientific, Waltham, MA, USA) and CellStack/ HyperStack (Corning, New York, NY, USA) systems are examples of this and have been used to expand MSC populations to clinically relevant scales (Bartmann et al. 2007; Schallmoser et al. 2008). Inflated facility size requirements and subsequent capital investment costs associated with 2-D culture scale up are challenges facing the application of traditional, planar technologies at a commercial scale (Brandenberger et al. 2011; Rodrigues et al. 2011).

Automated, closed-process systems such as the CompacT SelecT (Sartorius AG, Gottingen, Germany), capable of handling 90 x T175 flasks simultaneously, and the Nunc Automatic Cell Factory Manipulator (ACFM) (ThermoFisher Scientific, Waltham, MA, USA), capable of manipulating 4 x 40 layer vessels, may help increase the throughput of 2-D cell therapy bioprocess strategies during expansion and differentiation (Thomas et al. 2009). Automated systems allow processing to take place in smaller, lower grade clean rooms compared to manual processing. The

closed processing offered by automation systems provides greater process control and reproducibility compared to manual processes (Veraitch et al. 2008). The Xpansion series of bioreactors (Pall Life Sciences, Port Washington, NY, USA), offers planar culture in a fully contained, bioreactor type environment. These vessels stack thin plates, which support cell growth, on top on one another, akin to the multi-layered vessels mentioned above. This vessel is suitable for the culture of adherent cells (e.g. MSCs and PSCs) (Collignon 2012). An overview of planar cell culture platforms is contained within Table 2.1.

It is unlikely that planar vessels will be used in any commercial bioprocess designed for the manufacture of CAR-T cells. As stated above, CAR-T cells are grown in suspension. Restrictions in the physical depth of the media in T-flasks and stacked planar vessels mean that the volume of media per surface area, and thus achievable cell population sizes, of such vessels is limited. T-cell populations grown in T-flasks must therefore be passaged more frequently even that if a static culture bag was employed as the cell culture platform.

The scale-up of any bioprocesses that employ manual, planar technologies is likely to prove challenging. However, planar processing platforms may continue to have a place in commercial cell therapy bioprocesses. The application of planar technologies in the production of autologous and low-dose allogeneic cell therapies (such as those targeting AMD (Table 1.1), should not be discounted. 2-D platforms are also likely to prove useful for the production of phenotype-specific hPSC-derived cells for personalised medicine drug screening that necessitate a scale-out, rather than a scale-up approach to bioprocess design (Rowley et al. 2012).

Table 2.1 (continued overleaf) Cell culture platforms for cell-based therapy production and a summary of their characteristics

Technology	Scale	Advantages	Disadvantages	CAR-Ts	MSCs	PSCs
T-flasks	$25cm^2$ – $225cm^2$	Low cost per unit Low capital investment costs	Labour intensive Open system Low process reproducibility Limited scalability	Y	Y	Y
Multi-layer vessels (no automation platform)	$500cm^2$ – 60,000 cm2	Low capital investment costs Reduced facility footprint	Labour intensive Open system Difficult to achieve homogeneous media distribution Low process reproducibility	Y	Y	Y
CompacT SelecT (for T-flask/ Cell Factory manipulation)	Up to 90 x $175cm^3$	Closed system Automated Process reproducibility	High capital investment costs Complex operation Additional media consumption Multiple units needed for large doses	N	Y	Y
Automated Cell Factory Manipulator	Up to 4 x 60,000 cm^2	Automated media exchange Increased reproducibility Reduced facility footprint	High capital investment costs Difficult to harvest cells	N	Y	Y

Integrity Xpansion	6,120cm^2 – 122,400cm^2	Closed system Automated Control of growth environment Low capital investment costs Small facility footprint	High cost per unit	N	Y	Y
Static Culture Bags	1L – 50L	Cheap Low capital investment costs Easy to use	Labour intensive Poor control of culture environment	Y	N	N
Microcarrier culture in single-use bioreactors (SUBs)	1L – 1000L+	Fully controlled culture environment Automated Closed system High process reproducibility High surface area: media volume ratio	High capital investment costs on control unit High cost of SUB Few studies carried out at commercial scale	N	Y	Y
Aggregate culture in SUBs	1L – 1000L+	Fully controlled culture environment Automated Closed system High surface area: media volume ratio	High capital expenditure on control unit High cost of SUB Few studies carried out at commercial scale Difficulties controlling aggregate size	N	N	Y
G-Rex	10cm^2 – 500cm^2	High cell densities achievable Cheap Efficient use of media Low capital investment costs	Multiple units likely to be required	Y	N	N

Rocking motion bioreactor	1L – 50L+	Fully controlled culture environment Automated Closed system High process reproducibility High surface area: media volume ratio	High capital investment costs for control unit High cost of cell bag High media consumption	Y	N	N

2.2.2 Three dimensional culture systems for human cell culture

There are two main methods of 3-D human cell culture; the use of suspended microcarriers as adherent surfaces for anchorage-based cell growth (Oh et al. 2009; Chen et al. 2013) or the growth of cells in either single cell suspension cultures, or as aggregates (Gerecht-Nir et al. 2004; Somerville et al. 2012). Microcarrier systems are only appropriate for the culture of MSCs or PSCs. T-cells grow naturally in suspension. Many 3-D, bioreactor based cell culture systems allow online process monitoring, provide greater scalability potential and reduce facility size requirements when compared to conventional planar technologies. Advanced bioreactor systems also permit strict control of environmental conditions during bioprocesses (Olmer et al. 2012). A challenge to implementation of 3-D culture systems is exposure of cells to shear forces, which must be tightly controlled as they can impact upon cell viability and fate determination in the case of hPSCs (Chisti 2001; Leung et al. 2011).

A range of 3-D culture platforms exist for culture of cells for cell therapies, these are displayed in Table 2.1. These include static culture bags (sometimes used for bioprocesses involving T-cells), rocking motion, automated bioreactors such as the Xuri Cell Expansion System (GE Healthcare, Chicago, IL, USA), the G-Rex system, which is a gas permeable membrane-based culture vessel that can be vertically scaled (Wilson Wolf, New Brighton, MN, USA), and stirred suspension bioreactors that employ single use, closed bioreactors such as the CultiBag STR (Sartorius Stedim). The sections below are split into microcarrier-based culture systems for MSC and PSC culture, followed by a section on suspension-based culture of PSCs and T-cells. The latter of the two sections has been split into two sub-sections, one on PSCs, and one focusing on T-cells. This is because whilst some cell culture principals remain the same, the variety of supporting platforms available for T-cell culture in suspension varies greatly from that of PSCs, which are grown as cell aggregates, rather than single-cell suspensions.

Microcarrier-based systems for therapeutic cell expansion

Microcarriers are small beads or discs which permit propagation or directed differentiation of PSCs and MSCs within a 3-D bioreactor. hPSC studies investigating microcarriers have recently achieved expansion folds as high as 28-fold over 6 days (Marinho et al. 2012). MSC studies have also achieved high expansion folds, with values as high as 20-fold expansion per passage reported (Hewitt et al. 2011). Microcarrier-based expansion folds are often higher than those in 2-D expansion studies across similar timescales (Phillips et al. 2008; Fernandes et al. 2009; Oh et al. 2009; Thomas et al. 2009; Serra et al. 2010; Heathman et al. 2015).

A critical property of microcarriers is their high surface area to volume ratio, on which large populations of hPSC cells may be cultured in a relatively small vessel, alleviating the costs associated with expensive media and supplements necessary for hPSC bioprocessing (Serra et al. 2010; Serra et al. 2012). Indeed, microcarriers can offer up to $30cm^2$ growth area per cm^3 of media, around 10 times greater than that achievable on conventional T-flasks and multi-layered vessels (Panchalingam et al. 2015). Microcarriers are able to support expansion and long-term self-renewal of both hPSCs and hMSCs over multiple passages, proving the platform's capability to support production of clinically relevant cell numbers (Oh et al. 2009). Microcarrier culture of hPSCs also results in cell colonies that generally have less than 10 layers; thus concentration profiles of nutrients and signalling molecules are less likely to occur than in aggregate-based cultures (Chen et al. 2014). This is not a concern for MSC culture, which grow as anchorage-dependent monolayers.

There are a variety of commercially available microcarriers that have been successfully implemented for culture of both hPSCs and MSCs (Chen et al. 2013; Rafiq et al. 2013). Microcarriers that contain animal-derived components are unsuitable for use in the manufacture of cell therapies. Serum-free and feeder-free microcarrier platforms are available cell therapy processing, although many of these

utilise the microcarrier coating, Matrigel, which is derived from murine origins (Want et al. 2012). Recombinant human proteins can now be used as a substitute for animal-derived microcarrier coatings in planar and 3-D microcarrier cultures (Rodin et al. 2010; Chen et al. 2011; Rafiq et al. 2016). However, such proteins can be difficult to isolate, expensive to produce, and prone to lot-to-lot variation. Synthetic substrates, which circumvent consistency issues associated with recombinant substrates, have been developed in planar conditions and successfully applied to microcarrier-based culture of both hPSCs and hMSCs (Melkoumian et al. 2010; Villa-Diaz et al. 2010; Fan et al. 2013).

Xeno-free microcarrier coatings designed to support hPSC culture utilise polymers to mimic Matrigel and feeder layer properties in order to encourage attachment and self-renewal of cells. Expansion folds on xeno-free microcarriers comparable to those coated with Matrigel have been reported (Chen et al. 2011; Fan et al. 2013). It has been proposed that positively charged microcarriers can be used to successfully support hPSC expansion at clinically relevant scales and similar cell concentrations and expansion folds to coated microcarriers were achieved (Chen et al. 2014). Xeno-free (XF) cell therapy culture methods represent a regulatory compliant approach to the production of hPSCs for clinical applications; they also reduce additional expenses incurred by the use of supplementary serums. Xeno-free and serum-free microcarrer cultures have also been applied to hMSC cultures. Cell concentrations of up to $3x10^5$ cells per mL and 10-fold expansion have been achieved in XF conditions (Heathman et al. 2015). Generally xeno-free and serum-free conditions resulted in comparable growth kinetics and cell densities to serum-based culture (Santos et al. 2011; Hervy et al. 2014; Heathman et al. 2015).

Development of xeno-free microcarrier coatings is one area where a quality-by-design (QbD) approach to product development has allowed elucidation of specific properties of microcarriers that affect hPSC self-renewal. Microcarrier selection

impacts the whole bioprocess as it can affect harvest operations as well as cell culture operations. Few existing studies, excluding those referred to above that aim to identify the effects of a specific microcarrier property on hPSC culture, specify the reasoning behind the choice of microcarrier used for cell culture, or indeed mention screening of microcarriers prior to cell culture. Rafiq et al. (2016) developed a screening mechanism that was shown to identify optimal microcarriers for a specific hMSC cell culture and harvest.

Parallel to developing GMP-based cell culture protocols, research has focused on optimizing bioreactor conditions for dynamic hPSC expansion processes so as to increase achievable expansion folds and cell concentrations. This will help reduce COG associated with manufacture of cell therapies. Controlling the dissolved oxygen levels has been found to be critical during hPSC culture on microcarriers in SUBs; 2.5 higher expansion folds and ~85% improvements in maximum cell concentrations were reported in a hypoxic environment when compared to uncontrolled conditions (Serra et al. 2010). Culture of MSCs in hypoxic conditions has been shown to increase their secretion of bioactive factors, leading to suggestions that this might improve their clinical efficacy (Chang et al. 2013; Binder et al. 2014). However, the effect of hypoxic cell culture on MSC growth kinetics has not been studied in detail.

The attachment of hPSCs to microcarriers as single cells can improve seeding efficiency from 30% to over 80% and reduce durations associated with microcarrier loading compared to clump seeding (Fan et al. 2013). Seeding densities have also been shown to have an effect on MSC culture. Lower seeding densities have been shown to result in increased proliferation compared to higher seeding densities (Fossett and Khan 2012). It has been suggested that approximately 5 cells per microcarrier bead may be the optimal inoculation ratio in MSC studies (Forestell et al. 1992; Eibes et al. 2010).

Despite a growing bank of research examining the culture of MSCs and PSCs on microcarriers, very few studies have demonstrated culture of cells at clinically relevant, commercial scales. Rafiq et al. (2013) produced functional MSCs in a 5L stirred tank reactor. The maximum cell density achieved (1.7×10^5 cells per mL), was comparable to that achieved in a 100mL spinner flask (1.5×10^5 cells per mL).

Aggregate Suspension Culture of hPSCs

hPSCs can be cultured as suspended aggregates in bioreactors. When hPSCs are grown as aggregates the rho-associated protein kinase inhibitor (ROCKi), Y-27632, is used to protect single cells from dissociation-induced apoptosis(Watanabe et al. 2007). Each cell aggregate is treated as a de facto colony. Aggregate sizes must be controlled in suspension bioreactors to prevent differentiation of cells in larger colonies (Krawetz et al. 2010; Ungrin et al. 2012; Abbasalizadeh and Baharvand 2013). It has been reported that aggregate culture of stem cells increases the therapeutic potential and the differentiation efficiency of hPSCs via the sustainment of endogenous signalling within cell colonies (Sart et al. 2014). Aggregate expansion of hPSCs also negates the need for expensive (and sometimes undefined) components of substrates upon which hPSCs are cultivated in adherent cultures (Ungrin et al. 2012). Aggregate culture of hPSCs rely more heavily on the expensive media supplements (such as GFs) compared to microcarrier culture (Marinho et al. 2012).

Several groups have proposed methods of hPSC culture through the use of cell aggregates with the potential to be scaled up in order to produce clinically relevant cell numbers (Abbasalizadeh et al. 2012; Chen et al. 2012; Ungrin et al. 2012). 25-fold expansion has been achieved over 14 days during aggregate-based hPSC culture (Olmer et al. 2012) and studies into expansion of hPSCs as aggregates yield similar expansion-folds when compared to microcarrier systems (Olmer et al. 2010; Amit et al. 2011; Zweigerdt et al. 2011). Long-term maintenance of hPSCs in

aggregates in dynamic bioreactor conditions over several passages has also been proven to be feasible (Abbasalizadeh et al. 2012; Olmer et al. 2012). Aggregate-based hPSC cultivation necessitates frequent manual interactions in order to control aggregate sizes which could hamper its application within the cell therapy industry (Singh et al. 2010; Amit et al. 2011; Serra et al. 2012).

Agitation rates can be used to successfully modulate uniform aggregate size in order to improve expansion of hPSCs as aggregates and reduce cell loss due to shear forces (Abbasalizadeh et al. 2012; Wang et al. 2013). This is also the case with microcarrier cultures, where impeller speeds of between 45 and 60rpm were found to promote optimal cell population doubling times (Lock and Tzanakakis 2009). The effects of shear on hPSC self-renewal and lineage determination is an area of intensifying research, although currently this is a poorly understood area in terms of the effect of mechanical strain on hPSC fate determination (Abbasalizadeh et al. 2012; Fridley et al. 2012).

The importance of cell inoculation concentration has been demonstrated during aggregate culture of hPSCs in dynamic bioreactor conditions; seeding concentrations of 2-3x10^5 cells/mL were found to maximise viability of hPSCs (Kehoe et al. 2010; Abbasalizadeh et al. 2012). Single cell inoculation has also been estimated to reduce cell losses by up to 60% (Abbasalizadeh et al. 2012). Cell concentrations of up to 3.4 x 10^6 hPSCs/mL have been achieved using dynamic, aggregate-based culture techniques (Kehoe et al. 2010). This represents 1.9 fold improvement over maximum cell concentrations achieved in planar systems, although it is significantly lower than the maximum cell concentrations achieved in xeno-free hPSC cultures performed in microcarrier-based systems (6 x 10^6 cells/mL) (Bardy et al. 2012).

A few aggregate hPSC expansion processes combine xeno-free conditions with defined media (Amit et al. 2011; Chen et al. 2012; Wang et al. 2013). These investigations represent a valuable effort to remove media supplements that either

introduce the risk of xenogeneic material to hPSCs or expose media to lot-to-lot variability, although early attempts resulted in relatively modest expansion folds (Chen et al. 2012).

Three-dimensional culture of T-cells for CAR-T cell therapies

CAR-T cell therapies are a relatively new development in the field of cell therapy. Much of the available work on T-cell expansion has been carried out on unmodified cells, also intended for the use of adoptive cell therapies. However for the purposes of T-cell expansion, they can be considered equivalent and thus citations in this section may not refer directly to CAR-T bioprocesses. T-cells are grown in suspension as single cells. This naturally makes them more amenable to large-scale culture platforms than MSCs, which are anchorage-dependent, and PSCs, which must be grown as aggregates, or on microcarriers.

Static culture bags have previously been used for the expansion of therapeutic T-cells (Sadeghi et al. 2011). However, like T-flasks, these systems are labour-intensive, can suffer from vessel-to-vessel variability in performance, and present an open culture system which will are not compatible with large-scale cGMP cell therapy manufacture.

The G-Rex system is a static culture system in which cells grow on a gas permeable membrane, providing a highly oxygenated environment. This culture system allows removal and replenishment of media without disturbing cells within the reactor. G-Rex culture systems are compatible with standard tissue culture incubators, and have been shown to have the potential to significantly reduce the number of man hours associated with a T-cell culture process compared to T-flask based culture (Vera et al. 2010). The G-Rex 500 allows expansion of T-cell populations of up to $6x10^{10}$ in a single vessel (Bajgain et al. 2014), providing enough cells for autologous dose sizes. G-Rex devices consume less media volume than standard T-flasks and Xuri expansion systems. Therapeutic cells within the G-Rex have been safely

administered to patients (Somerville and Dudley 2012). Whilst G-Rex systems show comparable, sometimes even improved expansion folds relative to that of the Xuri, multiple vessels are likely to be required for the production of cell populations required for allogeneic and large dose autologous CAR-T therapies. A fully automated platform, capable of handling multiple G-Rex flasks in a closed environment is currently under development, which may alleviate concerns regarding the need for multiple vessels.

Rocking motion bioreactors, such as the Xuri (previously WAVE) cell expansion system (GE Healthcare, Chicago, USA), provide all of the advantages of a closed-system, fully automated bioreactor (see Table 2.1). Reliable and reproducible T-cell culture has been reported in rocking motion bioreactors (Hollyman et al. 2009; Sadeghi et al. 2011; Somerville et al. 2012; Janas et al. 2015). Rocking motion platforms provide agitation of the cell culture; this negates the need for impellers that can introduce shear stress that affects T-cell growth and expression of surface markers. Larger final cell population sizes and expansion folds have been reported using rocking motion bioreactors, as compared to static culture bags by Hollyman et al. (2009) and Sadeghi et al. (2011), whereas Somerville et al. (2012) reported that final cell population and expansion folds were equivalent to static bags. Daily media perfusions of between 500mL and 1000mL (in a 1L bioreactor) depending on viable cell concentrations were found to increase final cell counts by over 100% in comparison to cultures where no perfusion was performed (Janas et al. 2015). Cell concentrations of up to 2 x 10^7 cells/mL have been achieved using rocking motion bioreactors (GE Healthcare 2014). Culture vessels with volumes of up to 50L may be obtained using these systems. Like the G-Rex system, rocking motion bioreactors have been used to generate cells that have proven safe and efficacious when administered to patients (Somerville & Dudley 2012).

2.3. Differentiation of hPSCs

2.3.1 Planar strategies for hPSC differentiation

Traditional stem cell differentiation protocols were designed around bench-scale research paradigms and little effort was made to incorporate reproducibility and process robustness into these experiments (Mordwinkin et al. 2013). Directed differentiation strategies often involve exposing hPSCs to a cocktail of morphogens, at specific time-points throughout the differentiation process (Karumbayaram et al. 2009; Zhang et al. 2009; Ghodsizadeh et al. 2010; Sullivan et al. 2010). Directed differentiation can reduce both the timescale and direct resource utilisation associated with a differentiation unit operation relative to spontaneous differentiation (Surmacz et al. 2012).

Similar to hPSC expansion, early differentiation strategies relied heavily upon the use of xenogeneic materials (Martinez et al. 2012). Planar differentiation protocols, that are free of xenogeneic material, have been reported (Surmacz et al. 2012). Despite such progress, many differentiation protocols are inherently variable owing to the laboratory idiosyncrasies of individual technicians, thus reliable and robust differentiation processes are still in their infancy. Timescales and efficiencies also vary significantly between experiments even when the same cell type is targeted for production (Table 2.2).

The use of small molecules within differentiation protocols has helped to improve their reproducibility via reduced use of recombinant growth factors (Zhu et al. 2011; Li et al. 2012). Several groups have created highly simplified protocols, whilst still improving the efficiency and processing times of 2-D differentiation processes, by replacing growth factors with small molecules in the preliminary stages of differentiation protocols (Burridge et al. 2011; Chambers et al. 2012; Surmacz et al. 2012). A protocol with the specified aim of creating a differentiation process capable

of creating dopaminergic neurons for transplantation in T-flasks has been developed (Liu et al. 2013). This strategy enabled the production of cryopreservable dopaminergic neurons with a high level of efficiency, allowing better control of time management in within the differentiation process. This approach is well served to reduce bottlenecks in the downstream phases of autologous hPSC processes. Further advances have proven it is possible to derive progenitor cells, suitable for transplantation as cell therapies at high efficiencies (Diekmann et al. 2015) and in xeno-free and small-molecule free, defined conditions (Lippmann et al. 2014). Negation of the need for small molecules and growth factors also has the potential to drastically reduce the cost of differentiation procedures.

Table 2.2 (continued overleaf) A summary of the key performance characteristics of planar and bioreactor-based differentiation protocols

Derived Cell-Type	Method	Time (days)	Number of Target Cells per Input hPSC (Ratio)	Reported Efficiency (%)	Max Cell Concentration (Cells/mL)[a]	Source
Cardiomyocytes	2D Monolayer	9	ND	64.8±3.3	2.5 - 5 x 10^4	(Burridge et al. 2011)
Cardiomyocytes	2D EB formation	60	0.81	10±2 - 22±4	ND	(Zhang et al. 2009)
Hepatocytes	2D EB formation	ND	ND	50±2	1-5 x 10^4	(Ghodsizadeh et al. 2010)
Hepatocytes	2D Monolayer	14	ND	73±18	ND	(Sullivan et al. 2010)
Motor Neurons	2D Monolayer	14	ND	33.6±12	ND	(Karumbayaram et al. 2009)
Neural Nociceptors	2D Monolayer	15	ND	61±2	1 x 10^4	(Chambers et al. 2012)
Neurons	2D Monolayer	~7	ND	ND	4.5 x 10^4	(Surmacz et al. 2012)
Dopaminergic Neurons	2D Monolayer	~28	ND	30±2	ND	(Liu et al. 2013)
Neural Progenitor Cells	2D Monolayer	6	ND	90±1	5 x 10^4	(Lippmann et al. 2014)

Endoderm Progenitors	2D Monolayer	4	ND	73.2±1.6	1.3 x 10^5	(Diekmann et al. 2015)
Cardiomyocytes	2D EB formation	16-18	70	87±3.4	4.5 -6 x10^4	(Weng et al. 2014)
Cardiomyocytes	SUB Microcarriers	16	0.33	15.7±3.3	1.36 x 10^6	(Lecina et al. 2010)
Haematopoietic Cells	SUB Microcarriers	7	4.41	ND	ND	(Lu et al. 2013)
Cardiomyocytes	SUB Cell Aggregates	18	23	100 % Beating Aggregates	4.3 x 10^5 – 5.2 x 10^5	(Niebruegge et al. 2008)
Hepatocyte-like cells (HLCs)	SUB Cell Aggregates	21	ND	18±7	3-5 x 10^5	(Vosough et al. 2013)

2.3.2 Bioreactor-based systems for hPSC differentiation

Concentrated research into bioreactor-based differentiation strategies has stemmed from the need to translate differentiation from a lab-scale area of research into processes capable of producing industrially relevant cell numbers in a reproducible manner. A number of studies in which hPSCs have been successfully differentiated in bioreactor conditions have been carried out, either attached to microcarriers (Lu et al. 2013) or in the form of cell aggregates (Lecina et al. 2010; Vosough et al. 2013). Differentiation strategies developed in 3-D bioreactors, particularly stirred-tank vessels, lend themselves to large-scale processes far better than their planar counterparts as labour-intensive tasks, such as media exchanges, can be fully automated in such vessels, which also offer processing advantages such as online environmental monitoring and control. Research carried out on SUB-based differentiation of mPSCs suggests that the use of spinner flasks resulted in a 12-fold reduction of the man hours spent in the laboratory when compared to planar techniques (Zwi-Dantsis et al. 2011).

hPSCs can be differentiated towards a number of clinically relevant lineages in SUBs including cardiac (Niebruegge et al. 2008), haematopoietic (Lu et al. 2013), neuronal (Bardy et al. 2012) and hepatocyte-like (Vosough et al. 2013) (summarised in Table 2.2). Bioreactor-based differentiation will be necessary in order to produce certain hPSC-derived cell products at commercially relevant scales, however it must be considered that such processes will only be made more cost-effective by making concurrent improvements in differentiation efficiencies and through the reduction of expensive media supplements in such protocols. Bioreactor-based differentiation would benefit from the translation of highly efficient protocols demonstrated in planar systems (Chambers et al. 2012; Surmacz et al. 2012; Weng et al. 2014) to SUB systems. Such protocols have the potential to result in differentiation efficiencies that are higher than those achieved with SUB-based bioreactors alone. A novel,

microparticle-based approach to morphogen delivery to PSC aggregates was reported as a method to achieve up to a 12-fold reduction in morphogen use during bioreactor-based differentiation protocols (Bratt-Leal et al. 2013). Such systems provide a valuable method by which to reduce material costs associated with SUB-based hPSC culture.

One question arising from the birth of SUB-based hPSC differentiation is how a dynamic, controlled environment might be harnessed to augment processing strategies in this area (Leung et al. 2011). One of the reasons for the lack of characterisation with regards to the effects of shear on hPSCs, is that different dynamic culture systems result in different shear profiles. Thus, drawing comparisons across separate studies is difficult (Fridley et al. 2012). However, scale-down studies suggest that shear stress during early hPSC differentiation promotes mesodermal, endothelial and haematopoietic phenotypes even when the presence of morphogens promoting these lineages were absent (Ahsan and Nerem 2010; Wolfe et al. 2012; Wolfe and Ahsan 2013). Interestingly, in early stages of differentiation, hPSCs lineage determination seems to be insensitive to the magnitude of shear stress; however in later stages, progenitor cell activity appears to be more magnitude-sensitive (Adamo et al. 2009; Wolfe and Ahsan 2013). Shear forces have been shown to partially negate the need for costly media supplements in published studies (Wolfe et al. 2012; Wolfe & Ahsan 2013); broadening our knowledge of the way that shear stress impacts upon hPSC culture must be seen as an important factor in bioprocess optimization. Hypoxic environments, which can be tightly controlled within SUBs, have also been shown to enhance differentiation of hPSCs towards both ectoderm and mesoderm cell lineages (Niebruegge et al. 2008; Bae et al. 2012).

Novel, microfluidic systems could be a key tool in elucidating the effects of specific environmental parameters on hPSC propagation and differentiation. Microfluidic bioreactors provide an ultra-scale down, high throughput platform by which to study

single cells or colonies in strictly defined conditions (Cimetta et al. 2009; Wang and Bodovitz 2010; Prabhakarpandian et al. 2011; Reichen et al. 2012). The cellular processes governing hPSC fate are complex and cannot be attributed to a single given parameter. Microfluidic devices are well placed, as a low cost development platform, to enhance our understanding of how defined microenvironmental conditions can affect hPSC activity (Macown et al. 2014).

The effect of the biochemical properties of microcarriers on hPSC fate determination is poorly understood. It has also been suggested that the mechanical properties of microcarriers, such as their stiffness and size can also be investigated and optimised for specific purposes (Sart et al. 2013). Rational design of microcarriers could provide an optimized bioprocess platform with which to manufacture specific hPSC-derived cell lineages. This would enable better control of cells' microenvironment and thus allow more efficient differentiation processes that do not rely as heavily on expensive media supplements as current platforms do.

2.4 Genetic engineering of cells for cell therapies

Genetic engineering and phenotype modification techniques have a significant role to play in the production of efficacious cell therapies. Human induced pluripotent stem cells (hiPSCs) can be derived from adult stem cells by forced expression of defined transcription factors (Takahashi et al. 2007). This has led to the possibility of autologous hiPSC-derived therapies (Kimbrel and Lanza 2015). Cellular reprogramming of hiPSCs is a labour intensive, lengthy process. Efficiencies, or the percentage of somatic cells successfully reprogrammed to pluripotency, are generally in the region of 0.1-1%, with some notable exceptions (see Table 2.3). CAR-T cells are also produced through genetic modifications that cause the expression of the CAR on the surface of the T-cell protein (Gross et al. 1989). Furthermore, allogeneic CAR-T cell therapies depend on genetic engineering techniques to ensure the knockout of TCRs that are known to cause graft versus host disease. CAR-T cells

can be further modified to prevent the expression of surface proteins known to interact with combination drugs that are sometimes administered alongside cell therapies in cancer patients (Valton et al. 2015). Expression rates of CARs in genetically modified T-cells are far higher than iPSC reprogramming efficiencies; expression rates can vary from 20%-80% depending on the delivery system used (Table 2.3).

The majority of approaches to genetically modify T-cells and to derive hiPSCs have relied upon transgene expression via viral transduction (Rao and Malik 2012; Kalos and June 2013). Gammaretroviruses have been used extensively for the delivery of transgenes to both T-cells and somatic cells for hiPSC derivation (Takahashi et al. 2007). In immunotherapy, gammaretroviruses have been well-established as safe and efficacious in clinical settings (Rosenberg et al. 1990). Gammaretroviruses are belived to be less prone to silencing in hESCs and somatic cell lines; they are also believed to minimize the risk of producing immunogenic peptides, which may make them more suitable for therapuetic applications than other retroviral systems (Maetzig et al. 2011).

Gammaretroviral and lentiviral vectors are examples of integrating viruses. In hiPSC production, integrating viral vectors are seen as a disadvantage due to the integration of exogenous sequences into the host genome. Integrating vectors drive long-term expression of transgenes, which is a safety concern for cell therapies (Rao & Malik 2012). However, such characteristics can be harnessed in CAR-T cell therapy production as it can boost long-term expression of CARs following viral transduction. Integrating vectors have been shown to be safe in long-term adoptive cell transfer studies (Scholler et al. 2012). Lentiviral vectors, another example of an integrating viral vector, have also been explored for use in CAR-T cell therapy production. Both gammaretroviral and lentiviral vectors are characterised by their high transduction rates. However, whereas retroviruses only transduce replicating cells, lentiviruses can also transduce quiescent cells and thus result in a higher percentage of CAR-

bearing T-cells (Sandrin et al. 2002; June et al. 2009; Vannucci et al. 2013). Indeed 60-80% of a cell population expressing a CAR has been reported using lentiviral vectors (Cribbs et al. 2013; Cellectis 2014) (Table 2.3).

The focus of derivation of hiPSCs using viral vectors has moved towards non-integrating viral vectors such as adenoviruses and the Sendai Virus. Adenoviral vectors only allow expression of the transcription factors required to drive cells towards pluripotency for a short period of time; this results in reprogramming efficiencies that are several magnitudes lower than that of other vectors (Table 2.3) (Stadtfeld et al. 2008; Zhou and Freed 2009). Adenoviral vectors have been applied to T-cells for CAR expression with only limited success (June et al. 2009). Sendai vectors are able to derive hiPSCs at efficiencies comparable to that of lenti- and retroviral vectors (Fusaki et al. 2009; Ban et al. 2011), and are readily available as off-the-shelf cGMP grade reprogramming kits. Viral vectors are hampered by high costs and their complex production process, which represents a field within the bioprocess industry in its own right. T-cells that bear a specific type of CAR require the creation of a bespoke viral vector in order to deliver transgenes to the cell. The design of these vectors is not trivial, and requires highly skilled personnel.

Non-viral vectors benefit from lower manufacturing costs and are theoretically safer because no viral elements are introduced to the host cell's DNA (Kalos and June 2013). Non-viral methods of transgene expression include episomal vectors, microplasmid DNA, and transposon technology (Rao and Malik 2012; Singh et al. 2013). Electroporation and mechanical membrane disruption techniques have been used to deliver non-viral vectors to cells (Manuri et al. 2009; Sharei et al. 2015). Electroporation is a conventional method to introduce transposons, such as the piggyBac and Sleeping Beauty, to T-cells. Delivery of transposons to T-cells via electroporation results in CAR expression levels similar to those observed when transgene delivery is carried out using retroviral vectors (Nakazawa et al. 2011; Singh

et al. 2013). A novel approach to cytosolic delivery of cargo to T-cells involves passing cells through microfluidic channels to cause temporary membrane disruption. Molecules can then pass through the disrupted membrane into the cytoplasm of the cell (Marx 2016). The CellSqueeze platform (SQZBiotech, Boston, MA, USA) has been used to deliver functional macromolecules to T-cells, resulting in higher expression rates compared to electroporation (Sharei et al. 2015). In the field of hiPSC derivation, mRNA and miRNA molecules have been used for highly efficient reprogramming of somatic cells (Table 2.3) (Anokye-Danso et al. 2011). The simplicity of such systems makes them attractive candidates for derivation of iPSCs.

Vessels that are impermeable to gas, such as disposable bioreactors that are designed to fit rocking motion bioreactors, are not ideal for transduction of cells via viral vectors. Therefore, transduction is currently carried out in static cell culture bags, or static planar vessels. Retronectin-coated culture vessels are used during transduction of T-cells. This promotes co-localisation of virus' and T-cells, which enhances the levels of CAR expressing T-cells (Hanenberg et al. 1996; Dodo et al. 2014). Transduction can be carried out within the CliniMACS Prodigy (Miltenyi Biotec) as part of a fully integrated bioprocess (see Section 8 for details). Microfluidic membrane disruption technologies, such as CellSqueeze (SQZBiotech) may also allow transduction to be carried out as part of an integrated bioprocess. However, the microfluidic nature of such devices might limit their throughput and their subsequent applicability to large-scale bioprocesses. Higher expression rates of transgenes delivered to T-cells will result in the production of higher numbers of functional CAR-T cells in a given culture vessel, leading to more efficient manufacturing processes.

Derivation of hiPSCs is hampered by low reprogramming efficiencies and it technical difficulty (Rao & Malik 2012). It is a lengthy, labour intensive process that can take many weeks. As such many reprogramming protocols depend on the use of well-plates, rather than bioreactors. hiPSC lines are often generated from single colonies

following reprogramming in order to create homogeneous cell banks, therefore only a small number of hiPSCs are required. For allogeneic hiPSC cell therapies, viewing hiPSC-derivation as a precursor to the bioprocess may be adequate; once a cell line is created, a working cell bank can be maintained to satisfy demands of a bioprocess. However, for autologous cell therapies, reprogramming must be carried out for every patient, it is therefore important to consider its incorporation into an integrated bioprocess. Section 8 will cover the limited efforts made to integrate reprogramming into a full bioprocess.

Table 2.3 Vectors used for genetic modification of cells and their efficiencies when applied to CAR expression in T-cells and hiPSC reprogramming

Vector Type	Genome Integrating	Transgene expression rates in T-cells (%)	Reference	hiPSC reprogramming efficiency (%)	Reference
Retrovirus	Yes	23-51	(Quintás-Cardama et al. 2007; Pule et al. 2008)	0.02-0.08	(Takahashi et al. 2007; Park et al. 2008)
Lentivirus	Yes	38-80	(Zhou et al. 2003; Tumaini et al. 2013; Cellectis 2014)	0.02	(Yu et al. 2009)
Adenovirus	No			0.0002	(Zhou and Freed 2009)
Sendai Virus	No	ND	N/A	0.1-1	(Fusaki et al. 2009; Seki et al. 2010)
Transposon (Electroporated)	No	20-50	(Manuri et al. 2009; Singh et al. 2013)	0.02	(Kaji et al. 2009)
siRNA (CellSqueeze)[a]	No	50-70	(Sharei et al. 2015)	ND	N/A
mRNA/ miRNA	Dependent on delivery mechanism	ND		1.4-10	(Warren et al. 2010; Anokye-Danso et al. 2011)

a) CellSqueeze technology has not yet been shown to facilitate the expression of CARs on CAR-T cells in published studies, results here indicate gene knockout of surface proteins, which have application in the production of allogeneic CAR-T therapies.

2.5 Downstream processing of cell therapies

2.5.1 Cell harvesting, washing and concentration

The harvest of cells take place following cell culture based unit operations such as expansion or differentiation and is usually carried out in two stages. For MSCs and PSCs the first harvest step is detachment, or dissociation of cells from the cell culture anchorage material (for example tissue culture plastic or microcarriers). If aggregate culture is used, then aggregate dissociation must first take place in order to create a suspension of single cells. Secondly, 'separation' takes place, separation is generally not necessary for aggregate-based culture. This stage involves removing any microcarriers from the cell culture broth so as to produce a cell-only suspension. CAR-T cell expansion employs single-cell suspension culture and therefore does not require a detachment or dissociation step.

Detachment of cells from microcarriers is usually carried out using proteolytic enzymatic separation. In PSC-based cultures, this has been done using a recombinant trypsin enzyme (TrypLE Express) (Oh et al. 2009; Santos et al. 2011), or collagenase (Lock and Tzanakakis 2009). MSCs have been dissociated from microcarriers via the use of trypsin, accutase, trypsin-accutase mixtures, and collagenase (Weber et al. 2007; Goh et al. 2013). Thermo-sensitive polymers have also been used to negate the use of dissociation enzymes, which have been shown to affect cell viability and hPSC differentiation if cells are exposed to them for too long (Yang et al. 2010; Tamura et al. 2012). The culture broth is reduced to below 32^{o}C to allow cell detachment in this instance (Tamura et al. 2012). Yang et al. (2010) reported harvest yields of 82.5% (92% viability) for MSCs grown on thermo-sensitive microcarriers. Thermo-sensitive polymers may affect the growth characteristics and fate determination of MSCs and PSCs. Furthermore, it may be difficult to achieve homogenous polymer coatings of commercially available microcarriers.

Different enzymes have been shown to perform with varying degrees of success depending on the type of microcarrier being used during harvest protocols (Rafiq et al. 2016). However, there has been little focus in published studies on scalable harvest strategies and protocols for cell therapy manufacture (Chen et al. 2013). Many of the studies referred to above relied on the use of sieves to separate cells from microcarriers; this approach is not one which can be translated to GMP cell therapy manufacturing. Nienow et al. (2014) and Heathman et al. (2015b) presented a scalable protocol for the harvest of MSCs from microcarriers. Detachment was carried out using trypsin-EDTA (Nienow et al. 2014) or TrypLE (Heathman et al. 2015b) accompanied by agitation in a SUB. Harvest efficiencies of greater than 95% were reported in these studies (>99% viability). Separation of microcarriers to form a cell-only suspension can be carried out using volume reduction techniques, such as tangential flow filtration (TFF). TFF offers a scalable platform for cell harvesting that result in high cell viability rates, even when scaled and adapted for cGMP conditions (Brandenberger et al. 2011). Cunha et al. (2015) explored the use of different filtration devices and found that polypropylene filters with pore sizes of greater than 75μm resulted in the removal of microcarriers and recovery of over 80% viable cells. The concentration of cells in the retentate was 10-fold that of the feed stream.

Other volume reduction techniqes, such as centrifugation can also be used for the separation of cells. The kSep system (Sartorius Stedim) is a fluidised bed centrifugation (FBC) machine, which operates in a similar manner to small-scale, conventional cell separation systems used for blood-product processing such as the COBE 2991, or Elutra Cell separation system (these systems are small scale and inappropriate for allogeneic cell therapy bioprocesses). The kSep system can handle volumes of up to 1,000L in a single run (Brandenberger et al. 2011). Few studies have investigated the separation stage in detail. Nienow et al. (2014) reported that filtration resulted in the build-up of microcarriers on the filter, acting as a de facto ‘filter-cake’

which resulted in reduced harvest yield due to the entrapment of cells. One solution to this issue is to provide a larger surface area for the filtration; this would reduce the depth of the microcarrier build up. Hassan et al. (2015) considered the use of tangential flow filtration (TFF) and fluidised bed centrifugation in the form of the kSep system for downstream processing of allogeneic MSC therapies in a bioprocess economic appraisal. It was observed that TFF is generally considered more appropriate for smaller lot sizes, whilst FBC proved economically viable for large lot size (>~10^{11} cells per lot).

In the manufacture of CAR-T cell therapies, the detachment (or dissociation step) is unnecessary as cells are grown in single-cell suspension. However, beads, matrices, or gels used for activation of T-cells must be removed from the culture broth. This can be done by a washing, or separation stage in a manner similar to microcarrier separation in MSC and PSC therapy bioprocesses. Indeed, there are many cell processors that have been applied to blood product processing for many years that can be used in CAR-T cell therapies. Autologous CAR-T cell therapy products are only likely to result in media volumes of 5-10L, therefore small scale systems such as the Haemonetics CellSaver, COBE system from Terumo, and LOVO (Fresnius Kabi, Germany) can be integrated into a closed and sterile bioprocess for washing and concentration stages (Kaiser et al. 2015; Levine 2015). For large-scale production of allogeneic cell therapies, it is likely that scalable system such as the kSep will need to be employed to handle the media volume associated with this form of manufacture. Similar to the fields of MSC and PSC bioprocessing, there are few available examples of studies that focus on the washing and concentration of therapeutic T-cells following cell culture.

It is important to consider the timescale available for washing and concentration of cells. It has been observed that holding times of greater than six hours can adversely affect the viability of both MSC and PSC populations (Pal et al. 2008; Veraitch et al.

2008). A maximum of four hours can therefore be permitted for dissociation and separation (or volume reduction) of cells followed by holding in ambient culture medium (Veraitch et al. 2008; Hassan et al. 2015; Heathman et al. 2015b).

2.5.2 Purification of cells for cell therapies

The purification of therapeutic cell populations is essential to most cell therapy bioprocesses. Obtaining a pure population of the therapeutic cell type helps to ensure the safety and efficacy of cell therapy products. Mesenchymal stem cell therapies can be manufactured without the need for purification; a single, homogenous population of cells is the start point of MSC-based bioprocesses, and these same cells are the final therapeutic entity. In the case of allogeneic CAR-T cell therapies and many PSC-derived therapies purification is an essential step.

There are a range of techniques for separation of specific human cells from a general population. These include physical separation (using density gradients or exploiting physical variations in the size of cell populations), immuno-separation techniques and novel approaches such as microfluidic platforms (Table 2.4) (Diogo et al. 2012; González-González et al. 2012; Weil and Veraitch 2013).

Physical separation techniques include some of those described in Section 2.5.1. Examples of these include centrifugation using the COBE 2991 Cell Processor (Terumo BCT), counter flow elutriation using the Elutra Cell Separation System (Terumo BCT) (Powell et al. 2009) and density gradient separations using the Sepax (GE Healthcare). Such systems are low resolution and are generally only used as preparative isolation steps in USP operations, such as the isolation of lymphocytes following apheresis. Apheresis technology is well established, and has evolved to become relatively cheap, closed off, high throughput processes (Levine 2015). Centrifugation techniques can also be used for removal of materials used for T-cell activation. Aqueous two phase systems can also be used for cell separations; ATPS is a highly scalable platform and is used in many other chemical and biological

processes. However, it is hampered by low specificity which limits its use in DSP operations (Weil & Veraitch 2013).

Immuno-separation techniques rely on the use of antibodies specific to target cell surface proteins. Magnetic activated cell sorting (MACS) and fluorescent activated cell sorting (FACS) are two widely used immuno-affinity platforms. Immuno-separation techniques (particularly those which are affinity-based) result in higher selectivity than physical purification strategies and are therefore appropriate for DSP unit operations which demand a homogeneous cell population.

FACS is achieved by first tagging target cells with an antibody linked to a fluorescent marker. Cell samples are then passed through a laser; this causes excitation of the fluorescent marker and results in light emission. Phenotype-specific cells are then separated by the application of either a positive or negative charge to cells tagged with light emitting fluorophores. FACS is a binary sorting system that processes single cells in sequence. FACS results in the highest target cell purities of any available purification technology; typical purities are in the region of 98% (McIntyre et al. 2010). However, its throughput is limited to cell numbers in the magnitude of 10^7 per hour (Weil and Veraitch 2013). This makes it unsuitable as a purification option for all but low-dose autologous cell therapies due to the process times associated with the technology. Additionally, fluorescent markers must be removed from cells following a FACS operation. The cost of cGMP-grade antibodies and the capital costs associated with FACS equipment are a challenge to its applications beyond analytical purposes. Furthermore, FACS has proven a more complex platform to use than technologies such as MACS. It therefore requires the use of highly trained staff, and necessitates a significant time period for set-up before each run.

Table 2.4 Summary table of cell separation and purification techniques and their advantages and limitations

Category	Platform	Separation criteria	Advantages	Limitations
Physical-based separation techniques	Density-gradient centrifugation	Size and density	- Label free - High throughput - High cell concentrations achievable	- Low selectivity
	Aqueous two-phase systems	Hydrophobicity, size, net charge	- Label free - Scalable - High cell viability	- Low selectivity - Requires repeated extraction steps - Difficulties recovering separated cells
Immuno-separation techniques	Magnet-activated cell sorting (MACS)	Expression of surface proteins	- High selectivity - High throughput - Closed system & automated platforms - Commercially available	- May require multiple steps - Magnetic bead removal - High antibody costs
	Fluorescent-activated cell sorting (FACS)	Expression of surface proteins	- High selectivity - Capacity for multiparameter sorting - Automated	- Low throughput - Flurouphore removal from cells - Skilled technicians required - High capital expenditure - High antibody costs
Novel platforms	Microfluidic devices	Cell size, expression of surface proteins	- Cheap fabrication - Can be automated - Efficient use of antibodies - Can create lab-on-a-chip systems for analytical & scale-down purposes	Low capacity, difficult to scale

Cells are prepared for MACS by incubation with paramagnetic beads that are coated in antibodies specific to a surface protein on the target cell type. This creates labelled target cells that are held by a magnetic field. Unlabelled cells then pass through the device and are disposed of. Other than resultant cell populations that are of a high purity, advantages of MACS include its ease of use and high throughput; 2 x 10^{10} cells can be processed within 30 minutes (Grützkau and Radbruch 2010). The latter two characteristics of MACS listed above place it at the forefront of existing platforms for the purification of cells for cell therapy; particularly where large lot sizes are required. The CliniMACS platform (Miltenyi Biotec, Germany) is the most commonly used MACS technology. Typical purities and viable cell yields achieved using CliniMACS range from 70-99% and 93%-99% respectively, although these values do depend on the cell type targeted for isolation (Lang et al. 2004; Chou et al. 2005; Schriebl et al. 2010; Weil and Veraitch 2013).

Whilst MACS has been shown to be capable of separating cardiomyocytes and undifferentiated hPSCs following differentiation (Uosaki et al. 2011), Schriebl et al. (2010) predict that it would still require 31 stages to eradicate every non-target cell from a differentiated PSC therapy. This would prove impractical due to the cell losses encountered in each stage. A combination of positive and negative selection techniques during MACS-based separation could be used to boost the purity of target cell populations (Weil & Veraitch 2013).

Novel purification systems are predominated by the use of microfluidic devices, which offer a ‘lab on a chip’ platform for cell processing. Microfludic devices are low-cost due to the ease of their fabrication. They can also harness existing immuno-separation techniques such as FACS and MACS (Didar and Tabrizian 2010). Microfluidic devices may offer reduced antibody costs compared to the systems described above. Owing to the limited loading volume that can be handled by a single unit, microfluidic devices may be limited to analytical purposes, unless run in parallel

(González-González et al. 2012). In order to run in parallel, more must be done to ensure the robustness and reproducibility of purifications carried out on microfluidic devices.

Production of allogeneic CAR-T cells involves the knockout of genes that prevent the expression of T-cell receptors (TCRs) that cause GvHD in patients. The gene knockout process is not 100% efficient. Specific T-cells, namely those that still express unwanted TCRs, must be separated from the final cell population before the therapy is administered to a patient (Yang et al. 2015). Separation of TCR- cells from the cell population cannot be carried out using apheresis methods employed in autologous CAR-T cell therapy production; they will therefore depend on high resolution, immuno-separation techniques (Valton et al. 2015). Similarly, the production of PSC-derived therapies requires the isolation of target cells that are specialist, progenitor cells. Depending on the performance of the differentiation unit operation, these cells may not be the majority cell type within a given population. Where passive separation techniques are not appropriate, PSC-derived therapies will depend on high-resolution purification platforms to provide a homogeneous population that are free of undifferentiated, or partially differentiated PSCs (which have the potential to form teratomas in vivo (Brederlau et al. 2006).

Occasionally, PSC-derived therapies can be purified through the use of culture, or formulation-based techniques. For example, in the production of retinal-pigment epithelial cell therapies for AMD, cells are sometimes transplanted as patches, whereby differentiated retinal pigment epithelium (RPE) cells are cultured as a monolayer in order to allow cell-cell interactions to form. These culture conditions do not support the viability of cells other than the patchwork RPE cells, and thus can usually be transplanted as a single cell type without the need for cell sorting.

Purification of cells at high resolution is among the most challenging areas within cell therapy bioprocessing. On the one hand, cells must be recovered at very high purities;

higher even than those currently being achieved using MACS systems (Schriebl et al. 2010). One the other hand, the time available for purification is limited. High throughput, high capacity solutions are required in order to not exceed the maximum holding time whereby cell viability and function is affected. The development of large-scale cell culture technologies discussed in Section 4 will only further this requirement. Leading academics in the cell therapy field have acknowledged that at present there is no gold standard cell purification system for achieving a homogeneous cell population (Schriebl et al. 2010; Diogo et al. 2012; González-González et al. 2012; Weil & Veraitch 2014). Future improvements in this field will be required for the translation of cell therapies to the clinic.

2.6 Integrated and continuous bioprocess strategies for cell therapies

Integrated bioprocesses, whereby multiple unit operations are carried out in a self-contained piece of equipment, are being explored as an alternative to segregated bioprocess strategies. Integrated bioprocesses negate the need for labour-intensive processes that usually take place following cell culture operations, such as hold steps and transfer of cellular material. Processing cell therapies in this manner can help to reduce bottlenecks and increase the throughput associated with cell therapy bioprocesses. Additionally, integrated bioprocess protocols offer greater containment capabilities, reducing the potential for contamination within the bioprocess.

To date, work in the cell therapy field has focused predominantly on integration of culture-based unit operations, such as expansion and differentiation of hPSCs. Several studies have reported integrated expansion and differentiation operations where continuous culture strategies have been employed (Lock and Tzanakakis 2009; Bardy et al. 2012; Ungrin et al. 2012; Fonoudi et al. 2015). Figure 2.3 illustrates how these strategies differ from segregated culture and differentiation of hPSCs. Only a handful of investigations into this relatively new area of hPSC bioprocess research

have been published and these are summarised in Table 2.5. Early investigations incorporating expansion and differentiation focused on overcoming the technical hurdles of carrying out two different operations in one integrated process step; as such only modest yields of target cells were achieved (Lock & Tzanakakis 2009). Recent studies have sought to optimize integrated iPSC bioprocesses via strategies such as the determination of optimal aggregate size during hPSC culture and differentiation (Ungrin et al. 2012). Switching feeding regimes from once to twice per day was found to double the achievable cell density during the expansion phase of an integrated bioprocess, although process economic analysis comparing the two approaches was not offered (Bardy et al. 2012). The reported expansion folds and differentiation efficiencies for integrated bioprocesses compare well with separated systems of a similar nature.

One of the challenges facing fully integrated cell therapy bioprocessing is a lack of technologies and bioprocess designs that support end-to-end bioprocessing in a fully contained manner. To date, no studies have produced an integrated process for hPSCs from derivation all the way through to differentiation. This has been achieved with mouse iPSCs (miPSCs) in a SUB (Fluri et al. 2012). Few studies exhibiting "suspension culture reprogrammed iPSCs" exist, all of which are carried out with miPSCs (Fluri et al. 2012; Baptista et al. 2013). Translation of integrated miPSC production techniques described by Baptista et al. (2013) to hiPSC processing may be particularly useful, as continuous derivation of large numbers hiPSCs would help reduce the bottlenecks bought about by cellular reprogramming. Moreover, it may provide a "black box" platform to derive, expand and differentiate a patient's cells in a single, contained unit that could be installed at point-of-care centres for relevant disease types.

a)

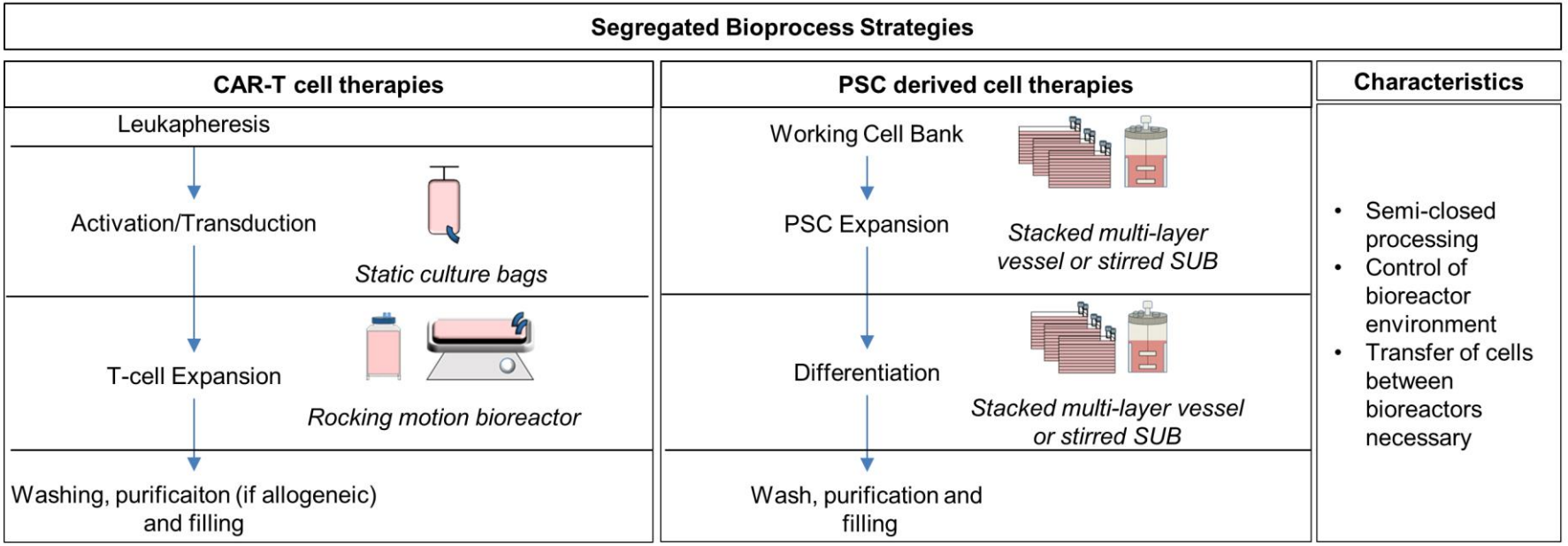

Figure 2.3 Continued overleaf

b)

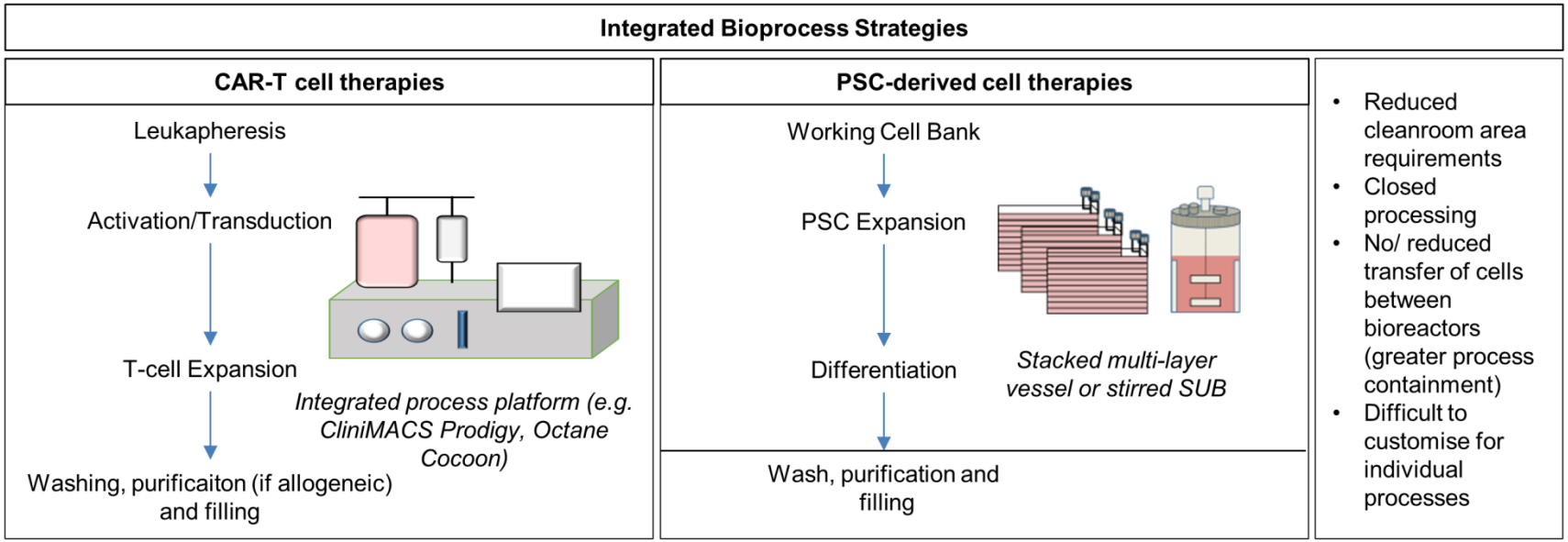

Figure 2.3 Cell therapy bioprocess strategies and their characteristics. **a)** Segregrated bioprocess strategies for CAR-T cell therapies (left upper panel) and hPSC-derived therapies (right upper panel) and typical technologies that are used in these processes. **b)** Integrated bioprocess strategies, which allow unit operations to be carried out as a single process in a self-contained system, for CAR-T cell therapies (left lower panel) and hPSC-derived therapies (right lower panel). Unit operations which are segregated in each bioprocess strategy (i.e. those that require transfer of cellular material between pieces of equipment) are separated by horizontal lines.

The potential for perfusion based culture has been described for MSC therapies (dos Santos et al. 2014). Perfusion culture supports continuous, integrated bioprocess systems for MSCs, whereby up-stream and downstream processing operation can be run in a fully contained manner at large scale. (Cunha et al. 2015), describe perfusion MSC culture followed by continuous TFF, in order to provide higher cell concentrations than batch methods.

The development of single-use bioreactors and culture-ware with ports and manifolds to support sterile tubing connections has allowed the conjunctive use of sterile plastic tubing to create bespoke closed systems for the transfer of cells between two pieces of equipment without exposing the cells to the open environment (Tumaini et al. 2013). Such systems allow a reduction in the necessary grade of cleanroom (usually to Class C/D from Class A/B). However, tubing and seals must be set-up for each individual lot. For autologous processes this is likely to be a time consuming task, especially if a single facility handles large numbers of patient samples on a daily basis. When a specific type of tubing is required (i.e. for CliniMACS machinery), the cost of a single tubing set is greater than £1,000, and this can add significantly to the direct costs associated with a bioprocess.

The CliniMACS Prodigy is a device which offers a fully integrated, contained cell therapy bioprocess platform (Figure 2.3). It provides a potential solution to the needs of CAR-T cell therapy bioprocess and has been shown to perform T-cell enrichment, activation, transduction, and expansion and formulation of T-cell therapies in a single-use tubing set (Apel et al. 2013). The cell culture chamber is also capable of performing differentiation protocols, although the Prodigy has yet to be applied to cells beyond lymphocytes. Platforms such as the CliniMACS may prove invaluable to the cell therapy industry. The self-contained environment that the Prodigy offers allows multiple devices to operate within the same cleanroom area, even for autologous processes, resulting in a reduced facility footprint (Kaiser et al. 2015). The automated

nature of the Prodigy will likely reduce the labour-intensive nature of many current bioprocesses. At present, the approximate cost of individual CliniMACS machines is approximately £250,000 (US$360,000). This represents a sizeable capital investment on single piece of equipment, which may impair the speed of its uptake, especially until its effectiveness and robustness can be assured. Furthermore, the size of the cell culture chamber in the CliniMACS, which allows T-cell populations of up to $2x10^9$ cells to be produced (Apel et al. 2013), is likely to restrict its application to autologous cell therapy bioprocesses. Another device which targets the production of 'device-based' production of autologous cell therapies is the Octane Cocoon (Octane Biotech Inc., Ontario, Canada). Similar to the Prodigy, the Octane seeks to allow automated, closed-off production of cell therapies in a single, turn-key based device. The Octane can be adapted for production of different types of cell therapies.

At the time of writing, there are no solutions to the need for fully contained bioprocess platforms capable of handling large lot sizes. Innovations in cell culture platforms and integrated process protocols have allowed SUBs to be used for integrated expansion and differentiation processes. Furthermore, multiple unit operations can now be carried out in a single, contained process platform, including DSP operations such as volume reduction and enrichment of target cell population. However, the novel, contained process platforms discussed in this section face a challenge in terms of their scalability and applicability to allogeneic and large-dose autologous cell therapies.

Table 2.5 (continued overleaf) Summary of studies investigating the integrated expansion and differentiation of hPSCs

Culture Conditions	Cell Type (iPSC/ESC)	Target Cell Type	Expansion Max Cell Density (cells/mL) (Fold Expansion)	Differentiation Max Cell Density (cells/mL) (Fold Expansion)	Reported Differentiation Efficiency (%)	Process Time (Days)	Target cells produced per input hPSC	Xeno-free (Y/N)	Source
Microcarrier (DE53 Whatman)	hiPSC	Neural Progenitor Cells (NPCs)	6.1×10^6 (20)	1.1×10^6 (16.6)	78±4.7	25	333	N	(Bardy et al. 2012)
Microcarrier (DE53 Whatman)	hESC	NPCs	4.3×10^6 (21.3)	1×10^6 (17.7)	83±8.5	23	371	N	(Bardy et al. 2012)
Aggregate Culture	hESC	Definitive Endoderm Progenitors (DEPs)	ND (5000)[a)]	ND (23.5)	>80%	22	65,000[a)]	N	(Ungrin et al. 2012)
Microcarrier (Collagen coated Hyclone)	hESC	DEPs	1×10^6 (34-45)	4×10^5 (ND)	84.2±2.3%	12	4	N	(Lock and Tzanakakis 2009)

Aggregate Culture	hESC	Cardiomyocytes	8-9 x 10^5 (4-4.5)	ND	85-95%	12-35	ND	Y	(Fonoudi et al. 2015)

Parameters given for both expansion and differentiation. ND = No data given

a) hESC cells underwent four round of expansion during this study, followed by differentiation as oppose to one round of expansion that took place in the other studies shown in the table. This may explain the disparity in performance parameters when compared to other studies in the table.

2.7 Manufacturing and distribution models for cell therapies

Specific challenges arise from the fact that cell therapies must be delivered to the patient as viable populations of living cells. Traditional manufacturing and distribution models may not be appropriate for some cell therapies due to this unique characteristic. This section will briefly cover the different options available to CBT manufacturers; namely centralised, and decentralised manufacturing.

Centralised manufacturing (Figure 2.4) involves the use of one large facility to cater for a large area of the global market (e.g. one facility in Europe, and a further facility in the USA to cater for North America, and so on). This is a traditional model that is often employed by the pharmaceutical industry. The advantages of centralisation include spreading indirect costs over large production volumes and minimising interactions with suppliers and customers (Medcalf 2016). Furthermore, centralised manufacturing could represent less of a regulatory burden in that a product is manufactured at one facility and quality control and assurance mechanisms need only demonstrate consistency across manufacturing lots, rather than consistency across multiple facilities A carefully designed manufacturing process operated at a single site is the easiest to implement. Conversely, this approach might also represent a greater risk; in the rare instance of a facility shutdown the production process is halted entirely at a high cost. Decentralised manufacturing models would de-risk the process from this perspective (Trainor et al. 2014).

Decentralised manufacturing models utilise multiple manufacturing facilities, these are generally positioned close to point-of-care centres and clinics licensed to administer the cell therapy in question. Decentralised facilities offer several potential benefits compared to centralisation. Foremost, decentralised facilities may offer greater market access for cell therapies by delivery of a product to a greater number of clinics (and therefore patients) than centralised models. Decentralised facilities also offer a reduction in delivery distances and times from a manufacturing facility to

a patient. This can be particularly useful for both ‘made to order’ therapies, for which the short supply chain will enhance the responsiveness of the manufacturing process, and fresh products (Medcalf 2016). Fresh products have a limited viable lifespan, usually in the order of hours rather than days or weeks associated with cryopreserved therapies; short supply chains associated with decentralised models allow these products to be delivered to a wider market than would be feasible using a centralised model. Even for cryopreserved products, centralised facilities can result in the need for long distance supply chains that are reliant on cold chain storage which can be difficult to validate and maintain. Furthermore, not all clinics have the capability to handle incoming cryopreserved materials (Medcalf 2016).

Trainor et al. argue that true decentralisation would be represented by a manufacturing model that allows autologous cell therapies to be manufactured within the same clinic from which patient biopsies are sourced (Figure 9.3). This would require the use of bench-top culture units that would be fully contained and at least partially automated. The arguments for such manufacturing models include their ability to reduce logistics and shipping costs associated with transportation of autologous cell therapies and patient materials, additionally they avoid the risk of cross-patient contamination. Realisation of manufacturing models such as this may come in the form of the ‘autonomous microfactory’, such as the Octane Cocoon (Octane Biotech Inc.), which could be utilised in a franchise-based model to produce cell based therapies (Trainor et al. 2014; Medcalf 2016). Whilst this model may prove to be an attractive prospect for low demand, autologous therapies due to a highly responsive manufacturing process set-up, it is currently unclear as to how this sort of business model and manufacturing facility would be regulated. It may therefore prove infeasible as a manufacturing option in the near-term. As technical advances in cell therapy manufacturing progress, it may be possible to realise the conceptual ‘GMP-in-a-box’ manufacturing model. In this case, autologous cell therapies can be

produced on a bench-top module outside of a cleanroom. This would involve a tissue acquisition being loaded into a fully automated module that could then carry out all the necessary steps to produce a cell therapy. Whilst not currently available, the GMP-in-a-box manufacturing model would prove advantageous as it would negate labour and transportation costs associated with autologous cell therapies. However, it is as yet unclear how such a model could be achieved from a regulatory perspective. It is also unclear how the business model for such a system would work as this might create a scenario where clinics act as de facto franchises for cell therapy manufacturers.

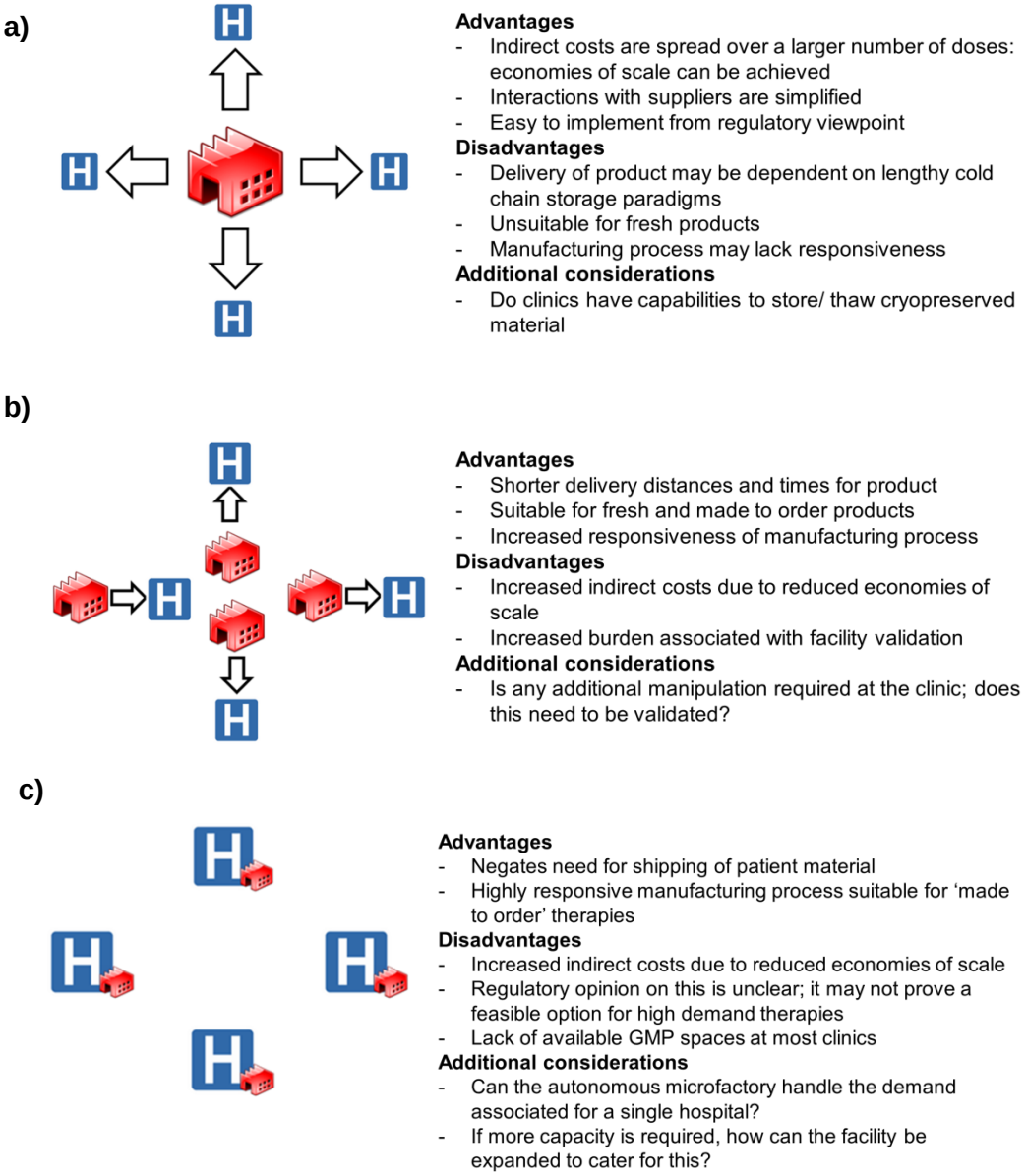

Figure 2.4 Cell-based therapy manufacturing and distribution strategies and the advantages, disadvantages and additional considerations associated with these. **a)** Centralised manufacturing: one facility is used to cater for a single market area and the therapy is then distributed to multiple clinics. **b)** Decentralised manufacturing (off-site): multiple facilities are used to cater for a single market area; one facility may cater directly for an individual clinic, or a small number of clinics within a specific location. **c)** Decentralised manufacturing (on-site): a manufacturing facility, most likely using 'GMP in a box' piece of equipment, is based at a clinic and the production process is carried out on site.

2.8 Conclusion

In this chapter, the basic properties of cell therapy bioprocesses have been outlined, including their structure, key unit operations, and key similarities and differences between bioprocesses for cell therapies of different types. Furthermore, the techniques and technologies currently available for use within each stage of a cell therapy bioprocess have been summarised.

Traditionally, low throughput, manual technologies such as T-flasks were used for cell culture-based unit operations (such as expansion and differentiation). However, the recent emergence of contained, automated bioreactors that negate the need for manual interventions coupled with the development of xeno-free, defined culture conditions have made robust, cGMP processes easier to attain for cellular products.

The downstream unit operations contained within a bioprocess are dependent upon the type of cell therapy that is to be manufactured. MSCs are anchorage-dependent cells; enzymatic removal of cells from growth surfaces is the preferred method of achieving dissociation within a bioprocess. Optimised protocols are being developed in this area. Further to this, high-throughput volume reduction equipment is now available for bioprocesses involving all types of cell therapy. Fluidised bed centrifugation (FBC), spinning membrane filtration (SMF), and tangential flow filtration (TFF) are three popular, scalable methods by which to achieve concentration of therapeutic cells.

Options for high-resolution enrichment, or purification, of target cell sub-populations from a varied input population are currently limited. Whilst MACS technologies offer the current gold standard in the industry in the form of a robust and relatively high throughput process platform, further improvements must be made to accommodate process options for the enrichment of rare cell types within a population.

Integrated contained process platforms, such as the Cocoon (Octane) and the Prodigy (Miltenyi), now offer automated, closed processing options for autologous cell therapies, particularly in the CAR-T cell space. Platforms such as these may afford the opportunity to de-risk cell therapy bioprocesses by reducing human error and contamination associated with transfer of process materials between separate pieces of equipment.

Finally, the nuances of cell therapy bioprocessing are forcing manufacturers to rethink traditional manufacturing and distribution models. Whereby traditional pharmaceutical and biopharmaceutical products have often been produced at a large, centralised facility, the time-sensitive nature of fresh cell therapy products may necessitate a different approach. Decentralised, satellite facilities have been proposed as an option for the production of autologous therapies and fresh, allogeneic therapies that have a limited lifespan following formulation.

This chapter has highlighted that while there has been progress in improving bioprocesses for cellular products, challenges exist still to achieving cost-effective manufacture. Current and future cell therapy bioprocess practices, as summarised in this chapter, were used as the problem domains for the decisional tools developed within this thesis. The generic processes outlined in this chapter were used as the basic inputs for the unit operations to be included in the tools, as Chapter 3 describes, with adjustments made to capture the specifics of different bioprocesses considered within this work.

Chapter 3: Materials and Methods

3.1 Introduction

The field of human cell bioprocessing is a relatively nascent, emerging field. Pressures to deliver both cell therapies and human stem cell-derived cells for use as research tools at affordable prices have, and will continue to, drive efficient manufacturing strategies and bioprocess platforms.

In Chapter 1, the importance of making effective decisions with regards to manufacturing strategies and process designs early on in product development was highlighted. Such decisions must be made with due consideration given to both technical and financial aspects of bioprocess design. Process simulation tools are a valuable asset to companies seeking to identify cost-effective manufacturing strategies and process designs in the early stages of product development.

This chapter introduces the tools that have been developed for the research presented in this thesis. Section 3.2 outlines the architecture of the models developed. This is followed by a description of the models used to compute mass balances and process costs within the decisional tools in Section 3.3 & 3.4. Section 3.5 details the different approaches to the identification of optimal process designs that have been employed. Stochastic modelling approaches that were used to deal with process uncertainty are outlined in Section 3.6. Finally, the data collection methods used throughout this research are highlighted in Section 3.7.

3.2 Model Architecture

A series of decisional tools have been developed to allow the identification of cost-effective process designs within the cell therapy sector. The tools developed all follow a similar architecture and (unless stated otherwise) consist of a deterministic bioprocess economics model and linked database, an algorithm used to identify

optimal manufacturing strategies and/or bioprocess designs, and a stochastic analysis algorithm (Figure 3.1).

The information database houses not only key input information associated with the specific bioprocess that is being evaluated by the decisional tool, but also technical and cost data pertaining to technologies, materials and media to be tested by the case studies reported in Chapters 3, 4 & 5.

The bioprocess economics model is used to compute mass balances and process costs for a given manufacturing strategy or bioprocess design. An overview of the bioprocess economics model developed is given in Section 3.3.

Specific bioprocess designs or manufacturing strategies can be encoded manually into the bioprocess economics model, however the algorithms that were developed were designed to generate possible process configurations (within set constraints), from the database of specified technologies and bioprocess designs. Key output parameters for each process configuration generated by the algorithm were then evaluated using the bioprocess economics model. Cost-effective process designs and manufacturing strategies were identified in this manner; the outputs of the bioprocess economic model were used to evaluate and assess each bioprocess configuration from a financial perspective.

The stochastic analysis algorithm was also linked to the bioprocess economics model in order to capture variations in key outputs of the bioprocess economics model under manufacturing uncertainty.

Figure 3.1 shows an how the components described above work together to provide meaningful outputs associated with a bioprocess such as process costs, resource utilisation, cost-effective process designs and information on process robustness under uncertainty.

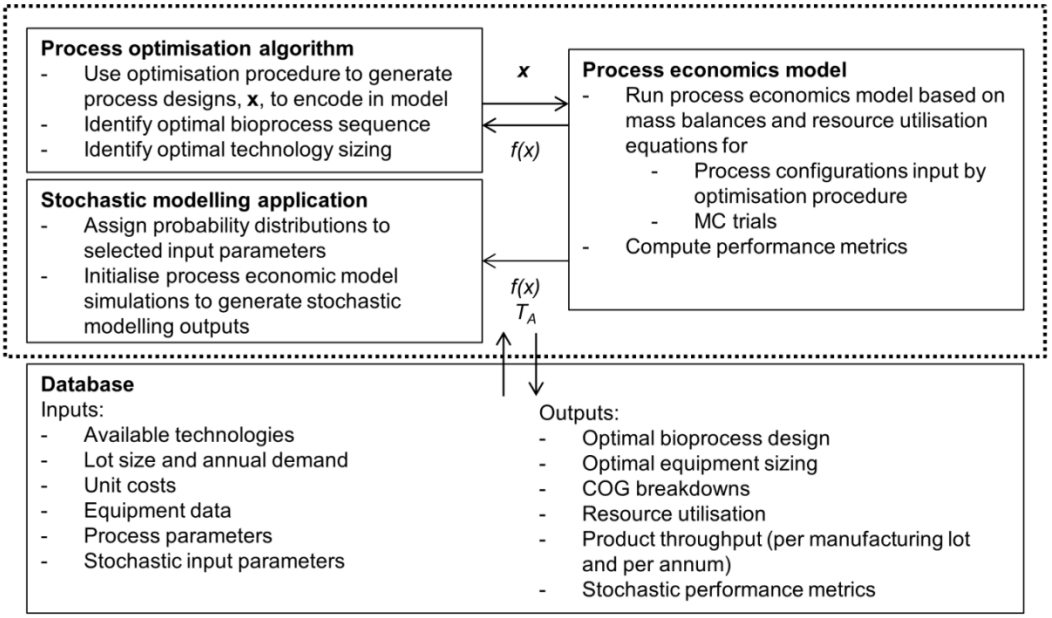

Figure 3.1 Schematic of the model architecture employed for the computational tools. An optimisation algorithm is linked to a detailed process economics model. The process economics model performs mass balancing and equipment sizing calculations, and computes key performance metrics. The optimisation algorithm identifies the best sequence of process technologies to use within a given manufacturing strategy. The stochastic analysis algorithm is also linked to the process economics model. Random values are assigned to variable inputs according to the probability distributions assigned in the stochastic analysis algorithm. The outputs of each individual simulation from the stochastic modelling process are used to draw conclusions about the robustness of a bioprocess under manufacturing uncertainty.

3.3 Process Models

Previously published process models have focused on a mass balance of materials across specific unit operations within a bioprocess. However stem cell and cell therapy bioprocesses present a unique scenario in that the final population of living cells is the product. Therefore, the focus of the process models developed in this thesis is on the flow of viable target cells through the process. Consequently a set of

equations has been constructed to model this parameter for each specific unit operation; i.e. in this case a ‘mass balance’ of cells has been developed.

The process models described in this chapter were used to calculate the composition and size of cell populations within each stage of the bioprocess. The process models described in this section allowed target product yield to be determined rapidly under different scenarios. This information fed directly into the number of manufacturing lots required to meet product demands and in turn the cost-effectiveness of a bioprocess. Furthermore, the process models detailed in this section provided an insight into resource utilisation and the impact that different process designs have upon this. The identification of the impacts of different process designs upon the utilisation of key resources allowed a deeper analysis of how and why certain process designs proved more cost-effective than others.

The process models outlined in this section reflect those that were used in a variety of decisional tools created as part of this work. For the most part, the generic calculations can be applied to every case study outlined in subsequent chapters; however alterations in these models that are specific to an individual case study will be presented in the relevant chapter. Furthermore, the process models listed below present some unit operations that are specific only to a bioprocess utilised for a certain type of cell therapy (e.g. CAR-T cell, or hiPSC-derived cell); information on the process models applied in each case study is given in subsequent chapters where these case studies are presented.

3.3.1 Cell Culture (Expansion)

Expansion, or cell culture, operations are inherent in almost all cell therapy bioprocesses. It is the process by which cell populations are systematically increased to clinically relevant cell numbers. The achievable increase in cell population size is a function of the daily growth rate of a population of cells; this determines the

expansion fold. The expansion fold refers to the fold-increase in the number of cells in a population over a given time-period of cell culture.

Passaging is a common technique in order to prevent cell concentration from becoming the limiting factor on the expansion fold that is achievable within a cell culture unit operation. Passaging involves transferring the population of cells to fresh culture vessels (this could be a single, larger vessel, or multiple vessels of the same size) in order to disperse cells at the standard seeding density (or concentration if suspension culture is employed). This allows the populations to continue to expand without exceeding limitations in the maximum viable cell density or concentration.

The output of a cell culture unit operation, in terms of the number of cells, n_F, can therefore be described as:

$$n_F = n_0 * (f) * h \quad (3.1)$$

where n_0 = starting number of cells

f = expansion fold of the cell population

h = harvest yield of the unit operation (%)

Equation 3.1 gives the output of a single stage of a cell culture unit operation. Where multiple passages were assumed, the total output of a cell culture operation (with all passages accounted for) was calculated as follows:

$$n_F = n_0 * f^{\rho} * h^{\rho} \quad (3.2)$$

where ρ = number of passages in a cell culture unit operation

The application of Eq. 3.1 and 3.2 to each individual passage within a cell culture unit operation (where applicable) allows computation of the resource utilisation associated with each individual passage, and allows cost-effective technologies to be selected for each phase of the cell culture operation.

3.3.2 Viral Transduction

Genetic engineering of cells is used to alter cell phenotype for a variety of purposes. A detailed overview of the techniques used to achieve this, and the reasons behind their applications can be found in Chapter 1. Viral transduction is a genetic engineering technique that has applications in the production of hiPSCs from a population of somatic cells and also in the generation of CAR-T cells.

The efficiency of a viral transduction process can be defined as the percentage of cells in a starting population (N_0) that are converted to the desired phenotype. Viral transduction does not result in 100% conversion of a starting cell population to the target cell phenotype. Therefore a process model has been developed to capture both the number of target cells produced by this process, but also the number of non-target (or contaminating cells) remaining in the cell population.

The final number of target cells, $n_{F\ target}$, from a viral transduction, or electroporation unit operation was calculated as follows:

$$n_{F\ target} = e_{VT} * e_{\mathrm{F}} \qquad 0 < e_{VT} \leq 1 \qquad (3.3)$$

where e_{VT} = efficiency of the transduction process

The number of non-target cells produced within a viral transduction unit operation can therefore be described thus:

$$N_{F\ non-target} = (1 - e_{VT}) * n_{\mathrm{F}} \qquad 0 < e_{VT} \leq 1 \qquad (3.4)$$

The composition of the cell populations computed using this method could be used to estimate the yield of target cells within a bioprocess and the level of whole cell impurities present in a bioprocess stream.

3.3.3 Electroporation

Electroporation, in addition to viral transduction, is a technique by which genetic modifications can be made to cells in order to alter their phenotype. Electroporation

can be used to deliver non-viral vectors to cells. Typical non-viral vectors include transposons, which are used to deliver mRNA encoding transgenes into cells. Similar to transduction, the efficiency of an electroporation process is represented by the percentage of a population of cells that successfully exhibit a target phenotype following the unit operation. In order to capture the composition of the cell population following electroporation, the following equations were applied:

$$n_{F\ target} = e_{EP} * n_{\mathrm{F}} \qquad 0 < e_{EP} \leq 1 \qquad (3.5)$$

where x_{EP} = efficiency of the transduction process

$$n_{F\ non-target} = (1 - e_{EP}) * n_{\mathrm{F}} \qquad 0 < e_{EP} \leq 1 \qquad (3.6)$$

3.3.4 Differentiation

Differentiation is the process by which a target cell phenotype, for example RPE cells to treat macular degeneration, is derived from a population of stem cells. In the work presented here only hPSC differentiation towards somatic cell types is considered. Differentiation efficiencies vary according to both the differentiation strategy employed, and the phenotype of the target cell that is required (as discussed in Chapter 1). In this work, the differentiation efficiency is represented by the ratio of target cells produced to the total number of cells in the differentiation feed stream. Therefore the differentiation efficiency was defined as follows:

$$e_{diff} = \frac{n_{F\ target}}{n_o} \qquad 0 < e_{diff} \leq 1 \qquad (3.7)$$

where e_{diff} = efficiency of the differentiation process

However, differentiation is predominantly a cell culture-based unit operation. Therefore, the yields, in terms of the number of target cells produced by a

differentiation process, $N_{F\,target}$, and the total number of undifferentiated, or non-target cells ($N_{F\,non\text{-}target}$) , was calculated as follows:

$$n_{F\,target} = n_{\mathrm{F}} * e_{diff} * h \qquad 0 < e_{diff} \leq 1 \qquad (3.8)$$

$$n_{F\,non-target} = (n_{\mathrm{F}} * \left(1 - e_{diff}\right) + n_0 * f * h \qquad 0 < e_{diff} \leq 1 \qquad (3.9)$$

where f = expansion fold of the differentiation culture as defined in equation 3.2

The calculations above provide an estimation as to the yield of target cells that exit the differentiation process. Some differentiation protocols rely on the fact that non-differentiated cells can be removed by 'culture-based' purification, whereby culture conditions mean that non-differentiated cells are unable to survive. Note, that for some culture-based purification protocols such as this, the expansion fold, *f*, is essentially negligible as the number of cells that die off negates any increase in the overall cell population, hence $n_F \leq n_0$ in some cases.

3.3.5 Concentration

Concentration, sometimes referred to as washing, involves separation of media (and in some cases support materials such as microcarriers) from a cell population. The cells are concentrated in this stage as media is removed from the process stream.

The performance of a concentration step can be quantified using a concentration factor (CF) and the yield of the unit operation (or percentage of target cells that are retained in the process stream (x_{conc})). The volume retained within the process stream can be calculated as a function of the concentration factor that can be achieved using a given technology:

$$v_{ret} = \frac{v_0}{CF} \qquad (3.10)$$

where v_0 = volume of the feed stream

The yield of target cells present as an output of the concentration step can be defined as

$$n_{ret\ target} = n_{0\ target} * e_{conc} \qquad 0 < e_{conc} \leq 1 \qquad (3.11)$$

where e_{conc} = percentage yield of viable cells that are retained following volume reduction

Devices used for volume reduction can employ either centrifugation techniques, or filtration in order to concentrate cell populations. Occasionally, this can result in a reduction in the number of non-target cells within the process stream, which may be separated from target cells on the basis of size or density. The number of non-target cells in retained in the process stream, $n_{ret\ non\text{-}target}$, was computed as follows:

$$n_{ret\ non-target} = \frac{n_{0\ non-target} * e_{conc}}{R_f} \qquad R_f \geq 1 \qquad (3.12)$$

where R_f = factor by which the number of non-target cells are reduced during the volume reduction stage

For volume reduction operations whereby target cells cannot be separated from non-target cells, an R_f of 1 is assumed. An example of this is in allogeneic CAR-T cell manufacture where a mixed population of CAR-T cells, some of which are TCR- or TCR+ cells, is subject volume reduction following cell culture. In this instance the target TCR- cells cannot be separated from TCR+ cells during the volume reduction phase.

In this instance, the composition of the feed stream, both in terms of percentage and number of target cells as well as the concentration of cells, is important as it may have an impact upon the feasibility of subsequent unit operations such as affinity purification and vialling of cryopreserved product (if applicable).

3.3.6 Purification

Purification is an essential part of many cell therapy bioprocesses whereby a population of pure target cells which form the cell therapy must be extracted from a mixed population of cells. In this work high resolution, affinity purification techniques have been evaluated within case studies laid out in subsequent chapters. Affinity purification techniques rely on the separation of cells based on the presence (or lack thereof) of surface antigens.

The performance of a purification process can be characterised using three key performance parameters; the total viable cell yield; z_{pur} (%), the percentage yield of target cells retained in the process stream following purification; x_{pur}, and the purity of the final cell population, p_F (%).

The total number of cells in the final cell population can therefore be described as:

$$n_F = n_0 * z_{pur} * x_{pur} \qquad 0 < x_{pur}, z_{pur} \leq 1 \qquad (3.13)$$

The number of target cells collected from the purification process was therefore derived from the initial cell population using the equation;

$$n_{F\,target} = n_0 * p_o * x_{pur} * z_{pur} \qquad 0 < p_0, x_{pur}, z_{pur} \leq 1 \qquad (3.14)$$

where p_o = the purity of the starting cell population (% of target cells)

And the number of non-target cells, $n_{F\,non\text{-}target}$ may be described as

$$n_{F\,non-target} = [n_0 * (1 - p_0)] * z_{pur} * (1 - p_F) \qquad 0 < p_0, p_F, z_{pur} \leq 1 \qquad (3.15)$$

3.3.7 Resource Utilisation

It was necessary to quantify the utilisation of resources within a bioprocess; in this case the utilisation of media, reagents, single-use culture vessels, fixed equipment,

and labour were computed by the process model. The consumption and utilisation of such resources determines the overall cost of a bioprocess and the capacity required of the facility housing the bioprocess.

In order to quantify the number of manufacturing lots per year, l_a, the annual demand, t, was divided by the output of an individual manufacturing lot, m, thus;

$$l_a = \left\lceil \frac{t}{m} \right\rceil \tag{3.16}$$

The number of manufacturing lots per year, and the duration of the bioprocess has a significant impact upon the utilisation of both direct and indirect resources associated with a bioprocess; the number of manufacturing lots run in parallel, l_p, was determined as a function of both the length of the bioprocess, b_l, and the length of time that the bioprocess facility is in operation over the course of a year, b_f ;

$$l_P = \frac{l_a}{\left\lceil \frac{b_f}{b_l} \right\rceil} \tag{3.17}$$

A key parameter when evaluating equipment sizing strategies is the type of technology to be used within each unit operation and the number of units required to process the required number of cells in each manufacturing lot.

For a cell population of maximum size n, the number of disposable units (u_{con}) required of a particular technology, j, for a given unit operation, i, was computed as;

$$u_{con\ j,i} = \left\lceil \frac{n_i}{s_j} \right\rceil \tag{3.18}$$

Where s_j = the capacity of a given technology (number of cells)

For cell culture based unit operations, whereby multiple, disposable vessels may be required, s_j, was defined as;

$$s_j = d_{h,i} * a_j \quad (3.19)$$

where $d_{h,i}$ = maximum cell density (for adherent culture) (cm^2) or cell concentration (for suspension culture) (mL) allowable in a given technology used within a given unit operation

a_j = surface area (for adherent culture) (cm^2) or volume (for suspension culture) available within a given technology (mL)

For many DSP operations it is necessary to constrain the number of process units required to one per manufacturing lot, particularly for back-end operations such as purification. This is because whilst units could be run in parallel, the pooling of samples together after purification was deemed an unlikely practice to be employed in a clinical setting owing to cGMP guidelines on product consistency. Therefore a constraint was placed on process designs such that:

$$u_{con\ i,j} = 1 \qquad \frac{n_i}{s_j} < 1, v_i \leq v_{j\ max} \quad (3.20)$$

where v_i = feed volume of a unit operation

$v_{j\ max}$ = surface area (for adherent culture) or volume (for suspension culture) available within a given technology

The volume of the DSP technology has been considered here because some technologies evaluated in the case studies presented in subsequent chapters had a maximum capacity given as a volume and some had a maximum capacity given as a total cell number.

It is also important to note that for DSP equipment, $u_{con\ j}$, may refer to disposable tubing sets, membranes and/or cartridges rather the 'vessels' characteristic of cell culture operations.

Following computation of the number of disposable units required per manufacturing lot for each unit operation, it was possible to estimate the number of skids, or pieces of fixed equipment, $u_{fixed\ j}$, required to support a given disposable technology. The number of skids required was calculated as function of the maximum number of relevant disposable vessels in use at any one time, across all unit operations. This was considered the best approach so that the utilisation of skids could be maximised by using the same skid to support the whole bioprocess, rather than a single unit operation, thus minimising 'dead' time of fixed equipment. The number of skids/ pieces of ancillary equipment required was therefore computed as;

$$u_{fixed\ j} = \left\lceil \frac{\max(u_{con\ i,j})_{i=1}^{k}}{m_j} \right\rceil * L_p \qquad (3.21)$$

where m_j = capacity of ancillary equipment, in terms of the number of disposable vessels that one piece of equipment can support at a given time

$\max(u_{con\ i,j})_{i=1}^{k}$ = maximum number of units of a given disposable technology, *j*, required at any point in the bioprocess (for unit operations *i = 1,…,k*)

It was assumed that separate equipment would be required for parallel lots to avoid the risk of cross-contamination between different manufacturing lots.

The number of operators required for a given technology was calculated as a function of the maximum number of units required, u_j, and the number of units of a given technology that a team of 2 operators could handle, y_j. A factor of 2 is included in equation 3.22 because operators were assumed to work in teams of 2, as per cGMP guidelines.

$$W_j = \left\lceil \frac{\max(u_{i,j})_{i=1}^{k}}{y_j} \right\rceil * 2 \quad (3.22)$$

where $\max(u_{i,j})_{i=1}^{n}$ = maximum number of units required of a specific technology, *j*, for unit operations i = 1,…,k

The total number of operators was calculated as a function of the number of parallel manufacturing lots per year; it was assumed that lots in series could be handled by the same operators. Therefore;

$$w_{ann} = [\max(W_j)_{j=1}^{k}] * l_p \quad (3.23)$$

where $\max(w_j)_{j=1}^{l}$ = maximum number of operators required to handle any technology, *j = 1,…,k* used in a bioprocess

3.4 Cost Models

The previous section focused on process models associated that were used to compute mass balances and calculate resource utilisation associated with a bioprocess. This section introduces the cost models, which utilise data generated by the process models described in the previous section to evaluate the financial performance of a bioprocess. The cost models presented in this section have been adapted from Farid (2002), where two key cost parameters fixed capital investment (FCI) and cost of goods (COG) are measured. Cost models have been adapted from the originals presented in (2002) in order to reflect the differences in cell therapy bioprocessing from biopharmaceutical protein manufacturing (as was their original function).

3.4.1 Fixed Capital Investment

Fixed capital investment costs represent the cost of any fixed equipment, along with the costs associated with building a facility to support a bioprocess. A Lang factor method was used to approximate fixed capital investment (Lang 1948). The Lang

factor method assigns a proportionality constant to the total equipment purchase cost (TEPC) in order to provide an estimate of the FCI required of a bioprocess. Therefore;

$$FCI = F_{Lang} * TEPC \quad (3.24)$$

where F_{Lang} = Lang factor that appropriately approximates the cost of a cell therapy/stem cell bioprocess facility

3.4.2 Cost of Goods

The COG represents the cost to manufacture a cell therapy, or stem cell product. COG comprises direct and indirect costs. Direct costs (DC), comprise of expenditure on materials and labour; they are a function of utilisation. Indirect costs (IDC), are expenditures that are independent of resource utilisation; they consist of depreciation costs (or amortisation), and miscellaneous costs such as equipment maintenance, tax and insurance.

Factors proposed by Farid (2002) were used to provide estimations of additional direct cost categories (namely, miscellaneous materials and QC/QA labour costs), and standard factors used in chemical engineering textbooks (e.g. Sinnott, XXXX) were used for indirect cost categories (namely maintenance, taxes, and insurance). These factors are presented in Table 3.1.

The total COG for a bioprocess can be described as;

$$COG = c_{direct} + c_{indirect} \quad (3.25)$$

Where c_{direct} = direct costs

$c_{indirect}$ = indirect costs

Direct costs are computed thus;

$$c_{direct} = c_{lab} + c_{mat} \quad (3.26)$$

Where c_{lab} = labour costs

c_{mat} = materials costs

Table 3.1 Cost of goods model overview

Cost Category	Parameter	Cost Factor
Direct	Supervisors	0.2 * Operating Labour
	QC/QA	1.0 * Operating Labour
	Management	1.0 * Operating Labour
	Misc. materials	0.5 * Materials
	Materials	*f* (utilisation)
Indirect	Maintenance	0.1*Capital Investment
	Local Taxes	0.02* Capital Investment
	Insurance	0.01* Capital Investment
	Depreciation	$\frac{\text{Capital investment}}{\text{Depreciation period (years)}}$

Labour costs are approximated from the value describing the number of operators required to run a bioprocess, w_{ann} and the annual cost of employment for one operator per annum, c_{op}. The cost QC/QA, supervisory, and management staff are also accounted for by the factor, $F_{lab:}$

$$c_{lab} = \left(w_{ann} + c_{op}\right) * F_{lab} \quad (3.27)$$

Materials costs are calculated as function of utilisation, on a unit operation basis. The calculation of direct costs associated with each unit operation was performed in order

to allow in depth analysis of a bioprocess, allowing focused efforts on cost reduction at stage of the bioprocess where it is likely to have the most impact. Generally materials costs were calculated thus:

$$c_{mat\ j} = \left[\left(\sum_{k=1}^{n_1} v_{m\ k} * c_{m\ k}\right) + \sum_{i=1}^{n_2} u_{con\ i} * c_{con\ i}\right] * F_{mat} \quad (3.28)$$

where $c_{m\,j}$ = cost of a reagent, *k*, used within a unit operation, *j*

c_{con} = cost of any consumable technology, *i*, used within a unit operation, *j*

v_m = volume of any reagent, *k*, required within a unit operation, *j*

F_{mat} = A factor to describe the cost of miscellaneous materials such as PPE

Total material costs are then calculated by aggregating material costs from each unit operation;

$$c_{mat} = \sum_{j=1}^{n_3} c_{mat\ j} \quad (3.29)$$

The calculation of overall annual costs on a cost category basis is important as it allows the process development teams to envisage how changes in process design will not only affect the total COG, but also the breakdown of the COG into its constituent parts.

Annual indirect costs were calculated as a function of the capital investment required of a facility and the depreciation period, δ, or lifespan of the facility;

$$c_{indirect} = FCI * (\frac{1}{\delta} + F_{indirect}) \quad (3.30)$$

where $F_{indirect}$ = factor which describes the cumulative cost of insurance, depreciation, local taxes and maintenance of a bioprocess facility

3.4.3 Distribution and Shipping costs

In Chapter 4, shipping costs were calculated as part of a representative case study seeking to compare different manufacturing strategies for an allogeneic cell therapy.

When overland distribution was considered, shipping costs, τ, were calculated as a function of the number of secondary facilities, μ, and the number of hospitals, ε:

$$\tau = \mu * (\alpha_{pf} * \beta_{pf}) + \varepsilon * \mu * (\alpha_{sf} * \beta_{sf}) \quad (3.31)$$

where α_{pf} = number of deliveries made from primary to secondary facility

α_{sf} = number of deliveries made from secondary facility to clinic

β_{pf} = factor representing road transportation costs from primary to secondary facility

β_{sf} = factor representing road transportation costs from secondary facility to the clinic

Where overseas shipping, via air transportation, was required, shipping costs, τ, were calculated as follows:

$$\tau = \alpha_{pa} * \beta_{pa} + \mu * (\alpha_{w} * \beta_{w}) + \varepsilon * \mu * (\alpha_{sf} * \beta_{sf}) \quad (3.32)$$

where α_{pa} = number of deliveries made from primary to airport

α_{w} = number of air shipments

β_{pa} = factor representing road transportation costs from primary facility to airport

β_{w} = factor representing air transportation costs inclusive of road transportation costs to secondary facility on arrival

The cost factors used to represent transportation costs can be found in Chapter 4, where the case study that utilises the shipping cost model is described.

3.5 Identification of optimal process designs and manufacturing strategies

The work presented in this thesis focuses on the identification of cost-effective bioprocess designs. The bioprocess economics model described in Sections 3.3 & 3.4 is capable of computing COG per unit for a specified process design. In order to ensure that the most cost-effective bioprocess design or manufacturing strategy, within a defined design space, was identified efficiently, algorithm-based search and/or optimisation tools were applied to each of the case studies presented in subsequent chapters. This section will focus on the algorithms and optimisation procedures used to carry out this process.

The methodologies presented here involve the generation of candidate solutions for a given bioprocess. Within these candidate solutions, a technology, *i*, is assigned to a unit operation, *j*. Figure 3.2 shows a candidate solution, **x**, for a hypothetical bioprocess consisting of number of unit operations, *k*. The algorithms outlined below link with the bioprocess economics model using the closed-loop model architecture displayed in Figure 3.1 to generate candidate solutions and compute performance metrics for each solution.

Each stage, or unit operation, within the bioprocess in the case shown above is subject to one discrete variable, which is the candidate technology to be used. As shown in Figure 3.2, the candidate technologies are encoded using an integer value

from a set of technologies specific to that unit operation. Therefore the design space, *X*, in terms of the number of available solutions, for the above bioprocess can be computed as;

$$X = \left(\prod_{i=1}^{k} q_i \right) - X_{con} \tag{3.33}$$

where q_i = number of candidate technologies available for each unit operation, *j*

X_{con} = number of solutions that are not assessed due to constraints on process designs

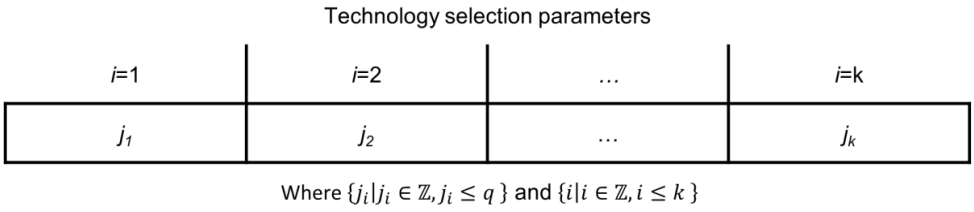

Figure 3.2 A candidate solution for a bioprocess containing *i=k* unit operations. Each step, *i* = 1,…, *k* is defined by a technology j_i. Candidate technologies are taken from a set of technologies specific to each unit operation and are encoded using an integer value.

3.5.1 Brute-force search algorithm

Brute-force search algorithms are an exhaustive means of assessing all solutions within a given design space. All possible solutions, $\boldsymbol{x_1},\ldots,\boldsymbol{x_N}$, are evaluated sequentially by a brute force search algorithm such that the number of iterations necessary to complete the procedure is equal to *X* (defined in equation 3.31).

Brute-force search algorithms hold an advantage over optimisation procedures outlined in subsequent sections in that they are simple to set-up in order to generate

results rapidly. This approach is particularly useful where a design space is relatively small, where approaches such as evolutionary algorithms would require a significant amount of effort to set-up for little gain in terms of computational effort and procedure run time. Brute-force search algorithms were initially used in a case study presented in this work (see Chapter 3). The brute-force approach was also selected in a subsequent case study which resulted in a small design space (i.e. few available solutions); this did not necessitate the use of a more advanced search and/or optimisation procedure (see Chapter 5).

Figure 3.3 illustrates the framework by which a brute-force search algorithm interacts with the bioprocess economics model to allow the evaluation of every available bioprocess design, but also allows the identification of the most cost-effective process design within this search area.

The bioprocess economics model described in Section 3.3 and 3.4 is able to calculate the COG per unit of production for a specific process design; the brute force search algorithm then develops every available bioprocess design ($\boldsymbol{x_1,\ldots,x_N}$) within a set of constraints. Key output metrics associated with each process design are then computed using the bioprocess economics model. The brute-force search algorithm then evaluates the candidate solution, $\boldsymbol{x}$, on the basis of an objective function (in most cases presented here this is the COG per unit of product). Once the search algorithm has ensured that all bioprocess designs have been tested, the procedure is halted and the 'fittest' solution, or optimal bioprocess design, is identified.

3.5.2 Evolutionary Algorithms

An evolutionary algorithm (EA) represents a population-based optimisation procedure, which employ models of biological evolution. Evolutionary algorithms mimic biological evolution in that the 'fittest' (or best) members of a population are passed on to future generations. Variations, as in nature, occur in the form of mutation

and crossover. Specific nomenclature is applied to EAs that reflects their relationship to biological evolutionary processes. A short glossary is provided in Table 3.2.

EAs hold significant advantages over brute-force approaches to identification of cost-effective process designs. These advantages are most apparent when the number of possible solutions, X, for a given problem is large. As detailed in section 3.5.1, a brute-force search algorithm must assess every possible solution, $\boldsymbol{x}$, within a design space. In contrast, an EA will only have to compute a fraction of the possible solutions within this domain. This is because EAs rely on the fitness, or effectiveness, of previously evaluated solutions; the optimal solution can therefore be found using fewer iterations than brute-force approaches. The increase in efficiency achieved through the use of an EA as compared to a brute-force search algorithm varies depending on the values selected for key EA parameters outlined in Table 3.3, as these dictate the number of iterations required to complete the EA procedure. In this work, a specific type of EA, known as a genetic algorithm (GA), was developed in order to perform optimisation of a bioprocess based on financial performance.

The procedure by which the GA developed is shown in the pseudo-code contained in Algorithm 3.1, a basic outline of the main loop of this procedure is given in Figure 3.4, along with visual representations of key operations within the GA. In the algorithm, N denotes the size of the current solution P, also referred to as the parent population in Figure 3.5. The GA begins by initialising a population, Pop, of fixed size, ψ, with randomly generated solutions (or chromosomes) which satisfy bioprocess sequence constraints (introduced in Chapter 4). A solution, $\mathbf{x}$, is evaluated via the method *evaluate*($\mathbf{x}$, H); this serves as the interface between the bioprocess economics model and the optimisation procedure. The method *evaluate*($\mathbf{x}$, H), allows a candidate solution, $\mathbf{x}$, to be encoded in to the bioprocess economics model so that the fitness of $\mathbf{x}$ can be evaluated using the objective function.

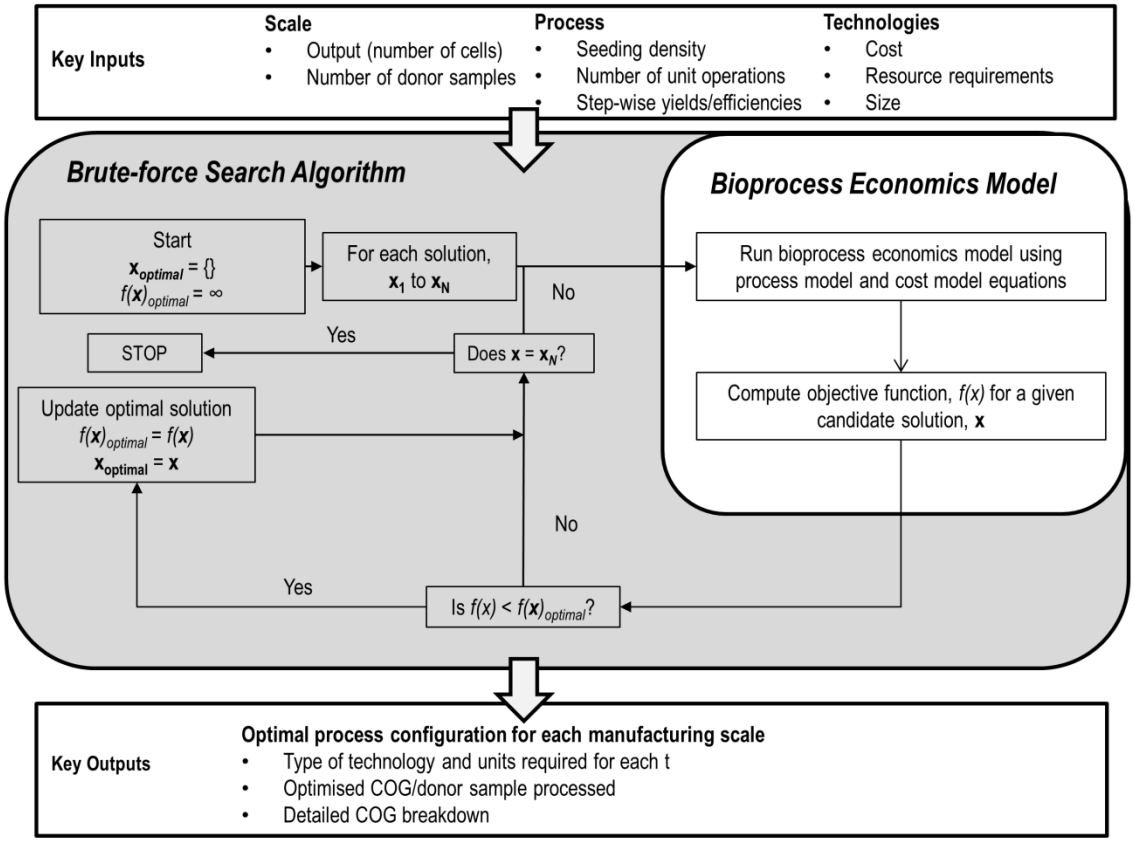

Figure 3.3 Schematic displaying the interaction between the brute-force search algorithm and a bioprocess economics model. Each solution, **x**, is encoded into the bioprocess economics model and key outputs are computed. The solutions are then evaluated on the basis of an objective function, *f(x)*, and the optimal bioprocess design is identified. The algorithm continues until all feasible solutions, $\mathbf{x}_1$,…, $\mathbf{x}_N$ have been evaluated.

Table 3.2 Glossary of terms associated with evolutionary computing

Term	**Definition**
Population	A set of solutions
Fitness	The quality of a solution
Objective function	Function used to quantify the fitness of a solution
Chromosome	An encoded solution; usually represented as a string of values
Gene/ locus	An individual piece of information that makes up a chromosome
Crossover	Process by which two solutions exchange sections of their genetic information in order to introduce variation into a population
Crossover rate	The probability of crossover occurring between two parent solutions
Mutation	Process by which the individual gene's within a solution are subjected to random change
Mutation rate	The probability of mutation occurring at each locus within a solution
Parent	Solution used to generate new solutions
Offspring	Solution resultant of a crossover operation
Generation	One iteration of the evolutionary procedure (involving selection, crossover & mutation)
Environmental selection	Process by which solutions are selected to either form a parental population, or process by which solutions are selected to form the population of a successive generation

.

Following this, in the main loop (Figure 3.4), binary tournament selection is used to select parents from the randomly generated population, *Pop*. This gives rise to the population, *PopTournament*, of size ψ. A visual representation of binary tournament selection is given in Figure 3.5a. Genetic operators are then used to create an

offspring population, *OffPop*, of size N. Crossover is used, whereby two parents are subjected to single-point crossover (Figure 3.5b) in order to generate two offspring solutions. Following this, variation is introduced into *OffPop* by subjecting chromosomes to random bit mutation (Figure 3.5c).

Table 3.3 Key parameters associated with a GA and their assigned values

Parameter	**Value Assigned**
Population size (ψ)	30
Number of generations (G)	30
Mutation rate (r_m)	0.1
Crossover rate (r_c)	0.7
Algorithm runs (R)	10

Mutation is applied at random according to a fixed probability, r_m, (Table 3.3) to any stage of the bioprocess ($j = 1,\ldots,k$), within a solution, **x**. The parent and offspring populations are combined and then subjected to elitist sorting, whereby the fittest solutions are carried over to form 90% of ψ for the next generation. Elitist sorting ensures that any offspring that only the fittest members of the combined parent and offspring populations are passed on to the successive generation. The remaining 10% of the population in the subsequent generation are randomly generated immigrant solutions. Immigrant solutions are usually reserved for dynamic optimisation problems, where the objective function may change during optimisation; they were included in this study as localised convergence was observed when random immigrants were omitted from the algorithm. The introduction of immigrant chromosomes into a population represents an instance of GA fine tuning. Tuning of evolutionary approaches to optimisation is a common practice used to maximise the efficiency and effectiveness of a procedure (2012). The procedure described in the

text above and the pseudo-code presented in Algorithm 3.1 represents a single GA 'run'. In order to ensure that the optimal solution was indeed identified, multiple runs for each scenario tested by the GA were carried out, so that the convergence of the optimal solutions could be tested. The values assigned to r_m and r_c in Table 3.3 were decided upon as a result of the use of standard values for basic GAs. The number of generations, runs and population size were derived as a result of tuning of the GA in order to ensure that an optimal solution could be reached using the minimal number of iterations.

Whilst EAs often prove significantly more efficient to run (in terms of the time take to complete a procedure) than brute-force algorithms, they are considerably more complex to set-up and often require fine tuning to ensure that they do in fact find the optimal, or 'fittest' solution within a given design space (Allmendinger 2012). For smaller design spaces, the increased effort associated with compiling an EA sometimes means that brute-force approaches can be more appropriate in order to generate rapid results. An EA was applied in the case study presented in Chapter 4 because the size of the design space meant that the computing time required to carry out a brute-force procedure proved infeasible.

Measuring the accuracy and reliability of the evolutionary algorithm

In order to ensure that the evolutionary algorithms used in this work did capture the optimal solutions in an accurate and reliable manner, measures of convergence were used during EA fine-tuning. Metrics such as the average fitness for each generation across all runs and the standard error associated with these values were measured. The convergence across all runs was also measured for each generation in order to ensure that the optimal solution could be found within an acceptable number of generations.

Finally, different scenarios evaluated by the EA were selected to be tested via brute-force analysis. This was done to ensure that the optimal solution identified by the EA could be reproduced via brute-force analysis; this would ensure its accuracy. Only selected scenarios were tested in this way, as running all scenarios tested by the EA using a brute-force search procedure would consume too much time for the purposes of this study.

In order to measure the savings in processing time that were achieved through the use of an EA, compared to brute-force procedures, a timer function was encoded into the algorithms used to run both the EA and brute-force analysis. This was used to extrapolate total savings in processing time across all the scenarios tested using the EA.

The results of the analysis of the accuracy and reliability of the EA are presented in Chapter 4, along with the results of the case study to which the EA was applied.

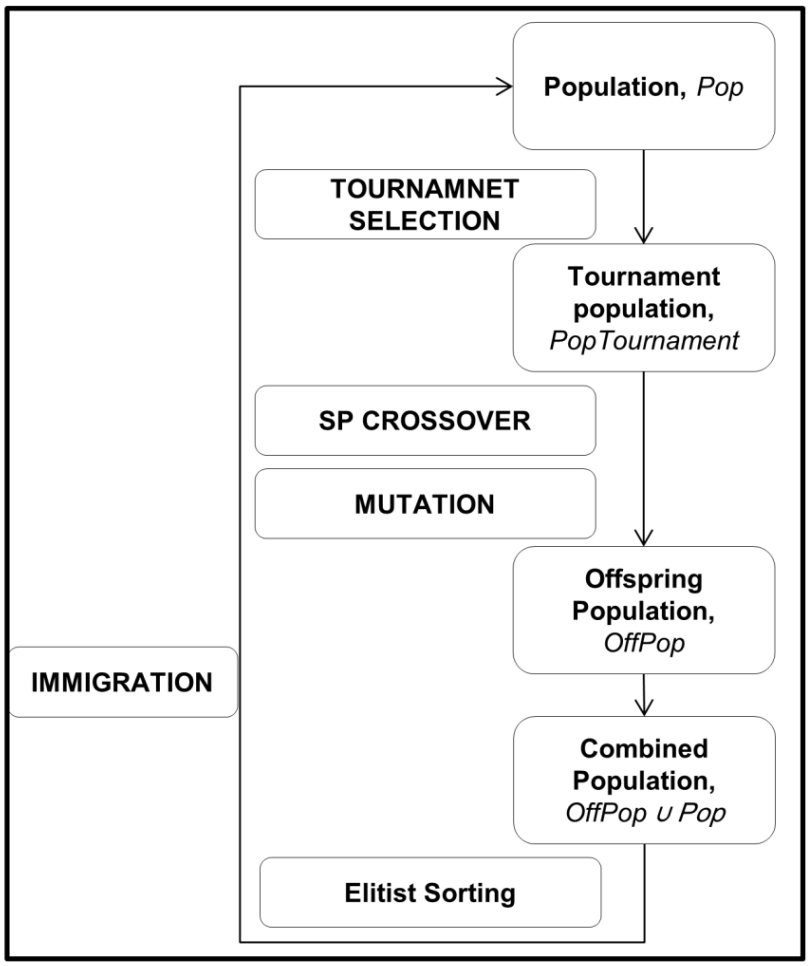

Figure 3.4 Visual representation of the path taken by the main loop EA procedure. *Pop* in each generation is subject to tournament selection to produce *PopTournament*, a parental population. *PopTournament* is subject to single-point crossover and mutation, which gives rise to *OffPop. OffPop* is then combined with *Pop* and elitist sorting is conducted in order to preserve the fittest solutions from each generation. Immigration allows new, randomly generated solutions to form part of *Pop* for the successive generation.

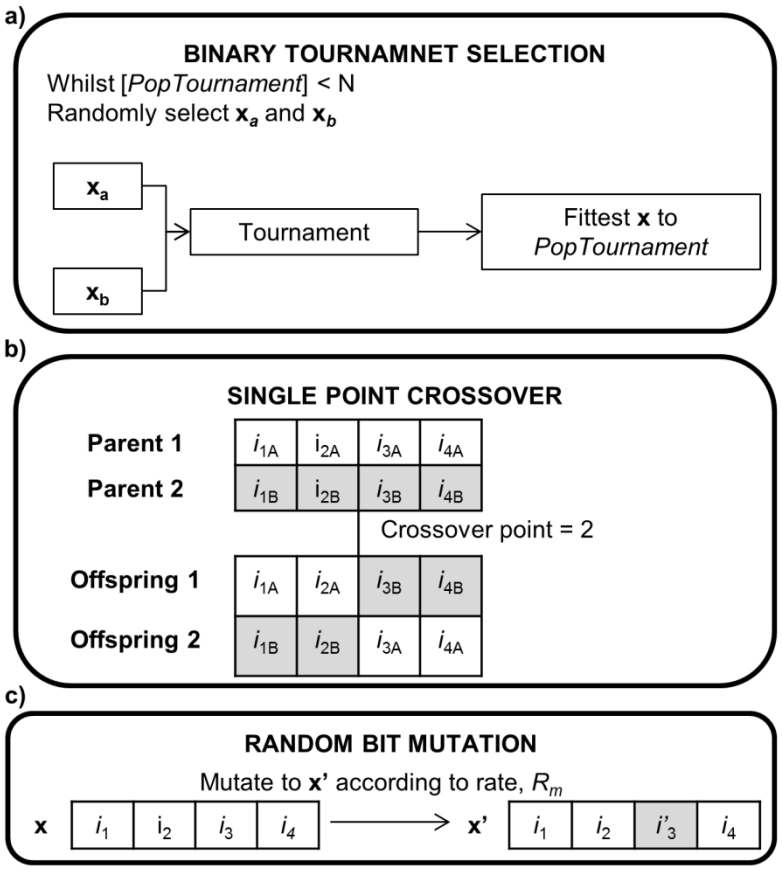

Figure 3.5 Visual representations of **a)** binary tournament selection, **b)** single point crossover and **c)** random bit mutation. In **a)** binary tournament selection, two solutions are selected randomly from *Pop* and the fittest of the two solutions is entered into the parental population, *PopTournament*. In **b)** single-point crossover, two hypothetical parent solutions are shown. A crossover point is assigned at random (e.g. 2 in this instance) and all genes beyond this point are swapped between the two parents to create two offspring solutions. Crossover occurs according to the probability r_c. In **c)** random bit mutation causes alleles associated with randomly selected genes in a chromosome to change value according to some probability, r_m.

Algorithm 3.1 The GA procedure and its interaction with the bioprocess economics model

Required: Objective function; *f*, population size; ψ, maximum number of generations; *G*, historical solutions; *H*, number of available technologies, *T*.

1: g= 0 (generation counter), *Pop* = Ø, *OffPop* = Ø, *PopTournament* = Ø

// initialise population:

2: **while** [*Pop*] < ψ **do**

3: Randomly generate **x** // ensure **x** satisfies sizing constraints

4: **x** = evaluate (**x**,*H*); *Pop* = *Pop* ∪ {**x**}

5: **end while**

6: g = g +1

//Main loop

While *g* <*G* **do**

7: *PopTournament* = Ø

OffPop = Ø

8: **repeat**

9: Choose two parent solutions $\mathbf{x_p}$ from *Pop* and select solution which best satisfies the objective function; *PopTournament* = *PopTournament* ∪ {$\mathbf{x_p}$}

10: **until** [*PopTournament*] **=** ψ

11: **repeat**

12: Generate two offspring $\mathbf{x}^{[1]}$ and $\mathbf{x}^{[2]}$ by selecting two parents from PopTournament, and then recombine and mutate the offspring with one another // ensure offspring satisfies Eq. X

13: evaluate($\mathbf{x}^{[1]}$, *H*); evaluate ($\mathbf{x}^{[2]}$,*H*); *OffPop* = *OffPop* ∪ {$\mathbf{x}^{[1]}$} ∪ {$\mathbf{x}^{[2]}$}

14: **until** [*OffPop*] **=** ψ

15: *Merge* = *Pop* ∪ *OffPop*; *Pop* = Ø

16: Applying elitist sorting to *Merge* according to f_1

17: Re-generate *Pop* by selecting the best 0.9*ψ solutions from *Merge*

18: **while** 0.9*ψ < [*Pop*] < ψ **do**

19: Randomly generate **x** // ensure **x** satisfies sizing constraints

end while

20: g = g+1

end while

//interface with BEM:

21: evaluate (**x**, *H*)

22: embed **x** into bioprocess shown in Fig.1

23: run BEM and check if **x** satisfies utilisation constraints

24: Compute f_1 for **x**

25: Update *H* by returning **x** and f_1

3.5.3 Constraint handling strategies

Virtually all bioprocesses are subject to constraints in one form or another. In order that the solutions to the bioprocess design evaluated by the bioprocess economics model be feasible, constraint handling strategies were built into the optimisation procedures described above. Two types of constraints were applied to bioprocess designs in this study; sizing (or sequential) constraints and utilisation constraints.

Sizing constraints refer to constraints placed on the size of a technology used for a unit operation, or set of unit operations. It was determined that for expansion unit operations that involve multiple stages (or passages), technologies in the process train must follow an ascending order in terms of their available growth area, or volume such that;

$$^{i=n+1}a_j \geq {}^{i=n}a_j \tag{3.34}$$

Utilisation constraints refer to constraints placed on the minimum, and or maximum feasible utilisation of the available capacity within a piece of equipment. Furthermore, many large-scale SUBs, particularly those used for microcarrier-based and suspension bioreactors have a minimum utilisation threshold, below which their use is deemed infeasible (Sartorius Stedim 2012; GE Healthcare [no date]). It was therefore necessary to apply a utilisation constraint on the use of a technology such that;

$$\omega_{j\,min} \leq \omega_j \leq \omega_{j\,max} \qquad 0 < \omega_j < 1 \tag{3.35}$$

Where $\omega_{j\,min}$ = maximum utilisation for a given technology, *j*

$\omega_{j\,max}$ = minimum utilisation for a given technology, *j*

When dealing with brute-force search algorithms, it is relatively easy to deal with constraints; any solution, **x**, which does not comply with the sizing constraints can be

skipped so that it is not even considered in the optimisation procedure. For the utilisation constraint, a penalty function was put in place such that any solution, **x**, which does not comply with the utilisation constraint above, then $f_1(\mathbf{x}) \rightarrow \infty$. This resulted in any solutions that did not comply with the above constraints being assigned a poor objective function value relative to others that were tested; this ensured that infeasible solutions were not put forward as the optimal process design when brute-force procedures were employed.

The GA procedure generated random solutions, all of which were required to form part of a population in order for the GA to progress. To ensure that the technologies selected for expansion followed the ascending order described in Eq 3.32, a sorting algorithm was used to arrange the random technologies selected for the expansion stages into ascending order of size (as determined by available growth area and/or volume for cells). This is a strategy known as forcing in common evolutionary computation parlance. Whilst it is useful as it eliminates the possibility of non-feasible solutions being evaluated, its drawbacks include the fact that it may destroy and rearrange a piece of solution that would have resulted in a high fitness value. This is likely to reduce the efficiency of the GA in terms of the computational effort required (Allmendinger 2012).

Similar to the strategy outlined above for brute-force procedures, utilisation constraints were handled using the penalty function described above. Penalty functions are of particular use when elitist sorting is applied within a GA, as is the case in this work, because they will be eliminated from the combined parent and offspring population within each generation owing to their poor fitness.

3.6 Dealing with Uncertainty

A deterministic bioprocess economics model, such as the one described in Sections 3.3 & 3.4 is capable of computing key output parameters (such as COG and product

throughput) for a given solution, **x**, to a bioprocess design problem. However, deterministic analysis alone cannot offer an evaluation of process robustness under manufacturing uncertainty. Process reproducibility and robustness are key considerations in cell therapy and stem cell bioprocess design (Veraitch et al. 2008; Placzek et al. 2009; Jenkins and Farid 2015). Furthermore, autologous bioprocess designs must take into consideration donor-to-donor variability and its effect on bioprocess performance. Stochastic modelling techniques provide a tool by which to quantify the robustness and reproducibility of bioprocess strategies by simulating real-life variation within key bioprocess performance parameters and measuring the effect on this of key output parameters.

A basic technique for dealing with uncertainty is the use of sensitivity analyses. Sensitivity analyses are used to evaluate the effect of ±% changes to uncertain inputs in a bioprocess design problem. Sensitivity analyses are a basic tool and were primarily used to identify key bioprocess economic drivers (namely those that resulted in the largest % change in COG when varied).

The Monte Carlo simulation method is a more complex stochastic modelling technique, which produces a range of possible outcomes for a bioprocess design problem, and allows conclusions about the likelihood these will occur to be drawn. Monte Carlo methods rely on repeated random sampling in order to simulate processes for which the value of key inputs is uncertain. The Monte Carlo method requires estimates of probability distributions for uncertain input parameters; these probability distributions are assigned to key process parameters. A sample outcome is randomly generated by assigning a value to each parameter tested in the simulation according to its specific probability distribution. This process is repeated a large number of times in order to generate frequency distributions of simulation outcomes. The output distributions of the Monte Carlo experiment can then be used to determine

the probabilistic properties associated with the key performance metrics of a bioprocess design or manufacturing strategy.

Monte Carlo analysis was used in order to imitate the randomness and uncertainty inherent in cell therapy and stem cell manufacturing processes. The impact of uncertainty in input parameters according to the choice of manufacturing strategy was evaluated using Monte Carlo analysis in order to help facilitate effective decision making in bioprocess design.

3.7 Multi-attribute decision making

3.7.1 Multi-attribute decision-making models

Previous sections have focused on selection, or identification of optimal bioprocess strategies from a large number of alternatives based on an objective function. Bioprocess design models, and business models in general often focus on improvements in process yields or a single financial measure, such as manufacturing COG or a project valuation metric (e.g. NPV) (Farid et al 2005; Simaria et al. 2014; Hassan et al. 2015; Hassan et al. 2016).

It is sometimes necessary to carry out a more holistic analysis of available methods, so as to arrive at a preferred bioprocess design having considered multiple attributes, not just economic metrics. One means of achieving this is via multi-attribute decision making (MADM). MADM analysis provides a mechanism for qualitative, as well as quantitative attributes of a solution to a bioprocess design problem to be evaluated. MADM requires that all attributes are considered across an equivalent measurement scale, this is usually done by converting all attributes to dimensionless units on a finite rating scale. This method therefore allows preference decisions to be made on the basis of multiple attributes for an array of different problem solutions (Yoon and Hwang 1995).

MADM analyses have previously been applied within various decision-support tools in the biopharmaceutical sector in order to evaluate bioprocess designs on the basis of operational, environmental, and economic attributes (Farid et al. 2005a; Pollock et al. 2013).

3.7.2 Additive weighting technique

In this work, a simple additive weighting technique was applied to a multi-attribute bioprocess design problem where economic and operational attributes were considered (Chapter 6). In this method an aggregate score, *W*, for each alternative, *j*, can be computed by multiplying the normalised rating for each attribute included in the analysis by the weight (representing the importance of each attribute) assigned to each attribute; these products are then summed over all the attributes (Yoon & Hwang 1995). This can be represented mathematically as;

$$W_j = \sum_{i}^{n} w_i r_{ij} \qquad (3.36)$$

Where w_i = The normalised weight assigned to attribute *i*

r_{ij} = The dimensionless rating of attribute *i* for alternative *j*

The additive weighting technique relies on assigning weightings to all attributes; these weightings are relative to the importance of each attribute within a given field. A greater weighting that an attribute is given, the more important it is. Weightings are normalised on a 0-1 scale in order to allow an aggregate score to be computed.

Prior to computation of the aggregate score using Eqn. 3.34, each alternative (*j*) had to be assigned a rating (*x*) for each attribute (*i*), which then had to be standardised. Economic attributes (e.g. manufacturing COG, FCI) were calculated using the bioprocess economics model described in Section 3.4. Operational attribute ratings,

and their relative importance, were collated from responses to a survey delivered to industry experts.

Different types of attributes were assigned ratings based on a number of different dimensions and measurement units. All attribute ratings were therefore standardised by converting them to a dimensionless, 0-100, scale. Standardisation was achieved by giving each attribute a rating that was a fraction of a feasible range of the best and worst attainable value for any given attribute. The dimensionless rating for each attribute, r_{ij}, was therefore calculated thus;

$$r_{ij} = \left| \frac{x_{ij} - x_{i\,worst}}{x_{i\,best} - x_{i\,worst}} \right| \tag{3.37}$$

where x_{ij} = rating value assigned to alternative *j* for attribute *i*

$x_{i\,best}$ = best attainable value for attribute *i*

$x_{i\,worst}$ = worst attainable value for attribute *i*

3.7.3 Weighted financial and operational scores

The relative importance of the total weighted economic and operational scores was captured using combination ratios, whose sum was equal to one. Overall aggregate scores for each alternative solution, W_j, were therefore calculated as follows:

$$W_{j\,overall} = \left(\frac{\sum_{i=1}^{n} r_{ij\,economic}}{n} * R_1 \right) + \left(\frac{\sum_{i=1}^{n} r_{ij\,operational}}{n} * R_2 \right) \tag{3.38}$$

where R_1 = economic combination ratio

R_2 = operational combination ratio

R_1+R_2 = 1

3.7.4 Stochastic additive weighting

Input variables in MADM analysis include weightings assigned to each attribute and the ratings assigned to each attribute for each process strategy tested using the analysis. In order to capture uncertainty that may be associated with these input variables, stochastic modelling (in the form of the Monte Carlo analysis described in Section 3.6) was applied to the MADM analysis. This allowed probability distributions for the final scores of each alternative to be generated. This allowed for more informed decision making, and the level of confidence associated with such a decision (Farid 2002).

3.8 Data Collection Methods

As highlighted in previous sections of this chapter, default input values are assigned to parameters within the models described. Default values have been derived from a thorough scoping analysis using sources such as historical literature data, vendor information, and personal correspondence with industry experts.

All input values were sanity checked during interviews and meetings with experts (T. Allsopp, J. Bilsland, P. Whiting, J. Kirby, Yajin Ni, M. Leonard, R. Fedechko, S. Ho; all of Pifzer, Cambridge, England or Pfizer, St. Louis, United States at the time of consultation). Further to this, industry experts were called upon to consult on assumptions made regarding the operation of the bioprocess facilities that have been evaluated in case studies presented in subsequent chapters.

Default input values defined within each case study were encoded such that automated alteration could be easily achieved. This was done in order to allow

stochastic modelling to be carried out without the need for manual intervention (aside from initialising the procedure). The fact that default values could easily be altered also made sense from a programming perspective; the model could be re-run easily in light of new information without the requirement for major adaptation of the tool.

Chapter 4 Patient-specific hiPSC bioprocessing for drug screening: bioprocess economics and optimisation

4.1 Introduction

In addition to the potential of hiPSCs to offer a raw material for the production of treatments for a variety of disorder with unmet clinical needs, they offer a near term application where drug discovery, phenotypic screen and safety testing programmes might be qualitatively improved (Rubin 2008; Mason and Dunnill 2009; Wu and Hochedlinger 2011; Robinton and Daley 2012) (See Chapter 1). Furthermore, hiPSC-derived somatic cells offer a humanised platform to current animal models, for pre-clinical efficacy and toxicity studies for the development of novel therapeutics (Ebert and Svendsen 2010). Current animal-based paradigms have proven to be of limited predictive value due to fundamental biochemical, physiological and genomic variations from humans (Pearson 2006; Kiskinis and Eggan 2010; Scott et al. 2013). hiPSC-derived cells also afford a predictive platform at the preclinical to clinical interface, pinpointing drug responders from non-responders and stratifying patients into treatment groups.

This case study investigates the production of patient-specific hiPS-cell lines, namely a cell line which is derived from a single patient in order to capture their individual genotype and phenotype. Manufacture of patient-specific cell lines requires scale-out of the process, whereby the manufacturing scale or lot size is kept constant and replicated for each cell line. In contrast, manufacture of non patient-specific cell lines can benefit from scale-up, whereby the manufacturing scale or lot size is increased when larger demands of a cell line are required (see Figure 4.1a). Non patient-specific cell lines are more likely to be used for purposes that are independent of the specific genotype or phenotype of a cell.

Automation systems designed to accommodate planar culture vessels, such as the CompacT SelecT (CTS) (Sartorius, Royston, UK), have the potential to reduce the labour requirements, potential points of contamination, and to improve the reliability associated with autologous hiPSC bioprocessing (Veraitch et al. 2008; Thomas et al. 2009; Hambor 2012) (see Chapter 2). Such systems could be implemented to help achieve large-scale manufacture of patient-specific stem cell products.

An integrated decisional tool that combines both bioprocess economic modelling and optimisation of the manufacture of patient-specific iPSC-derived neurons for use as a tool in the screening of NCEs is described. The bioprocess economics model and integrated brute-force search algorithm are designed to identify the process design that minimises the COG. The use of specified automation equipment such as the CTS for iPSC cell bioprocessing and its impact upon the overall COG is also evaluated as an alternative to existing, manual bioprocessing options (Figure 4.1b).

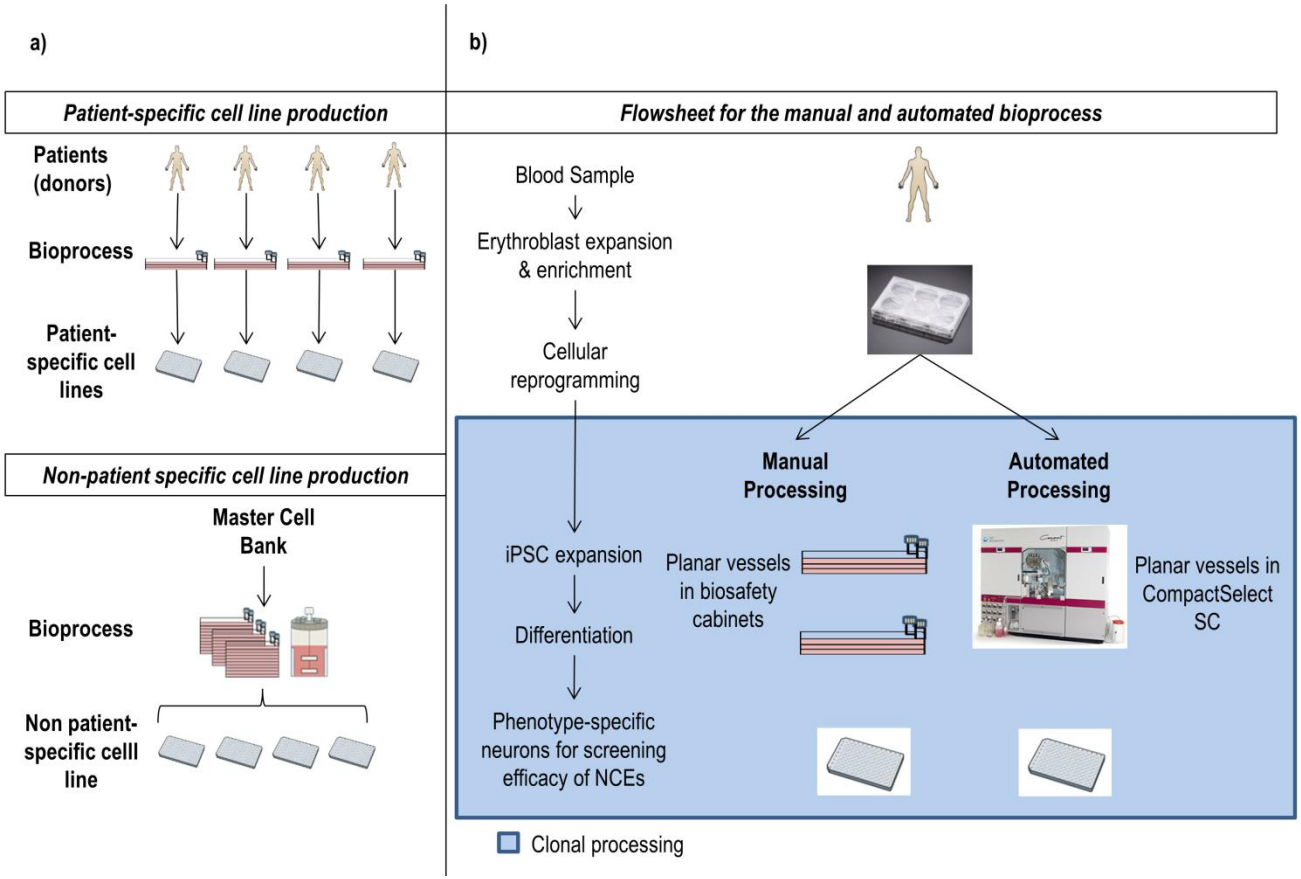

Figure 4.1 Process techniques for patient-specific and non-patient-specific cell lines. **a)** Outline of process techniques for patient-specific cell lines and non-specific cell lines. The bioprocess for a single patient-specific cell line is scaled-out to achieve a higher throughput. Non-specific bioprocesses are scaled-up to achieve a higher throughput. **b)** An overview of the bioprocess strategies considered within this case study. Clonal processing is employed following cellular reprogramming, therefore the technology used to process each donor sample remains constant until this point, regardless of the scale of the bioprocess.

4.2 Case study set-up

4.2.1 Tool Application

A representative case study was developed in partnership with Pfizer's Neuroscience and Pain Research Unit (Great Abington, Cambridge, UK) that focused on optimising the production of patient-specific iPSC-derived cells for drug screening. Specifically, it addressed the generation of iPSC-derived neurons to supply patient drug responder versus non-responder, "trial in a dish" screening platforms with which to augment clinical trials for NCEs. It is estimated that cell lines from 50 separate donors could be required to run such a screening programme. To investigate the effect of scale-out on the COG associated with the bioprocess, throughputs of 10, 50 & 100 cell lines per year were investigated by this study.

There are a variety of analytical methods by which to carry out drug screening. Currently, the resting or active status of the membrane potential in functional iPSC-derived neurons are analysed by patch-clamp analysis (PCA), a manual technique which requires a small sample population of iPSC-derived neurons (10^5). Whilst this is a data-rich analytical method, it samples only a small number of cells and is therefore a poor representation of whole cell populations (Yajuan et al. 2012). Powerful, automated analytical techniques such as high throughput screening (HTS) and plate-based pharmacological analysis (PBP) are also available methods by which to screen cells' reactions to NCEs. These techniques require larger sized cell populations (2×10^6 and 10^7 cell respectively), but offer high throughput analytical platforms. The level of scale-up required of the bioprocess required to manufacture each individual cell line is dependent on the analytical technique used for drug screening, along with characteristics of different analytical techniques (Figure 4.2).

Two different manufacturing strategies were considered during this case study; manual bioprocess techniques were evaluated alongside an automated iPSC

bioprocess, whereby iPSC expansion and differentiation were carried out using the CompacT SelecT SC (Sartorius, Royston, UK). A decisional tool was applied primarily in order to select the most cost-effective process design in both instances. In this case study a brute-force search algorithm was used to identify cost-effective bioprocess designs (see Chapter 3). This was linked to a bioprocess economics model (defined in Chapter 3), and a database housing relevant information on candidate technologies. Process reproducibility in stem cell bioprocessing is a significant challenge. As such, stochastic modelling was also employed in this case study to ascertain the robustness of both manufacturing strategies using the Monte Carlo simulation method (see Chapter 3 for methods).

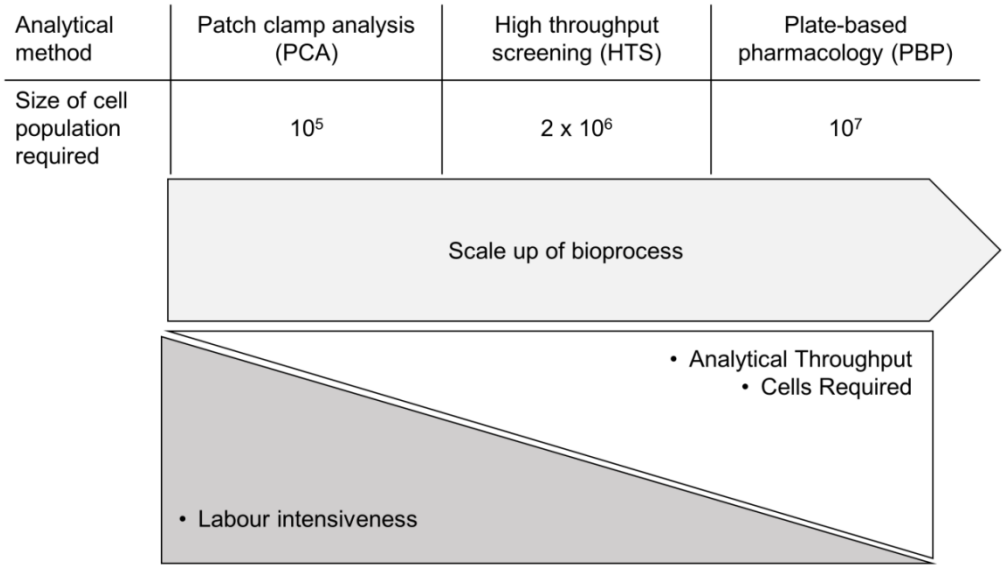

Figure 4.2 iPSC-derived neuron population sizes required to satisfy the demands of different analytical drug screening techniques. The required population size dictates the scale of the bioprocess required to produce cells for each analytical method. The lower panels illustrate graphically key characteristics of each analytical technique.

4.2.2 Process Overview

The process flowsheet used for the case study (Figure 4.1) employs processing of individual clones following the reprogramming stage; as such, the preliminary unit operations are of a constant scale regardless of the final number of iPSC-derived neurons produced from each cell line. Therefore, the main focus of this case study comprises the iPSC expansion and differentiation unit operations. Further details regarding the methods used and feeding regimes assumed for each unit operation can be found in (Table 4.1). Media changes are assumed to involve a full exchange of media within a process vessel.

The planar technologies considered within the case study included well plates (WP) as well as standard and compact multi-layer versions of T-flasks (T, cT, 3-F, 5-F) and stacked vessels (L, cL). Their key input parameters are stored within the tool's database (Table 4.2). This data was compiled using vendor websites and consultation with industry experts so as to properly capture the characteristics of each candidate technology. Key process and cost assumptions are summarised in Tables 4.3 & 4.4. These values have been compiled via a thorough review of available literature on planar bioprocessing of iPSCs and their derivatives. All assumptions listed in Tables 4.3 & 4.4 were then corroborated with industry experts to ensure they were representative. While sensible inputs and assumptions were sought, the primary aim of the paper was to demonstrate the application of the proposed methodology to provide visibility of the cost structure and the most significant process economics drivers for iPSC generation for drug screening applications. Hence, the actual inputs and answers should not be seen as definitive but an illustration of how to approach such an assessment. The risk of batch failure was also considered. The manual bioprocess strategy was assumed to exhibit a higher probability of batch failure (4%) compared to the automated strategy (2%) given the greater human intervention and degree of open processing in the manual strategy. Failure rates were assumed to capture the worst-case scenario, i.e. failure occurs during the final stages of

differentiation. Therefore, the direct costs of iPSC expansion and differentiation for additional donor samples required due to process failure were added to the final COG figure within the deterministic model to account for additional processing as a result of the batch failure rate. Only iPSC expansion and differentiation were assumed to be repeated following a failed lot because of the cell banking procedure in place.

Table 4.1 Methods and feeding regimes used within bioprocess unit operations in this case study

Unit Operation	Method	Feeding Regime
Erythroblast Expansion & Enrichment	Culture-based expansion and purification of erythroblasts	- Daily media replacement
Cellular Reprogramming	Sendai Virus transduction of Yamanaka factors	- Media replacement every two days during transduction - Daily media replacement during iPSC generation period
iPSC Expansion	Monolayer 10% of viable cells banked to safeguard against process failure during differentiation	- Daily media replacement
Differentiation	Monolayer, small molecule based	- Twice weekly media replacement

Table 4.2 Process technologies tested in this case study and their associated performance and cost parameters

Technology Type (i)	**Surface Area (cm^2/unit) (a_i)**	**Cost (£/unit) ($C_{con\ i}$)**	**Media Requirements (mL/unit) ($V_{req\ i}$)**	**Max units per Operator ($\omega_{op\ i}$)**	**Incubator Capacity (Double Stack) ($\delta_{inc\ i}$)**	**Requires BSC Cabinet (Y/N)**	**CompacT SelecT Capacity**
T-25	25	£1.54	7	4	100	Y	-
T-75	75	£2.21	18.75	4	100	Y	90
T-175	175	£4.95	50	4	100	Y	90
T-225	225	£5.27	56.25	4	100	Y	-
6-WP[a]	9.5	£2.10	2	24	600	Y	-
24-WP[a]	1.9	£2.66	0.5	48	2400	Y	-
L-2[b]	1272	£55.08	315	2	60	Y	-
L-5[b]	3180	£180.49	787.5	2	24	Y	-
cL-12[c]	6000	£287.69	1300	2	24	Y	-
3-F[d]	525	£10.20	150	-	-	N	90
5-F[e]	875	£17.00	250	-	-	N	90
cT[f]	1720	£63.58	500	-	-	N	90

[a]Well plate
[b]Multilayer planar vessels e.g. CellSTACK (Corning)
[c] Compact multilayer vessel e.g. 12-layer HYPERStack (Corning)
[d]3-layer T-flasks e.g. Triple Flask (Nunc) or Falcon Multi-Flask (Corning)
[e]5-layer T-flasks e.g. Falcon Multi-Flask (Corning)
[f] Compact multilayer flask e.g. 10-layer HYPERFlask (Corning)

Table 4.3 Assumed values for key process parameters

Unit Operation (*j*)	Seeding Density (cells/cm^2)	Harvest Density (cells/cm^2) ($d_{h,i}$)	Yield/Harvest Yield/ Efficiency (%)	Fold Expansion
Erythroblast Enrichment	$1.5 * 10^5$	$3.2 * 10^5$	25 (Yield)	N/A
Erythroblast Expansion	$1.5 * 10^5$	$3.2 * 10^5$	95 (Harvest Yield)	2
Reprogramming (Transduction)	$2.6 * 10^5$	$2.6 * 10^5$	95 (Harvest Yield)	N/A
Reprogramming (Generation)	10^4	10^4	0.5 (Efficiency)	N/A
iPSC Expansion	$4.2 * 10^4$	$3 * 10^5$	90 (per passage)	7
Differentiation	$3 * 10^5$	$3 * 10^5$	35 (Efficiency)	N/A

Table 4.4 Key process cost assumptions

Cost Parameter		**Value**[a]
Media		
	Differentiation Media	£0.55-£0.67/mL
	Expansion Medium	£0.43/mL
	Reprogramming Vector	£664/ donor
Labour		£60/hr
Fixed Equipment		
	Incubator (Large)	£11,890
	Incubator (Small)	£5,175
	CompacT SelecT	£550,000
	Biosafety Cabinet	£11,390
Depreciation Period		10 Years
Lang Factor (Manual Bioprocess Strategy)		23.7
Lang Factor (Automated Bioprocess Strategy)		16

[a]Price ranges are provided where more than one type of media is used within a unit operation

4.2.3 Specific methodologies applied to this case study

Labour Costs

In this case study, labour costs, c_{lab}, are calculated as a function of the time required to carry out tasks specific to each unit operation of the iPSC bioprocess (t_i). This is in contrast to methods detailed in Chapter 2 and applied in Chapters 4 & 5, where labour costs are considered a function of the number of operators to run a process. Labour has been calculated in the following manner in this case study because it was assumed that operators might have duties beyond this process. It is assumed that for each technology type an operator could handle a given number of units, ω_j, within this time period. Therefore:

$$c_{lab} = \left({}^{u_{ij}}/_{\omega_j}\right) * \ t * w \qquad (4.1)$$

where w represents the hourly cost of labour. Individual labour tasks and their durations can be found in Table 4.1.

Stochastic modelling input distributions

The probability distributions assigned to the values of process parameters are given in Table 4.2. For details on the stochastic modelling methodologies employed please refer to Chapter 3.

Table 4.5 Labour tasks associated with the bioprocess and their duration

Labour Task	**Time Required (h) (t_i)**
Media preparation	1
Cell harvest	0.75
Cell seeding	0.5
Media replacement	0.5
Viral transduction	1.5
CompacT SelecT setup	2
CompacT SelecT termination	2
Culture check (manual)	0.5
Culture check (automated)	0.25

Table 4.6 Probability distributions assigned to key bioprocess performance parameters in the stochastic Monte Carlo analysis of the manual and automated bioprocess strategies.

Parameter	**Probability Distribution Type**	**Manual Bioprocess Probability Distribution Profile (Min, Most Likely, Max)**	**Automated Bioprocess Probability Distribution Profile (Min, Most Likely, Max)**
iPSC Expansion Harvest Yield	Triangular	75%, 90%, 95%	85%, 90%, 95%
iPSC Expansion Harvest Density	Triangular	2.5×10^5, 3×10^5, 3.5×10^5	2.7×10^5, 3×10^5, 3.3×10^5
iPSC Expansion Fold	Triangular	6.3, 7, 7.7	6.6, 7, 7.4
Differentiation Efficiency	Triangular	20%, 35%, 45%	30%, 35%, 40%
Differentiation Harvest Yield	Triangular	80%, 90%, 95%	85%, 90%, 95%
Differentiation Seeding Density	Triangular	0.8×10^4, 1×10^5, 1.1×10^5	0.9×10^5, 1×10^5, $1{,}1 \times 10^5$

Note: 'Most likely' values in the distribution profiles are taken from the base case scenario from the deterministic bioprocess economics model

4.3 Results and Discussion

The decisional tool was used to assess the cost-effectiveness of alternative bioprocess designs across a range of different scales of production. A deterministic model was developed in order to carry out COG comparisons between different process designs and sensitivity analyses were used to further investigate economic drivers associated with the iPSC bioprocess. The tool was then adapted for stochastic modelling in order to evaluate the robustness under uncertainty of automated and manual bioprocessing strategies using the Monte Carlo simulation method.

4.3.1 Deterministic Cost Modelling

The optimal combination of process technologies for the final iPSC expansion stages and differentiation operation, for both the manual and automated bioprocess are depicted in Figure 4.3. The number of iPSC-derived neurons produced per cell line is representative of the size of cell populations needed to satisfy the demands of PCA, HTS and PBP analysis (moving vertically from the top to the bottom of the matrices). The cell population outputs per cell line required for each of these analytical methods are shown in Figure 4.2, and also in Figure 4.3. Annual throughputs of 10, 50 and 100 cell populations have been shown to depict the effects of scale-out on optimal bioprocess design. The bioprocess throughput, in terms of cell lines produced per year, increases horizontally from left to right across each matrix. The matrices show the optimal technology size and the number of units required (in square brackets) per cell line for each scale tested.

a)

		Cell lines produced per year	
Analytical Method [required output (iPSC-neurons/cell line)]	Unit Operation	50	100
Patch Clamp Analysis [10^5]	Expansion (final stage)	6-WP [4]	6-WP [4]
	Differentiation	T-25 [1]	T-25 [1]
High Throughput Screening [2 x 10^6]	Expansion (final stage)	T-75 [4]	T-75 [4]
	Differentiation	T-175 [1]	T-175 [1]
Plate-Based Pharmacological Assay [10^7]	Expansion (final stage)	L-2 [2]	L-2 [2]
	Differentiation	T-225 [4]	T-225 [4]

b)

		Cell lines produced per year	
Analytical Method [required output (iPSC-neurons/cell line)]	Unit Operation	50	100
Patch Clamp Analysis [10^5]	Expansion (final stage)	T-75 [4]	T-75 [4]
	Differentiation	T-75 [1]	T-75 [1]
High Throughput Screening [2 x 10^6]	Expansion (final stage)	T-75 [4]	T-75 [4]
	Differentiation	T-175 [1]	T-175 [1]
Plate-Based Pharmacological Assay [10^7]	Expansion (final stage)	T-175 [25]	3-F [11]
	Differentiation	5-F [1]	5-F [1]

Figure 4.3 Matrices which illustrate the optimal bioprocess configuration for the final stage of expansion and differentiation. Matrices show the most cost-effective technologies for **a)** Manual bioprocess strategies and **b)** Automated bioprocess strategies across the range of scale investigated in this study. Lighter shaded cells indicate cheaper COG per cell line relative to other bioprocess designs shown in the matrices, where the lightest shade indicates the cheapest COG per cell line output value.

Depicting optimal technology sizing for manual bioprocessing shows that as the size of cell populations produced increases, there is a trend towards technologies with a larger surface area (Figure 4.3a). Larger technologies, which require fewer vessels, are selected as the optimal bioprocess design. For example 2 x 2-layer CellSTACK vessels (L-2) are preferred for the final expansion stage when producing 10^7 cells per cell line (for PBP), as opposed to 4 x T-75 flasks if $2x10^6$ cells per cell line were to be produced (for HTS analysis). Larger vessels are preferred when larger cell populations are produced when a manual bioprocess strategy is employed as depicted by the direct cost breakdown for optimal technologies for the manual bioprocess at different production scales at a throughput of 50 donor samples per year for the final expansion stage and differentiation (Figure 4.4). The utilisation of available surface area in smaller technologies is higher, thus they make more efficient use of media. Material expenditures can be reduced if smaller cell populations are produced (such as those required for PCA and HTS analysis) if smaller technologies are used. This is exhibited by a 39% reduction in direct costs if T-75 flasks are used as opposed to L-2 vessels for the final iPSC expansion stage at the HTS scale (Figure 4.4a).

However, when satisfying the demands of PBP, the additional labour costs incurred by the use of large numbers of units of smaller vessels far outweigh the incremental reduction in material costs that such technologies offer within the manual bioprocess. The COG per cell line for the differentiation can be reduced by 76% if T-225 flasks are employed rather than T-25 flasks (Figure 4.4b). This is due to the reduction in the resultant labour costs associated with the use of T-225s. Darker shades within each area of the matrices (Figure 4.3) are illustrative of higher COG/cell line. Thus, the matrix also demonstrates the economies of scale that can be achieved when the number of cell lines produced per year increases. This is particularly true with regards to automated processing (Figure 4.3b), where a greater range in the COG between

different annual donor sample throughputs can be observed than for the manual bioprocessing strategy.

A COG breakdown for the different equipment sizing configurations available for use in the final stage of expansion and differentiation for the automated bioprocess strategy, whereby 10^7 iPSC-derived neurons are produced per cell line at a throughput of 50 cell lines per year is shown in Figure 4.5. The use of smaller vessels, such as T-75s, necessitates the use of multiple CTS machines due to the number of vessels required for such technologies, which corroborates results displayed in Figure 4.3b, in that larger technologies are preferred for this throughput in the optimal technology matrix. This is particularly true of vessels used during differentiation, a lengthy process that occupies equipment capacity for long periods of time.

The optimal process configuration, where the technologies selected were 11 x T-75 flasks for the final iPSC expansion stage and 1 x 5-F (5-layer T-flask) for differentiation, results in a maximum requirement of 1 CTS machine. However, were T-75s and T-175s to be used for the respective process steps above (as is optimal for producing cells for HTS analysis), then 4 CTS machines would be required to produce cell populations satisfying the demands of PBP analysis. The latter of these options results in only an incremental direct costs reduction (~1%), whereas the resultant indirect costs are 375% higher than the optimal process design. Larger technologies, which can house cell populations in a smaller number of vessels, are preferred as they do not have as significant an impact on automated processing equipment utilisation. Owing to the automated nature of this processing strategy, the use of multiple vessels does not impact significantly upon labour costs, unlike manual processing, where it is important to minimise the number of units required in order to drive down labour costs.

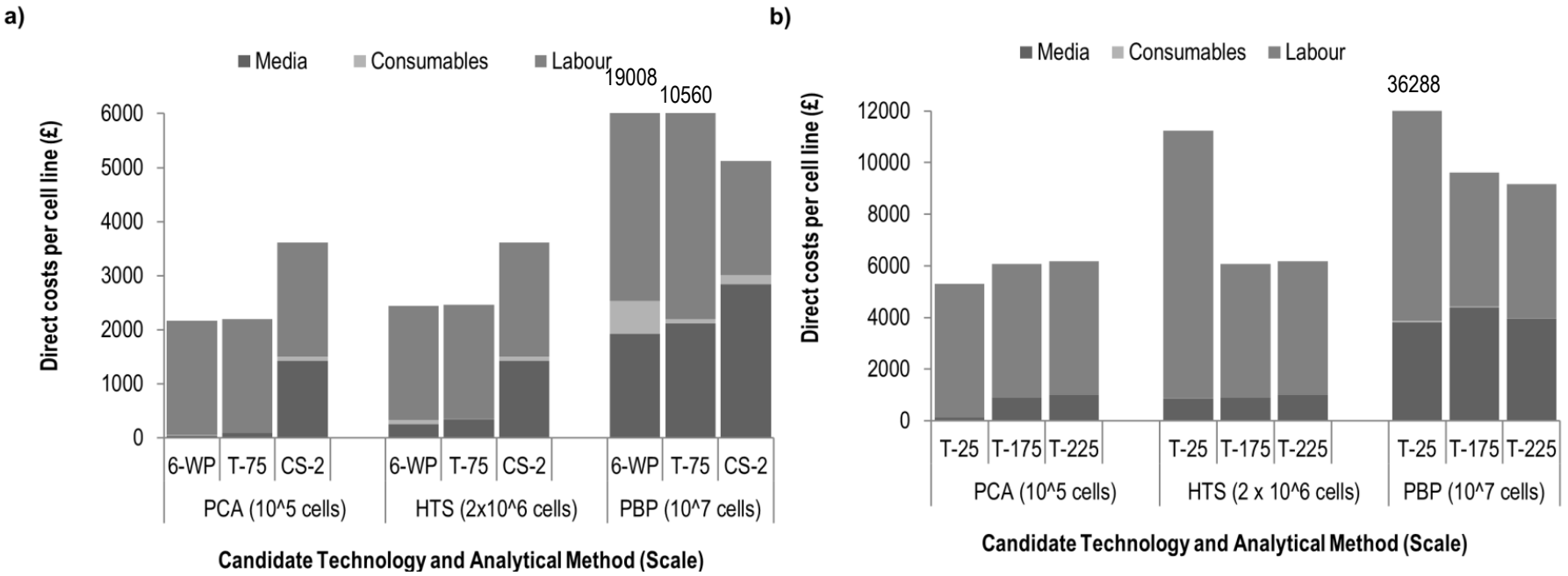

Figure 4.4 Direct cost breakdown for the optimal technologies at scales satisfying the demands of the three analytical drug screening techniques (PCA, HTS & PBP). Cost breakdowns are shown at a throughput of 50 cell lines/yr for **a)** the final stage of expansion and **b)** differentiation. Required iPSC-derived neuron outputs per donor are shown in brackets on the x-axis. Maximum values on the y-axis have been assigned to maintain scales whereby data can be clearly seen. Therefore for scales satisfying demands of PBP, direct costs beyond these values are labelled above the relevant column.

Analysis of COG breakdowns for manual and automated bioprocesses when the demands of HTS and PBP analysis at throughputs of 50 and 100 cell lines per year are satisfied shows that automated processing can significantly reduce labour costs associated with stem cell bioprocesses (Figure 4.6). This is particularly due to additional ancillary tasks associated with manual bioprocess strategies, such as media changes and cell seeding and harvesting. Material costs do not fluctuate greatly between manual and automated processing. However, savings on the cost of labour are outweighed by the additional indirect costs (a function of fixed capital investment required) for the automated bioprocess when 50 cell lines are produced. A 10% COG per cell line reduction is offered by manual processing when cells are produced for PBP analysis. At a throughput of 100 cell lines per year, the additional indirect costs associated with automated bioprocess strategies are spread across enough cell lines to provide significant COG reductions (19% at PBP scale) against the manual bioprocess - the cost of which is heavily weighted by labour costs. This is supported further by percentage COG breakdowns for the manual and automated bioprocesses when cell lines are produced to satisfy the demands of PBP analysis. At higher annual throughputs, direct costs make up a higher percentage of the COG breakdown. For the automated bioprocess, direct costs account for 41% of COG (70% for manual processing) when 50 cell lines are produced per year, compared to 58% (72% for manual processing) if 100 cell lines are produced annually. This analysis provides evidence that automation of patient-specific iPSC bioprocesses can provide significant COG reductions at scales sufficient to warrant the additional capital expenditure. Indirect costs dominate the COG breakdown for the automated bioprocess (Figure 4.5) hence minimisation of the number of pieces of automation equipment must be achieved in order to curtail COGs.

There is no significant reduction in either the labour costs or material costs for both the manual and the automated bioprocess at throughputs of 50 and 100 cell lines per

year (Figure 4.6). However, when the process is scaled out, smaller COG figures are realised as a result of reductions in the indirect costs per cell line. This suggests that economies of scale can only be achieved for patient-specific hiPSC bioprocesses requiring scale-out through shared use of fixed equipment. Bioprocess scheduling and equipment sizing in order to maximise use of fixed equipment and minimise the required size of cleanrooms must therefore be considered during process design in this area.

It can be concluded that a threshold throughput exists where automated bioprocesses offer a COG reduction compared to a manual bioprocesses. This is in accordance with previous studies in stem cell bioprocess design (Simaria et al. 2014). When assessing the COG per cell line for both the automated and manual bioprocess at throughputs ranging from 50 to 200 cell lines, the point at which the automated bioprocess becomes more cost-effective than the manual bioprocess is at a throughput of 65 cell lines (Figure 4.7). The spike on the line representing COG per cell line for automated bioprocesses also depicts the throughput at which it is necessary to purchase additional automated processing equipment (a throughput of 110 cell lines). The switchpoints identified between automated and manual processing are specific to the modelling assumptions made in this particular case study.

The assumed cost of automation equipment is based upon the current purchase cost for a functional CTS machine. At the time of writing, this was the only piece of automation equipment that could fully support this bioprocess. In the future, other pieces of equipment may become available and competition may drive down the cost of automation equipment. The effect of the price of automation equipment price on bioprocess COG can be seen in Figure 4.8.

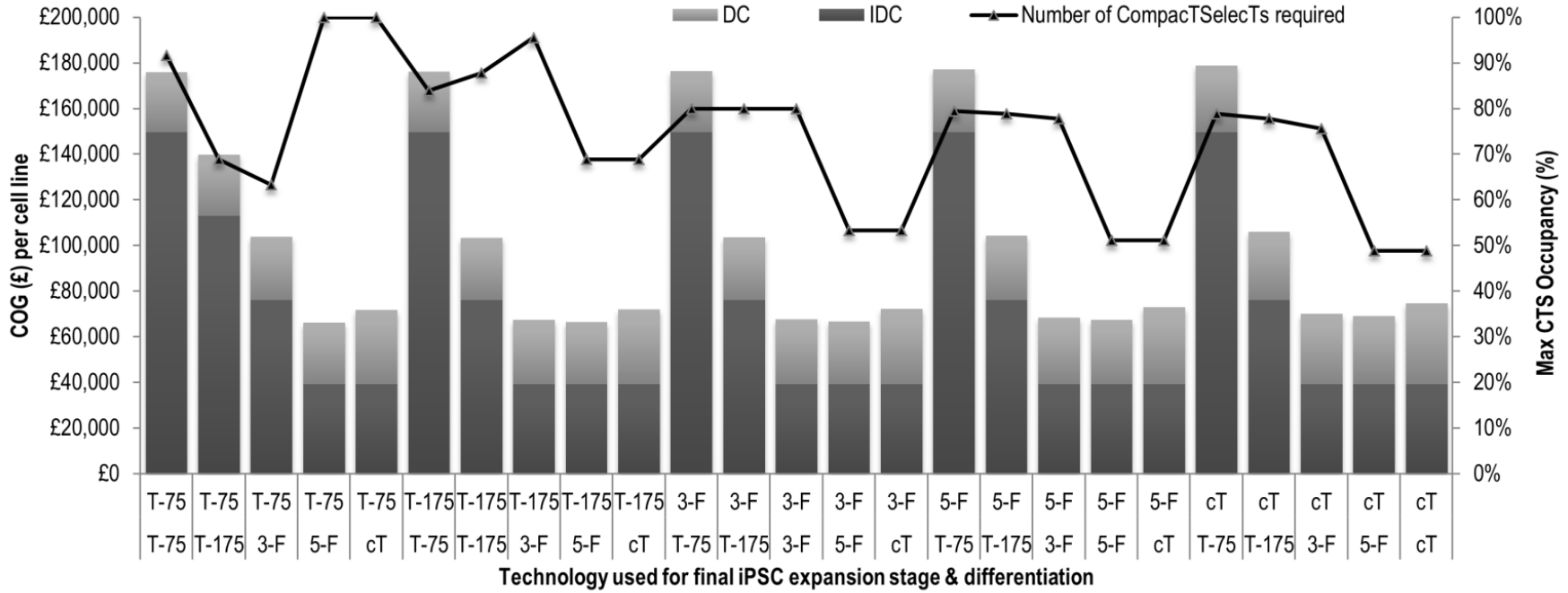

Figure 4.5 Brute-force algorithm outputs. COG breakdowns are shown for possible equipment sizing configurations for an automated process strategy. The x-axis displays different process platforms for the final expansion stage (top line) and differentiation (bottom line) at a throughput of 50 cell lines/yr, whereby populations of 10^7 cells are produced to satisfy the demands of PBP analysis. The scatter points on the chart show the number of Compact Select SC machines required for each process configuration.

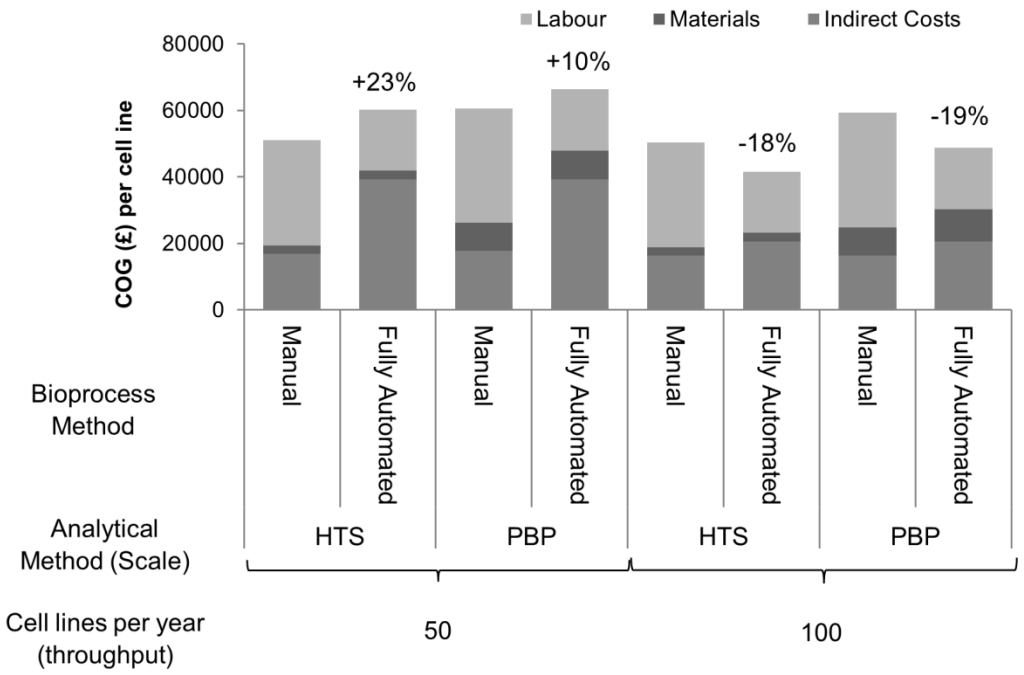

Figure 4.6 COG breakdowns for manual and automated bioprocess strategies at throughputs of 50 and 100 cell lines. COG breakdowns are shown for the production of populations of 10^7 iPSC-derived neurons in order to satisfy the demands of PBP. Percentage changes in COG/cell line caused by implementing an automated bioprocess strategy are shown above columns representing automated bioprocess COG breakdowns.

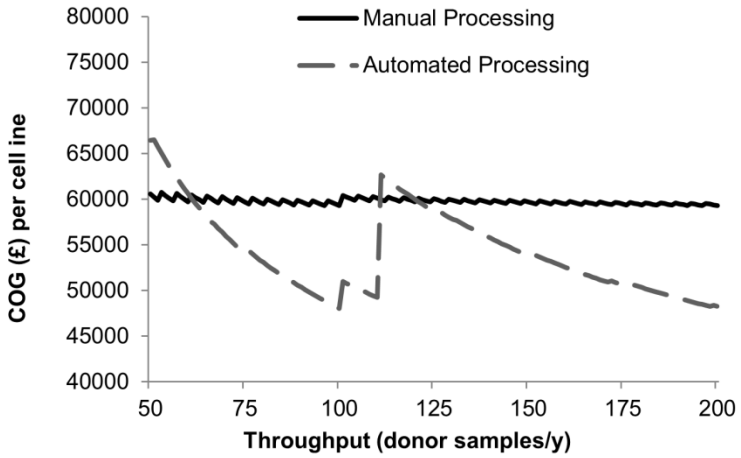

Figure 4.7 COG per cell line at annual throughputs ranging from 50 to 200 cell lines of 10^7 iPSC-derived neurons for manual and automated processing.

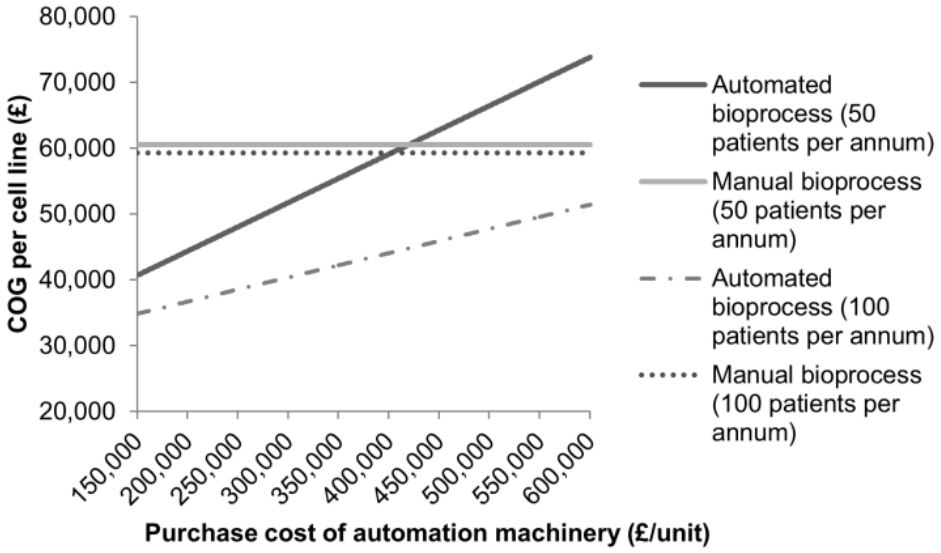

Figure 4.8 Line chart displaying COG per cell line when purchase cost of automation machinery is varied. This chart shows the cost of goods per cell line for the automated and manual bioprocesses at throughputs of 50 and 100 cell lines when the purchase cost of an automation unit is varied from £150,000 to £600,000 per unit (default setting is £550,000).

4.3.2 Sensitivity Analysis

In order to further identify key economic drivers associated with the iPSC-derived bioprocess, and to provide further understanding of where process development and optimisation resources might be best focused, a sensitivity analysis was carried out. Several process and cost parameters were varied to reflect their best and worst case values. The tool was used to test the resultant change upon the COG per cell line values that these variations. The Tornado charts (Figure 4.9) illustrate the effect on COG that variations in key parameters caused for a) the manual bioprocess and b) the automated bioprocess at a throughput of 50 cell lines per year (where cell populations that satisfy the demands of PBP are produced). The number of iPSC expansion stages required was the greatest economic driver for both the manual and automated bioprocess strategies (Figure 4.9). Variations in the number of iPSC expansion stages can occur due to fluctuations in key performance parameters. The impact of this parameter upon COG can be significant, as each additional iPSC expansion stage necessitates additional direct resources and fixed equipment capacity. Thus, a change in the number of iPSC expansion stages required within a bioprocess will significantly affect COG per cell line.

Labour costs are also a significant cost driver for the manual bioprocess, resulting in an 18% difference in COG between the best and worst case scenarios. The fact that labour costs have been identified as a key process economic driver is perhaps unsurprising; this parameter dominates the COG breakdown at high cell line throughputs (see Figure 4.6). Similarly, the secondary cost driver for the automated bioprocess is FCI costs, which are the largest contributor to the COG breakdown for this process strategy (Figure 4.6).

a)

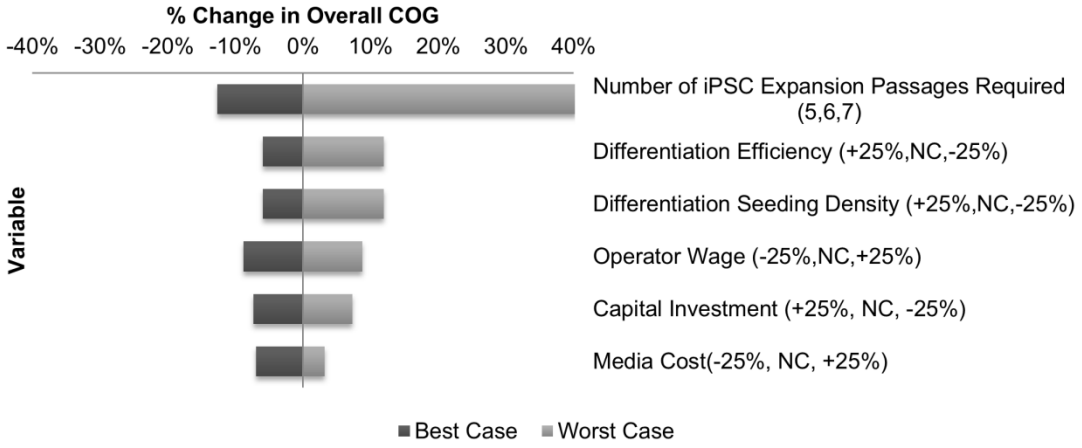

b)

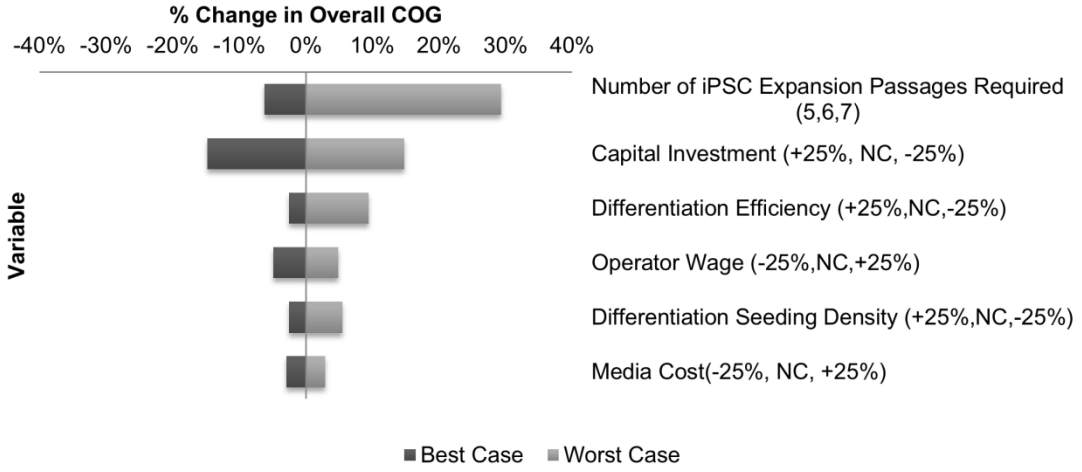

Figure 4.9 Tornado plots showing the effect of variations in key bioprocess parameters on COG for **a)** the manual bioprocess strategy and **b)** the automated bioprocess strategy at a throughput of 50 cell lines/ year. Best case, base case, and Worst case values are shown in brackets on the Y-axis labels. Percentage changes represent the percent change as proportion of the base case value (e.g. for differentiation efficiency base case = 30%, therefore worst case differentiation efficiency = 30%*75%, the worst case value is therefore a differentiation efficiency of 22.5%). NC = no change.

4.3.3 Stochastic Modelling

The mean COG/cell line value for the automated bioprocess is higher than that of the manual bioprocess when producing 50 cell lines per year, whereas at 100 cell lines per year, this value is higher for the manual bioprocess, as described by the stochastic analysis (Table 4.7). These figures are consistent with the deterministic model results, which also show the same trend (Figure 4.6).

The results of the Monte Carlo analysis (Table 4.7, Figures 4.10a & 4.10b) show that the standard deviation and range of COG values for the automated bioprocess strategy at throughputs of both 50 and 100 cell lines per year (£3,025 (GBP) and £3,221 respectively) are significantly lower than those of the manual bioprocess strategy (£8,481 and £9,493 at 50 and 100 cell lines per year, respectively). This suggests that the automated bioprocess is more robust from a bioprocess economics standpoint than the manual bioprocess. The frequency density curves and COG distributions (Figure 4.10a & 4.10b) follow a distinct pattern. They are bimodal with a positive skew and hence the majority of COG values are concentrated at the lower end of the distribution and are followed by a long tail with a smaller peak at the upper end of the distribution with higher COG values. This is particularly true of the frequency distribution curves of the manual bioprocess, where the peaks at the upper end of the distribution where high COG values occur are larger compared to those for the automated bioprocess. One explanation of the shape of the frequency distributions can be illustrated in Figure 4.10c, which shows the relative frequency at which the number of iPSC expansion passages required for the manual bioprocess (at a throughput of 50 cell lines per year) rises from six (as in the base case) to seven based on process variability modelled in Monte Carlo analysis. The frequency distribution of the COG per cell line for the manual bioprocess from Figure 4.10a is also displayed on Figure 4.10c. This shows that the minor peak with high COG values that appears in Figures 4.10a & 4.10b is due to the requirement of an additional stage

of iPSC expansion owing to process variations modelled during the Monte Carlo simulation. Figure 4.10c also emphasises the importance of minimising the number of iPSC expansion stages as a strategy for minimisation of COG.

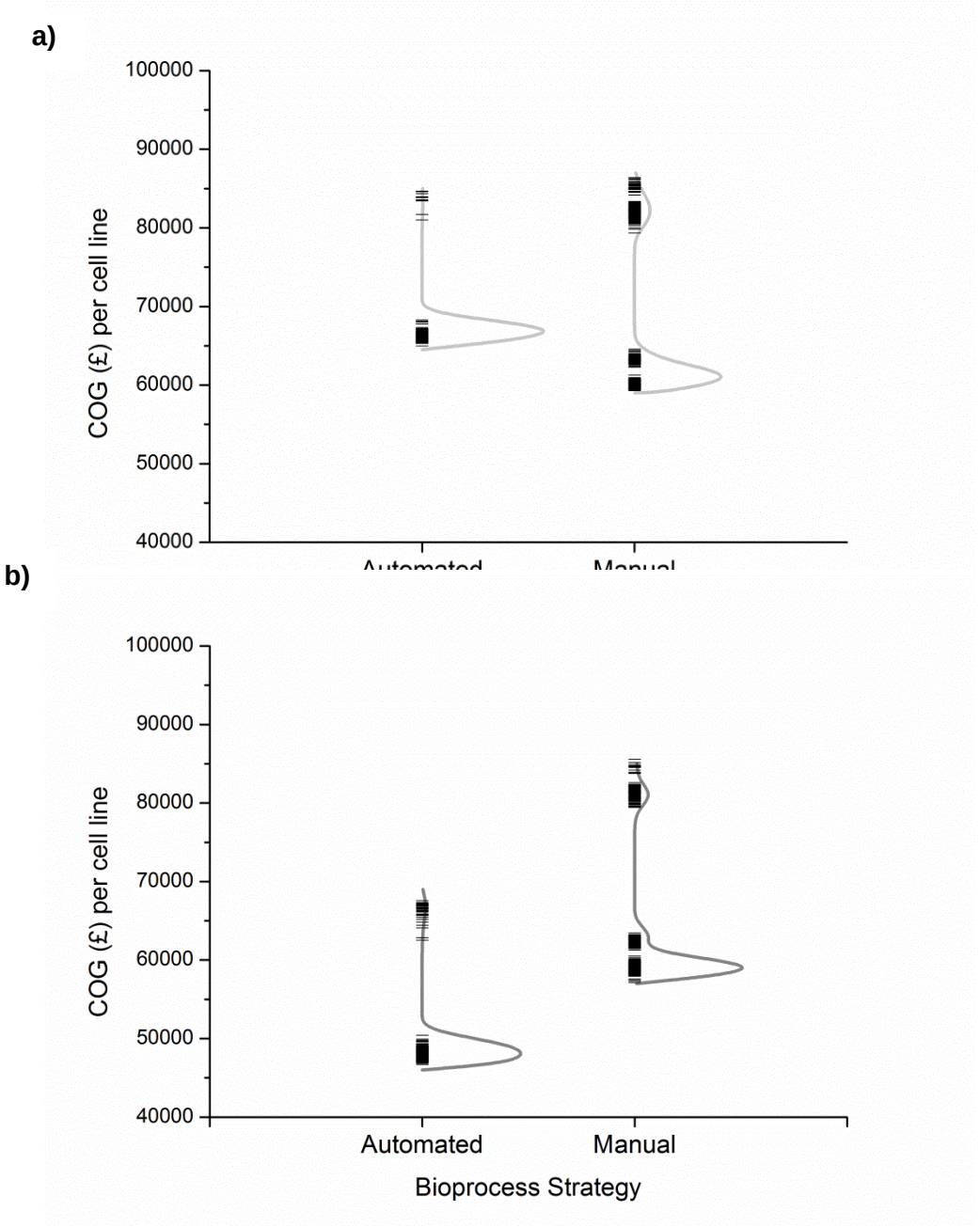

Figure 4.10 A & B Please see overleaf for full legend

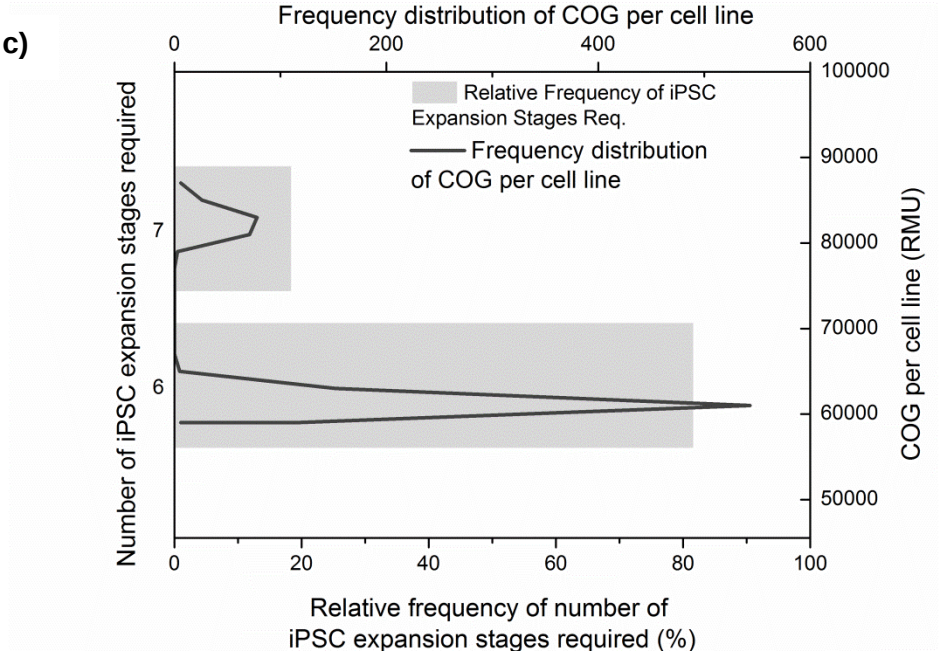

Figure 4.10 Frequency distributions for the COG per cell line outputs for the automated and manual bioprocess strategies under uncertainty. **a)** Bioprocess scale of 50 cell lines per year and **b)** Bioprocess scale of 100 cell lines per year. Dashed lines depict individual COG per cell line outputs and continuous curves represent the frequency distributions of the COG per cell line outputs. **c)** Relative frequency of the different number of iPSC expansion stages for the manual bioprocess strategy for 50 cell lines per year superimposed onto the COG per cell line frequency distribution. Bars represent the relative frequency of the number of iPSC expansion passages shown (bottom x-axis and left-hand y-axis) and lines represent the frequency distribution of COG per cell line (top x-axis & right-hand y-axis).

Table 4.7 Statistical parameters of the COG per cell line values for the manual and automated bioprocess strategies from the stochastic Monte Carlo analysis

	50 cell lines per year		**100 cell lines per year**	
	Manual bioprocess	Automated bioprocess	Manual bioprocess	Automated bioprocess
Mean (μ)	£64,841	£66,655	£65,405	£48,601
Standard deviation	£8,481	£3,025	£9,493	£3,221
P(COG < $\mu_{automated}$)	0.81	0.93	0	0.89

4.3.4 Can an acceptable COG for in-house manufacture of patient-specific hiPSC derived cell lines be achieved?

List prices from vendors for a vial containing 10^6 non patient-specific hPSC-derived cells currently lie in the region of US$1000-2000. This study shows that, unlike non patient-specific stem cell bioprocesses, where both direct and indirect cost savings can be achieved on a per million cells basis via appropriate scale-up strategies (Simaria et al. 2014), economies of scale can only be achieved in patient-specific cell lines through shared use of fixed equipment. Direct costs per cell line do not fluctuate significantly, regardless of throughput (Figure 4.6). The market price of patient-specific cell lines may therefore be assumed to be higher than their non-specific counterparts; not only because of the added expenditure as a result of scale-out processing, but also the added analytical value provided by such products in

responder vs non-responder studies and potential personalised medicine regimes (see Chapter 1). This is reflected in the fact that patient-specific hPSC-derived cell lines are marketed for ~US$50k (~£35k) for 10^7 cells, including the additional costs of iPSC derivation and genetic engineering.

This case study reflects an in-house hiPSC-derived cell line manufacturing regime. According to the stochastic modelling above, the minimum COG per cell line that can be achieved is ~£45,000. This is significantly higher than current market prices for such products. In order for in-house production of cell lines for drug screening to be worthwhile, an acceptable COG per cell line must be below current market prices. A scenario analysis was designed to identify the process improvements required to reduce COG per cell line to below £35,000. Within the scenario analysis, reductions in the indirect costs and media costs have been assumed. A one-off new-build facility has been assumed for this case study in order to capture the fixed equipment costs associated with manufacturing patient-specific cell lines. In reality, such an in-house facility would likely be used for multiple research activities. To reflect this, indirect costs of 60% and 75% of the base case value have been investigated in this analysis. Established Big Pharma companies might also make use of existing experience in pharmaceutical reagent manufacturing in order to produce media components and small molecules required for certain unit operations in-house. This would allow some media components to be produced at cost price, rather than purchasing them at vendor list prices (as assumed in base case results).

COG per cell line at both base case media costs and a 25% reduction in media costs have been modelled in this analysis. The process parameters varied in this analysis were the differentiation efficiency and iPSC expansion fold per stage. These parameters were chosen for two reasons; primarily they both impact upon the number of iPSC expansion stages required. This was identified as a key process economics driver in the sensitivity analysis (Figure 4.9). Secondly, advances in media

composition and morphogen delivery systems during iPSC expansion and differentiation are areas of concentrated research. Innovations in these areas have proven that improvements in these parameters are achievable on the base case values assumed in this case study(Chambers et al. 2009; Bardy et al. 2012; Chen and Thomson 2012; Surmacz et al. 2012; Ungrin et al. 2012; Lippmann et al. 2014).

The in-house scenario considered in this project was for a single drug screening project application and hence the indirect costs were only spread across this activity. In future it is possible to envisage several drug screening applications where the investment is offset across several projects similar to how a vendor may achieve economies of scale. Hence the impact of lowering the indirect costs was explored. If indirect costs are 60% of base case value, there is a large window of operation whereby a COG <=£35k per cell line, even when media costs remain at the base case value (Figure 4.11a). Indeed, if the achievable iPSC expansion fold can be increased from 7to 10, then it would be acceptable for differentiation efficiency to remain at 35%. If media costs could be reduced by 25%, then a differentiation efficiency of 50% (up from 35% in the base case scenario) would be required for COG<=£35k per cell line, even if the iPSC expansion fold could not be improved (Figure 4.11b). The windows of operation shrink significantly at both base case and reduced media cost values when indirect costs increase from 60% to 75% of the base case values (Figure 4.11c & 4.11d). In this instance, improvements in both differentiation efficiency and iPSC expansion to 76% and 11, respectively, would be required. Less dramatic improvements would be necessary if media costs could be reduced by 25%. In this scenario differentiation efficiencies as low as 52% and iPSC expansion folds of 10 could allow COG<=£35k per cell line to be achieved.

The maximum indirect cost (% base case) whilst media costs remain at base case value whereby a COG<=£35k per cell line is still feasible was found to be 77%. When media costs are 75% of the base case values, this value increases to 81%. Both of

these instances would require improvements to produce a 12-fold expansion during iPSC culture and a differentiation efficiency of 79%. Conversion of hiPSCs to neurons at efficiencies beyond 80% have been reported (Lippmann et al. 2014) as have iPSC expansion folds of up to 11.3 over 7 days in planar conditions, or up to 28 in bioreactor conditions (Bardy et al. 2012; Marinho et al. 2012) Therefore, realising the windows of operation discussed above is not infeasible. In the event that fixed capital investment (or indirect costs) can be reduced by 25% or more there are realistic scenarios whereby in-house manufacture of patient-specific, iPSC-derived cell lines could be worthwhile for companies wishing to carry out responder vs non-responder studies as part of drug development regimes. Lower indirect cost values could be achieved by either retrospective fitting of an existing research facility, or by diversifying the functionality of a new-build facility. The scenarios analysed above also illustrate how changes to the bioprocess in terms of the key process parameters might impact upon COG and shows how the findings of this study might be applied to bioprocesses other than the one that is the focus of this work.

The scenarios examined here determine an acceptable COG to be less than current market prices for patient-specific, hiPSC-derived cell lines. This is because this case study examines production of such cell lines for use in in-house studies. Were the cell lines discussed in this case study to be manufactured for sale, the acceptable COG figure would be far lower in order to take into account COG as a percentage of sales. Smith (2010) determines this value to be in the range of 40-60% for autologous products. It is possible to conclude that acceptable COG for patient-specific hiPSC-derived cell lines designed for sale is in the region of £14,000-£21,000 per cell line (whereby 10^7 cells are produced for each line). It is assumed that a process producing cell lines for commercial sale would be of a far greater scale than the bioprocess examined in this study (i.e. 100 cell lines per year). Identification of process improvements required to reduce the COG derived in this study to such values is

therefore beyond the scope of this paper. However, future work will focus upon large-scale bioprocess design strategies in order to maintain a supply chain of hPSC-derived cell lines to a number of clients.

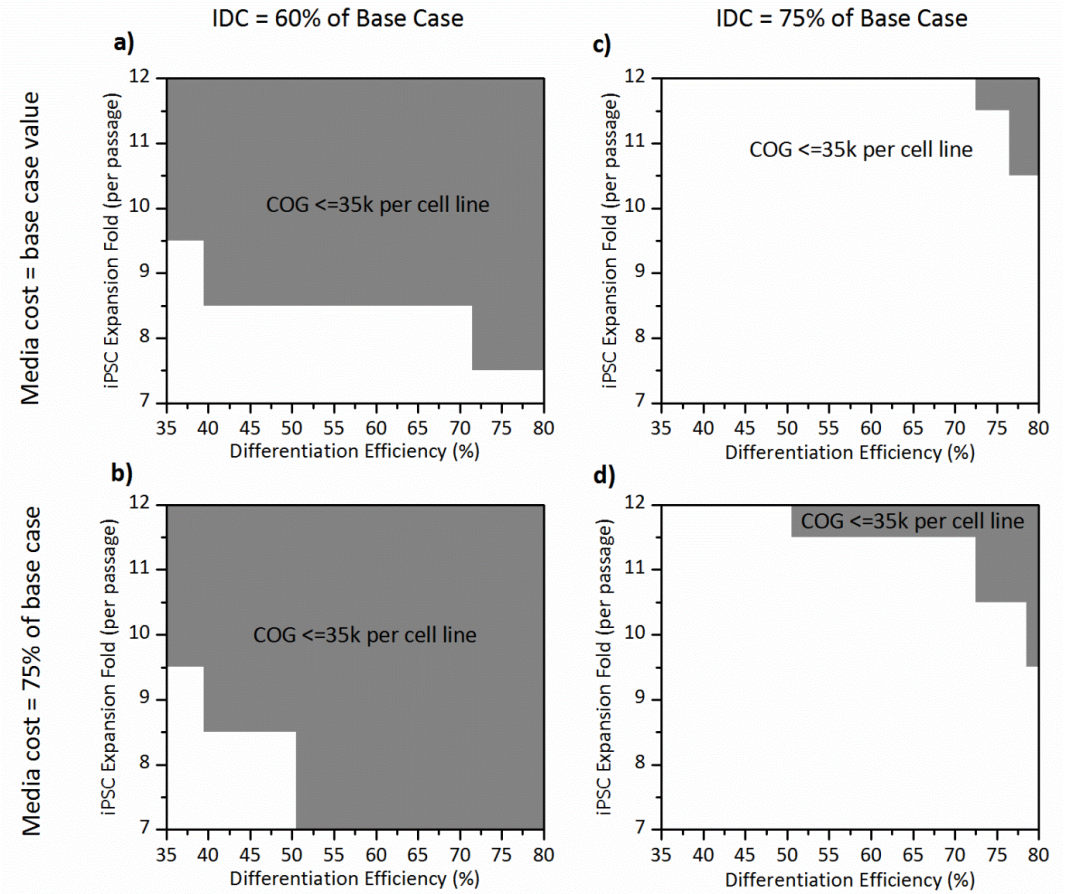

Figure 4.11 Scenario analysis to identify windows of operation where COG <=£35k/ cell line. Contour plots show the windows of operation where COG <=£35k/ cell line when **a)** media cost = base scenario and IDC = 60% of base case values **b)** media cost = 75% of the base scenario and IDC = 60% of base case values **c)** media costs = base case value and IDC = 75% of base case values **d)** media costs = 75% of base case value and IDC = 75% of base case. Shaded areas on the plots show windows of operation whereby COG<= £35,000/cell line, white areas of the plots represent windows of operation whereby COG>£35k/ cell line. IDC = indirect costs.

4.4 Conclusion

A decisional tool is presented that consists of a bioprocess economics model with an integrated brute-force search algorithm. The tool has been applied to an industrial case study, in which patient-specific iPSC-derived neurons are produced for use in responder vs. non-responder studies as part of the development of NCEs to be used in personalised medicine regimes. Via the use of this tool, optimal equipment sizing regimes were identified for both a manual and an automated hPSC bioprocess. Furthermore, it can be concluded that whilst the most cost-effective option of the two process strategies tested is dependent on the throughput of the process, the use of automation equipment was found to result in a more robust bioprocess in terms of COG values when tested under uncertainty. Indirect cost reductions are required in order to achieve acceptable manufacturing COG. This might be done by retrospectively fitting existing facilities, or diversifying functionality of a new-build facility in order to offset some of the required fixed capital investment to other projects. Were an existing full-scale process to be adapted from a manual to an automated bioprocess it would be wise to take into account the cost and time required to train staff to use automated equipment. Furthermore, the logistics and costs of updating facility infrastructure to cope with automated processing should be considered in the case of retro-fitting an existing facility. This work modelled a relatively small scale bioprocess in commercial terms. However, the outputs can be of use in aiding decision making early on in bioprocess design for patient-specific cell line production at a variety of scales.

Chapter 5: An evolutionary optimisation approach to identify the cost-effective bioprocess strategies for the manufacture of an allogeneic hESC-RPE therapy

5.1 Introduction

Globally, AMD is the leading cause of vision loss. Its onset is brought about by degeneration a layer of cells known as the retinal pigment epithelium (RPE). AMD is an ideal target for a hESC-derived cell therapy for several reasons. First of all, it is a condition which is currently devoid of a curative treatment; at best current treatments can halt the progress of wet-AMD and there is no available treatment for dry-AMD (Nazari et al. 2015). Furthermore, current stem cell technology allows the derivation of hESC-RPE cells in a potentially unlimited supply (Klimanskaya et al. 2004; Schwartz et al. 2012) for the production of cell-based curative treatments. Finally, and perhaps most significantly, several proof-of-concept studies where a certain amount of visual function was restored using hESC-RPEs in rat models have led to the launch of several clinical trials which have begun to demonstrate that these cells can be safely implanted into human patients (Lund et al. 2006; Lu et al. 2009; Schwartz et al. 2012; Ilic et al. 2015; Nazari et al. 2015). In the UK, the annual incidence of AMD is estimated to be greater than 70,000 cases per year (Owen et al. 2012). This represents a large target market for cell therapy manufacturers in this sector.

Allogeneic cell therapies are amenable to scale-up strategies, whereby larger lot sizes can be manufactured to realise the economies of scale that can be associated with commercial-scale manufacture of a product (Brandenberger et al. 2011). As discussed in Chapter 2, larger lot sizes may necessitate the need for larger, more scalable bioreactors and culture strategies including culture of cell on suspended microcarriers. This chapter therefore considers the use of both planar and

microcarrier-based cell culture strategies in order to evaluate potential inflection points where one culture platform may become more cost-effective than another.

This study describes the development and application of a decisional tool that is capable of determining the optimal process flowsheet for an allogeneic hESC-RPE cell therapy across a variety of lot sizes and annual demands. The tool was applied to an industrial case study examining the manufacture of a low dose, allogeneic hESC-RPE therapy, the target indication of which is age-related macular degeneration. Four different bioprocess strategies were considered: spontaneous differentiation supported by planar technologies; a spontaneous differentiation supported by microcarrier-based bioprocessing; directed differentiation supported by planar technologies, and finally directed differentiation supported by microcarrier-based bioprocessing. An evolutionary algorithm, introduced in Chapter 3, was used to determine the optimal process flowsheet across different manufacturing lot sizes and annual demands for each of these strategies.

5.2 Case Study Set-up

A case study was designed in order to examine four different bioprocess strategies by which to manufacture a hESC-derived RPE therapy that is to be delivered as a fresh patch of cells. The final product is delivered as a 6mm x 3mm patch of hESC-RPE cells, implanted surgically onto the patient's retina.

5.2.1 Process overview

Figure 5.1 outlines the stages of the manufacturing process for the product considered within this case study. The final product has a validated life-span of 8 hours once the patch is cut. For this reason, it was decided that patch formation (whereby hESC-RPEs are plated on a permeable membrane and cultured in order for cell-cell junctions crucial to efficacy to form), should take place at secondary facilities close to point-of-care centres (Figure 5.1). Manufacturing must usually be

decentralised in some manner for fresh cell-based therapies due to time constraints on the shipment of such products (Medcalf, 2016).

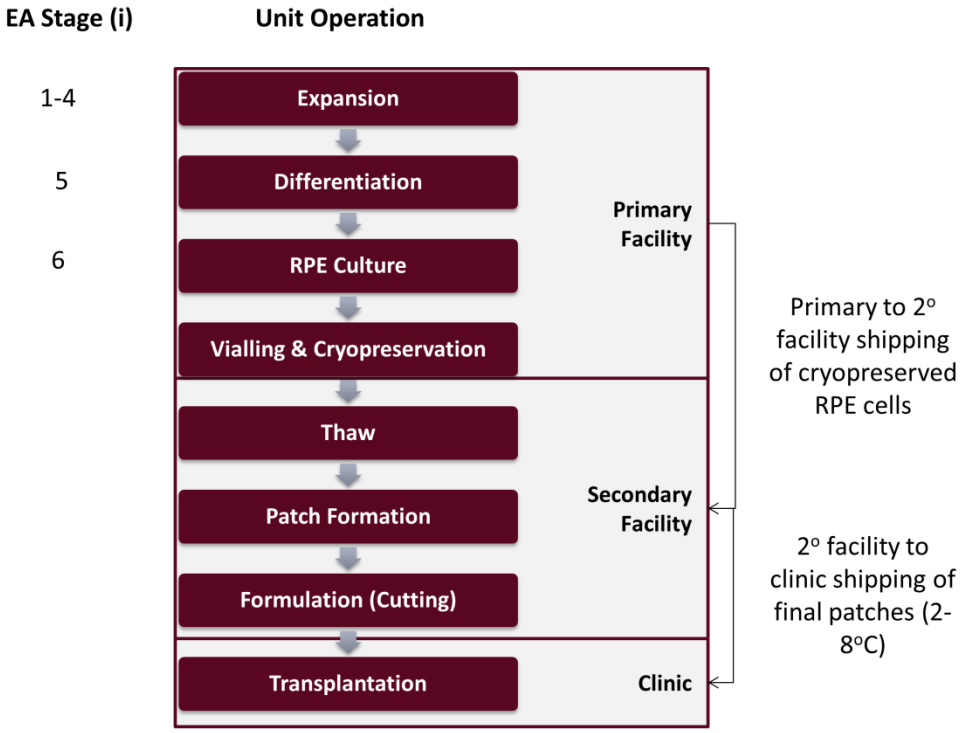

Figure 5.1 Process flowsheet considered in the RPE case study, including unit operations to be carried out at the primary manufacturing facility and secondary manufacturing facility. The left hand column refers to the stages of the unit operation (i=1,…,k) that were assigned as part of the evolutionary algorithm.

5.2.2 Spontaneous vs. directed differentiation

Two differentiation protocols were considered within the case study; an incumbent spontaneous differentiation (SD) process and a novel, directed differentiation process. The directed differentiation (DD) is characterised by an improvement in the efficiency (% target cells out/ % target cells in) of the differentiation process as compared to the spontaneous differentiation process. The DD protocol also results in an expedited process, reducing the total differentiation time to 19 days compared to 12 weeks (84 days) for the SD process. However, the DD protocol involves the use

of a more costly media and this case study aimed to examine what trade-offs, if any, there were between the two protocols. Table 5.1 summarises the key process parameters assumed for all bioprocess strategies, all values have been corroborated with industry experts.

Table 5.1 Key bioprocess parameters associated with different manufacturing strategies tested in this chapter

Unit Operation	Harvest density (cells per cm^2)	Yield/Harvest yield/ efficiency (%)				Fold expansion	Time (days)			
		SD-PL	SD-MC	DD-PL	DD-MC		SD-PL	SD-MC	DD-PL	DD-MC
hESC expansion (per passage)	$3x10^5$	93	93	93	93	7	7	7	7	7
Differentiation	$3x10^5$	0.75	0.75	90	90	N/A	84	84	19	19
RPE Culture	$5.5x10^5$	93	90	93	90	6.18	42	42	42	42
Vialling & Cryopreservation	N/A	70	70	70	70	N/A	<1	<1	<1	<1
Product Formation	$5.5x10^5$	99	99	99	99	N/A	42 -140	42 -140	42 - 140	42 - 140

5.2.3 Comparison of different bioprocess strategies for manufacturing at primary facilities

Two different cell culture techniques were considered for the differentiation and RPE culture unit operations within the bioprocess. The use of 2-D processing in planar vessels (PL) throughout the bioprocess was considered against the use of microcarrier-based (MC) differentiation and RPE culture in single-use bioreactors (SUBs); here it was assumed hESC expansion would still be carried out in planar vessels. Microcarrier-based culture allows a higher surface area to media volume ratio to be achieved for cell seeding (Jenkins & Farid 2015). Previous COG analyses have shown MC-based culture to be a more cost-effective process strategy than planar culture for stem-cell product manufacturing (Simaria et al. 2014; Hassan et al. 2015). This case-study examined whether MC-based culture proves more cost-effective than planar culture for small dose, allogeneic cell therapies. The cell culture platforms tested for hESC expansion, differentiation to RPEs, and hESC RPE culture are shown in Table 5.2. Additionally, cost parameters for reagents used within the bioprocess and unit prices of fixed equipment required to support the cell culture systems summarised in Table 5.2, can be found in Table 5.3

Planar and MC-based differentiation and RPE culture were considered for the use of both the spontaneous and directed differentiation protocols described above. Thus, four bioprocess strategies were considered for the manufacture of the hESC-RPE cell therapy, these are shown in Table 5.4.

Table 5.2 Bioprocess technologies tested within this case study and their associated input parameters

Technology Type	Abbreviated name	Surface area (cm^2/unit) (*a*)	Cost (US$/unit)	Media requirements (mL/unit)	Technology number (*t*)
T-25	T-25	25	$2	7	1
T-75	T-75	75	$2	18.75	2
T-175	T-175	175	$9	50	3
T-225	T-225	225	$10	56.25	4
Triple Flask	TrF	500	$14	150	5
CellSTACK	L-1	636	$59	787.5	6
2-layer CellSTACK	L-2	1,272	$74	315	7
HYPERflask	cT	1,720	$19	560	8
5-layer CellSTACK	L-5	3,180	$241	787.5	9
12-layer HYPERStack	cL-12	6,000	$575	1320	10
Xpansion bioreactor (10-layer)	XP-10	6,360	$2,506	1399.2	11
40-layer CellSTACK with automated cell factory manipulator	L-40	25,440	$1,265	6360	12
Xpansion bioreactor (50-layer)	XP-50	31,800	$5,586	6996	13
120-layer CellSTACK with automated cell factory manipulator	L-120	60,000	$3,000	13200	14
Xpansion bioreactor (200-layer)	XP-200	122,400	$13,980	139920	15
1L single-use bioreactor with microcarriers	MC-1L	13,844	$250	750	16
5L single-use bioreactor with microcarriers	MC-5L	69,221	$700	3750	17
20L single-use bioreactor with microcarriers	MC-20L	276,885	$2,000	16000	18
50L single-use bioreactor with microcarriers	MC-50L	692,212	$2,000	37,500	19

Table 5.3 Key cost parameters for the bioprocess including media and reagent costs, unit prices of fixed equipment used within the bioprocess, and assumptions regarding shipping costs associated with the bioprocess

Cost parameter		**Value**
Media		
	Expansion medium	US$690/L
	Spontaneous differentiation medium	US$355/L
	Directed differentiation medium	US$1280/L
	RPE Culture and Formulation medium	US$645/L
	CellStart coating (RPE Culture)	US$1535/L
Labour		US$120/hr
Fixed Equipment		
	Standard incubator	US$17,850
	CF40 incubator	US$30,000
	Biosafety cabinet	US$17,100
	ACFM	US$425,000
	Xpansion series controller	US$56,000
	SUB rig	US$45,000-US$105,000
	Aseptic vialling machine	US$340,000 – US$1.48m
	Controlled rate freezer	US$136,500
Depreciation period		5 years
Shipping Costs		
	Air transport (A_w)	US$60 per dose
	Road transport from 1^o to 2^o facility (R_{pf})	US$725 per shipment
	Road transport from 2^o facility to hospital (R_{sf})	US$50 – US$430 per shipment
	Road trasnsport from 1^o facility to an airport (R_{pa})	US$600 per shipment
	Road transport from airport to 2^o facility (R_w)	US$600 per shipment

Table 5.4 Description of the four bioprocess strategies that were tested using the EA in this case study

SD-PL (existing process): Spontaneous differentiation with planar vessels used throughout.	**SD-MC:** Spontaneous differentiation with microcarrier-based differentiation and RPE culture in 3-D SUBs (planar vessels used for all other unit operation).
DD-PL: Directed differentiation with differentiation with planar vessels used throughout.	**DD-MC:** Directed differentiation with microcarrier-based differentiation and RPE culture in 3-D SUBs (planar vessels used for all other unit operations).

The different bioprocess strategies were tested at a variety of annual demands and manufacturing lot sizes, outlined in Table 5.5. There are estimated be over 70,000 new cases of AMD in the UK annually (Owen et al. 2012). It is not unusual for first-to-market therapies to achieve a 40% market share, particularly in a specialised sector; however this market capture might not be as significant when lead times are short (Mckinsey & Company 2014). This is likely to be the case because there is concentrated product development activity related to hESC-RPEs for AMD treatment. Therefore, a modest estimate of market capture for a new product such as this would be 8%-15% of the market. The scales tested were therefore representative of the different phases of product development and different commercial scales, depending on the product's share of the market. Early and late-phase clinical trial manufacture (10-100 doses per annum) is captured, through to commercial scale manufacturing to satisfying the UK market (1,000 – 10,000 doses per annum). Annual demands of up to 50,000 doses were tested in order to capture the optimal bioprocess design that could be used to satisfy a large percentage of the UK market, and also sections of the European market.

The optimal bioprocess design for each strategy (at each production scale) tested in this study from a COG perspective was identified using the decisional tool described in Section 2. Annual demands ranging from the clinical scale to commercial manufacturing scales were tested in order to evaluate which bioprocess strategy was most appropriate from a COG perspective for different scenarios.

Table 5.5 Matrix illustrating the number of manufacturing lots required per annum for the annual demands and lot sizes tested in this chapter, red boxes indicate infeasible scales of production where the number of lots/year exceeds 50

	Doses /lot								
Doses /yr	1	10	50	100	500	1,000	5,000	10,000	50,000
1	1								
10	10	1							
100	100	10	2	1					
1000	1,000	100	20	10	2	1			
5,000	5,000	500	100	50	10	5	1		
10,000	10,000	1,000	200	100	20	10	2	1	
50,000	50,000	5,000	1,000	500	100	50	10	5	1

5.2.4 Comparison of different manufacturing schedules at secondary facilities

Patch formation necessitates the use of small-scale, planar vessels in order to support culture of differentiated hESC-RPEs on specially adapted polyester membranes in order to allow the formation of cell-cell junctions and adhesions; this provides functionality and viability to the final product following transplantation to the patient. Due to the fact that only small-scale well-plates are suitable for this operation, a rigorous analysis of different technologies was not performed for manufacturing at the secondary facility. Rather, different process schedules were evaluated.

Three different process schedules have been evaluated using a bioprocess economics model, which calculates COG associated with patch formation and harvesting in the manner described for the BEM described in 2.3. The Gantt charts in

Figure 5.2 illustrate each of the proposed process schedules which are summarised in Table 5.6.

Table 5.6 Description of the three proposed process schedules for operations at the secondary production facility

Process Schedule	Description
Schedule A (Figure 5.2a)	Enough patches to satisfy a single day's demand undergo formation for the minimum validated period of 6 weeks (Table 3). A complete lot of patches are cut and harvested for delivery to the clinic on a daily basis.
Schedule B (Figure 5.2b)	Schedule B: Enough patches to satisfy weekly demands undergo formation for between the minimum validated formation period of 6 weeks and 7 weeks. Patches are cut and harvested on a daily basis from the end of week 6 to the end of week 7 within a single lot schedule.
Schedule C (Figure 5.2c)	Schedule C: Enough patches to satisfy the demands of 14 weeks of doses undergo formation for between the minimum validated period of 6 weeks and the maximum validated period of 20 weeks (Table 3). Patches are cut and harvested on a daily basis from the end of week 6 to the end of week 20 with a single lot schedule.

Different process schedules have been evaluated in order to test their effect on manufacturing COG they were also analysed to test their ability to de-bottleneck manufacturing at secondary facilities.

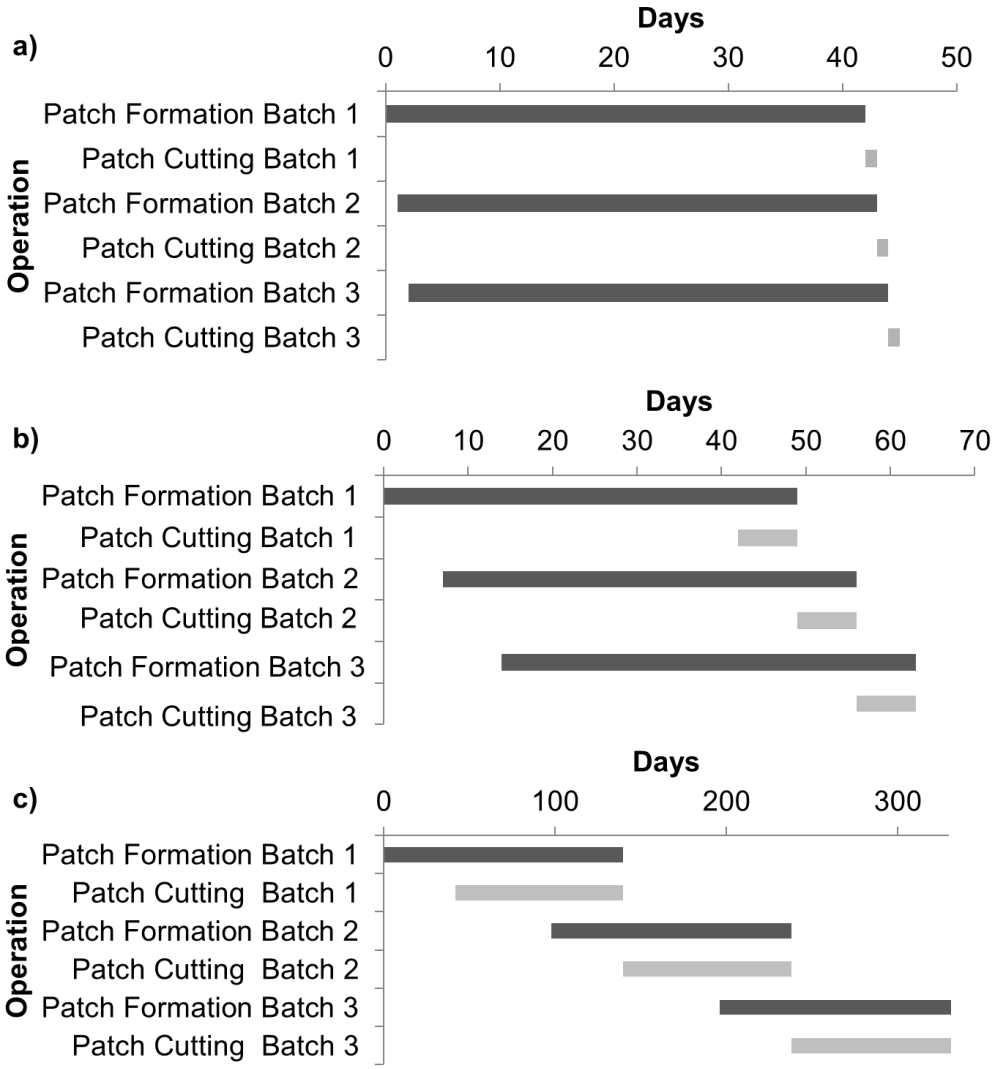

Figure 5.2 Gant charts representing patch formation and patch cutting for **a)** Schedule A, **b)** Schedule B, **c)** Schedule C. Details of each schedule can be found in Table 5.6. Patch cutting and harvest periods are illustrated by lighter shaded bars in the Gantt charts.

5.2.5 Comparison of different distribution strategies

The bioprocess and intended manufacturing strategy outlined in Figure 5.1 resulted in a variety of different distribution strategies. Two variables were considered to assess the impact of distribution on the COG associated with the manufacture of the cell therapy: the number of hospitals served by each secondary facility and the number of secondary facilities whereby patch formation is to occur.

In order to capture the time constraints associated with transfer of the final product in the form of a patch of hESC-RPE cells from the secondary facility to the clinic, a series of assumptions were made regarding the number of patients that could be treated by a single surgery team depending on the number of hospitals served by a secondary facility. These are shown in Table 5.7. If the number of clinics served by a secondary facility is larger, it was assumed that fewer patients could be treated in a single day. This is because it was assumed that the product would have to travel a greater distance to the clinic from the secondary manufacturing facility in these conditions. Therefore less time is available to perform the implantation surgery within the viable lifespan of the product once it arrives at the clinic.

Table 5.7 Number of patients that can be treated in a single day depending on number of clinics served by a single 2^0 facility

Parameter	Conditions	Value
Number of clinics per 2^o facility	N/A	1 to 5
Max treatments per surgery team	One hospital per 2^o facility	5
Max treatments per surgery team (2-4 hospitals per secondary facility)	2 to 4 hospitals per 2^o facility	3
Max treatments per surgery team (5 hospitals per secondary facility)	5 hospitals per 2^o facility	2

In addition to an evaluation of the available technologies and strategies for primary manufacturing operations and scheduling options for secondary manufacturing, centralised versus de-centralised primary manufacturing was also assessed. The distribution scenarios in this study consider manufacturing and delivery of the cell therapy to clinics in both the UK and mainland member nations of the EU in mainland Europe. As discussed previously, the fact that the product must be delivered as a fresh entity to the clinic dictates that secondary, decentralised facilities must be employed. Therefore, distribution models were used to evaluate the impact that the number of secondary facilities have upon cost of goods and whether the use of a single centralised facility, or multiple de-centralised facilities for primary manufacturing would be more cost-effective. Figure 5.3 shows the distribution models that were evaluated within this study. The centralised model (Figure 5.3a) involves distribution from a single primary facility based in the UK to secondary facilities within the UK and mainland Europe. Process material is transported from the primary facilities to UK-based secondary facilities by road. Transport from the primary facility to EU-based secondary facilities was assumed to involve transport to airport by road, air-shipment to an airport within the EU, before final road transportation to the secondary facility. The decentralised model assumes that two primary facilities will be built; one in the UK and one within the EU on mainland Europe. Shipment of process material from the primary manufacturing facilities to secondary facilities will be by road transport. In all instances delivery of the final product from the secondary facility to the clinic is carried out by road transport. The costs associated with shipping can be found within Table 5.3, road transport costs were derived from quotes obtained from NHS-contracted couriers who regularly transport medicinal products under cGMP conditions. Air shipment costs were derived from conversations with industry experts.

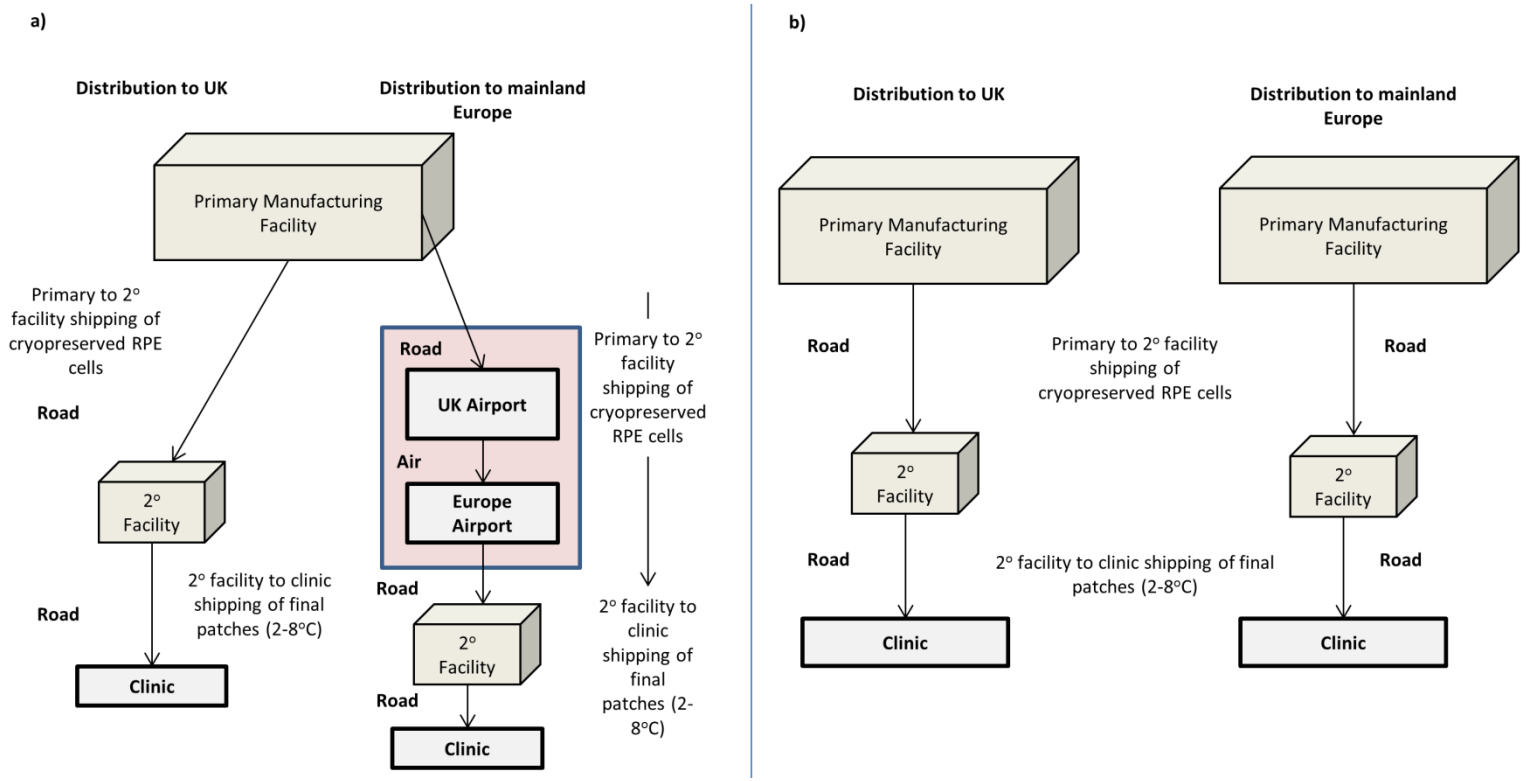

Figure 5.3 Flowcharts illustrating the flow of process materials between primary and secondary manufacturing facilities, and then on to the clinic within the UK and mainland Europe when a) a single centralised primary facility is built in the UK, and b) two separate primary facilities are built; one located in the UK and one located in mainland Europe.

5.3 Case Study Results and Discussion

5.3.1 Comparison of bioprocess strategies: selection of cost-effective technologies

Figure 5.4 shows the outputs the decisional tool derived from the functioning of the evolutionary algorithm (EA). The text matrices depict the most cost-effective technologies to be used for the final passage of expansion, differentiation and RPE culture for each bioprocess strategy tested, with the number of units required per lot given in square brackets.

Figure 5.4 illustrates the impact of both the bioprocess strategy used and the scale of the bioprocess, in terms of demand and lot size, upon the type of technology selected as the optimal technology. The colours used in the matrix represent different categories of process technologies (see legend inset). For the directed differentiation and planar (DD-PL) option, the DD-PL matrix (Fig 5.4b) illustrates that single-layer T-flasks remain the most cost-effective technology, even at lot sizes of 500 doses. Beyond this, multi-layer planar vessels, such as 2-layer CellStacks (L-2), or 5-layer CellStacks (L-5) are preferred. In comparison, the matrix representing the spontaneous differentiation route (SD-PL) (Fig 5.4a) shows that for both expansion and differentiation single-layer T-flasks are only the most cost-effective technologies at lot sizes of 10 doses. The switch to multi-layer planar vessels must be made at smaller lot sizes than if the DD-PL bioprocess were employed. Technologies used for RPE culture are generally the same across all scales for the SD-PL and DD-PL processes because the cell population size that is output from the differentiation unit operation is the same between the two strategies. Caveats to this rule do exist and instances where the optimal technology differs between the two RPE culture steps are due to the fact that the selected technology is more cost-effective to run in sequence with technologies used in previous unit operations. For example, at an annual demand of 50,000 doses where 5 x 10,000 doses per lot are manufactured,

one cL-12 unit is preferred for RPE culture in the SD-PL process (Fig. 5.4a) compared to one XP-10 unit for the DD-PL process (Fig. 5.4b). Solutions were found for lot sizes of 50,000 doses for the SD-PL bioprocess, however these have been marked as infeasible in Figure 5.4a as they exceeded the maximum number of vessels allowable per lot from a QC point of view in this instance.

Figures 5.4c and 5.4d represent the microcarrier routes for both the spontaneous and directed differentiation (SD-MC and DD-MC) bioprocess strategies, respectively. Juxtaposed with the high-seeding densities reported for successful hESC differentiation and RPE culture, the small dose sizes required for a hESC-RPE therapy mean that microcarrier-based differentiation is infeasible at lot sizes below 500 doses when SD is considered, this lower limit increases to 10,000 doses when DD is considered. This is because the cell population sizes required to satisfy demands in these scenarios result in suspension bioreactor utilisation rates lower than 25%; this is the minimum allowable utilisation as defined by the vessels' manufacturer (Sartorius Stedim 2017). Furthermore, RPE culture in SUBs is infeasible at lot sizes of 10,000 doses and below and thus was not considered for the SD-MC process at lot sizes ranging from 500 to 10,000 doses (inclusive).

Similar to the data presented in Figures 5.4a and 5.4b (at feasible lot sizes), the SD-MC bioprocess strategy necessitates the use of larger vessels than the DD-MC bioprocess strategy. At lot sizes of 5,000, 10,000 and 50,000 doses, SUBs with volumes of 5L, 20L, and 50L respectively are the preferred differentiation technology for the SUB-based bioprocess. Comparatively, at lot sizes of 10,000 and 50,000 doses, single SUBs with respective volumes of 1L and 5L are preferred for the differentiation unit operation for the DD-MC bioprocess strategy.

Examination of Figure 5.4 shows that SD-based bioprocesses necessitate the need for larger culture vessels during the expansion and differentiation unit operations. This is due to the fact that SD-based bioprocesses result in lower differentiation

efficiencies compared to their DD counterparts; therefore larger cell population sizes must be handled during the expansion and differentiation unit operations.

a)

SD-PL

Demand (doses/yr)		Lot Size (doses/ lot) 10	50	100	500	1,000	5,000	10,000	50,000
10	Expansion	T225 [1]							
	Differentiation	T175 [1]							
	RPE Culture	T-25 [1]							
100	Expansion	T225 [1]	L-2 [1]	L-5 [1]					
	Differentiation	T175 [1]	L-2 [1]	cT [1]					
	RPE Culture	T-25 [1]	T-25 [1]	T75 [1]					
1,000	Expansion		L-2 [1]	L-5 [1]	cL-12 [2]	cL-12 [3]			
	Differentiation		L-2 [1]	cT [1]	cL-12 [2]	cL-12 [3]			
	RPE Culture		T-25 [1]	T75 [1]	T225 [1]	TrF [1]			
5,000	Expansion			L-5 [1]	cL-12 [2]	cL-12 [3]	XP-50 [3]		
	Differentiation			cT [1]	cL-12 [2]	cL-12 [3]	XP-50 [3]		
	RPE Culture			T75 [1]	T225 [1]	TrF [1]	cL-12 [1]		
10,000	Expansion				cL-12 [2]	cL-12 [3]	XP-50 [3]	XP-200 [1]	
	Differentiation				cL-12 [2]	cL-12 [3]	XP-50 [3]	XP-50 [6]	
	RPE Culture				T225 [1]	TrF [1]	L-5 [1]	cL-12 [1]	
50,000	Expansion					cL-12 [3]	XP-50 [3]	XP-50 [6]	cL-120 [16]
	Differentiation					cL-12 [3]	XP-50 [3]	cL-120 [3]	cL-120 [16]
	RPE Culture					TrF [1]	L-5 [1]	cL-12 [1]	XP-50 [1]

b)

DD-PL

Demand (doses/yr)		Lot Size (doses/ lot) 10	50	100	500	1,000	5,000	10,000	50,000
10	Expansion	T-25 [1]							
	Differentiation	T-25 [1]							
	RPE Culture	T-25 [1]							
100	Expansion	T-25 [1]	T-25 [1]	T-25 [1]					
	Differentiation	T-25 [1]	T-25 [1]	T75 [1]					
	RPE Culture	T-25 [1]	T-25 [1]	T75 [1]					
1,000	Expansion		T-25 [1]	T-25 [1]	T175 [1]	T225 [1]			
	Differentiation		T-25 [1]	T75 [1]	T225 [1]	L-2 [1]			
	RPE Culture		T-25 [1]	T75 [1]	T225 [1]	TrF [1]			
5,000	Expansion			T75 [1]	T175 [1]	T175 [1]	L-2 [1]		
	Differentiation			T175 [1]	T225 [1]	L-2 [1]	L-5 [1]		
	RPE Culture			T75 [1]	T225 [1]	TrF [1]	L-5 [1]		
10,000	Expansion				T175 [1]	T225 [1]	L-2 [1]	cT [1]	
	Differentiation				T225 [1]	L-2 [1]	L-5 [1]	cL-12 [1]	
	RPE Culture				T225 [1]	TrF [1]	L-5 [1]	cL-12 [1]	
50,000	Expansion					T225 [1]	L-2 [1]	cT [1]	L-5 [3]
	Differentiation					L-2 [1]	L-5 [1]	XP-10 [1]	cL-12 [4]
	RPE Culture					TrF [1]	L-5 [1]	XP-10 [1]	cL-12 [4]

Figure 5.4 a) & b) Continued overleaf

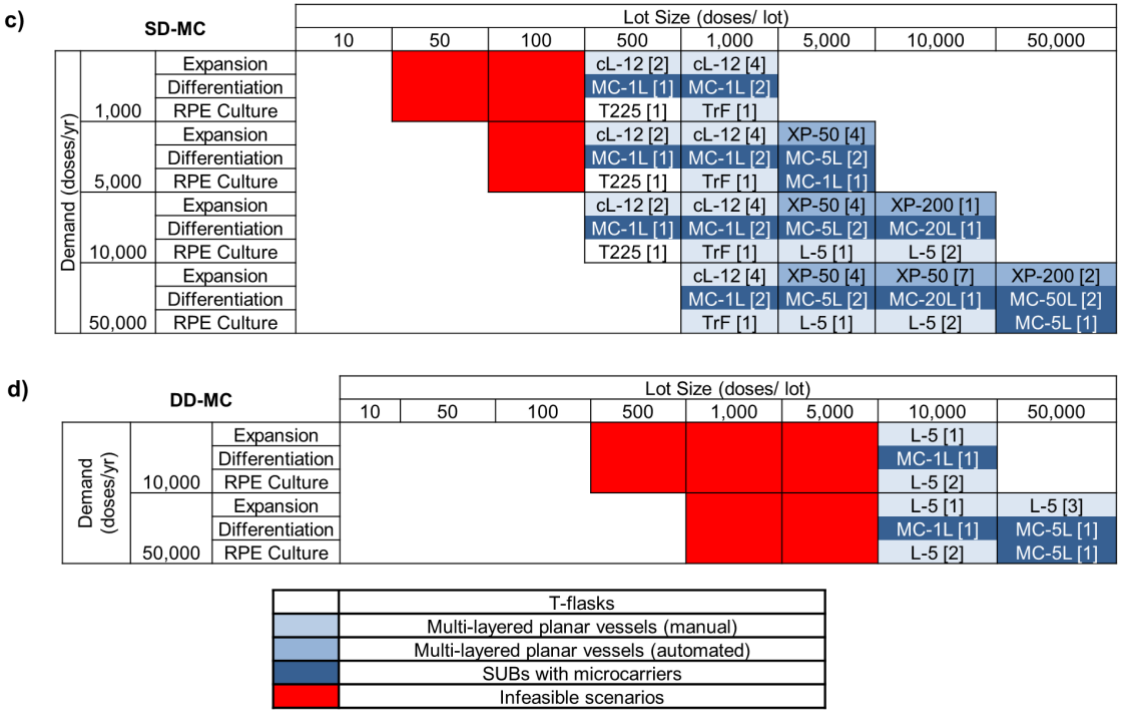

Figure 5.4 Matrices showing the impact on the optimal process technology for the final passage of expansion, differentiation and RPE cell culture unit operations when a) SD-PL, b) DD-PL, c) SD-MC, d) DD-MC bioprocess strategies are employed at different lot sizes and annual demands. For SUBs, the values represent the size of the bioreactor selected as optimal. For all technologies the number in square brackets represents the number of units required per lot. Only feasible annual demands are shown in c) and d).

5.3.2 Comparison of the manufacturing cost of goods associated with each bioprocess strategy

Figure 5.5 offers a comparison between the four bioprocess strategies tested from a COG perspective. The values given in Figure 5.5a are the minimum COG per dose values for primary manufacturing for each given annual demand and lot size, as evaluated by the EA. Figure 5.5a illustrates the economies of scale that can be achieved in allogeneic cell therapy processing. This is evident from the difference in COG per dose from an annual demand of 100 doses (US$20,497 for 10 lots per year) and an annual demand of 10,000 doses (US$397 at 10 lots per year). This is possible because the bioprocess can be scaled-up in an allogeneic setting, as opposed to the scale-out strategy necessitated by autologous processes (Jenkins & Farid 2015).

Figures 5.5b, c and d illustrate the percentage change in COG when use of the DD-PL, SD-MC and DD-3D bioprocess strategies, respectively, is considered against the SD-PL strategy. Figure 5.5b illustrates that COG associated with the DD-PL process strategy are less than those associated with the SD-PL process strategy at all scales tested. In comparison, switching to the SD-MC bioprocess (Fig. 5.5c) from the SD-PL process only proves more cost-effective at lot sizes of 5,000 doses and beyond. Furthermore, the DD-MC bioprocess strategy proves more cost-effective than the SD-PL bioprocess strategy in all feasible scenarios (Fig. 5.5d).

A comparison of the DD-PL and DD-MC matrices (Fig 5.5b & 5.5d, respectively) shows that there is no significant difference in the COG associated with these two bioprocess strategies at lot sizes of 10,000 doses. Relative to the SD-PL bioprocess, a 1% reduction in COG can be achieved by using the DD-MC bioprocess strategy as oppose to the DD-PL strategy, at a lot size of 50,000 doses (1 lot per annum). In real terms, this is a 6% COG reduction when comparing the COG values for the two bioprocesses (US$54 for DD-MC vs. US$58 for DD-PL) (see Fig 5.6b). Both DD

bioprocesses prove more cost-effective than the SD bioprocess in all scenarios tested.

a) **SD-PL**

Demand	Lot Size							
	10	50	100	500	1,000	5,000	10,000	50,000
10	110,324							
100	20,497	13,323	11,167					
1,000		3,218	2,211	1,500	1,335			
5,000			1,363	623	535	553		
10,000				523	397	399	456	
50,000					300	233	216	205

Process change results in COG reduction

Process change results in COG increase

b) **DD-PL**

Demand	Lot Size							
	10	50	100	500	1000	5000	10000	50000
10	-1%							
100	-5%	-5%	-3%					
1,000		-16%	-12%	-13%	-12%			
5,000			-24%	-32%	-30%	-34%		
10,000				-44%	-44%	-48%	-50%	
50,000					-63%	-74%	-73%	-72%

c) **SD-MC**

Demand	Lot Size							
	10	50	100	500	1,000	5,000	10,000	50,000
10								
100								
1,000				3%	17%			
5,000				3%	22%	-13%		
10,000				-3%	26%	-13%	-35%	
50,000					18%	-26%	-36%	-43%

d) **DD-MC**

Demand	Lot Size							
	10	50	100	500	1,000	5,000	10,000	50,000
10								
100								
1,000								
5,000								
10,000							-50%	
50,000							-73%	-74%

Figure 5.5 Matrices showing the impact on bioprocess COG when different bioprocess strategies are employed at different annual demands and lot sizes. **a)** COG per dose values (US$) when the most cost-effective process flowsheet is selected for the SD-PL bioprocess strategy. **b) – d):** Percentage change in the minimum COG/dose for given annual demands and lot sizes as compared to the values calculated for the SD-PL bioprocess strategy if the **b)** DD-PL, **c)** SD-MC, **d)** DD-MC bioprocess strategy were employed. Green cells within the matrices indicate a COG per dose decrease compared to the SD-PL bioprocess, red cells indicate a COG per dose increase compared to the SD-PL bioprocess.

In order to further investigate the trends featured in Figures 5.4 and 5.5, a detailed analysis of the COG and its constituent components was carried out (Figure 5.6a, 5.6b, 5.6e and 5.6f). At annual demands of 5,000 doses, satisfied by 10 manufacturing lots, the SD-PL bioprocess strategy proves to be more cost-effective than the SD-MC bioprocess. This is because the SD-MC bioprocess results in an increase in the indirect costs associated with production of the hESC-RPE therapy at this scale. SUBs require expensive fixed capital equipment; this is in contrast to the type of disposable vessel (2 x 12 cl-12 (12-layer CellStack)) used for the SD-PL at this scale. Despite resulting in an overall increase in COG at this scale, the SD-MC strategy results in a decrease in materials and labour costs (Figure 5.6a). This is because a single SUB can be used for the differentiation unit operation in each lot, as oppose to the multiple vessels required for the SD-PL bioprocess strategy (Fig. 5.4). SUB culture using microcarriers offers greater growth surface area per volume of media used for adherent cells, therefore less media is required for the SD-MC bioprocess, hence materials costs are reduced if this bioprocess strategy is used. Furthermore, SUBs run in an automated manner, therefore less manual interaction is required when the SD-MC strategy is employed. This, along with the fact that only one unit is required for the differentiation process in the SD-MC bioprocess (compared to two for the SD-PL bioprocess strategy), results in decreased labour costs directly associated with this strategy when compared with the SD-PL bioprocess strategy.

In contrast, at annual demands of 50,000 doses, satisfied by 5 manufacturing lots per year, it is the SD-MC bioprocess strategy that proves more cost-effective than the SD-PL strategy. At this production scale, the SD-MC strategy offers reductions in both direct (DC) and indirect (IDC) costs compared to the SD-PL strategy (Figure 5.6e). At this scale automated planar vessels in the form of 3 x 120-layer Cell Factories are required, along with an Automated Cell Factory Manipulator (Nunc, USA). The

additional cost of this machinery outweighs the capital expenditure associated with the 20L SUB control rig required for the SD-MC process strategy at this scale (Figure 5.4).

Figures 5.6e and 5.6f show that the DD-PL and DD-MC bioprocess can drastically reduce bioprocess COG by 73% compared to the SD-PL bioprocess at an annual demand of 50,000 doses. The DD bioprocess strategies utilise an improved differentiation protocol, whereby differentiation efficiencies are improved as a result of an improved media composition. Hence, smaller cell populations are required to be output from the hESC expansion unit operation and smaller cell populations are process during the differentiation unit operation. This is why materials costs are dramatically reduced if the DD-PL bioprocess strategy is used compared to either the SD-PL, or SD-MC bioprocess strategy at an annual demand of 5,000 doses (Figure 5.7a). Labour costs are also reduced as a result of selecting either of the DD bioprocesses when compared to the SD-PL or SD-MC bioprocess because the length of the differentiation protocol is reduced from 84 days to 19 days. This reduction in the length of the bioprocess also affects materials costs (this equates to fewer media exchanges using DD protocols). Capital expenditure is also reduced when DD is employed; equipment utilisation is improved because more lots can be produced in a shorter period of time.

There is only a 5% difference in direct costs between the DD-MC process strategy and the DD-PL strategy at an annual demand of 50,000 doses (Figure 5.6b & 5.6d). This is reflective of the fact that the cell populations required at this scale result in low utilisation of the 1L-SUB that is the preferred DD-MC technology for differentiation, which means that the bioprocess is unable to achieve full advantage of the increased surface area to volume ratio that is offered by SUBs.

Figure 5.6b & 5.6f illustrate the effects that different bioprocess strategies have on the direct costs associated with each unit operation in the process. Here, the dramatic

direct costs reductions that can be achieved through use of the DD-PL and DD-MC bioprocess are depicted. Whilst the RPE culture costs remain the same as those for the SD-based bioprocesses, direct costs associated with the expansion and differentiation unit operations are significantly reduced (97% and 90% compared with the SD-PL and SD-MC strategies respectively). This is illustrative of the reduced cell populations required when DD is used as opposed to SD. The direct costs associated with differentiation are also significantly reduced with use of the SD-MC bioprocess strategy when compared the SD-PL bioprocess, whereas those associated with RPE culture and expansion remain approximately constant. This confirms that reductions in materials costs discussed in Figure 5.6a and 5.6b derive from SUB usage during the differentiation unit operation.

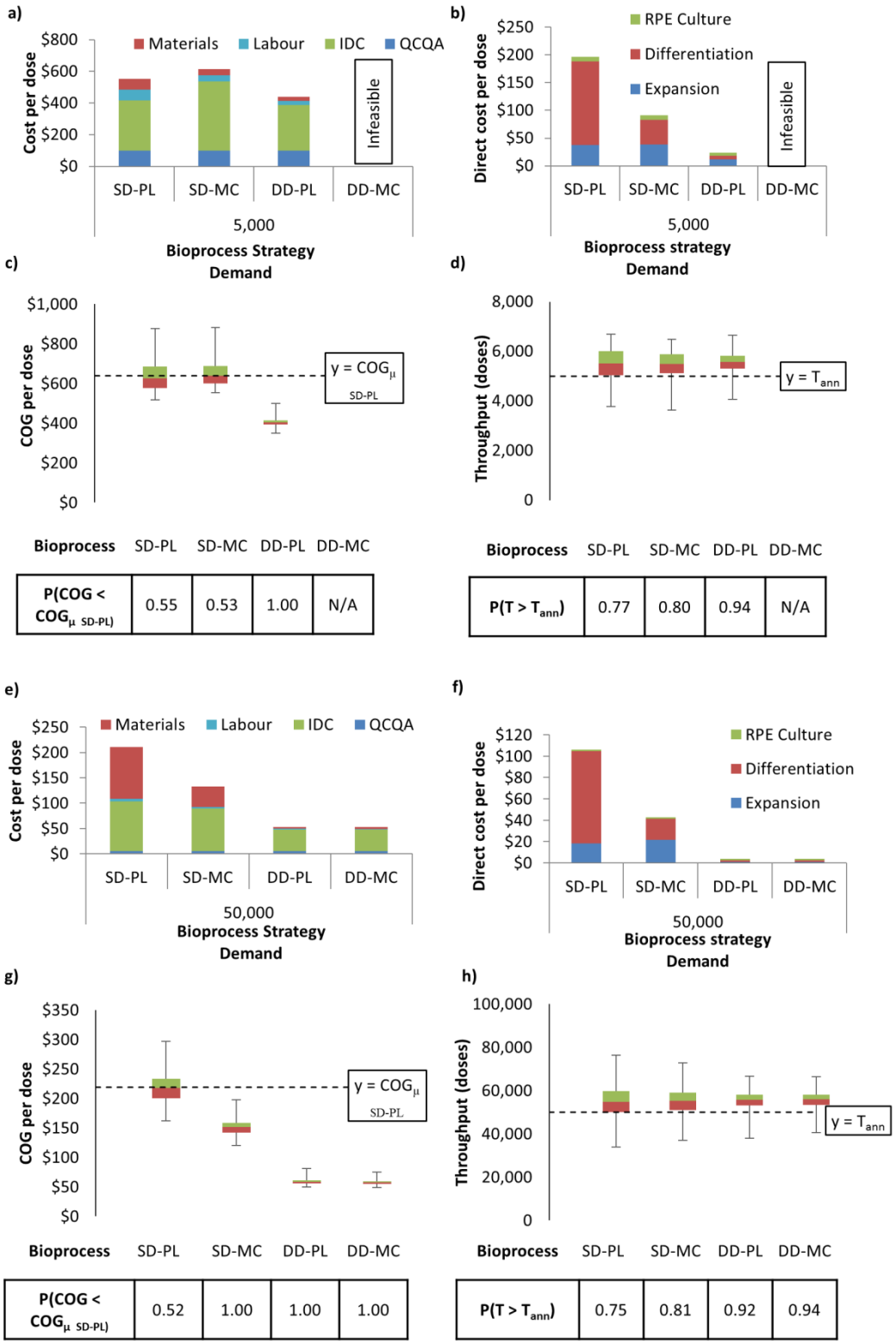

Figure 5.6 See overleaf for legend

Figure 5.6 Charts showing the effect of process scale and bioprocess strategy choice on COG and process robustness at annual demands of **a) – d)** 5,000 doses produced across 10 manufacturing lots and **e) – h)** 50,000 doses produced across 5 manufacturing lots . **a) & e)**: COG breakdown at **c)** an annual demand of 5,000 doses produced across 10 manufacturing lots and **e)** an annual demand of 50,000 doses produced across 5 manufacturing lots. **b) & f):** Direct cost breakdown by unit operation at **b)** an annual demand of 5,000 doses produced across 10 manufacturing lots and **f)** an annual demand of 50,000 doses produced across 5 manufacturing lots. **c) & g):** Box and whisker plots illustrating the effects of process variation on COG per dose at an annual demand of **c)** 5,000 doses produced across 10 manufacturing lots and **g)** 50,000 doses produced across 5 manufacturing lots. The dashed intercept on the y-axis displays the mean COG per dose value for the SD-PL bioprocess, the boxed values below the chart illustrate the probability (as assessed by Monte Carlo analysis) that the COG for a given bioprocess strategy will fall below the mean value of SD-PL bioprocess at an annual demand of 5,000 doses per annum. **d) & h):** Box and whisker plots illustrating the effects of process variation on annual throughput at an annual demand of **d)** 5,000 doses produced across 10 manufacturing lots and **h)** 50,000 doses produced across 5 manufacturing lots. The dashed intercept on the y-axis of each plot displays the annual demand and the boxed values below the plots illustrate the probability (as assessed by Monte Carlo analysis) that the annual throughput for a given bioprocess strategy will satisfy the annual demand.

5.3.3 Stochastic modelling of different bioprocess strategies under uncertainty

Further to the deterministic bioprocess economics model that was used to capture the data shown in Figs. 5.6a, 5.6b, 5.6e & 5.6f, the Monte Carlo stochastic modelling technique was employed in order to assess the performance of the different bioprocess strategies under manufacturing uncertainty.

The results of the Monte Carlo analysis show that at an annual demand of 5,000 doses (Figure 5.6c), the median COG per dose of the SD-PL process (US$627) is slightly lower than that of the SD-MC bioprocess (US$640). This is consistent with the results of the deterministic cost model, whereby the SD-PL strategy proved more cost-effective than the SD-MC strategy (Fig. 5.6a). However, the spread of values shown by the whiskers of the box plots in Figure 5.6c illustrate that there is greater variation in the bioprocess COG for the SD-PL process than there is when the SD-MC bioprocess is employed. This is reflective of the fact that bioprocesses in SUBs generally allow much greater control of a cells microenvironment and therefore process variation can be reduced if the SD-MC bioprocess is employed.

Similar to the deterministic model, the median value for the COG of the DD-PL strategy proves to be significantly lower than that of both the SD bioprocess strategies. The greater process control allowed by the use of the DD strategy is reflected by the narrow range of COG values for this strategy as compared to the SD values (Figure 5.6c).

Even under uncertainty the DD-PL strategy proved to be more cost-effective than both the SD strategies, indeed the Monte Carlo analysis found that $COG_{DD\text{-}PL} < COG_{\mu\ SD\text{-}PL}$ in 100% of the simulations carried out, where COG_{μ} = the cost of goods value for a given process strategy determined by the Monte Carlo analysis; i.e. in all instances tested by the Monte Carlo analysis, COG for the DD-PL process was less than the COG found for the SD-PL process under base case conditions. The increased robustness of the DD-PL strategy compared to the SD-PL and SD-MC

strategies is also illustrated in Fig. 5.6d, which consists of box and whisker plots the output of the Monte Carlo analysis representing the number of doses produced per annum. The Monte Carlo Analysis shows that there is a 94% probability that the throughput of the bioprocess (T) will be greater or equal to the target annual demand (T_{ann}) when the DD-PL bioprocess is employed, as compared to probabilities of 80% and 74% for the SD-MC and SD-PL bioprocesses respectively.

At an annual demand of 50,000 doses the COG per dose output values of the Monte Carlo Analysis also follow a similar trend to that of the deterministic model in that the median value of the COG of the SD-MC, DD-PL and DD-MC bioprocesses (US$151, US$58 and US$57 respectively) are significantly lower than that of the SD-PL bioprocess (US$218). Indeed, the Monte Carlo outputs show that in all 1,000 simulations the COG per dose values calculated for the SD-MC, DD-PL and DD-MC bioprocesses were lower than the COG value calculated for the SD-PL bioprocess in the deterministic model ($COG_{\mu\ SD\text{-}PL}$). Similar to the Monte Carlo analysis outputs at an annual demand of 5,000 doses, the Monte Carlo outputs at 50,000 doses per annum show a narrower spread of values for the MC bioprocess strategies as compared to their PL counterparts; this owes itself to the tighter process control of a cell population's environment offered by SUBs. This pattern was observed for both output values of COG per dose (Fig. 5.6g) and output values of the number of doses produced per annum (Fig. 5.6h).

Finally, the DD-MC bioprocess was shown to be the most robust of the four strategies tested under uncertainty at this scale; there was a 94% probability that the annual throughput (T) of this process will exceed the target annual demand (T_{ann}) when tested at 50,000 doses per annum (Fig. 5.6h). This is compared to 92%, 81% and 75% for the DD-PL, SD-MC, SD-PL bioprocess respectively. A wider range of values for the SD-PL and SD-MC strategies were observed than for the DD-PL and DD-MC process for both the COG per dose and annual throughput outputs of the Monte Carlo

analysis (Fig. 5.6c, 5.6d, 5.6g & 5.6h). This illustrates that when manufacturing uncertainty and variations in critical process parameters are taken into account directed differentiation platforms prove to be more robust from both a process performance and bioprocess economic standpoint. It is unsurprising that the DD bioprocess strategies proved more robust than their SD counterparts; numerous empirical studies have shown that the use of directed differentiation offers greater control of the differentiation process than spontaneous differentiation strategies.

5.3.4 Appraisal of the four bioprocess strategies tested within this study

Two differentiation strategies have been compared; spontaneous differentiation and directed differentiation. Empirical data shows that directed differentiation is both a more efficient and more robust means of generating hESC-RPE cells (Idelson et al. 2009; Buchholz et al. 2013), as well as other types other progenitor cell type including neuronal cells and cardiomyocytes (Surmacz et al. 2012; Burridge et al. 2011).

It can be concluded that in addition to generating larger number of target cells in a shorter timeframe, directed differentiation offers a significantly more cost-effective route to producing hESC-RPEs for cell therapies than spontaneous differentiation. Furthermore, the Monte Carlo analysis illustrates that directed differentiation protocols prove to be a more robust platform than their spontaneous counterparts from both a bioprocess economics and bioprocess performance perspective.

A bioprocess economic comparison of microcarrier-based differentiation and RPE culture versus planar-based bioprocessing was carried out. Previous analyses have shown that microcarrier-based processing of cells for cell therapies can significantly reduce cost of goods compared to the use of planar technologies, particularly at large manufacturing lot sizes (Simaria et al. 2014; Hassan et al. 2016). Here we found that for a low-dose, allogeneic therapy microcarrier-based differentiation does not offer significant cost of goods savings, even at annual demands in the order of 10^4 doses if a directed differentiation protocol is employed. As stated previously, this is because

the small cell populations required for this strategy do not allow full realisation of the increased efficiency in media usage that has been shown to be offered by microcarrier-based processing (Wang et al. 2013; Panchalingam et al. 2015). 3-D bioprocess strategies do offer other advantages over many planar technologies, including the fact that the microenvironment of the cells can be better controlled, and the bioreactor environment more tightly controlled (Olmer et al. 2012). This can result in greater process robustness from both a process performance and economic standpoint, as illustrated by the stochastic modelling employed in this study.

However, more advanced planar technologies, which have more in common with traditional bioreactors than manual planar vessels such as T-flasks, can also offer a well-controlled, robust process platform when directed differentiation protocols are employed. This study found that the differences between the DD-MC and DD-PL strategies were not significant from a COG perspective. Indeed for low-dose cell-based therapies, such as the one investigated in this study, planar bioreactors may be a more suitable platform due to the cell population sizes involved in the bioprocess if they can be run in a controlled and contained manner. This is certainly true if the cell therapy development pathway is taken into account; the DD-MC bioprocess is unsuitable for lot sizes below 1,000 doses as this results in utilisation values below 25%; the minimum advised by the manufacturer of such platforms (Sartorius Stedim 2017). Therefore, in pre-clinical, and early phase trials the DD-PL bioprocess will likely need to be employed. Switching to the DD-MC bioprocess either in late-phase clinical trials or post approval will represent a significant investment (and large risk if done pre-approval). This investment will unlikely be recouped as the differences in cost of goods between the two strategies is not significant, even at annual demands of up to 10,000 doses.

5.3.5 Comparison of bioprocess schedules for manufacturing at secondary facilities

Figure 5.7 displays the COG breakdown of manufacturing carried out at the secondary facility. It is clear from Figure 5.7a that at small, clinical production scales (10 and 100 doses per annum), schedule C, whereby patches undergo formation from between 6 weeks and 20 weeks, proves less cost-effective than schedules A and B (see Table 5.5/ Fig. 5.2 for production schedules), whereby each patch undergoes formation for 6 weeks, or 6 to 7 weeks respectively. This is largely due to increased IDC, which also prove to be significantly higher for process schedule C at commercial production scales (5,000 and 50,000 doses per annum, Figure 5.7b). The number of doses that must be processed at any given time in Schedule C is larger than the other process schedules. 14 weeks of doses must be incubated at any given time, which drives up the required incubator capacity, and subsequently IDC, at this stage of the process. Furthermore, the need to handle more doses at a single time means that more operators are required for Schedule C. This in turn results in the need for more biosafety cabinets to allow operators to work in Class A/B conditions required for manual processing. This is also why labour costs are higher for schedule C compared to schedules A and B; the fact that more patches must have their media replenished over a longer time period also results in slightly increased materials costs for Schedule C. Schedule A proves more cost-effective than schedule B at commercial production scales (Figure 5.7b). This owes itself to similar reasons as those described previously for schedule C, although they are less pronounced when schedules A and B are compared.

There are logistical arguments for and against both schedule A and B. It could be argued that Schedule A offers more flexibility, for example fewer doses could be prepared for weekend surgeries (if these were considered at all). However, this option could be worked into schedule B without great difficulty. Schedule B is less challenging logistically; a maximum of 7 lots will be handled at a single time. This number rises to 42 with schedule A. The therapeutic material will need to be tracked

carefully throughout the duration of manufacturing at the secondary facility. Barcode tracking software packages such as Trakcel (Cardiff, UK) have made tracking and tracing of individual samples (or patches in this case) far simpler and therefore the logistical challenge presented by schedule A may not be the barrier that it once might have been.

Given the insignificant differences in cost between production schedules A and B, the decision of which schedule to proceed with would likely depend on whether a manufacturer prefers a more responsive manufacturing schedule (process schedule A) or a schedule that offers greater logistical simplicity within the secondary facility (process schedule B).

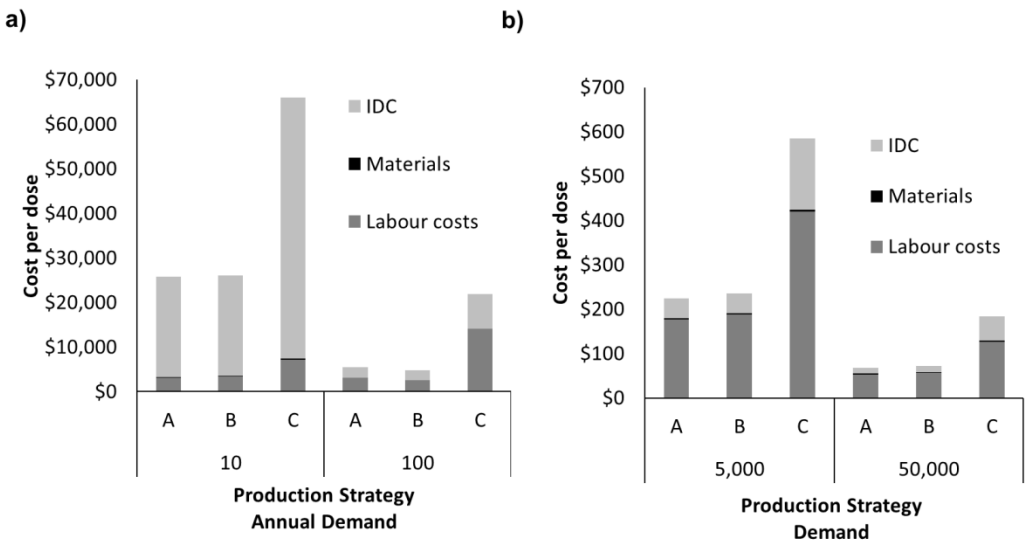

Figure 5.7 Bar charts representing COG breakdowns at the secondary manufacturing facilities for **a)** annual demands of 10 and 100 doses per year and **b)** annual demands of 5,000 and 10,000 doses per year. The process strategies refer to Schedules A, B and C; details of which can be found in Table 5.5.

5.3.6 Effect of distribution strategies on shipping and manufacturing costs

Figure 5.8 illustrates the effect that both the number of secondary facilities and the number of hospitals per secondary facility have on COG at the secondary facility and shipping costs. A reduction in the number of facilities is advantageous because it reduces IDC associated with product manufacture. Furthermore, labour costs are reduced because the number of operators required at a single secondary facility remains the same regardless of the scale of the facility at the annual demand tested for this scenario (10,000 doses).

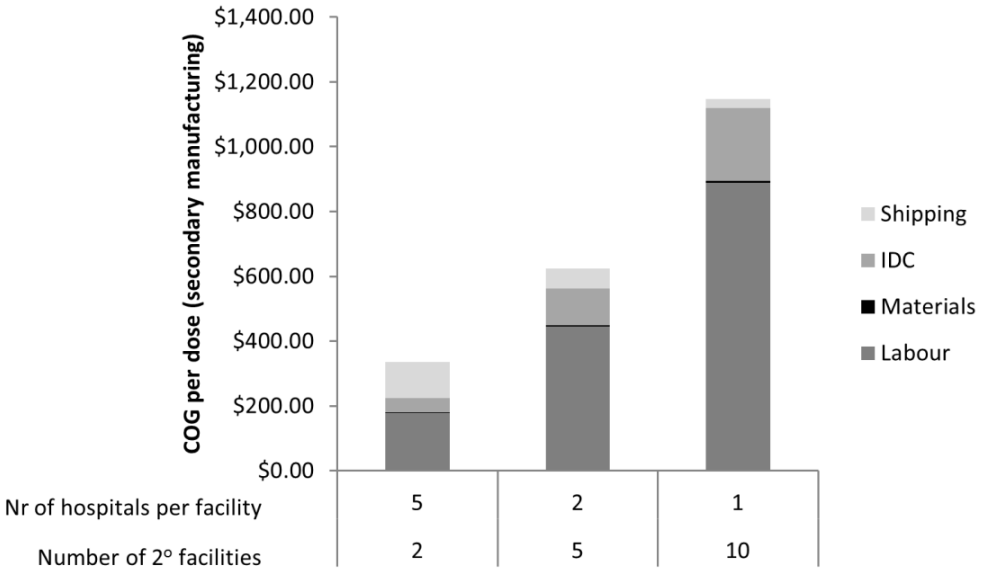

Figure 5.8 Bar chart representing the COG breakdowns for secondary manufacturing and shipping costs (inclusive of transportation costs from 1^0 facility to 2^0 facility) when it is assumed that the therapy is administered at 10 hospitals within the UK. The assumed annual demand is 10,000 doses per year.

Minimising the number of hospitals per facility proves more expensive because IDC and labour costs are increased as the number of required secondary facilities increases. Shipping costs are decreased in this scenario. Although the number of journeys from the primary facility to secondary facilities is increased when the number

of secondary facilities is increased, there is a reduction in both the distance and in the number of journeys required between the secondary facility and the clinic. Thus, the number of time-sensitive transports of the finished product that is required is reduced. Furthermore, small secondary facilities may be able to be built within, or adjacent to clinics; this would negate the need for a final road transport from the secondary facility to the clinic altogether. However, placing a manufacturing area within a hospital would not always prove feasible. This is particularly true of clinics based in city centres, or densely populated areas where space on hospital premises is likely to be at a premium.

Increasing the number of clinics at which the product is available would likely increase the availability of the therapy to a larger proportion of a target market. However when dealing with public healthcare systems, it is likely to be the decision of the health services as to which hospitals will be licensed to administer a specialist therapy, or whether it will be added to local formularies. Furthermore, even in a private healthcare model, cell therapy manufacturers may be liable for patient transfer to and from specialist clinics that are able to administer the therapy in question and this may incur added costs.

Figure 5.9a illustrates the COG breakdowns for the centralised primary manufacturing model and the decentralised primary manufacturing model at annual demands of 20,000 and 50,000 doses. At annual demands of 20,000 doses (5,000 in the UK, 15,000 in mainland Europe) it proves more cost-effective to use a centralised primary manufacturing model, whereby a single facility is based in the UK. However, at higher annual demands of 50,000 doses it proves more cost-effective to employ a decentralised primary manufacturing model whereby one primary facility is based in the UK and one primary facility is based in mainland Europe. This is because the reductions in shipping costs that are achieved using the decentralised primary manufacturing model (as compared to the centralised one), outweigh the additional

primary manufacturing COG that are inherent in the decentralised primary manufacturing strategy (Figure 5.9b). Whereas if a smaller target market is expected, a centralised primary manufacturing model may be a more appropriate strategy to employ for this type of cell therapy. At both annual demands tested, the decentralised primary manufacturing model resulted in a significant increase in primary manufacturing COG. This is a reflection of both the increased capital expenditure required to build multiple facilities and the reduction in economies of scale (discussed above) by dividing primary manufacturing operations between two sites (Trainor 2016).

The decentralised primary manufacturing model also resulted in a reduction in shipping costs as compared to the centralised primary manufacturing model at both annual demands tested. This is because the decentralised model obviates the need for air transport, or overseas shipment of process material from the UK to mainland Europe (Figure 5.3).Figure 5.9b displays the COG breakdown for the centralised primary manufacturing model. In this case, shipping accounts for 28% of total costs. Whilst shipping to the EU accounts for 27% of total costs, UK shipping only accounts for 1% of the same figure. This suggests that overseas shipment of process material contributes heavily towards total costs. This is further illustrated in Figure 5.9c, which illustrates the COG breakdown for the decentralised primary manufacturing model. In this instance shipping only accounts 6% of the total costs (4% EU shipping, 2% UK shipping).

Although shipping costs can be reduced both in real terms and as a percentage if the decentralised primary manufacturing model is employed as opposed to the centralised model, the opposite is true of primary manufacturing COG (Fig. 5.9a-5.9c). Figure 5.9 suggests that the larger the annual demands, the more likely it is that a decentralised manufacturing model will prove more cost effective than a centralised manufacturing model. The decentralised model will reduce interactions

with courier companies as it obviates the need for overseas shipping, which can be difficult to validate (O'Donnell 2015). However if multiple facilities are employed, it is essential to fully validate the manufacturing process in order to ensure that critical quality attributes of the product are kept within the validation space; i.e. it must be ensured that the product manufactured at each facility is consistent (Trainor et al. 2016).

.

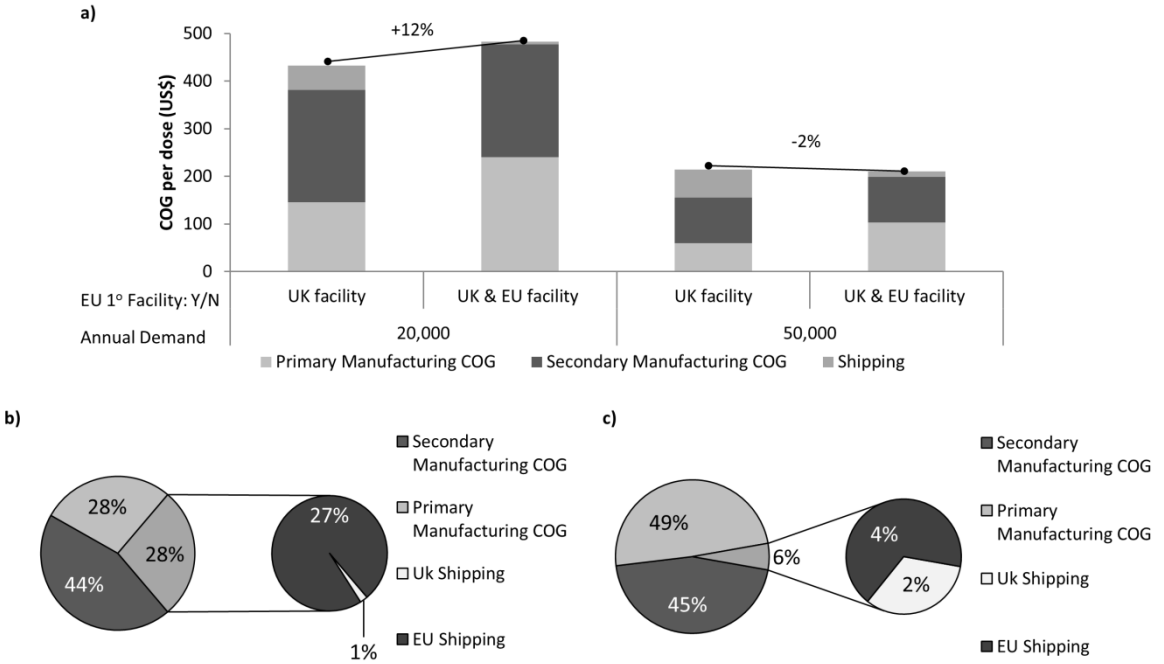

Figure 5.9 Comparison of COG breakdowns for centralised vs decentralised manufacturing. **a)** Bar chart comparing the COG breakdowns when a single, centralised primary facility is built in the UK to when two separate primary facilities are built: one located in the UK and one located in the EU at annual demands of 20,000 doses per year and 50,000 doses per year. It has been assumed that 25% of doses will be distributed to the UK and 75% of doses will be distributed to the EU. **b) & c)** Pie-charts illustrating the COG breakdowns (including shipping) when **b)** a single, centralised primary facility is built in the UK to when **c)** two separate primary facilities are built: one located in the UK and one located in the EU. An annual demand of 50,000 doses per year was assumed in figures b and c.

5.4. Case Study Conclusions

This chapter shows how an evolutionary algorithm can allow rapid identification of optimal bioprocess designs. A decisional tool was contextualised using a representative case study, in which a low dose, allogeneic hESC-RPE therapy is produced. The tool was used to appraise four different bioprocess strategies including cross comparison of spontaneous versus directed differentiation protocols, and planar versus microcarrier-based differentiation and RPE culture unit operations. The outputs show that directed differentiation protocols can significantly both reduce the cost of goods and increase the process economic robustness associated with hESC derived cell-based therapy manufacturing. Additionally, the study found that for low dose cell-based therapies, there is no significant difference in the cost of goods or process robustness between planar and microcarrier bioprocesses when directed differentiation is employed, even at larger lot sizes. However, when larger cell populations were required (i.e. for spontaneous differentiation) microcarrier-based processing can offer significant manufacturing COG reductions compared to planar technologies.

The tool was also used to evaluate whether centralised, or decentralised primary manufacturing would prove more cost effective. At lower annual demands (20,000 doses), centralised manufacturing proved more cost effective; the savings in shipping costs associated with decentralised manufacturing failed to outweigh the additional capital expenditure associated with building an additional facility. At larger annual demands (50,000 doses), the reverse of this proved to be the case. This work sought to model a bioprocess at scales ranging from clinical (i.e. 10-100 doses per annum) to commercial (1,000+ doses per annum).

5.5. Measuring the performance of the evolutionary algorithm

A single scenario was used to test the performance of the EA when applied to the MC and PL bioprocess strategies. This was done in order to provide a snapshot that was reflective of the EAs performance for both of these bioprocess strategies. In the scenario selected, the annual demand was assumed to be 5,000 doses and the lot size was assumed to be 500 doses. This scenario featured in the results and discussion of this case study, presented in Section 5.3. The EA was tested when it was applied to both the SD-PL and the SD-MC bioprocess strategies. This was to ensure that the algorithm was accurate and reliable when applied to both the PL and MC differentiation platforms, but also to test the performance of the EA against a brute-force search procedure in both instances. It was necessary to do this because the MC process strategy results in a smaller design space for the problem tested within this case study, therefore the performance of the EA relative to a brute-force algorithm would be different to that of the EA when applied to the PL process strategy.

5.5.1 Metrics used to evaluate EA performance

The performance of the evolutionary algorithm was measured using standard convergence metrics. The mean fitness (in this instance cost of goods) was measured for each generation across all algorithm runs, and the standard error of the mean (SEM) was used to quantify the convergence of the solutions produced by the EA. The standard error of the mean is the standard deviation of the sample mean's estimate of a population. Therefore, the smaller the standard error of the mean, the greater the convergence of the solutions found by the EA, a standard error of the mean value of zero indicates that the solutions for each generation across all EA runs have converged fully. Selected scenarios that have been highlighted in Section 5.3 were tested in order to ensure the reliability and accuracy of the EA.

5.5.2 EA Performance

Figure 5.10 shows the average fitness value (Fig 5.10a) and the standard error of the mean average fitness value (5.10b) for each generation across the five EA runs when it was applied to the SD-PL bioprocess respectively for the selected scenario. Figure 5.10a illustrates the optimisation carried out by the EA, with the average fitness value falling gradually across each successive generation, before it remains constant from generation 22 onwards (Point A). The steep gradients, which are apparent between early generations (e.g. 1 to 5), indicate that the EA is yet to find the optimal solution at this stage of the procedure, as each generation produces a solution that results in the cost of goods being minimised further as compared to the previous generation. The line representing the average fitness across all five EA runs has a gradient of zero from generation 22 onwards. This indicates the latest point at which the optimal solution was found by the EA across any of the five runs.

Figure 5.10b, which displays the standard error of the mean fitness value of the best solution after each generation across all the EA runs illustrates the convergence of the EA outputs towards the optimal solution. The SEM has a value of zero from generation 22 onwards (Point B). This indicates that by this point, the solutions produced across all five runs of the EA are consistent and, as shown by the fact that fitness values illustrated in Figure 5.10a remain constant from this point, have converged upon the optimal solution.

The mean fitness values across all five EA runs for each of the 25 generations and the standard error of these mean values for the MC bioprocess strategy are displayed in Figures 5.11a and 5.11b respectively. These figures follow the same pattern shown in Figures 5.10a and 5.10b; the gradient of the line representing the average fitness value for optimal solutions found by the EA remains 0 from generation number 20 onwards (Point A, Fig. 5.11a). The standard error of the mean of the best solution found by the EA reaches 0 at generation 20, and remains at 0 from this point forwards

(Point B, Figure 5.11b). Together, these trends indicate that the optimal solution identifiable with the EA is reached by generation 20 across all five runs.

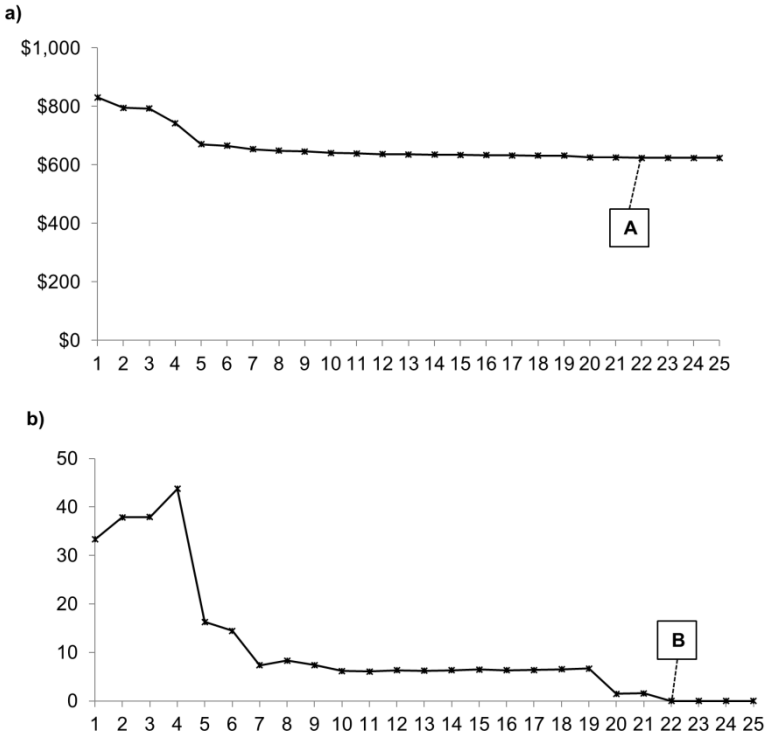

Figure 5.10 Line plots illustrating performance metrics for the EA when it was applied to the SD-PL bioprocess. **a)** Line plot that shows the mean fitness value (in this instance the cost of goods per dose) of the best solution found across all five runs of the EA for each of the 25 generations. Point A identifies the point by which the optimal solution is found within all five EA runs, and the mean fitness value remains constant. **b)** Line plot that shows the standard error of the mean fitness value across all five runs of the EA for each of the 25 generations. Point B identifies the point at which the solutions across all five runs become consistent, and that the standard error of the mean remains zero.

The fact that the EA solutions converged for both the SD-PL and SD-MC bioprocess within 25 generations indicates that the EA can reliably identify the optimal solution for a bioprocess design problem within the number of generations used within this study. The reason that the EA reached a consistent optimal solution in fewer generations for the MC bioprocess than the PL bioprocess is likely to owe itself to the fact that the design space is smaller for the MC bioprocess scenarios than for the PL bioprocess scenarios; therefore the problem evaluated by the EA is less complex in this instance.

The accuracy of the EA must was evaluated by comparing the optimal solution found using the EA against that produced by a brute-force procedure, which analysed every possible bioprocess design for a given scenario. Table 5.8 shows the optimal solution and fitness value found for the SD-PL bioprocess strategy, and the SD-MC bioprocess strategy using both the EA and a brute-force procedure. The solutions found using the EA are consistent with those found using the brute-force approach. This illustrates that the EA used here is capable of accurately determining the optimal solution to the bioprocess design problem to which it has been applied.

The final measure of EA performance was the reduction in processing time that could be achieved using the EA when compared to the use of a brute-force procedure. To achieve this, a timer function that measured the running time was encoded within the algorithms used to execute the evolutionary and brute-force procedures. Whilst only one scenario was run for the respective PL and MC bioprocess strategies, it was possible to extrapolate a percentage in reduction in overall processing time that could be achieved using the EA procedure.

Table 5.9 shows the processing time in hours required to run the EA and the brute-force procedure for a scenario where an annual demand of 5,000 doses is satisfied via the production of 10 manufacturing lots (500 doses per lot). The time taken to run the EA in the SD-PL and SD-MC scenario is 0.56 hours. This compares to a time of

192.9 hours, which is required to run the brute-force procedure for the SD-PL strategy and a time of 14.3 hours to run the brute-force procedure for the MC strategy. When applied to the PL strategy, the EA results in a 99.7% saving in processing time compared a brute-force approach. This value is 96.1% when the EA is applied to the MC strategy. The reason that the EA results in a greater reduction in processing time for the PL strategy is that there are 15 technologies available for the RPE and differentiation unit operations when planar processing is considered; only 4 technologies are available when microcarrier-based processing is assumed. Therefore more iterations are required when the brute-force procedure is applied to the PL bioprocess strategies compared to when it is applied to the MC bioprocess strategies. Contrastingly, the number of iterations required of the EA is reliant solely upon the population size, ψ, the number of generations, *g*, and the number of runs, *r*. Therefore, the processing time required to run the EA is constant regardless of the bioprocess strategy considered. This explains the difference in values describing the percentage reduction in processing time that can be achieved when the EA is applied to the respective PL and MC bioprocess strategies in place of a brute-force procedure.

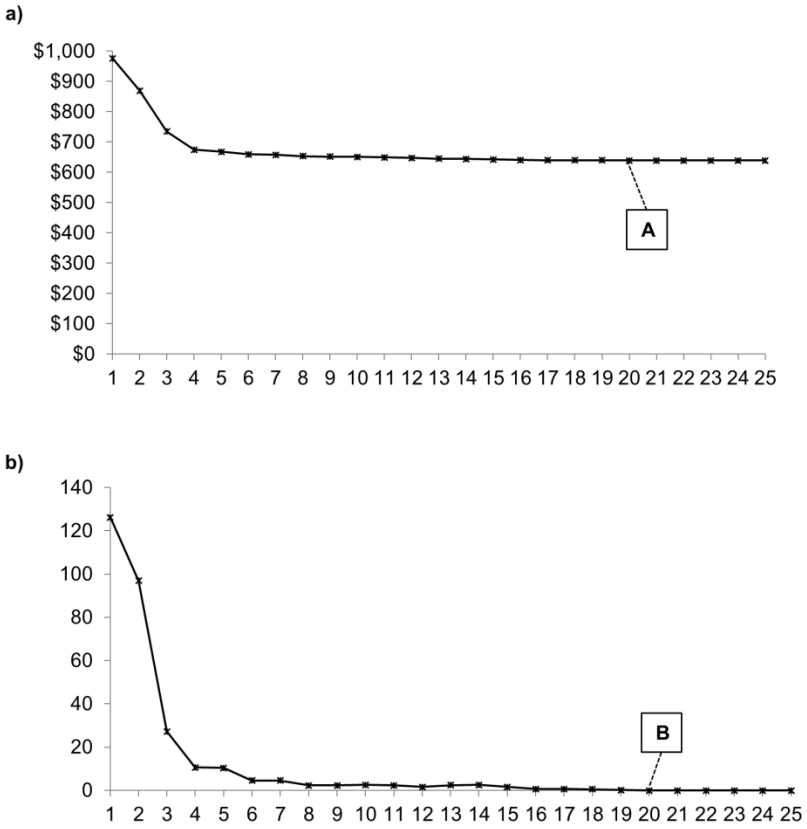

Figure 5.11 Line plots illustrating performance metrics for the EA when it was applied to the SD-MC bioprocess. **a)** Line plot showing the mean fitness value (in this instance the cost of goods per dose) of the best solution found across all five runs of the EA for each of the 25 generations. Point A identifies the point by which the optimal solution is found within all five EA runs, and the mean fitness value remains constant. **b)** Line plot showing the standard error of the mean fitness value across all five runs of the EA for each of the 25 generations. Point B identifies the point at which the solutions across all five runs become consistent, and that the standard error of the mean remains zero.

Table 5.8 Comparison of solutions found using brute-force algorithm compared to the EA at a lot size of 500 doses and annual demand of 5,000 doses

	SD-PL		SD-MC	
Algorithm used	Brufe-force	EA	Brute-force	EA
COG per dose	US$623	US$623	US$761	US$761
Optimal technologies (Expansion) (Diff 1) (RPE Culture)	cL-12[2] cL-12[2] T-225[1]	cL-12[2] cL-12[2] T-225[1]	cL-12[2] MC-1L [1] T-225[1]	cL-12[2] MC-1L [1] T-225[1]

Table 5.9 Comparison of the processing time required to run the EA as compared to the brute-force search algorithm at a lot size of 500 doses and annual demand of 5,000 doses

	SD-PL		SD-MC	
Percentage reduction in processing time as a result of using the EA as compared to brute-force algorithm	99.7%		96.1%	
Algorithm used	Brufe-force	EA	Brute-force	EA
Time taken (hrs)	192.9	0.56	14.25	0.56

Chapter 6: Application of multi-attribute decision making analysis to an allogeneic CAR-T cell bioprocess

6.1 Introduction

Many chimeric antigen receptor (CAR) T-cell therapies currently in development are autologous. This has been reflected by the focus of the majority of process design commentaries and analyses in this area to date (Kaiser et al. 2015; Levine 2015; Levine et al. 2017). However, recent advances have allowed the silencing of T cell receptor (TCR) expression on T cells derived from normal healthy donor so as to remove their alloreactive properties in order to avoid attacks on recipients' tissues and cells (Valton et al. 2015). This has paved the way for the development of allogeneic CAR-T cell therapies. A major advantage of an allogeneic CAR-T therapy is that it could be used as an off-the-shelf treatment in acute oncology cases if a patient is either too ill to provide their own T-cell sample, or if they cannot provide the requisite number of T-cells required for the manufacture of an autologous product. Further to this, universal cell therapies align with traditional scale-up strategies and greater economies of scale could be realised with such a product. Allogeneic CAR-T cell therapies have the potential to enable more affordable treatments when compared to their autologous counterparts that are estimated to command a price bracket of US$150k – US$650k (Pierson 2015; Walker and Johnson 2016; Hettle et al. 2017).

Advances in technologies have seen platforms such as the following being evaluated in cell therapy bioprocessing applications: gas-permeable vessels (e.g. G-Rex (Wilson Wolf, New Brighton, MN, USA)) (Vera et al. 2010), rocking motion bioreactors (e.g. Xuri Cell Expansion System (GE Healthcare, Chicago, IL, USA)), and contained, integrated bioprocess platforms (e.g. CliniMACS Prodigy (Miltenyi Biotec, Bergisch Gladbach, Germany)) (Kaiser et al. 2015). Further to this, technologies used for the

concentration of T-cell populations following cell culture have also improved. Spinning filter membrane technologies (Wegener 2014) (e.g. Lovo Cell Processing System (Fresenius Kabi, Lake Zurich, IL, USA)) and fluidised bed centrifuge systems (e.g. kSep (Sartorius, Göttingen, Germany)) (Sartorius Stedim 2016), along with integrated systems mentioned above where the cell culture chamber also acts as a centrifuge, now offer efficient means of cell concentration in a closed environment. This represents a welcome shift from more conventional, planar technologies that do not offer the process control, flexibility, or potential for scale-up associated with modern technologies. Despite these advances, cost of goods (COG) associated with the production of CAR-T cell therapies are still a major challenge facing products of this nature.

This chapter investigates bioprocess design associated with allogeneic CAR-T cell therapy manufacturing. Currently available technologies are considered from both an economic perspective (as shown in Chapters 4 & 5 for PSC-derived products), but also from an operational perspective in order to provide a representative case study demonstrating the application of multi-attribute decision making (MADM) analysis to the cell therapy bioprocessing field.

Multi-attribute decision-making (MADM) analysis provides a mechanism for qualitative, as well as quantitative attributes of a solution to a bioprocess design problem to be evaluated. MADM requires that all attributes are considered across an equivalent measurement scale, this is usually done by converting all attributes to dimensionless units on a finite rating scale. This method therefore allows preference decisions to be made on the basis of multiple attributes for an array of different problem solutions (Yoon and Hwang 1995). MADM analyses have previously been applied within various decision support tools in the biopharmaceutical sector in order to evaluate bioprocess designs on the basis of operational, environmental, and economic attributes (Suzanne S. Farid et al. 2005; Pollock et al. 2013).

This is the first instance of the application of a computational MADM analysis to a cell therapy bioprocess design problem.

6.2 Incorporation of MADM analysis into a decision support tool

MADM analysis was incorporated into the decision tool constructed in Microsoft Excel (Microsoft Corporation). This was done by adapting the typical tool architecture described in Figure 3.1 to include MADM analysis, as shown in Figure 6.1. In this instance, industry experts were asked to rate different process technologies on a scale of 1-10 for the operational attributes considered in this Chapter. These ratings made up the qualitative data described in Figure 6.1.

The bioprocess economics model was used to calculate quantitative data in order to compute the financial attributes (COG, fixed capital investment) considered in the MADM analysis. In order to capture the uncertainty in ratings and importance weightings assigned to each attribute considered within the MADM analysis, probability distributions were assigned a) to the ratings assigned to each attribute for each process design evaluated within the MADM analysis and b) the importance weightings assigned to each attribute considered in the MADM analysis. The probability distributions were then used as the inputs for a Monte Carlo simulation in order to characterise the variability in the weights and ratings of the financial and operational attributes.

The Monte Carlo simulation was set up and run as described in Section 3.6 of this thesis; the only difference being that input distributions were assigned to MADM inputs rather than process parameters in this instance. Section 3.7 recounts the methodology associated with the MADM analysis. This study aims to capture uncertainty associated with the MADM analysis. The resultant attribute weightings and decision matrix for the evaluation of allogeneic CAR-T cell therapy process designs can be found in Sections 6.3 & 6.4 of this chapter.

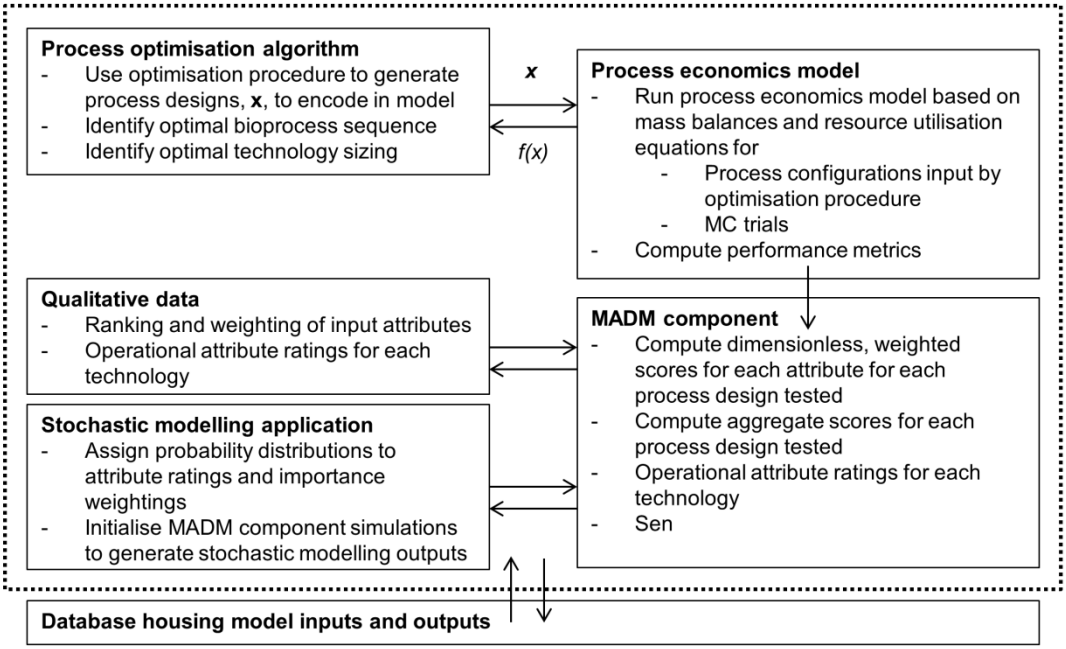

Figure 6.1 Decisional tool framework used within this chapter. The framework introduced in Section 2 has been adapted here to incorporate the MADM analysis. Information from the process economics model is fed into the MADM component of the tool, along with qualitative data obtained from responses to surveys completed by industry experts. Data was handled by the database in the same manner as previously described.

6.3 Case Study Setup

6.3.1 Tool Application

The decisional tool was applied to a case study designed to evaluate the use of different process technologies for the manufacture of an allogeneic CAR-T cell therapy product. At this time, and with limited clinical experience, it was estimated that CAR-T cell therapy dose sizes will vary depending on the target indication from ~10^4- 10^{12} cells per Kg, with the majority of those tested in the region of 10^6 – 10^9 cells per dose (Hartmann et al. 2017). The annual demand is also likely to vary dependent on target indication; rare haematological malignancies may only warrant an annual market size numbering in the low hundreds, whereas more common indications may

require thousands of doses per year. In this instance, a target dose size of 10^8 target cells and an annual demand of 1,000 doses was set as the base case scenario as these values are believed to be the near the midpoint. The effects of dose size and annual demand on COG were analysed using the bioprocess economics model; dose sizes ranging from 10^7 to 10^9 total cells and annual demands ranging from 500 to 5,000 doses were tested as the extremes using the model.

The bioprocess economics model was used to compute COG and FCI requirements for different bioprocess designs; these economic parameters were then combined with the operational ratings for different technologies in order to create a MADM rating for each process design tested using the tool.

The cost of manufacturing viral vectors is an important cost aspect in CAR T-cell therapy production, and more widely in gene therapy manufacturing. However, in this instance it was assumed the manufacturer outsoutced viral vector manufacturing to a CMO, the cost of viral vector produciton was therefore not considered in this case study and was considered as a 'per lot' cost. Furthermore, exploring the process economics of viral vector manufacturing is a subject for a significant body of research in itself and should be considered in future research.

6.3.2. Process Overview

The bioprocess in question is outlined in Figure 6.2, where it is broken down into unit operations. This process flowsheet differs from a typical autologous process in that additional unit operations in the form of electroporation and purification are required. Electroporation is utilised in order to transfer genetic material that silences the genes causing expression of T-cell receptor αβ (TCR). The silencing of TCR expression prevents alloreactivity of these cells upon transplantation to the recipient (Valton et al. 2015). Purification, or enrichment, of TCR^- cells at the end of the bioprocess is required (Figure 6.2) in order to attain a targeted level of purity of TCR^- cells amongst the total cell population that forms the therapy in this instance.

Three categories of cell culture technology were tested within the model; tissue culture flasks (TCFs), including T-flasks and manually operated stacked culture vessels; gas permeable vessels (GPVs); and finally rocking motion bioreactors (RMBs). Key input parameters regarding these technologies are Table 6.1.

The concentration technologies tested included fluidised bed centrifugation (FBC), spinning membrane filtration (SFM), automated media removal (AMR) – to be used in conjunction with GPVs only – and finally an integrated process technology offering the potential for cell culture, concentration and purification in a contained, all-in-one platform (INT). Key input parameters pertaining to concentration technologies can be found in Table 6.2, where data is also available for the purification technologies considered in this study; namely a standalone magnetic-activated cell sorting platform (MACS) and a MACS platform within the INT technology described above. Where INT is used for purification, the platform was also assumed to be used for concentration as well. Static cell culture bags were assumed to support transduction and activation unit operations, whereas electroporation was carried out using the AgilePulse machine (BTX, MA, USA).

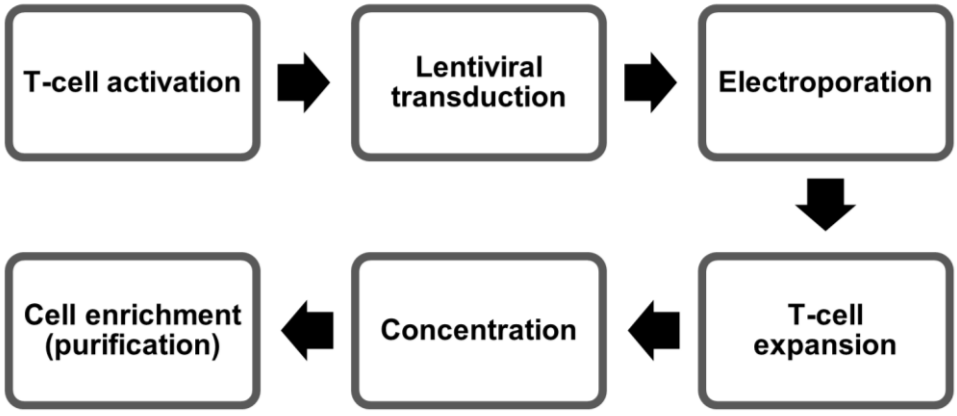

Figure 6.2 Process flowsheet for the production of an allogeneic CAR-T cell therapy.

A base case viral transduction efficiency of 70% was selected as it is within the range reported in (Yang et al. 2008), as well as consistent with values seen during process

development work carried out by Pfizer (data not shown). Within the sensitivity and scenario analyses, viral transduction efficiencies ranging from 50% to 90% were used. Key process and cost assumptions associated with the bioprocess, including reagent and material costs, labour costs, fixed capital equipment costs and specific process yields can be found in Table 6.2.

Table 6.1 Cell culture technologies considered within this case study and their associated performance and cost parameters

Equipment Type	Name	Volume (L)	Working culture volume (L)	Minimum Utilisation	Maximum Cell Density	Single-use vessel costs	Fixed equipment costs	Perfusion rate
Rocking Motion Bioreactor (RMB)	50L RMB	50	25	20%	3.50E+07	$793.75	67,500	30% - 100% of WV depending on cell concentration
	20L RMB	20	10	10%	3.50E+07	$778.13	67,500	
	10L RMB	10	5	10%	3.50E+07	$765.63	67,500	
	2L RMB	2	1	30%	3.50E+07	$739.06	67,500	
Planar culture flask (CF)	L-5	1575	1.6	100%	4.00E+06	$198.44	N/A[a]	Media addition based on cell population
	L-2	787.5	0.8	100%	4.00E+06	$183.59	N/A[a]	
	L-1	315	0.3	100%	4.00E+06	$73.57	N/A[a]	
	T225	50	0.05	100%	4.00E+06	$8.64	N/A[a]	
Gas permeable vessel (GPV)	GPC500	5.5	5.5	10%	4.00E+06	$951.50	15,000[a]	Media addition based on cell population
	GPC100	1.1	1.1	10%	4.00E+06	$190.30	15,000[a]	
	GPC10	0.1	0.1	10%	4.00E+06	$156.48	15,000[a]	
Integrated bioprocess platform (INT)	INT	3.8	0.65	4%	3.50E+07	$2,512.00	235,500	N/A

[a]Indicates that additional fixed equipment such as incubators and BSCs are required – please see table X for details on this equipment
WV = working volume

Table 6.2 – Cell concentration and cell purification (purification) technologies considered in this case study and their associated cost and performance parameters

Concentration Technologies							
Equipment Type	**Name**	**Maximum input**	**Maximum cell density**	**Viable cell yield**	**Target cell yield**	**Disposable equipment costs per run (US$)**	**Fixed equipment costs (US$)**
Fluidised bed centrifugation (FBC)	FBC	114	N/A	80%	N/A	1,800	281,000
LoVo	SFM	7.2L	1.6	85%	N/A	537	79,500
Integrated bioprocess platform (INT)	INT	3.5×10^{10} cells	0.65	86%	N/A	3,000	235,500
Purification Technologies							
Equipment Type	**Name**	**Maximum input**	**Maximum cell density**	**Viable cell yield**	**Target cell yield**	**Disposable equipment costs per run (US$)**	**Fixed equipment costs (US$)**
Stand-alone immuno-affinity purification	MACS	3.5×10^{10} cells	N/A	95%	80%	2,217	55,000
Integrated bioprocess platform-based immune-purification	INT	3.5×10^{10} cells	N/A	95%	80%	3,000	235,500

Table 6.3 Key cost assumptions used within the bioprocess economics model

Cost Parameter		Value
Media & Re-agents		
	Activation beads	US$454/mL
	Electroporation buffer	US$785/L
	TALEN plasmid	US$6,500/mg
	Expansion media	US$300/L
	LoVo buffer	US$100/L
	FBC buffer	US$80/L
	INT concentration buffer	US$300/L
	Purification buffer	US$2,157/L
	Purification re-agents	US$3,636 per 10^{10} cells
Labour		
	Operator cost	US$120,000/yr
Fixed Equipment		
	Incubator	US$27,000
	BSC	US$12,000
	AgilePulse electroporator	US$32,400
Process parameter		Value
Daily population doublings (cell culture)		1.38
Viral transduction efficiency		70%
Electroporation efficiency		70%

6.3.3 Multi attribute decision making under uncertainty: Attribute identification, ranking and weighting

The attributes tested within this case study fell into two categories; financial and operational. Attributes and their rank, in terms of importance, were determined via consultation with industry experts. The final list of attributes, the category to which they are assigned, and the importance weighting assigned to each attribute are listed in Table 6.4. Weightings have been assigned probability distributions to capture the uncertainty in these values. These distributions were utilised in the stochastic MADM analysis. The COG and fixed capital investment associated with each process design were selected as the financial measure used in the MADM analysis. The COG is a key quantitative measure of the cost-effectiveness of a bioprocess, and has therefore been included in this analysis. FCI represents the upfront costs required to build a new facility fit for housing a bioprocess. Typically, many companies involved in cell therapy product development are academic spin outs and SMEs (Maciulaitis et al. 2012). Many of these players are likely to view the upfront costs associated with a process design as a key factor to consider with regards to bioprocess design. Equally, larger companies may view high FCI costs as a significant risk associated with a particular project; FCI was therefore included in the MADM analysis.

Qualitative attributes, such as process control, and process containment are vital to the robustness and reproducibility of cell therapy bioprocesses. These are two areas upon which product quality is dependent. Furthermore, ease of scale-up and ease of operation are important attributes to capture in the MADM analysis. For instance, technologies such as AMRs are not commonly associated with high fixed equipment costs, unlike FBC and SFM units. It is important to translate these qualitative trade-offs into quantitative measures within the MADM analysis. The likely validation effort supported by different technologies is also important to capture. For example, technologies which rely on manual operators and are therefore more prone to human

error and may require additional validation studies in order to prove the consistency of product quality over multiple production lots.

Table 6.4 Attributes considered in the MADM analysis, along with their respective weightings and probability distributions

Attribute Category	Attribute Name	Importance Rank	Weighting
Financial	FCI	1	Uniform (90,100)
	COG per dose	2	Uniform (40, 100)
Operational	Process control	1	Uniform (85,95)
	Process containment	2	Uniform (65, 75)
	Ease of scale-up	3	Uniform (45, 65)
	Ease of validation	4	Uniform (30, 60)
	Validation effort	5	Uniform (10, 40)

6.4 Results and discussion

This section discusses insights from the process economics analysis of alternative whole bioprocess flowsheets for allogeneic CAR-T cell therapies. It provides a breakdown of the COG categories for each flowsheet as well as the bottlenecks and cost drivers in each case. The cost analysis is extended using a stochastic MADM analysis to weigh up the financial and operational attributes of each flowsheet.

6.4.1 Bioprocess economic analysis

The bioprocess economics model was used to compute COG and the achievable number of doses per lot (or per donor) for different bioprocess designs. The optimal equipment sizing regimes, where manufacturing COG was the objective function, for each of the process flowsheets was identified using the brute-force search method detailed in Section 3.5. The optimal equipment sizes for each process design (from

here on in referred to by their flowsheet number), in terms of category of technology used, are displayed in Table 6.5.

Figure 6.3 shows the relative COG per dose values, broken down into constituent cost categories, associated with each bioprocess flowsheet. Whilst the optimal process flowsheet (Flowsheet 2), in terms of COG, is highlighted in Figure 6.3, COG differences of <5% are considered insignificant due to the margin of error associated with the COG model. Percentage values above each column in the chart refer to the COG difference relative to the optimal flowsheet.

Table 6.5 Flowsheet configurations considered within the bioprocess case study (equipment sizes shown where relevant)

Flowsheet Number	Cell culture	Cell concentration	Cell purification (purification)
1	RMB (10L)	FBC	MACS
2	RMB (10L)	SMF	MACS
3	RMB (10L)	INT	INT
4	GPV500	AMR	MACS
5	L-5	FBC	MACS
6	L-5	SMF	MACS
7	L-5	INT	INT

Flowsheets 1-4, which all involve RMB or GPV as the cell culture platform, all lie within 10% of one another (Figure 6.3). However, Flowsheets 5-7, for which TCF is the cell culture platform, all have a COG value at least 20% larger than the Flowsheet 2 (optimal COG). Figure 6.3 shows that the major difference in the COG between flowsheets including TCF compared to those where cell culture is supported by RMB and GPV is the labour costs. Flowsheets 5, 6 and 7 require seven, seven and six cell

culture units respectively; this is compared to one unit for Flowsheets 1-3 and to two units for Flowsheet 4 (table insert, Figure 6.3). Hence, more operators are required for flowsheets that include TCF; this is reflected in the increased labour costs. This reinforces the greater scalability of RMBs compared to TCFs

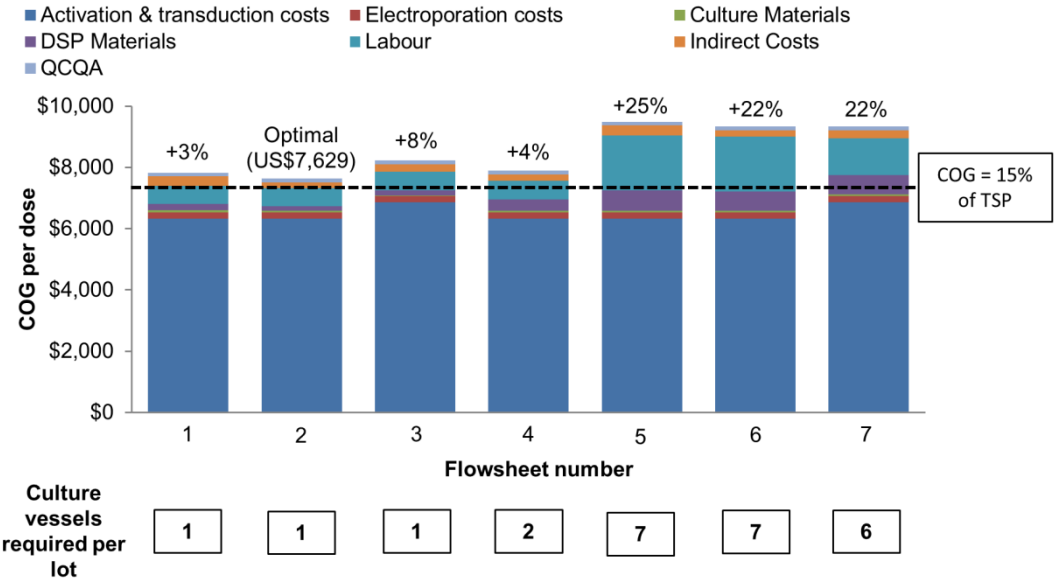

Figure 6.3 Stacked column chart displaying manufacturing COG breakdown per dose for each process design. Numbers on the x-axis refer to the process design numbers introduced in Table 6.5. The dashed line intersecting the y-axis at US$7,500 represents the COG value that is equal to 15% of target selling price. Panels inset below the x-axis indicate the number of culture vessels required per lot for each process design.

Capacity limitations and their consequences on lot size and number of lots required are illustrated by the capacity bottleneck schematics and inset panels for the four highest ranked flowsheets (determined by COG) in Figure 6.4. Indeed Flowsheet 3, where INT is used, can produce 78 doses per lot; this is compared to 90 doses per lot for Flowsheets 1, 2 & 4, where FBC, SMF and AMR are the respective concentration technologies. T. Therefore, because VT costs are calculated on a ‘per

lot' basis, Flowsheets 3 and 7 result in increased viral transduction costs compared to other flowsheets (Figure 6.3).

When INT is not considered for cell concentration, the capacity of current cell purification platforms is the limiting factor on the number of doses that can be produced per lot (Figure 6.4).

A target selling price (TSP) of US$50,000 was selected based on costs for marketed cellular therapies being in the range of ~US$1,000 to US$100,000 (Bravery 2012); an approximate midpoint of these values was chosen for calculations in this case study. However, at this time in the development of CAR-T cell therapies, it is not possible to determine what the actual selling price will be, but estimates are potentially in the several hundred thousand dollar range for autologous CAR-T cell products (Pierson 2015; Walker and Johnson 2016; Hettle et al. 2017). In the biologics industry typical values for COG as % sales are reported from 15% to 40% in order to recover R&D, sales and marketing costs (Smith 2012). In order to maximize the sensitivity model, a figure on the very low end of this range (15%) was selected (Smith 2012; Simaria et al. 2014; Hassan et al. 2015), which translates in to a COG target of US$7,500 in this case study.

6.4.2 Effect of dose size and annual demand on manufacturing COG

Different annual demands and dose sizes were investigated in order to test their effect on the manufacturing COG of the four highest ranked Flowsheets (according to COG), and whether the target of a COG value of less than 15% of TSP was realistic across these scenarios.

The trend displayed within Figure 6.5a, whereby COG per dose decrease as the annual demands increase in consistent with economies of scale that are associated with scale-up of allogeneic cell therapies; reductions in labour costs and the divestment of FCI costs across a larger annual demand are the causes of this. This

is concurrent with both current opinion in the field of cell therapy bioprocessing and previous analyses examining process economics in the cell therapy sector (Simaria et al. 2014), and data presented in Chapter 5.

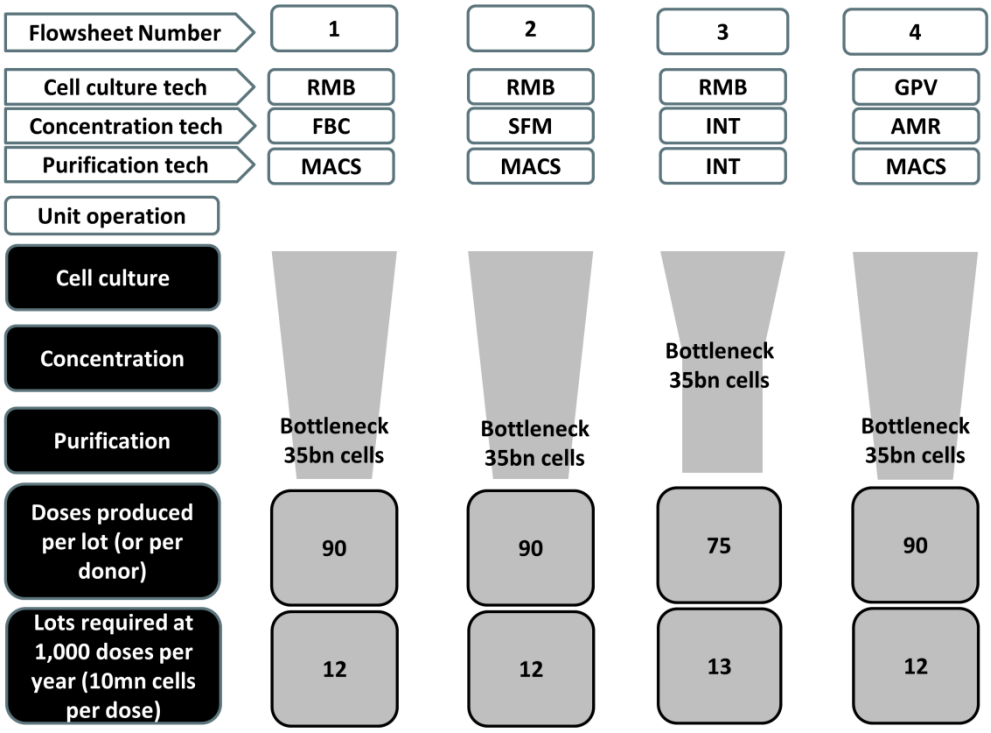

Figure 6.4 Schematic and inset panels summarising the capacity bottlenecks, doses produced per lot, and number of lots required per annum for the process flowsheets with the lowest COG per dose values. Unit operations are shown in the panels on the left of the figure. The capacity bottleneck (in terms of number of cells that can be handled) is overlaid for each process flowsheet and is positioned according to the unit operation where this occurs. This label indicates the unit operation whereby the number of cells that can be handled by the technology used within a given flowsheet is the limiting factor on the scalability of the process design.

At the highest tested annual demand of 5,000 doses per year, Flowsheet 2 still exhibits the lowest COG figure; this equates to ~13% of TSP, as shown by the scatter plot in Figure 6.5a – which displays COG values for the four flowsheets across the different annual demands. Flowsheets 1 and 4 also exhibit COG values that are less

than 15% of TSP. Only Flowsheet 3 exhibits COG > 15% of TSP; this is due to the increased viral transduction costs associated with this Flowsheet that are discussed in Section 6.4.1.

At annual demands of 500 doses per annum all four process flowsheets tested resulted in scenarios where COG>15% of TSP. As with other demands that were analysed, Flowsheet 2 resulted in the lowest COG figure, which was approximately 17% of TSP. Similarly, Flowsheet 3 proved to have the highest COG, whereby COG is equal to ~19% of TSP. At all annual demands the COG for Flowsheet 1 and Flowsheet 4 fell within 1% of each other's value, indicating that there is no significant difference between these process designs from a COG perspective.

Figure 6.5b shows that changes in COG associated with changes in dose size are more dramatic when compared with those associated with changes in annual demand (Figure 6.5a). For dose sizes less than 10^8 target cells, a COG per dose value of <=~15% of sales is achievable. For dose sizes of $5x10^8$ and above, manufacturing costs exceed far beyond this value; as high as 70% greater than TSP in the case of Flowsheet 3 at a dose size of 10^9 cells. As dose size increases, so too does the number of lots required per year. This is because number of doses produced per lot decreases as dose size increases. The dramatic rises in COG associated with increase in dose size observed in Figure 6.5b can be attributed to VT costs, which are carried out on a 'per lot' basis. Owing to the fact that large dose sizes result in COG that greatly exceed the 15% of TSP target set, therapies for indications that require increased dose sizes may prove challenging from a reimbursement perspective. The sales price achieved by a cell therapy will likely be determined by its quality and efficacy relative to currently available comparators, and key performance indicators as described by health technology assessments (HTAs).

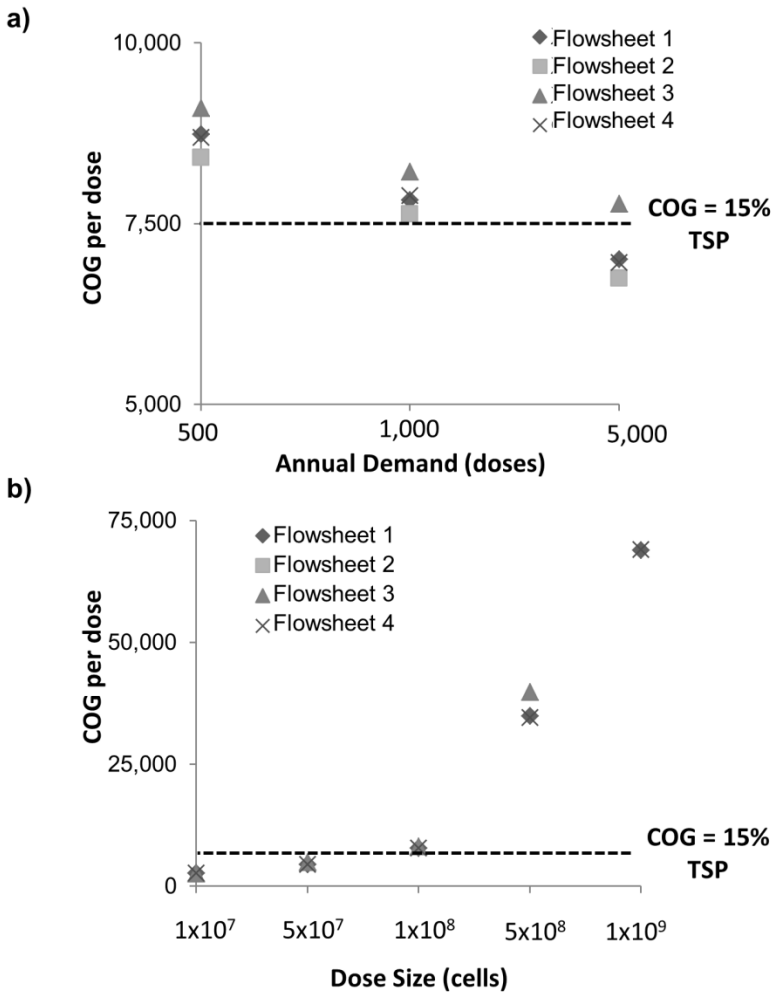

Figure 6.5 Scatter plots indicating the effect of **a)** annual demand and **b)** dose size on the manufacturing COG per dose for Flowsheets 1-4. Dashed lines on the plots that intersect the x-axis at US$7,500 indicate the COG value that is equal to 15% of target selling price.

6.4.3 Sensitivity analysis: identification of key process economic drivers

A sensitivity analysis was carried out in order to identify key process economic drivers associated with the process. Here, as with the same analysis carried out in Chapter 4, process input parameters were varied by ±15% of their original value in order to assess their impact on COG. For example, when the base case viral transduction efficiency, 70%, was varied by ±15% the worst case value was 59.5% and the best case value was 80.5%.

The tornado chart in Figure 6.6 illustrate the changes in COG that variations in input parameters effect. Transduction efficiency and electroporation efficiency proved to be the greatest economic drivers associated with this bioprocess, each resulting in a 30% swing in COG when altered by ± 15%. Both these parameters have a direct impact on the number of target cells that can be produced per lot; this is why they effect such a major change in COG when varied. Purification technology capacity was ranked third in the sensitivity analysis. Figure 6.4 shows that the capacity of currently available cell purification technologies causes a capacity bottleneck; therefore, an increase in this parameter would increase achievable lot sizes and thus reduce the number of viral transduction process required to satisfy annual demands. The tornado charts show that the cost of goods per lot of viral transduction has a significant impact on COG; it is the parameter ranked fourth in the sensitivity analysis. This is to be expected given the fact that the cost of viral transduction dominates the COG breakdowns shown in Figure 6.3.

Finally, it is of note that variations in the cell culture expansion fold have little impact on COG. This is in contrast to the data presented in Chapter 4, whereby cell culture expansion fold (expressed as number of expansion stages required) was a key process economic driver. However, in this instance it has little effect because of the DSP capacity bottlenecks mentioned in Section 6.4.1; a higher expansion fold may create incremental reductions in material costs associated with cell culture, but will not impact on the number of doses that can be produced per lot.

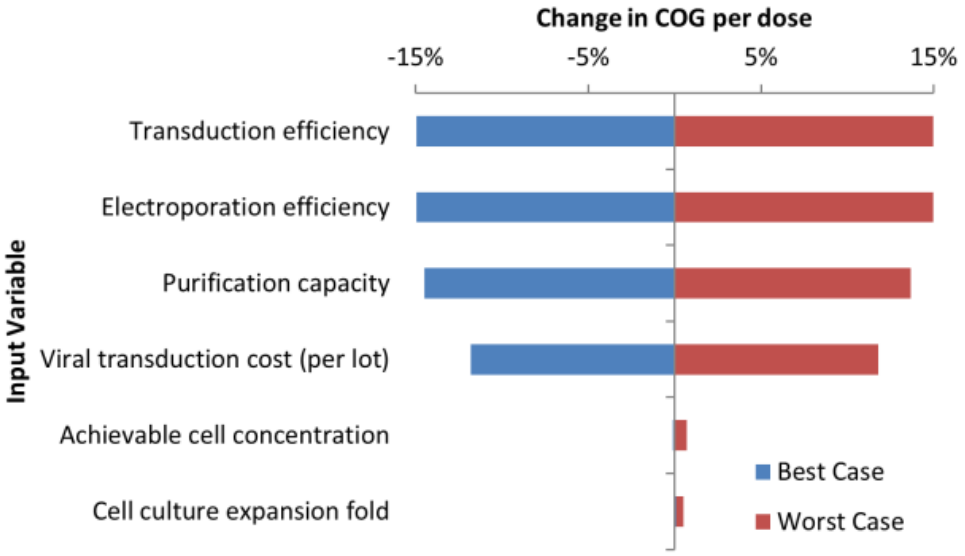

Figure 6.6 Tornado charts showing the effect that a ±15% change in key parameters has upon the manufacturing COG per dose in terms of a percentage change. Best case values, whereby COG per dose decrease relative to the base case are shown in blue. Worst case values are shown in red.

6.4.4 Scenario Analyses

Based on the results of the sensitivity analysis described in Section 6.4.3, scenario analyses, or gap analyses, were carried out in order to identify process improvements or cost reductions necessary to achieve a target COG value. In these analyses, the impact of simultaneously varying two or more key economic drivers upon the COG was measured. This allowed the identification of the amount by which current process yields and efficiencies, or process costs, need to improve in order to hit a target COG. Analyses were performed using Flowsheet 2 as the basis for improvements in COG as this design resulted in the minimum COG per dose value.

The process parameters varied in this analysis were the transduction efficiency and electroporation efficiency. These parameters were chosen because they were identified as key economic drivers by the sensitivity analysis. Furthermore, both viral transduction technologies and mRNA plasmids used in electroporation have seen

rapid advances in recent years and it is feasible that further improvements in the efficiencies observed in these unit operations could be achieved.

Additionally, the cost of viral transduction per lot was tested in the scenario analyses, as was the capacity (in terms of number of cells) of cell purification platforms. Again, these were shown to be key economic drivers in the sensitivity analysis (Section 6.4.3). The price to the cell therapy manufacturer in this instance is negotiated with a contract manufacturing organisation (CMO), which is assumed to produce the viral vector used in the transduction stage of the bioprocess. This results in a 'viral transduction cost per lot'. As with other bioprocess sectors (not least the cell therapy field); advances in the technologies and reagents used in the production of viral vectors are being made. This is likely to result in reduced COG for the CMOs producing viral vectors; it is therefore not unreasonable to assume that cell therapy manufacturers will put pressure on these CMOs to reduce the selling price to reflect this. Thus, the cost of viral transduction may be reduced.

Purification technologies are limited in capacity and throughput; this has been the subject of many commentaries and reviews within the cell therapy bioprocess field (Weil and Veraitch 2013; Weil et al. 2017). As competition amongst manufacturers of purification platforms increases, and as demand from the process sector increases, it is likely that the capacities of these technologies will increase.

Having explored whether current processes can meet a cost target of COG as 15% TSP earlier (Figure 6.3), further scenarios were then carried out to see how much better the performance would need to be if the target was COG had to be even lower, set at 10% TSP. Figure 6.7a indicates that viral transduction efficiency must be increased to 90% from 70%, along with a 22% increase in the purification capacity from the base case scenario, in order to achieve a COG as 10% TSP (Point B, Figure 6.7a). Alternatively, a 50% increase in purification capacity and a minor increase in viral transduction efficiency to 73% could achieve this target (Point A, Figure 6.7a).

This is a similar scenario to that where both reductions in the viral transduction cost per lot, and the viral transduction efficiency are varied. Point A in Figure 6.7b illustrates that a reduction in viral transduction costs per lot of 38% is required, assuming viral transduction efficiency remains at the base case value. However, as shown by Point B in Figure 6.7b, improvements in viral transduction costs alone are not sufficient to achieve COG equal to 10% of TSP. Furthermore, when both viral transduction and electroporation efficiencies are varied (Figure 6.7c), when electroporation efficiency is increased to 84%, viral transduction efficiency is required to be 90% for COG equal to 10% of TSP to be achieved.

Figures 6.7b and 6.7c indicate that significant process improvements are required in order to reach COG values equal to 10% of TSP, particularly if the capacity of cell purification platforms were to remain unchanged. Therefore, to analyse whether an increase in process capacity at the cell purification stage would have an effect on the required process improvements in other areas in order to achieve COG equal to 10% of TSP, the scenarios described by Figures 6.7b and 6.7c were re-run under the assumption that the capacity of the cell purification technology had increased by 25% (Figure 6.7d & 6.7e). Direct cost fluctuations that would be associated with this increasedl purification technology capacity were also considered in COG computations.

Figure 6.7d illustrates that if a 25% increase in cell purification technology capacity is assumed, then a 21% reduction in the viral transduction cost per lot will result in COG equal to ~10% of TSP (Point A, Figure 6.7d). Furthermore, if viral transduction costs can be improved from 70% to 88% then COG equal to 10% of TSP can be achieved (Point B, Figure 6.7d). If the capacity of cell purification platforms improved by 25%, electroporation efficiency must be improved from 70% to 89% to achieve COG equal to ~10% of TSP (Point B, Figure 6.7a).

The scenario analyses in this section offer evidence that allogeneic CAR-T cell therapies can achieve COG values as a percentage of TSP similar to early biopharmaceutical products. They also illustrate how COG of 10% of TSP may be achieved. Depending on what are deemed to be the most feasible or achievable process improvements, the window of operation will be directed towards different regions of the contour plots. For instance, if viral transduction efficiency can be easily improved then process engineers may target Point B in Figures 6.7a-e, however if improvements in other parameters prove more feasible, then a window of operation whereby COG ≈ 10% of sales close to Point A in Figures 6.7a-e may be targeted. However, at this time in development, it must be emphasized that both COG and TSP are not definitively known as there as currently no examples of marketed therapies in this space, and as such, the model should be used as a tool to determine the relative importance of altering various process parameters on COG

In order to reduce COG, it is likely that improvements in current process technologies will be required (Figures 6.7a, d & e). Previous case studies and reviews have commented on the lack of scalable, high resolution purification (sometimes referred to as purification) platforms (Weil and Veraitch 2013; Weil et al. 2017). The scenario analyses above indicate that improvements in this area of cell therapy bioprocesses, alongside the maximisation of potential yields of target cell types via the improvement of vector delivery systems, are key to reducing the manufacturing COG burden associated with allogeneic cell therapy bioprocessing. Whilst these scenario analyses provide an example of where process development efforts can be focused in order to provide maximum COG reductions, future work should also consider the cost of development in order to produce the improvements discussed above. The overall impact this might have on projet valuation metrics should be considered in order to fully understand the cost-benefit trade-off of such development efforts.

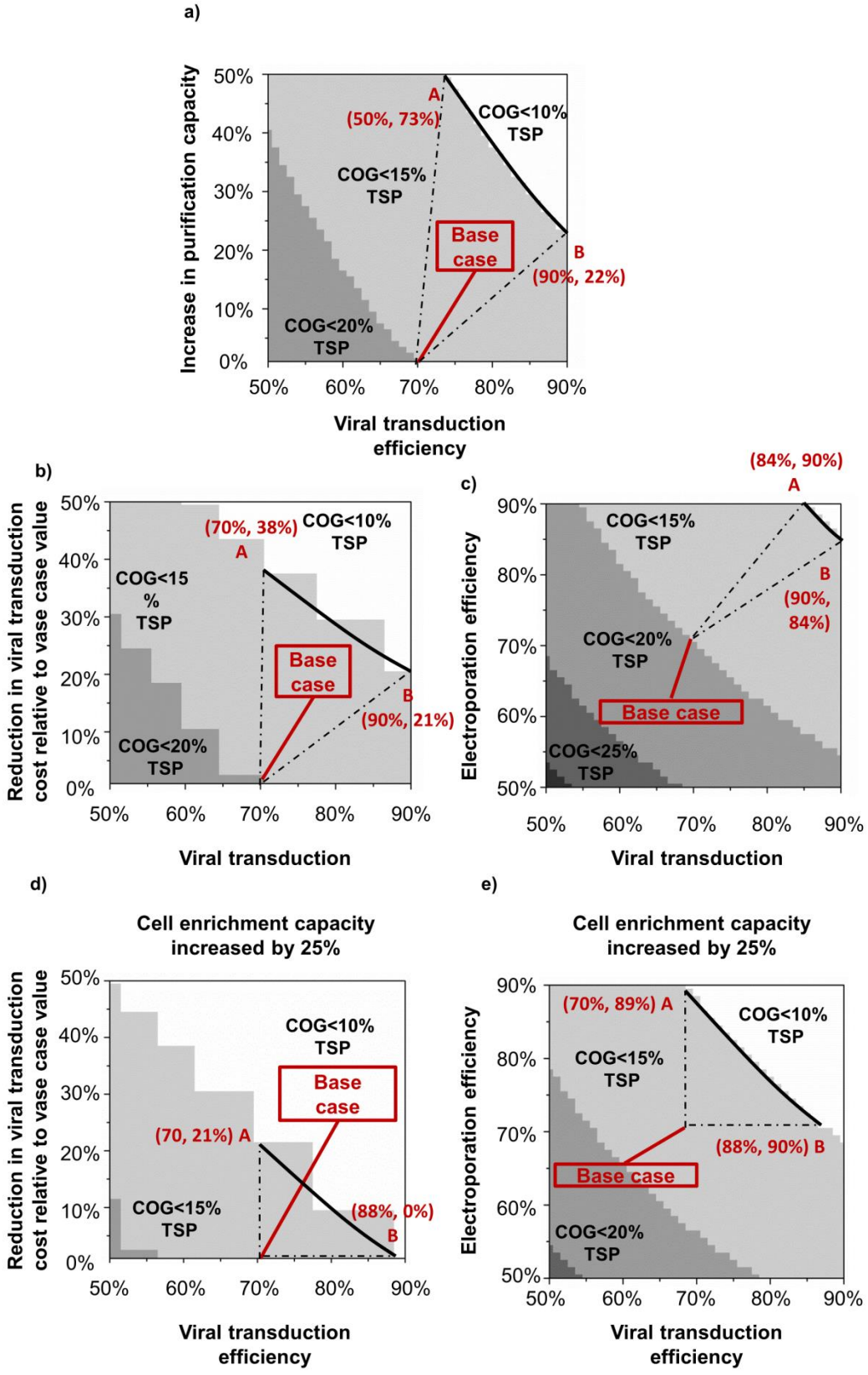

Figure 6.7 please see next page for figure legend

Figure 6.7 Contour plots that illustrate improvements in key process and cost parameters required to achieve COG value ≈ 10% of target selling price (TSP). Point A indicates the point on the contour lines shown in each plot whereby **a)** improvements in cell purification technology capacity, **b) & d)** the reduction in viral transduction cost per lot, and **c) & e)** electroporation efficiency is maximised in order to achieve COG ≈ 10% of TSP. Point B indicates the point on the contour lines shown in plots **a) – e)** whereby viral transduction efficiency is maximised in order to achieve COG ≈ 10% of TSP. Plots **b) & c)** consider scenarios where the capacity of cell purification technology remains at the base case value. Point A on the respective plots indicates the required bioprocess performance whereby COG is safely below 15% of TSP. Plots **d) & e)** consider scenarios where the capacity of cell purification technology is assumed to be 25% greater than the base case scenario.

6.4.5 The effect of parallel DSP processing on capacity bottlenecks and COG

In Chapter 3, the fact that only one DSP unit per process has been permitted was outlined, to prevent parallel processing of samples and pooling of process streams following DSP operations. In order to evaluate the effect that the permission of running DSP operations in parallel had upon the bottlenecks associated with the bioprocess basic equipment sizing calculations were run for a scenario whereby multiple DSP units were permitted to process each donor's sample. The results of this analysis for the four key process flowsheets are detailed in Figure 6.8. The results indicate that purification would no longer be the bottleneck or restricting factor on the scalability of the bioprocess and that the number of doses produced per lot would range from 311 to 334 as oppose to 75 to 90 as was previously described. Interestingly, Flowsheet 3, containing the Prodigy would now allow for the greatest number of doses to be produced per lot; previously this Flowsheet produced the smallest number of doses per lot.

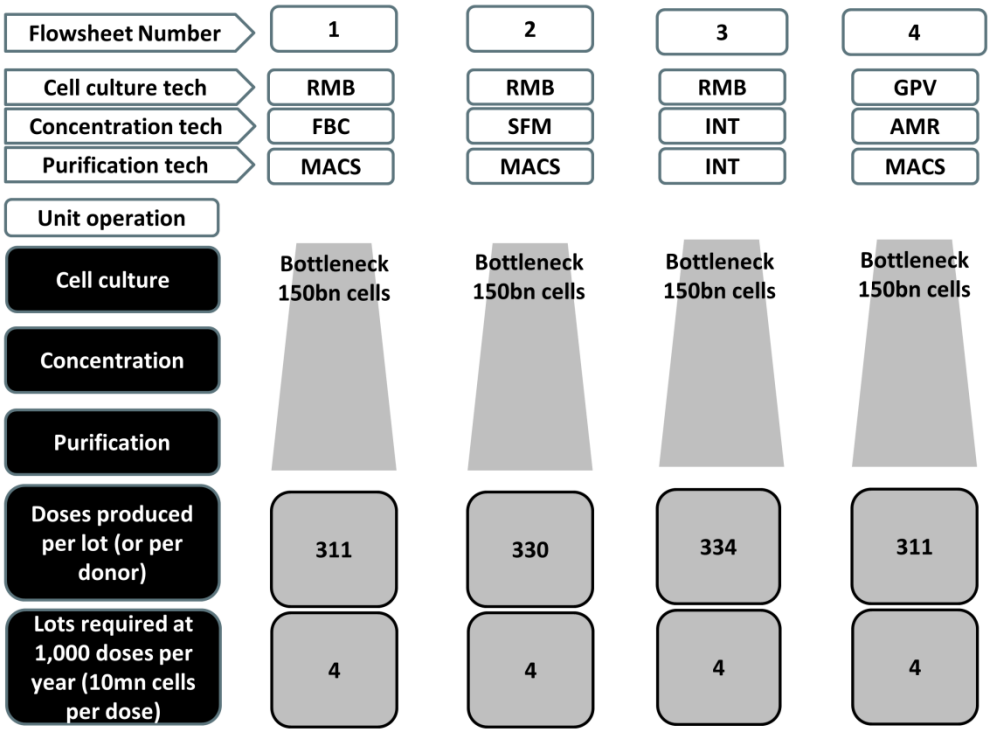

Figure 6.8 Schematic and inset panels summarising the capacity bottlenecks, doses produced per lot, and number of lots required per annum for the process flowsheets with the lowest COG per dose values. Unit operations are shown in the panels on the left of the figure. The capacity bottleneck (in terms of number of cells that can be handled) is overlaid for each process flowsheet and is positioned according to the unit operation where this occurs. This label indicates the unit operation whereby the number of cells that can be produced due to process limitations is a constraining factor on the scalability of the bioprocess.

The permission of parallel DSP processing also has a significant impact upon COG. This is evidenced in Figure 6.9, where Flowsheet 3 is now the optimal process platform from this perspective. Interestingly, it is possible to achieve a COG < 15% of TSP with Flowsheets 1-4 in this scenario. Multiple GPV reactros are required in order to culture the 150billion cells that the expansion process is capable of producing. Therefore labour costs increase significantly for this technology compared to larger technologies such as the RMB technology. The COG for Flowsheet 2, when only one

DSP unit per lot is permitted, have been included for comparison. Across all flowsheets in the new scenario, where parallel DSP is permitted, activation and transduction costs are reduced significantly compared to the scenario when only one DSP unit per lot is permitted. This is because the number of lots required to satisfy 1,000 doses per year has been reduced from 12 to four. Viral transduction costs are calculated on a per lot basis and can therefore be reduced in the number of lots per year can also be reduced. Overall, this analysis suggests the COG can be significantly reduced if parallel DSP processing is permitted. Equally, the process can be de-bottlenecked at the purification stage of the process in this scenario.

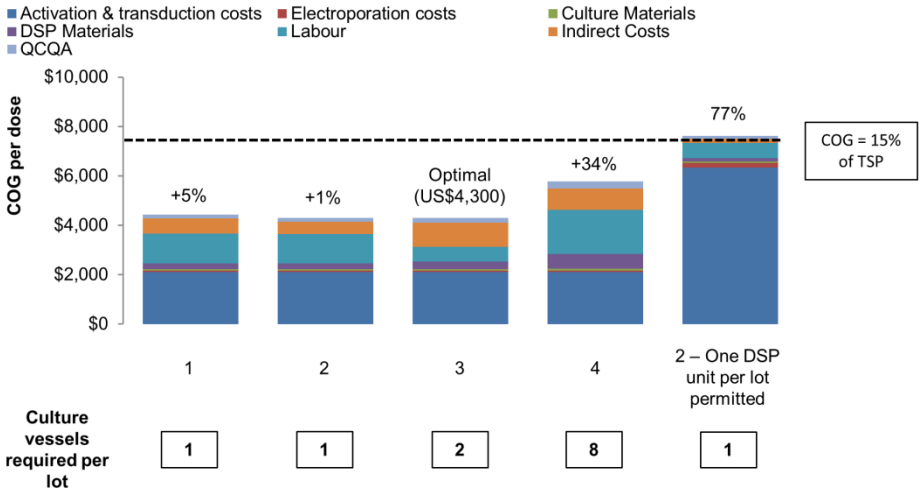

Figure 6.9 Stacked column chart displaying manufacturing COG breakdown per dose for each process design. Numbers on the x-axis refer to the process design numbers introduced in Table 6.5. The dashed line intersecting the y-axis at US$7,500 represents the COG value that is equal to 15% of target selling price. Panels inset below the x-axis indicate the number of culture vessels required per lot for each process design.

6.4.6 Multi attribute decision making analysis under uncertainty

MADM analysis was applied in this case study in order to evaluate potential process designs on the basis not only of financial attributes, but also operational attributes. In this case study, the use of MADM proved particularly instructive due to fact that the four top-ranked process flowsheets from a COG perspective all resulted in COG values within 10% of the optimal solution. MADM analysis was therefore be used to definitively select between different process designs in this instance. A stochastic MADM analysis was applied to Flowsheets 1, 2, 3 & 4, as defined in Section 6.3.2. An online of the methodology used to calculate aggregate scores can be found in Section 3.7.

Uncertainty data was incorporated into the ratings given to the qualitative operational attributes for each technology by assigning appropriate probability distributions. Triangular distributions were assigned to each attribute for each flowsheet, to represent their minimum, most likely, and maximum values. The resultant decision matrix for the evaluation of the four bioprocess flowsheets is therefore shown in Table 6.6.

Qualitative operational benefits

Table 6.7 contains the mean dimensionless ratings scored by each process flowsheet for each attribute when evaluated using the stochastic MADM analysis. The data contained within Table 6.7 indicates that Flowsheet 3 ranks highest for process control amongst the four flowsheets. This is due to the INT platform's ability to run both concentration and cell purification unit operations within a controlled environment in an automated manner. This attribute was ranked the most important amongst respondents to a survey sent to bioprocess professionals. Process containment, referring to a bioprocess' ability to run without exposure to the surrounding environment was also ranked high in terms of its importance amongst operational attributes. Flowsheets 1, 2 & 3 all achieved high ratings amongst

respondents for this attribute. Table 6.7 shows that Flowsheets 1, 2 & 3 containing rocking motion bioreactors were rated favourably compared to Flowsheet 4, containing GPV, for all operational attributes aside from ease of operation. This is due to the automated media removal device used for media exchanges associated with GPV as oppose to complex perfusion culture strategies used within the RMB platform. In order to test whether the apparent operational benefits associated with Flowsheets 1 and 3 outweigh the high score achieved for the FCI attribute achieved by Flowsheet 4, it was necessary to consider the aggregate scores achieved by each process flowsheet in the MADM analysis.

Table 6.6 Decision matrix for the evaluation of different process designs

Attribute	Original rating data				Feasible Range	
	Flowsheet 1	Flowsheet 2	Flowsheet 3	Flowsheet 4	Worst Value	Best Value
COG per gram	7,829	7,630	8,220	7,888	9,500	6,500
FCI	932,574	556,797	703,097	623,397	500,000	1,000,000
Process control	Triang(6.8, 7.3, 7.8)	Triang(6.8, 7.3, 7.8)	Triang(5.5, 6.0, 9.5)	Triang(5.2, 5.7, 6.2)	0	10
Process containment	Triang(8.2, 8.7, 9.2)	Triang(8.2, 8.7, 9.2)	Triang(8.5, 9.0, 9.5)	Triang(5.5, 6.0, 6.5)	0	10
Ease of scale-up	Triang(6.5, 7.0, 7.5)	Triang(5.8, 6.3, 6.8)	Triang(6.0, 6.5, 7.0)	Triang(5.0, 5.5, 6.0)	0	10
Ease of operation	Triang(6.2, 6.7, 7.2)	Triang(6.8, 7.3, 7.8)	Triang(6.5 ,7.0, 7.5)	Triang(7.8, 8.3, 8.8)	0	10
Validation effort	Triang(6.5, 7.0, 7.5)	Triang(6.2, 6.7, 7.2)	Triang(5.5 ,6.0, 6.5)	Triang(5.2, 5.7, 6.2)	0	10

Table 6.7 Summary of weighted dimensionless ratings for each attribute and process flowsheet tested within the MADM analysis

Parameter	Flowsheet			
	1	2	3	4
COG per dose	75	84	58	73
Fixed capital investment	5	40	26	34
Ease of operation	22	25	23	28
Process control	63	63	50	47
Validation effort	10	9	8	8
Ease of scale-up	37	32	34	28
Process containment	60	60	62	39

Multi-attribute decision making analysis under uncertainty

The cumulative frequency distribution of the aggregate score of the alternative process flowsheets was generated and is displayed in Figure 6.10. Initially, equal importance of operational and financial attributes was assumed (i.e. $R_1 = R_2 = 0.5$).

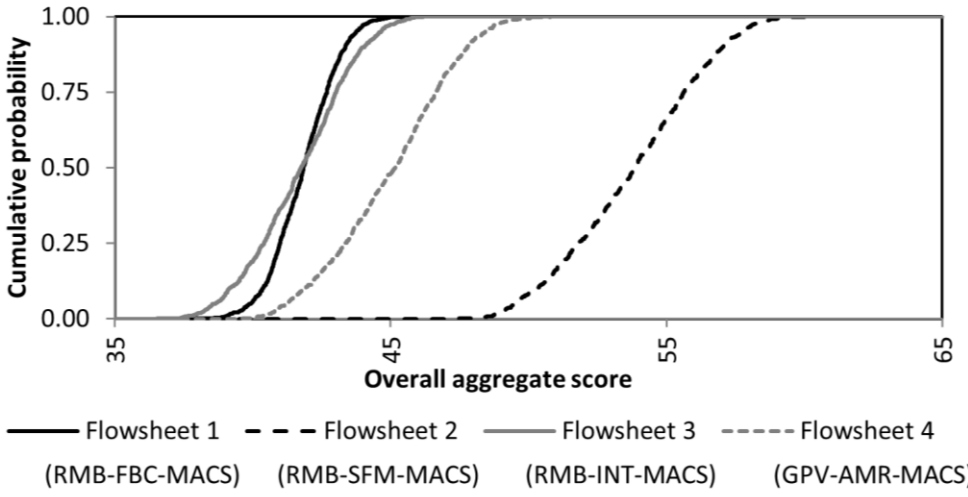

Figure 6.10 Cumulative frequency curves showing the spread of aggregate MADM scores as under uncertainty. Aggregate scores were generated over 1,000 Monte Carlo simulations.

The cumulative frequency curves for Flowsheets 2 and 4 do not intersect with each other, or any other curves on the chart. However, Flowsheets 1 and 3 intersect with one another just above the median value. Flowsheet 1 achieved a preferable aggregate score compared to Flowsheet 3 in 51% of Monte Carlo simulations. Flowsheet 3 also resulted in the greater range of values compared to Flowsheet 1. This indicates that the uncertainty associated with Flowsheet 3 is greater than Flowsheet 1, and therefore whilst the median aggregate scores are approximately equal, it may be that Flowsheet 1 is considered preferable to Flowsheet 3 due to the reduction in variability of its aggregate score. Flowsheet 2 is clearly the preferred alternative of all the options presented in Figure 6.10. It is therefore possible to rank the alternatives in order of preference; Flowsheet 2, Flowsheet 4, Flowsheet 1, Flowsheet 3.

Multi-attribute decision making analysis: Sensitivity to financial and operational weightings

The results of reconciling trade-offs between financial and operational outputs using a single multi-attribute score are discussed in this section. Previous sections of this work have focused on identification of the preferred process design when operational and financial attributes were given equal ratings. Here, overall strategy scores were calculated for each process design using MADM analysis across a range of combination ratios. These combination ratios reflect the relative importance of financial and operational attributes in process design. The financial combination ratio, $R_{1,}$ and the operational attribute combination ratio, R_2 were assigned such that $R_1 + R_2 = 1$ under any circumstance. Therefore if one combination ratio is varied, the other is adjusted to reflect this change.

In this instance, the weightings assigned to each individual attribute were kept constant and were not subject to uncertainty. The average weightings assigned to

each attribute during the Monte Carlo simulation described previously in this section, shown in Table 6.4, were applied for the purposes of this deterministic analysis.

The combination ratios were then assigned a values ranging from 0 to 1 (at intervals of 0.1). Figure 6.11 depicts the sensitivity of the overall aggregate score for each flowsheet to the financial and operational combination ratios at an annual demand of 1,000 dose per year and a dose size of 10^8 target cells per dose.

If the operational attributes are considered approximately twice as important as the financial attributes (R_2=0.65, R_1=0.35), Flowsheet 4 is ranked bottom of the four flowsheets tested using MADM. However, when financial attributes are considered at least as important as economic attributes (R_1=R_2=0.5), Flowsheet 4 is ranked above Flowsheets 1 and 3, despite all flowsheets obtaining a similar ranking for COG per dose. Flowsheet 4 is ranked favourably to Flowsheets 1 & 3 due to its superior FCI ranking; the GPV technology is characterised by low FCI costs. Flowsheets 1 & 3 are ranked approximately equally across scenarios tested; they scored similarly in both economic and operational categories. Flowsheet 3 is favoured slightly owing to the greater process containment offered by this strategy, and a reduction in FCI costs. Indeed in scenarios where operational attributes are considered 9 times (or greater) the importance of economic attributes, Flowsheet 3 is the top ranked technology, although the difference between the aggregate scores for Flowsheets 1, 2 and 3 in these instances are not significant. Flowsheet 2 is the top ranked flowsheet in all other scenarios tested; it offers significant operational and economic benefits in comparison to Flowsheet 4 due to the process containment and process control offered by RMB cell culture devices.

The FCI rating for Flowsheet 3 is also significantly higher than Flowsheets 1 and 2, due to the relatively low cost of the SMF technology, as opposed to FBC or INT, used for cell concentration.

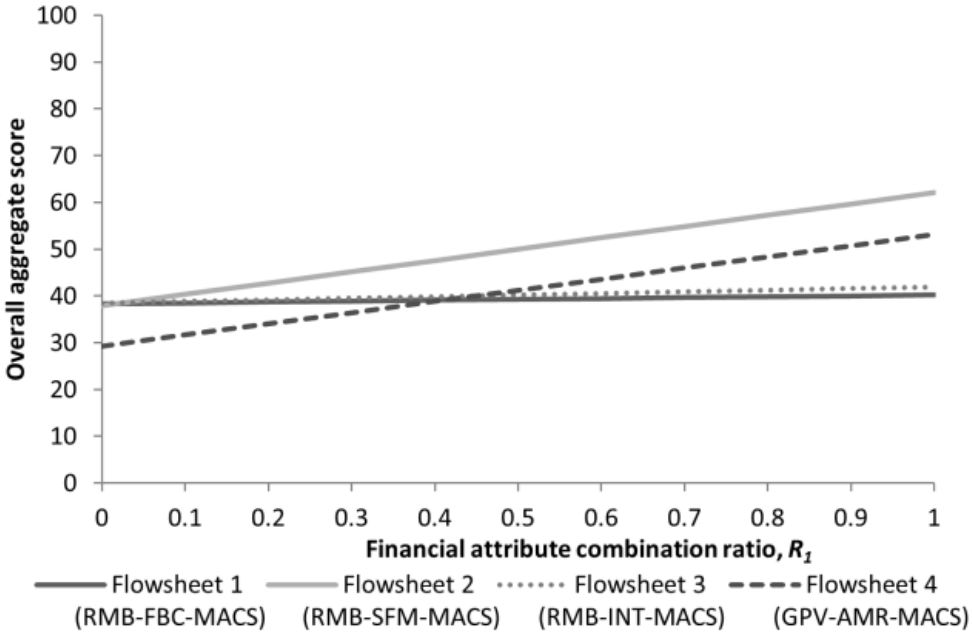

Figure 6.11 Spider plots showing depicting the sensitivity of the overall aggregate MADM score for each process design to variations in the financial attribute combination ratio, or the importance given to financial attributes within the MADM analysis. The sum financial attribute combination ratio (R_1) and operational attribute combination ratio (R_2) (not shown on chart) are always equal to 1.

6.5 Conclusion

A case study has been presented whereby a decisional tool, consisting of a bioprocess economics model, information database, and MADM analysis, has been developed in order to facilitate decision making with regards to process design for an allogeneic CAR-T cell manufacturing process. Cost-effective equipment sizing regimes were identified for alternative process flowsheets. Flowsheets consisted of a variety of different technology platforms to support cell culture, concentration of cells, and purification of target cell populations. The difference in COG values of three of the process designs evaluated within the study did not exceed 10% compared to the most cost-effective design (in terms of COG per dose). It was found that using tissue culture plastic cultureware such as T-flasks and multilayer vessels proved to be

significantly more costly than rocking motion bioreactors or gas permeable vessels. A sensitivity analyses indicated that viral transduction efficiency, electroporation efficiency, viral transduction cost per lot and the capacity of downstream processing equipment (in terms of cell numbers) were the key process economic drivers; improvements required to bring about a COG per dose value significantly below 15% of target selling price were subsequently identified using scenario analyses. MADM analysis was also able to identify that the flowsheet consisting of rocking motion bioreactor, spinning filter membrane, and a standalone MACS platform as the preferred process design when both financial and operational attributes were taken into account. Future work in this section may focus upon a more wide-ranging study of available technologies to consider additional process designs. Furthermore, comparisons between allogeneic and autologous CAR-T cell COG should be made in order to identify scales whereby one product type is more economically viable than the other. This analysis must also take into account the fact that both allogeneic and autologous therapies may not be feasible or indeed available depending on the condition of the patient and indication targeted.

7. Conclusion & Future Work

7.1 Conclusions

The work presented in this thesis has focused on the development of a series of decisional tools in order to demonstrate their applicability to the field of cell therapy bioprocessing. The tools developed within this work have aimed to capture the technical, financial and operational aspects of cell therapy bioprocessing. Additionally, process related uncertainties, inherent in current cell therapy bioprocess techniques, were captured using stochastic risk modelling.

The applicability of the tools was demonstrated through a series of industrially relevant case studies. Namely, a series of tools were developed that evaluated strategies for the production of patient-specific iPSC-derived cell lines for drug screening purposes, the manufacture and distribution of a low dose allogeneic hESC-derived therapy, and the production of an allogeneic CAR-T cell therapy.

An investigation into the techniques and technologies used to produce cell therapies enabled the identification of common unit operations, such as tissue acquisition, cell culture, and harvest of cells, across production processes for different cell therapies. In addition to the identification of common unit operations, processes specific to the manufacture of certain types of cell therapy were also identified. These included differentiation of hPSCs to target cell types, viral transduction and electroporation required for the genetic modification of T-cells in the production of allogeneic CAR-T cell therapies, and cell purification (or purification) steps in order to select for a subset of target cells amongst a broader population. The aforementioned investigation enabled the development of prototype bioprocess flowsheets for each case study; these flowsheets were subsequently used as the basis of which unit operations were included in the decisional tools that were developed.

Following the investigation into current practices within cell therapy bioprocessing, a series of computational tools were developed and were set-up according the methods and framework set up in Chapter 3. A Brute-force algorithm was applied in Chapter 4 as a means of identifying optimal bioprocess designs according to an objective function, in this instance this was the manufacturing cost of goods per unit. However, when faced with a case study that presented a large problem domain, as in Chapter 5, an evolutionary algorithm was developed in order to streamline the identification of optimal bioprocess design. Chapter 6 demonstrates the applicability of multi-attribute decision making (MADM) to cell therapy bioprocessing; here, a combination of financial and operational attributes were evaluated in order to provide a more holistic analysis of available process designs.

The bioprocess economics associated with manufacturing patient-specific iPSC-derived cell lines for the purposes of drug screening were investigated using a decisional tool in Chapter 4. A case study was developed that compared manual and automated bioprocess strategies. In this instance the tool was used to carry out equipment sizing calculations and produce data with which to carry out economic analyses of different process designs. Via the use of a decisional tool, it was determined that the most cost-effective process design (manual or automated) was dependent upon the scale and the throughput of the bioprocess. Key economic drivers were identified and stochastic modelling outputs suggested that automated platforms resulted in a more robust bioprocess. Finally, it was determined that indirect cost reductions are required in order to achieve an acceptable COG value for in-house manufacture of iPSC-derived cell lines for drug screening. Owing to the demonstration of the applicability of the tool to a non-GMP process, it was hypothesised that such a tool could also be applicable to GMP based production of cell therapies.

In Chapter 5, a decisional tool was applied to a process design problem involving the scale-up of a manufacturing process for a low dose, allogeneic, hESC-derived RPE therapy for the treatment of macular degeneration. An incumbent bioprocess, which contained a lengthy and inefficient spontaneous differentiation protocol, was compared to a directed differentiation protocol. Additionally, the use of planar-based technologies was compared, from a cost of goods perspective, to microcarrier-based differentiation in stirred suspension bioreactors. An evolutionary algorithm was incorporated into a decisional tool in order to streamline the identification of cost-effective bioprocess designs. Stochastic modelling was used to capture uncertainties associated with each manufacturing strategy and to establish the robustness of different process designs. Further to this the effects of centralised vs. decentralised manufacturing on COG associated with a fresh cell therapy product were evaluated. The results of Chapter 5 suggest that planar-based bioprocess platforms still have a large part to play in the production of low dose cell therapies, particularly at relatively small scales of production.

A decisional tool that combined metrics computed using a bioprocess economics model (e.g. COG per dose, fixed capital expenditure) with operational criteria (e.g. ease of scale-up, process containment) is presented in Chapter 6. Here, a range of alternative bioprocess designs for the manufacture of an allogeneic CAR-T cell therapy are considered from both a financial and operational perspective. A multi-attribute decision making approach was used so as to provide a more holistic evaluation of available process designs. This approach was able to capture a variety of factors that should be taken into consideration when making process design decisions, not just the manufacturing COG as in previous chapters. Combination ratios were used to demonstrate how the ranking of alternative process designs changed according to the priority given to either operational or financial metrics computed by the tool.

One of the most significant challenges to the cell therapy field is the development of bioprocesses that can manufacture products at a scale and cost relevant to market demands. Whilst manufacturing costs are just one piece of a complex jigsaw that determines the commercial success of a cell therapy product, they underpin many important commercial elements of a cell therapy; their consideration during bioprocess design is crucial. Therefore, this work has demonstrated how decision support tools, such as those introduced in this thesis, can help inform effective process design during the development of cell therapy products.

7.2 Future Work

The implementation of the decisional tools developed as part of this thesis within industrially relevant case studies demonstrates their application to the field of cell therapy bioprocessing. However, this thesis represents the early application of such tools to the cell therapy sector. Future work could therefore focus on either the development of the tools to provide further insight into the bioprocess economics of cell therapy development and manufacturing, or to establish the decisional tools developed in this thesis as a more generic, user-friendly, potentially commercially available platform.

The fixed capital investment cost estimates derived within this thesis were based initially on a Lang Factor derived by Pollock et al. (2013) for biopharmaceutical bioprocesses based on the use of disposable technologies (Chapter 4). Following this, a Lang Factor method currently under development at UCL, which is specifically tailored to the cell therapy bioprocess sector, was used (Chapters 5 and 6). Accurate representation of fixed capital investment costs is dependent on this Lang Factor system and its development should be at the forefront of future work programmes. This will require communication with cell therapy manufacturers and business leaders in order to obtain benchmark data that can be used to test the accuracy of a novel cell therapy Lang Factor for estimation of fixed capital investment. However, the Lang

Factor approach, and it relevance to the cell therapy sector, is not as clear as it is for the chemical and biochemical engineering industries. Ratios between facility costs and TEPC vary drastically for cell therapy bioprocess designs depending on the classification of cleanroom and surface area required for different types of equipment required in the cell therapy industry. Therefore in the future, facility costs may be more accurately estimated by approximating the surface area and classification of clean room required for a given bioprocess design. This approach may be more accurate, but would require a greater number of calculations than the Lang Factor approach; in turn, this could drive up computing times associated with bioprocess economics models. It may therefore be appropriate to try and identify suitable Lang Factor-type ranges dependent on cleanroom classifications.

Additionally, work carried out in parallel to this thesis by Hassan et al. (2016) has highlighted the effects of process changes during product development on the economic performance of cell therapy products, this was done using project performance metrics such as NPV. Moving forward, it is important to recognise that whilst a process design might be identified as more cost-effective than a given alternative, the effect of process change on the profitability of a product must also be considered. Therefore, one area of future work may be to integrate the work of Hassan et al. (2016) with the tools presented in this thesis in order to introduce the opportunity for broader analyses to be performed. This will also allow manufacturing design decisions to be made based on development timelines and costs, not only manufacturing cost of goods.

In Chapter 5, centralised vs. decentralised processing was considered. The choices available to cell therapy manufacturers with regards to available process technologies, manufacturing locations and distribution strategies are increasing. When considering decentralised facilities as a manufacturing strategy, future work should consider the additional costs behind the use of multiple facilities. For example,

the costs of commissioning and inspection of the facility as well as regional variations in the facility regulations should be considered. The requirement of Qualified Persons and the additional costs this might incur if multiple facilites are used should be also be considered in future models. Addiionally, the impact on validation and comparability studies across multiple sites should be considered, again this should take into account regional variations in regulatory requirements in these areas. Further studies could investigate novel distribution strategies, such as installing clean rooms in hospitals, or so called ‘GMP in a box’ manufacturing, and their impacts on shipping and manufacturing costs.

In Chapter 6, when considering the impact of percentage improvements in process paramaters on potential cost of goods reductions, the increased costs associated with process development efforts were not included within the modelling framework. In this instance, these scenarios were designed to give thought ‘spaces to play’ with regards to process development, future work should take into account the effects of process development efforts and resources associated with these when estimating potential impacts on manufacturing cost of goods.

Finally, consideration of the ‘per unit’ costs of viral vector manufacturing may be an important aspect for future work; in this study a ‘per lot’ cost was used. However, this proves difficult to justify when considering scale-up or scale-down of the bioprocess. A ‘per unit’ cost for a viral vector would allow a more flexible approach to the economic analysis.

From a programming perspective, the tool developed in Chapter 5 is somewhat complex; the size of the problem domain necessitated the use of an evolutionary algorithm. Even so, running the algorithm proved to be a lengthy process, taking up to 24 hours dependent on the number of scenarios (lot sizes and demands) run. Ideally, the process economics model, and linked algorithm, should be further

developed in order to reduce the time required for each simulation in order to improve the speed at which optimal process designs are identified.

The decisional tools developed as part of this thesis are very specific in their current form; they are tailored for the bioprocesses that they are designed to capture. Whilst this is an advantage in that they are sophisticated and thorough in their appraisal of a bioprocess, they do not offer a lot of flexibility. Their application may therefore be limited beyond the case studies described in this thesis (NB this is a note about the specific models, not the approaches described in this work, which are widely applicable to the whole cell therapy field). Future work could therefore focus on the development of the tools themselves. In order to further develop the tools, and potentially make them an attractive tool available for license by cell therapy manufacturers, future work should focus on the generification of the tools presented here. This is to say that whilst it is important to capture the specifics of individual bioprocesses, the tools presented here may be more widely applicable if they could be developed such that user interfaces would allow users to input their own process flowsheet and select technologies pertinent to a given process design from a central database. The effort involved in translating the tools described in this thesis to a product for general use in the cell therapy field would be considerable and require advanced expertise in computer programming. However, comparable products are available in the biopharmaceutical field in the form of BioSolve (Biopharm Services, Chesham, UK).

Bibliography

Abbasalizadeh, S. et al. 2012. Bioprocess Development for Mass Production of Size-Controlled Human Pluripotent Stem Cell Aggregates in Stirred Suspension Bioreactor. *Tissue Engineering Part C: Methods* 18(11), pp. 831–851. doi: 10.1089/ten.tec.2012.0161.

Abbasalizadeh, S. and Baharvand, H. 2013. Technological progress and challenges towards cGMP manufacturing of human pluripotent stem cells based therapeutic products for allogeneic and autologous cell therapies. *Biotechnology Advances* 31(8), pp. 1600–1623. doi: 10.1016/j.biotechadv.2013.08.009.

Adamo, L. et al. 2009. Biomechanical forces promote embryonic haematopoiesis. *Nature* 459(7250), pp. 1131–5. doi: 10.1038/nature08073.

Ahsan, T. and Nerem, R.M. 2010. Fluid shear stress promotes an endothelial-like phenotype during the early differentiation of embryonic stem cells. *Tissue engineering. Part A* 16(11), pp. 3547–53. doi: 10.1089/ten.TEA.2010.0014.

Allmendinger, R. 2012. *Tuning evolutionary search for closed-loop optimisation*. University of Manchester.

American Society of Gene & Cell Therapy [no date]. Cell and gene therapy defined.

Amit, M. et al. 2011. Dynamic suspension culture for scalable expansion of undifferentiated human pluripotent stem cells. *Nature protocols* 6(5), pp. 572–579. doi: 10.1038/nprot.2011.325.

Anokye-Danso, F. et al. 2011. Highly Efficient miRNA-Mediated Reprogramming of Mouse and Human Somatic Cells to Pluripotency. *Cell Stem Cell* 8(4), pp. 376–388. doi: 10.1016/j.stem.2011.03.001.

Apel, M. et al. 2013. Integrated Clinical Scale Manufacturing System for Cellular Products Derived by Magnetic Cell Separation, Centrifugation and Cell Culture.

Chemie Ingenieur Technik 85(1–2), pp. 103–110. doi: 10.1002/cite.201200175.

Bae, D. et al. 2012. Hypoxia enhances the generation of retinal progenitor cells from human induced pluripotent and embryonic stem cells. *Stem cells and development* 21(8), pp. 1344–55. doi: 10.1089/scd.2011.0225.

Bajgain, P. et al. 2014. Optimizing the production of suspension cells using the G-Rex 'M' series. *Molecular Therapy — Methods & Clinical Development* 1, p. 14015.

Ban, H. et al. 2011. Efficient generation of transgene-free human induced pluripotent stem cells (iPSCs) by temperature-sensitive Sendai virus vectors. *Proceedings of the National Academy of Sciences of the United States of America* 108(34), pp. 14234–14239. doi: 10.1073/pnas.1103509108.

Baptista, R.P. et al. 2013. High density continuous production of murine pluripotent cells in an acoustic perfused bioreactor at different oxygen concentrations. *Biotechnology and Bioengineering* 110(2), pp. 648–655. doi: 10.1002/bit.24717.

Bardy, J. et al. 2012. Microcarrier Suspension Cultures for High-Density Expansion and Differentiation of Human Pluripotent Stem Cells to Neural Progenitor Cells. *Tissue Engineering Part C: Methods* 19(2), p. 120904064742009. doi: 10.1089/ten.tec.2012.0146.

Bartmann, C. et al. 2007. Two steps to functional mesenchymal stromal cells for clinical application. *Transfusion* 47(8), pp. 1426–1435. doi: 10.1111/j.1537-2995.2007.01219.x.

Bernardo, M.E. et al. 2007. Optimization of in vitro expansion of human multipotent mesenchymal stromal cells for cell-therapy approaches: Further insights in the search for a fetal calf serum substitute. *Journal of Cellular Physiology* 211(1), pp. 121–130. doi: 10.1002/jcp.20911.

Binder, B.Y.K. et al. 2014. Reduced Serum and Hypoxic Culture Conditions

Enhance the Osteogenic Potential of Human Mesenchymal Stem Cells. *Stem Cell Reviews and Reports* 11(3), pp. 387–393. doi: 10.1007/s12015-014-9555-7.

Brandenberger, R. et al. 2011. Cell therapy bioprocessing. *Bioprocess Int* 9, pp. 30–37.

Bratt-Leal, A.M. et al. 2013. A microparticle approach to morphogen delivery within pluripotent stem cell aggregates. *Biomaterials* 34(30), pp. 7227–7235. doi: 10.1016/j.biomaterials.2013.05.079.

Bravery, C.A. 2012. Are biosimilar cell therapy products possible? Available at: http://advbiols.com/documents/Bravery-AreBiosimilarCellTherapiesPossible.pdf.

Brederlau, A. et al. 2006. Transplantation of Human Embryonic Stem Cell-Derived Cells to a Rat Model of Parkinson's Disease: Effect of In Vitro Differentiation on Graft Survival and Teratoma Formation. *Stem Cells* 24(6), pp. 1433–1440. doi: 10.1634/stemcells.2005-0393.

Brentjens, R.J. et al. 2011. Safety and persistence of adoptively transferred autologous CD19-targeted T cells in patients with relapsed or chemotherapy refractory B-cell leukemias. *Blood* 118(18), pp. 4817–4828. doi: 10.1182/blood-2011-04-348540.

Brock, A. et al. 2012. Cellular Reprogramming: A New Technology Frontier in Pharmaceutical Research. *Pharmaceutical Research* 29(1), pp. 35–52. doi: 10.1007/s11095-011-0618-z.

Burridge, P.W. et al. 2011. A universal system for highly efficient cardiac differentiation of human induced pluripotent stem cells that eliminates interline variability. *PLoS ONE* 6(4). doi: 10.1371/journal.pone.0018293.

Caplan, A.I. et al. 2016. The 3Rs of Cell Therapy. *Stem Cells Translational Medicine* 5, pp. 1–5. doi: 10.5966/sctm.2016-0180.

Carr, A.F. et al. 2013. Development of human embryonic stem cell therapies for age-related macular degeneration. *Trends in Neurosciences* 36(7), pp. 385–395. doi: 10.1016/j.tins.2013.03.006.

Cellectis 2014. Engineered T cell therapies. (March). doi: 10.1017/erm.2015.14.

Chambers, S.M. et al. 2009. Highly efficient neural conversion of human ES and iPS cells by dual inhibition of SMAD signaling. *Nat Biotech* 27(3), pp. 275–280.

Chambers, S.M. et al. 2012. Combined small-molecule inhibition accelerates developmental timing and converts human pluripotent stem cells into nociceptors. *Nature biotechnology* 30(7), pp. 715–20. doi: 10.1038/nbt.2249.

Chang, C.-P. et al. 2013. Hypoxic preconditioning enhances the therapeutic potential of the secretome from cultured human mesenchymal stem cells in experimental traumatic brain injury. *Clinical Science* 124(3), pp. 165–176.

Chen, A.K.-L. et al. 2013. Application of human mesenchymal and pluripotent stem cell microcarrier cultures in cellular therapy: achievements and future direction. *Biotechnology advances* 31(7), pp. 1032–46. doi: 10.1016/j.biotechadv.2013.03.006.

Chen, A.K.-L. et al. 2014. Inhibition of ROCK-myosin II signaling pathway enables culturing of human pluripotent stem cells on microcarriers without extracellular matrix coating. *Tissue engineering. Part C, Methods* 20(3), pp. 227–38. doi: 10.1089/ten.TEC.2013.0191.

Chen, A.K.L. et al. 2011. Critical microcarrier properties affecting the expansion of undifferentiated human embryonic stem cells. *Stem Cell Research* 7(2), pp. 97–111. doi: 10.1016/j.scr.2011.04.007.

Chen, G. and Thomson, J.A. 2012. *Simplified basic media for human pluripotent cell culture*.

Chen, V.C. et al. 2012. Scalable GMP compliant suspension culture system for human ES cells. *Stem Cell Research* 8(3), pp. 388–402. doi: 10.1016/j.scr.2012.02.001.

Chhatre, S. et al. 2007. A prototype software methodology for the rapid evaluation of biomanufacturing process options. *Biotechnology and Applied Biochemistry* 48(2), pp. 65–78. doi: 10.1042/BA20070018.

Chisti, Y. 2001. Hydrodynamic damage to animal cells. *Critical reviews in biotechnology* 21(2), pp. 67–110. doi: 10.1080/20013891081692.

Chou, T. et al. 2005. Isolation and transplantation of highly purified autologous peripheral CD34+progenitor cells: purging efficacy, hematopoietic reconstitution following high dose chemotherapy in patients with breast cancer: results of a feasibility study in Japan. *Breast cancer (Tokyo, Japan)* 12(3), pp. 178–88. doi: 10.2325/jbcs.12.178.

Cimetta, E. et al. 2009. Microbioreactor arrays for controlling cellular environments: design principles for human embryonic stem cell applications. *Methods (San Diego, Calif.)* 47(2), pp. 81–89. doi: 10.1016/j.ymeth.2008.10.015.

Collignon, F. 2012. Integrity ™ Xpansion ™ Multiplate Bioreactor : The Scalable Solution for Adherent Stem Cell Expansion Xpansion-One., p. 2012.

Cribbs, A.P. et al. 2013. Simplified production and concentration of lentiviral vectors to achieve high transduction in primary human T cells. *BMC Biotechnology* 13(1), pp. 1–8. doi: 10.1186/1472-6750-13-98.

Cunha, B. et al. 2015. Exploring continuous and integrated strategies for the up- and downstream processing of human mesenchymal stem cells. *Journal of Biotechnology* 213, pp. 97–108. doi: 10.1016/j.jbiotec.2015.02.023.

Darkins, C.L. and Mandenius, C.-F. 2013. Design of large-scale manufacturing of

induced pluripotent stem cell derived cardiomyocytes. *Chemical Engineering Research and Design* 92(August), pp. 1–11. doi: 10.1016/j.cherd.2013.08.021.

Didar, T.F. and Tabrizian, M. 2010. Adhesion based detection{,} sorting and enrichment of cells in microfluidic Lab-on-Chip devices. *Lab Chip* 10(22), pp. 3043–3053. doi: 10.1039/C0LC00130A.

Diekmann, U. et al. 2015. A reliable and efficient protocol for human pluripotent stem cell differentiation into the definitive endoderm based on dispersed single cells. *Stem cells and development* 24(2), pp. 190–204. doi: 10.1089/scd.2014.0143.

Diogo, M.M. et al. 2012. Separation technologies for stem cell bioprocessing. *Biotechnology and Bioengineering* 109(11), pp. 2699–2709. doi: 10.1002/bit.24706.

Dodo, K. et al. 2014. An efficient large-scale retroviral transduction method involving preloading the vector into a retronectin-coated bag with low-temperature shaking. *PLoS ONE* 9(1). doi: 10.1371/journal.pone.0086275.

Dodson, B.P. and Levine, A.D. 2015. Challenges in the translation and commercialization of cell therapies. *BMC Biotechnology* 15(1), pp. 1–15. doi: 10.1186/s12896-015-0190-4.

Drukker, M. et al. 2006. Human Embryonic Stem Cells and Their Differentiated Derivatives Are Less Susceptible to Immune Rejection Than Adult Cells. *STEM CELLS* 24(2), pp. 221–229. doi: 10.1634/stemcells.2005-0188.

Ebert, A.D. and Svendsen, C.N. 2010. Human stem cells and drug screening: opportunities and challenges. *Nat Rev Drug Discov* 9(5), pp. 367–372.

Eibes, G. et al. 2010. Maximizing the ex vivo expansion of human mesenchymal stem cells using a microcarrier-based stirred culture system. *Journal of Biotechnology* 146(4), pp. 194–197. doi: 10.1016/j.jbiotec.2010.02.015.

Eichler, H.-G. et al. 2012. Adaptive Licensing: Taking the Next Step in the Evolution

of Drug Approval. *Clinical Pharmacology & Therapeutics* 91(3), pp. 426–437. doi: 10.1038/clpt.2011.345.

Eiselleova, L. et al. 2008. Comparative study of mouse and human feeder cells for human embryonic stem cells. *International Journal of Developmental Biology* 52(4), pp. 353–363. doi: 10.1387/ijdb.082590le.

EMA 2016. *Final report on the adaptive pathways pilot*.

Engle, S.J. and Vincent, F. 2014. Small Molecule Screening in Human Induced Pluripotent Stem Cell-derived Terminal Cell Types. *Journal of Biological Chemistry* 289(8), pp. 4562–4570. doi: 10.1074/jbc.R113.529156 .

Fabre, D. et al. 2016. Successful Tracheal Replacement in Humans Using Autologous Tissues: An 8-Year Experience. *The Annals of Thoracic Surgery* 96(4), pp. 1146–1155. doi: 10.1016/j.athoracsur.2013.05.073.

Fan, Y. et al. 2013. Facile engineering of xeno-free microcarriers for the scalable cultivation of human pluripotent stem cells in stirred suspension. *Tissue engineering. Part A* 20, pp. 1–43. doi: 10.1089/ten.TEA.2013.0219.

Farid, S.S. et al. 2000. A tool for modeling strategic decisions in cell culture manufacturing. *Biotechnology Progress* 16(5), pp. 829–836. doi: 10.1021/bp0001056.

Farid, S.S. 2002. *A decision-support tool for simulating the process and business perspectives of biopharmaceutical manufacture*. University College London.

Farid, S.S. et al. 2005. Combining Multiple Quantitative and Qualitative Goals When Assessing Biomanufacturing Strategies under Uncertainty. *Biotechnology Progress* 21(4), pp. 1183–1191. doi: 10.1021/bp050070f.

Farid, S.S. et al. 2005. Decision-support tool for assessing biomanufacturing strategies under uncertainty: Stainless steel versus disposable equipment for

clinical trial material preparation. *Biotechnology Progress* 21(2), pp. 486–497. doi: 10.1021/bp049692b.

Farid, S.S. 2009. Process Economic Drivers in Industrial Monoclonal Antibody Manufacture. In: *Process Scale Purification of Antibodies*. John Wiley & Sons, Inc., pp. 239–261. doi: 10.1002/9780470444894.ch12.

Feric, N.T. and Radisic, M. 2016. Strategies and Challenges to Myocardial Replacement Therapy. *Stem Cells Translational Medicine* 5(4), pp. 410–416. doi: 10.5966/sctm.2015-0288.

Fernandes, A.M. et al. 2009. Successful scale-up of human embryonic stem cell production in a stirred microcarrier culture system. *Brazilian Journal of Medical and Biological Research* 42(6), pp. 515–522. doi: 10.1590/s0100-879x2009000600007.

Fluri, D. a et al. 2012. Derivation, expansion and differentiation of induced pluripotent stem cells in continuous suspension cultures. *Nature Methods* 9(5), pp. 509–516. doi: 10.1038/nmeth.1939.

Fonoudi, H. et al. 2015. A Universal and Robust Integrated Platform for the Scalable Production of Human Cardiomyocytes From Pluripotent Stem Cells. *Stem Cells Translational Medicine* 4(12), pp. 1482–1494. doi: 10.5966/sctm.2014-0275.

Forestell, S.P. et al. 1992. Development of the optimal inoculation conditions for microcarrier cultures. *Biotechnology and Bioengineering* 39(3), pp. 305–313. doi: 10.1002/bit.260390308.

Fossett, E. and Khan, W.S. 2012. Optimising human mesenchymal stem cell numbers for clinical application: A literature review. *Stem Cells International* 2012. doi: 10.1155/2012/465259.

Fridley, K.M. et al. 2012. Hydrodynamic modulation of pluripotent stem cells. *Stem cell research & therapy* 3, p. 45. doi: 10.1186/scrt136.

Fujita, Y. and Kawamoto, A. 2016. Regenerative medicine legislation in Japan for fast provision of cell therapy products. *Clinical Pharmacology & Therapeutics* 99(1), pp. 26–29. doi: 10.1002/cpt.279.

Fusaki, N. et al. 2009. Efficient induction of transgene-free human pluripotent stem cells using a vector based on Sendai virus, an RNA virus that does not integrate into the host genome. *Proceedings of the Japan Academy, Series B* 85(8), pp. 348–362. doi: 10.2183/pjab.85.348.

ge-sees-cell-therapy-industry-s-sales-at-10-billion-by-2021 @ www.bloomberg.com. [no date].

GE Healthcare 2014. Equivalent performance of Xuri ™ Cell Expansion System W25 and WAVE Bioreactor ™ System 2 / 10 for the culture of T lymphocytes., pp. 1–4.

GE Healthcare [no date]. Xuri Cell Expansion System Cellbag Perfusion, ph and DO. Available at: http://www.gelifesciences.com/webapp/wcs/stores/servlet/catalog/en/GELifeSciences-uk/products/AlternativeProductStructure_19859/29105498 [Accessed: 15 August 2016].

Gerecht-Nir, S. et al. 2004. Bioreactor cultivation enhances the efficiency of human embryoid body (hEB) formation and differentiation. *Biotechnology and Bioengineering* 86(5), pp. 493–502. doi: 10.1002/bit.20045.

Ghodsizadeh, A. et al. 2010. Generation of Liver Disease-Specific Induced Pluripotent Stem Cells Along with Efficient Differentiation to Functional Hepatocyte-Like Cells. *Stem Cell Reviews and Reports* 6(4), pp. 622–632. doi: 10.1007/s12015-010-9189-3.

Goh, T.K.-P. et al. 2013. Microcarrier culture for efficient expansion and osteogenic

differentiation of human fetal mesenchymal stem cells. *BioResearch open access* 2(2), pp. 84–97. doi: 10.1089/biores.2013.0001.

González-González, M. et al. 2012. Current strategies and challenges for the purification of stem cells. *Journal of Chemical Technology & Biotechnology* 87(1), pp. 2–10. doi: 10.1002/jctb.2723.

Gottipamula, S. et al. 2013. Serum-free media for the production of human mesenchymal stromal cells: a review. *Cell Proliferation* 46(6), pp. 608–627. doi: 10.1111/cpr.12063.

Gross, G. et al. 1989. Expression of immunoglobulin-T-cell receptor chimeric molecules as functional receptors with antibody-type specificity. *Proceedings of the National Academy of Sciences of the United States of America* 86(24), pp. 10024–10028. doi: 10.1073/pnas.86.24.10024.

Grskovic, M. et al. 2011. Induced pluripotent stem cells — opportunities for disease modelling and drug discovery. *Nature Reviews Drug Discovery* 10(12), pp. 915–929. doi: 10.1038/nrd3577.

Grupp, S.A. et al. 2013. Chimeric antigen receptor-modified T cells for acute lymphoid leukemia. *N Engl J Med* 368(16), pp. 1509–1518. doi: 10.1056/NEJMoa1215134.

Grützkau, A. and Radbruch, A. 2010. Small but mighty: How the MACS1-technology based on nanosized superparamagnetic particles has helped to analyze the immune system within the last 20 years. *Cytometry Part A* 77(7), pp. 643–647. doi: 10.1002/cyto.a.20918.

Hambor, J. 2012. Bioreactor design and bioprocess controls for industrialized cell processing. *Bioprocess Int* 10(6), pp. 22–33.

Hanenberg, H. et al. 1996. Colocalization of retrovirus and target cells on specific

fibronectin fragments increases genetic transduction of mammalian cells. *Nat Med* 2(8), pp. 876–882.

Hare, J.M. et al. 2009. A Randomized, Double-Blind, Placebo-Controlled, Dose-Escalation Study of Intravenous Adult Human Mesenchymal Stem Cells (Prochymal) After Acute Myocardial Infarction. *Journal of the American College of Cardiology* 54(24), pp. 2277–2286. doi: 10.1016/j.jacc.2009.06.055.

Hartmann, J. et al. 2017. Clinical development of CAR T cells — challenges and opportunities in translating innovative treatment concepts. 9(9), pp. 1183–1197. doi: 10.15252/emmm.201607485.

Hassan, S. et al. 2015. Allogeneic cell therapy bioprocess economics and optimization: downstream processing decisions. *Regenerative medicine* 10(5), pp. 591–609. doi: 10.2217/rme.15.29.

Hassan, S. et al. 2016. Process change evaluation framework for allogeneic cell therapies : impact on drug development and commercialization. 11, pp. 287–305.

Hay, M. et al. 2014. Clinical development success rates for investigational drugs. *Nature Biotechnology* 32, p. 40.

Heathman, T.R. et al. 2015. The translation of cell-based therapies: clinical landscape and manufacturing challenges. *Regenerative medicine* 10(1), pp. 49–64. doi: 10.2217/rme.14.73.

Heathman, T.R.J. et al. 2015. Expansion, harvest and cryopreservation of human mesenchymal stem cells in a serum-free microcarrier process. *Biotechnology and Bioengineering* 112(8), pp. 1696–1707. doi: 10.1002/bit.25582.

Herberts, C.A. et al. 2011. Risk factors in the development of stem cell therapy. *Journal of Translational Medicine* 9(1), pp. 1–14. doi: 10.1186/1479-5876-9-29.

Hervy, M. et al. 2014. Long term expansion of bone marrow-derived hMSCs on

novel synthetic microcarriers in xeno-free, defined conditions. *PLoS ONE* 9(3), pp. 1–7. doi: 10.1371/journal.pone.0092120.

Hettle, R. et al. 2017. The assessment and appraisal of regenerative medicines and cell therapy products: an exploration of methods for review, economic evaluation and appraisalssment. *Heatlh Technologoy Assessment* 21(7). doi: 10.3310/hta21070.

Hewitt, C.J. et al. 2011. Expansion of human mesenchymal stem cells on microcarriers. *Biotechnology Letters* 33(11), pp. 2325–2335. doi: 10.1007/s10529-011-0695-4.

Hochedlinger, K. 2013. Regenerative Medicine. 13(5), pp. 497–505. doi: 10.1038/ncb0511-497.Harnessing.

Hollyman, D. et al. 2009. Manufacturing validation of biologically functional T cells targeted to CD19 antigen for autologous adoptive cell therapy. *Journal of immunotherapy (Hagerstown, Md. : 1997)* 32(2), pp. 169–180. doi: 10.1097/CJI.0b013e318194a6e8.

Horwitz, E.M. et al. 2002. Isolated allogeneic bone marrow-derived mesenchymal cells engraft and stimulate growth in children with osteogenesis imperfecta: Implications for cell therapy of bone. *Proceedings of the National Academy of Sciences of the United States of America* 99(13), pp. 8932–7. doi: 10.1073/pnas.132252399.

Idelson, M. et al. 2009. Directed Differentiation of Human Embryonic Stem Cells into Functional Retinal Pigment Epithelium Cells. *Cell Stem Cell* 5(4), pp. 396–408. doi: 10.1016/j.stem.2009.07.002.

Ilic, D. et al. 2015. Human embryonic and induced pluripotent stem cells in clinical trials. *British Medical Bulletin* 116(November), pp. 19–27. doi: 10.1093/bmb/ldv045.

Janas, M. et al. 2015. Perfusion's role in maintenance of high-density T-cell cultures. *BioProcess International* 13(1)

Jenkins, M.J. and Farid, S.S. 2015. Human pluripotent stem cell-derived products: Advances towards robust, scalable and cost-effective manufacturing strategies. *Biotechnology Journal* 10(1), pp. 83–95.

Jørgensen, J. and Kefalas, P. 2015. Reimbursement of licensed cell and gene therapies across the major European healthcare markets. *Journal of Market Access & Health Policy* 3(1), p. 29321. doi: 10.3402/jmahp.v3.29321.

June, C.H. et al. 2009. Engineering lymphocyte subsets: tools, trials and tribulations. *Nat Rev Immunol* 9(10), pp. 704–716.

Kaiser, A.D. et al. 2015. Towards a commercial process for the manufacture of genetically modified T cells for therapy. *Cancer gene therapy* 22(2), pp. 72–8. doi: 10.1038/cgt.2014.78.

Kaji, K. et al. 2009. Virus-free induction of pluripotency and subsequent excision of reprogramming factors. *Nature* 458(7239), pp. 771–775.

Kalos, M. et al. 2011. T cells with chimeric antigen receptors have potent antitumor effects and can establish memory in patients with advanced leukemia. *Science translational medicine* 3(95), p. 95ra73. doi: 10.1126/scitranslmed.3002842.

Kalos, M. and June, C. 2013. Adoptive T Cell Transfer for Cancer Immunotherapy in the Era of Synthetic Biology. *Immunity* 39(1), pp. 49–60. doi: 10.1016/j.immuni.2013.07.002.

Karumbayaram, S. et al. 2009. Directed differentiation of human-induced pluripotent stem cells generates active motor neurons. *Stem Cells* 27(4), pp. 806–811. doi: 10.1002/stem.31.

Kawamata, S. et al. 2015. Design of a Tumorigenicity Test for Induced Pluripotent

Stem Cell (iPSC)-Derived Cell Products. *Journal of Clinical Medicine* 4(1), p. 159. doi: 10.3390/jcm4010159.

Kehoe, D.E. et al. 2010. Scalable Stirred-Suspension Bioreactor Culture of Human Pluripotent Stem Cells. *Tissue Engineering* 16(2), pp. 405–421.

Kimbrel, E. a. and Lanza, R. 2015. Current status of pluripotent stem cells: moving the first therapies to the clinic. *Nature Reviews Drug Discovery* 14(10), pp. 681–692. doi: 10.1038/nrd4738.

Kiskinis, E. and Eggan, K. 2010. Review series Progress toward the clinical application of patient-specific pluripotent stem cells. *The Journal of Clinical Investigation* 120(1), pp. 51–59. doi: 10.1172/JCI40553.with.

Klimanskaya, I. et al. 2004. Derivation and Comparative Assessment of Retinal Pigment Epithelium from Human Embryonic Stem Cells Using Transcriptomics. *Cloning and Stem Cells* 6(3), pp. 217–245. doi: 10.1089/clo.2004.6.217.

Ko, H.C. and Gelb, B.D. 2014. Concise Review: Drug Discovery in the Age of the Induced Pluripotent Stem Cell. *STEM CELLS Translational Medicine* 3(4), pp. 500–509. doi: 10.5966/sctm.2013-0162.

Kochenderfer, J.N. et al. 2012. B-cell depletion and remissions of malignancy along with cytokine-associated toxicity in a clinical trial of anti-CD19 chimeric-antigen-receptor-transduced T cells. *Blood* 119(12), pp. 2709–2720. doi: 10.1182/blood-2011-10-384388.

Kola, I. and Landis, J. 2004. Can the pharmaceutical industry reduce attrition rates? *Nat Rev Drug Discov* 3(8), pp. 711–716.

Krawetz, R. et al. 2010. Large-scale expansion of pluripotent human embryonic stem cells in stirred-suspension bioreactors. *Tissue engineering. Part C, Methods* 16(4), pp. 573–582. doi: 10.1089/ten.tec.2009.0228.

Lang, H.J. 1948. Simplified approach to preliminary cost estimates. *Chem. Eng.* 55, pp. 112–113.

Lang, P. et al. 2004. Transplantation of a combination of CD133+ and CD34+ selected progenitor cells from alternative donors. *British Journal of Haematology* 124(1), pp. 72–79. doi: 10.1046/j.1365-2141.2003.04747.x.

Lecina, M. et al. 2010. Scalable platform for human embryonic stem cell differentiation to cardiomyocytes in suspended microcarrier cultures. *Tissue engineering. Part C, Methods* 16(6), pp. 1609–1619. doi: 10.1089/ten.tec.2010.0104.

Leung, H.W. et al. 2011. Agitation can induce differentiation of human pluripotent stem cells in microcarrier cultures. *Tissue engineering. Part C, Methods* 17(2), pp. 165–172. doi: 10.1089/ten.tec.2010.0320.

Levine, B.L. 2015. Performance-enhancing drugs: design and production of redirected chimeric antigen receptor (CAR) T cells. *Cancer gene therapy* 22(2), pp. 79–84. doi: 10.1038/cgt.2015.5.

Levine, B.L. et al. 2017. Global Manufacturing of CAR T Cell Therapy. *Molecular Therapy: Methods & Clinical Development* 4(March), pp. 92–101. doi: 10.1016/j.omtm.2016.12.006.

Li, L. et al. 2004. Human Embryonic Stem Cells Possess Immune-Privileged Properties. *STEM CELLS* 22(4), pp. 448–456. doi: 10.1634/stemcells.22-4-448.

Li, W. et al. 2012. Concise review: A chemical approach to control cell fate and function. *Stem cells (Dayton, Ohio)* 30(1), pp. 61–8. doi: 10.1002/stem.768.

Lim, A.C. et al. 2006. A computer-aided approach to compare the production economics of fed-batch and perfusion culture under uncertainty. *Biotechnology and Bioengineering* 93(4), pp. 687–697. doi: 10.1002/bit.20757.

Lipowska-Bhalla, G. et al. 2012. Targeted immunotherapy of cancer with CAR T cells: Achievements and challenges. *Cancer Immunology, Immunotherapy* 61(7), pp. 953–962. doi: 10.1007/s00262-012-1254-0.

Lippmann, E.S. et al. 2014. Defined human pluripotent stem cell culture enables highly efficient neuroepithelium derivation without small molecule inhibitors. *Stem Cells* 32(4), pp. 1032–1042. doi: 10.1002/stem.1622.

Liu, Q. et al. 2013. Optimizing dopaminergic differentiation of pluripotent stem cells for the manufacture of dopaminergic neurons for transplantation. *Cytotherapy* 15(8), pp. 999–1010. doi: 10.1016/j.jcyt.2013.03.006.

Lock, L.T. and Tzanakakis, E.S. 2009. Expansion and Differentiation of Human Embryonic Stem Cells to Endoderm Progeny in a Microcarrier. *Tissue Engineering Part A* 15(8), pp. 2051–2063. doi: 10.1089/ten.tea.2008.0455.

Lu, B. et al. 2009. Long-Term Safety and Function of RPE from Human Embryonic Stem Cells in Preclinical Models of Macular Degeneration. *STEM CELLS* 27(9), pp. 2126–2135. doi: 10.1002/stem.149.

Lu, S.-J. et al. 2013. 3D microcarrier system for efficient differentiation of human pluripotent stem cells into hematopoietic cells without feeders and serum [corrected]. *Regenerative medicine* 8(4), pp. 413–24. doi: 10.2217/rme.13.36.

Lund, R.D. et al. 2006. Human Embryonic Stem Cell–Derived Cells Rescue Visual Function in Dystrophic RCS Rats. *Cloning and Stem Cells* 8(3), pp. 189–199. doi: 10.1089/clo.2006.8.189.

Maciulaitis, R. et al. 2012. Clinical Development of Advanced Therapy Medicinal Products in Europe: Evidence That Regulators Must Be Proactive. *Mol Ther* 20(3), pp. 479–482.

Macown, R.J. et al. 2014. Robust, microfabricated culture devices with improved

control over the soluble microenvironment for the culture of embryonic stem cells. *Biotechnology Journal* 9(6), pp. 805–813. doi: 10.1002/biot.201300245.

Maetzig, T. et al. 2011. Gammaretroviral Vectors: Biology, Technology and Application. *Viruses* 3(6), pp. 677–713. doi: 10.3390/v3060677.

Mahalatchimy, A. 2016. REIMBURSEMENT OF CELL-BASED REGENERATIVE THERAPY IN THE UK AND FRANCE. *Medical Law Review* 24(2), pp. 234–258. doi: 10.1093/medlaw/fww009.

Manuri, P.V.R. et al. 2009. piggyBac Transposon/Transposase System to Generate CD19-Specific T Cells for the Treatment of B-Lineage Malignancies. *Human Gene Therapy* 21(4), pp. 427–437. doi: 10.1089/hum.2009.114.

Marinho, P.A.N. et al. 2012. Xeno-Free Production of Human Embryonic Stem Cells in Stirred Microcarrier Systems Using a Novel Animal/Human-Component-Free Medium. *Tissue Engineering Part C: Methods* 19(2), p. 121016064607007. doi: 10.1089/ten.tec.2012.0141.

Martinez, Y. et al. 2012. Generation and Applications of Human Pluripotent Stem Cells Induced into Neural Lineages and Neural Tissues. *Frontiers in Physiology* 3(March), pp. 1–9. doi: 10.3389/fphys.2012.00047.

Marx, V. 2016. Cell biology: delivering tough cargo into cells. *Nat Meth* 13(1), pp. 37–40.

Mason, C. et al. 2012. The global cell therapy industry continues to rise during the second and third quarters of 2012. *Cell Stem Cell* 11(6), pp. 735–739. doi: 10.1016/j.stem.2012.11.013.

Mason, C. and Dunnill, P. 2008. A brief definition of regenerative medicine. *Regen Med* 3, pp. 1–5.

Mason, C. and Dunnill, P. 2009. Quantities of cells used for regenerative medicine

and some implications for clinicians and bioprocessors. *Regen Med* , pp. 153–157. doi: 10.2217/17460751.4.2.153.

Masuda, S. and Shimizu, T. 2016. Three-dimensional cardiac tissue fabrication based on cell sheet technology. *Advanced Drug Delivery Reviews* 96, pp. 103–109. doi: 10.1016/j.addr.2015.05.002.

McIntyre, C.A. et al. 2010. Fluorescence-activated cell sorting for CGMP processing of therapeutic cells. *BioProcess International* 8(6), pp. 44–53. doi: 10.1017/CBO9781107415324.004.

Medcalf, N. 2016. Centralized or decentralized manufacturing ? Key business model considerations for cell therapies. *Cell and Gene Therapy Insights* 2(1), pp. 95–109. doi: 10.18609/cgti.2016.012.

Melkoumian, Z. et al. 2010. Synthetic peptide-acrylate surfaces for long-term self-renewal and cardiomyocyte differentiation of human embryonic stem cells. *Nature biotechnology* 28(6), pp. 606–610. doi: 10.1038/nbt.1629.

Mordwinkin, N.M. et al. 2013. A review of human pluripotent stem cell-derived cardiomyocytes for high-throughput drug discovery, cardiotoxicity screening, and publication standards. *Journal of Cardiovascular Translational Research* 6(1), pp. 22–30. doi: 10.1007/s12265-012-9423-2.

Mount, N.M. et al. 2015. Cell-based therapy technology classifications and translational challenges. *Philosophical Transactions of the Royal Society B: Biological Sciences* 370(1680)

Nakazawa, Y. et al. 2011. PiggyBac-mediated cancer immunotherapy using EBV-specific cytotoxic T-cells expressing HER2-specific chimeric antigen receptor. *Molecular therapy : the journal of the American Society of Gene Therapy* 19(12), pp. 2133–43. doi: 10.1038/mt.2011.131.

Nasef, A. et al. 2008. Immunomodulatory effect of mesenchymal stromal cells: possible mechanisms. *Regenerative Medicine* 3(4), pp. 531–546. doi: 10.2217/17460751.3.4.531.

Nazari, H. et al. 2015. Stem cell based therapies for age-related macular degeneration: The promises and the challenges. *Progress in Retinal and Eye Research* 48, pp. 1–39. doi: 10.1016/j.preteyeres.2015.06.004.

Nguyen, H.N. et al. 2016. LRRK2 Mutant iPSC-Derived DA Neurons Demonstrate Increased Susceptibility to Oxidative Stress. *Cell Stem Cell* 8(3), pp. 267–280. doi: 10.1016/j.stem.2011.01.013.

Niebruegge, S. et al. 2008. Cardiomyocyte production in mass suspension culture: embryonic stem cells as a source for great amounts of functional cardiomyocytes. *Tissue engineering. Part A* 14(10), pp. 1591–1601. doi: 10.1089/ten.tea.2007.0247.

Nienow, A.W. et al. 2014. A potentially scalable method for the harvesting of hMSCs from microcarriers. *Biochemical Engineering Journal* 85, pp. 79–88. doi: 10.1016/j.bej.2014.02.005.

Novais, J.L. et al. 2001. Economic comparison between conventional and disposables-based technology for the production of biopharmaceuticals. *Biotechnology and Bioengineering* 75(2), pp. 143–153. doi: 10.1002/bit.1182.

O'Donnell, D. 2015. The cell therapy supply chain: Logistical considerations for autologous immunotherapies. *BioProcess International* 13(9)

Oh, S.K.W. et al. 2009. Long-term microcarrier suspension cultures of human embryonic stem cells. *Stem Cell Research* 2(3), pp. 219–230. doi: 10.1016/j.scr.2009.02.005.

Olmer, R. et al. 2010. Long term expansion of undifferentiated human iPS and ES cells in suspension culture using a defined medium. *Stem Cell Research* 5(1), pp.

51–64. doi: 10.1016/j.scr.2010.03.005.

Olmer, R. et al. 2012. Suspension Culture of Human Pluripotent Stem Cells in Controlled, Stirred Bioreactors. *Tissue Engineering Part C: Methods* 18(10), pp. 772–784. doi: 10.1089/ten.tec.2011.0717.

Pal, R. et al. 2008. Effect of holding time, temperature and different parenteral solutions on viability and functionality of adult bone marrow-derived mesenchymal stem cells before transplantation. *Journal of Tissue Engineering and Regenerative Medicine* 2(7), pp. 436–444. doi: 10.1002/term.109.

Palau, R. and Van Deusen, A.L. 2016. Compatibility of GxP with Existing Cell Therapy Quality Standards A2 - Vives, Joaquim. In: Carmona, G. B. T.-G. to C. T. G. ed. *Guide to cell therapy*. Boston: Academic Press, pp. 231–252. doi: http://dx.doi.org/10.1016/B978-0-12-803115-5.00006-1.

Panchalingam, K.M. et al. 2015. Bioprocessing strategies for the large-scale production of human mesenchymal stem cells: a review. *Stem Cell Research & Therapy* 6(1), p. 225. doi: 10.1186/s13287-015-0228-5.

Park, I.-H. et al. 2008. Reprogramming of human somatic cells to pluripotency with defined factors. *Nature* 451(7175), pp. 141–146.

Pearson, H. 2006. The bitterest pill. *Nature* 444(7119), pp. 532–533.

Phillips, B.W. et al. 2008. Attachment and growth of human embryonic stem cells on microcarriers. *Journal of Biotechnology* 138(1–2), pp. 24–32. doi: 10.1016/j.jbiotec.2008.07.1997.

Pierson, R. 2015. Safety concerns cloud early promise of powerful new cancer drugs. *Reuters* January

Pla, A. 2016. 1 - Overview of the Development Program of a Cell-Based Medicine A2 - Vives, Joaquim. In: Carmona, G. B. T.-G. to C. T. G. ed. Boston: Academic

Press, pp. 1–13. doi: http://dx.doi.org/10.1016/B978-0-12-803115-5.00001-2.

Placzek, M.R. et al. 2009. Stem cell bioprocessing: fundamentals and principles. *Journal of The Royal Society Interface* 6(32), pp. 209–232. doi: 10.1098/rsif.2008.0442.

Pollock, J. et al. 2013. Fed-batch and perfusion culture processes: economic, environmental, and operational feasibility under uncertainty. *Biotechnology and bioengineering* 110(1), pp. 206–19. doi: 10.1002/bit.24608.

Porter, D.L. et al. 2011. Chimeric Antigen Receptor–Modified T Cells in Chronic Lymphoid Leukemia; Chimeric Antigen Receptor–Modified T Cells for Acute Lymphoid Leukemia; Chimeric Antigen Receptor T Cells for Sustained Remissions in Leukemia. *New England Journal of Medicine* 365(8), pp. 725–733. doi: 10.1056/NEJMx160005.

Powell, D.J. et al. 2009. Efficient clinical-scale enrichment of lymphocytes for use in adoptive immunotherapy using a modified counterflow centrifugal elutriation program. *Cytotherapy* 11(7), pp. 923–935. doi: 10.3109/14653240903188921.

Prabhakarpandian, B. et al. 2011. Microfluidic devices for modeling cell-cell and particle-cell interactions in the microvasculature. *Microvascular Research* 82(3), pp. 210–220. doi: 10.1016/j.mvr.2011.06.013.

Prasad, V.K. et al. 2011. Efficacy and Safety of Ex Vivo Cultured Adult Human Mesenchymal Stem Cells (Prochymal™) in Pediatric Patients with Severe Refractory Acute Graft-Versus-Host Disease in a Compassionate Use Study. *Biology of Blood and Marrow Transplantation* 17(4), pp. 534–541. doi: http://dx.doi.org/10.1016/j.bbmt.2010.04.014.

Prescott, C. 2011. The business of exploiting induced pluripotent stem cells. *Philosophical Transactions of the Royal Society B: Biological Sciences* 366(1575),

pp. 2323–2328. doi: 10.1098/rstb.2011.0047.

Pule, M.A. et al. 2008. Virus-specific T cells engineered to coexpress tumor-specific receptors: persistence and antitumor activity in individuals with neuroblastoma. *Nature medicine* 14(11), pp. 1264–1270. doi: 10.1038/nm.1882.

Quintás-Cardama, A. et al. 2007. Multifactorial Optimization of Gammaretroviral Gene Transfer into Human T Lymphocytes for Clinical Application. *Human Gene Therapy* 18(12), pp. 1253–1260. doi: 10.1089/hum.2007.088.

Rafiq, Q.A. et al. 2013. Culture of human mesenchymal stem cells on microcarriers in a 5 l stirred-tank bioreactor. *Biotechnology Letters* 35(8), pp. 1233–1245. doi: 10.1007/s10529-013-1211-9.

Rafiq, Q.A. et al. 2016. Systematic microcarrier screening and agitated culture conditions improves human mesenchymal stem cell yield in bioreactors. *Biotechnology Journal* 11(4), pp. 473–486. doi: 10.1002/biot.201400862.

Rajamohan, D. et al. 2013. Current status of drug screening and disease modelling in human pluripotent stem cells. *BioEssays* 35(3), pp. 281–298. doi: 10.1002/bies.201200053.

Rao, M.S. and Malik, N. 2012. Assessing iPSC reprogramming methods for their suitability in translational medicine. *Journal of Cellular Biochemistry* 113(10), pp. 3061–3068. doi: 10.1002/jcb.24183.

Reichen, M. et al. 2012. Microfabricated Modular Scale-Down Device for Regenerative Medicine Process Development. *PLoS ONE* 7(12). doi: 10.1371/journal.pone.0052246.

Ringden, O. et al. 2006. Mesenchymal Stem Cells for Treatment of Therapy Resistant Graft-versus-Host Disease. 81(10), pp. 1390–1397. doi: 10.1097/01.tp.0000214462.63943.14.

Robinton, D.A. a. and Daley, G.G.Q. 2012. The promise of induced pluripotent stem cells in research and therapy. *Nature* 481(7381), pp. 295–305. doi: 10.1038/nature10761.The.

Rodin, S. et al. 2010. Long-term self-renewal of human pluripotent stem cells on human recombinant laminin-511. *Nature biotechnology* 28(6), pp. 611–615. doi: 10.1038/nbt.1620.

Rodrigues, C.A. V et al. 2011. Stem cell cultivation in bioreactors. *Biotechnology Advances* 29(6), pp. 815–829. doi: 10.1016/j.biotechadv.2011.06.009.

Römhild, A. 2016. Good Manufacturing Practice Compliance in the Manufacture of Cell-Based Medicines. In: Carmona, G. B. T. ed. *Guide to cell therapy*. Boston: Academic Press, pp. 107–175. doi: http://dx.doi.org/10.1016/B978-0-12-803115-5.00004-8.

Rosenberg, S.A. et al. 1990. Gene Transfer into Humans — Immunotherapy of Patients with Advanced Melanoma, Using Tumor-Infiltrating Lymphocytes Modified by Retroviral Gene Transduction. *New England Journal of Medicine* 323(9), pp. 570–578. doi: 10.1056/NEJM199008303230904.

Rowley, J. et al. 2012. Meeting lot-size challenges of manufacturing adherent cells for therapy. *BioProcess International* 10(SUPPL. 3), pp. 16–22.

Rubin, L.L. 2008. Essay Stem Cells and Drug Discovery : The Beginning of a New Era ?, pp. 549–552. doi: 10.1016/j.cell.2008.02.010.

Sadeghi, A. et al. 2011. Large-scale bioreactor expansion of tumor-infiltrating lymphocytes. *Journal of Immunological Methods* 364(1–2), pp. 94–100. doi: 10.1016/j.jim.2010.11.007.

Sandrin, V. et al. 2002. Lentiviral vectors pseudotyped with a modified RD114 envelope glycoprotein show increased stability in sera and augmented transduction

of primary lymphocytes and CD34+ cells derived from human and nonhuman primates. *Blood* 100(3), pp. 823–832.

Santos, F. dos et al. 2011. Toward a Clinical-Grade Expansion of Mesenchymal Stem Cells from Human Sources: A Microcarrier-Based Culture System Under Xeno-Free Conditions. *Tissue Engineering Part C: Methods* 17(12), pp. 1201–1210. doi: 10.1089/ten.tec.2011.0255.

dos Santos, F. et al. 2014. A xenogeneic-free bioreactor system for the clinical-scale expansion of human mesenchymal stem/stromal cells. *Biotechnology and Bioengineering* 111(6), pp. 1116–1127. doi: 10.1002/bit.25187.

Sart, S. et al. 2013. Engineering stem cell fate with biochemical and biomechanical properties of microcarriers. *Biotechnology Progress* 29(6), pp. 1354–1366. doi: 10.1002/btpr.1825.

Sart, S. et al. 2014. Process engineering of stem cell metabolism for large scale expansion and differentiation in bioreactors. *Biochemical Engineering Journal* 84, pp. 74–82. doi: 10.1016/j.bej.2014.01.005.

Sartorius Stedim 2012. *True scaleability in single-use True scaleability in single-use*.

Sartorius Stedim 2016. Scalable single-use centrifugation systems.

Sartorius Stedim 2017. BIOSTAT STR ® Bioreactors and Flexsafe STR ® Bags A Perfect Match for True Scalability in Single Use Single-Use Production Platform of the Future.

van Schalkwyk, M.C.I., Papa, S.E., Jeannon, J.-P., Urbano, T.G., et al. 2013. Design of a Phase I Clinical Trial to Evaluate Intratumoral Delivery of ErbB-Targeted Chimeric Antigen Receptor T-Cells in Locally Advanced or Recurrent Head and Neck Cancer. *Human Gene Therapy Clinical Development* 24(3), pp. 134–142. doi: 10.1089/humc.2013.144.

van Schalkwyk, M.C.I., Papa, S.E., Jeannon, J.-P., Guerrero Urbano, T., et al. 2013. Design of a phase I clinical trial to evaluate intratumoral delivery of ErbB-targeted chimeric antigen receptor T-cells in locally advanced or recurrent head and neck cancer. *Human gene therapy. Clinical development* 24(3), pp. 134–42. doi: 10.1089/humc.2013.144.

Schallmoser, K. et al. 2008. Rapid large-scale expansion of functional mesenchymal stem cells from unmanipulated bone marrow without animal serum. *Tissue engineering. Part C, Methods* 14(3), pp. 185–96. doi: 10.1089/ten.tec.2008.0060.

Schriebl, K. et al. 2010. Stem cell separation: A bottleneck in stem cell therapy. *Biotechnology Journal* 5(1), pp. 50–61. doi: 10.1002/biot.200900115.

Schulz, T.C. et al. 2012. A scalable system for production of functional pancreatic progenitors from human embryonic stem cells. *PLoS ONE* 7(5). doi: 10.1371/journal.pone.0037004.

Schwartz, S.D. et al. 2012. Embryonic stem cell trials for macular degeneration: a preliminary report. *The Lancet* 379(9817), pp. 713–720. doi: 10.1016/s0140-6736(12)60028-2.

Scott, C.W. et al. 2013. Human induced pluripotent stem cells and their use in drug discovery for toxicity testing. *Toxicology Letters* 219(1), pp. 49–58. doi: 10.1016/j.toxlet.2013.02.020.

Seki, T. et al. 2010. Generation of Induced Pluripotent Stem Cells from Human Terminally Differentiated Circulating T Cells. *Cell Stem Cell* 7(1), pp. 11–14. doi: 10.1016/j.stem.2010.06.003.

Serra, M. et al. 2010. Improving expansion of pluripotent human embryonic stem cells in perfused bioreactors through oxygen control. *Journal of Biotechnology* 148(4), pp. 208–215. doi: 10.1016/j.jbiotec.2010.06.015.

Serra, M. et al. 2012. Process engineering of human pluripotent stem cells for clinical application. *Trends in Biotechnology* 30(6), pp. 350–359. doi: 10.1016/j.tibtech.2012.03.003.

Sharei, A. et al. 2015. Ex vivo cytosolic delivery of functional macromolecules to immune cells. *PLoS ONE* 10(4), pp. 1–12. doi: 10.1371/journal.pone.0118803.

Shaw, R. et al. 2014. Business model considerations for development of cell therapies. *Bioprocess Int* 12(4), pp. 10–14.

Sherman, R.E. et al. 2013. Expediting Drug Development — The FDA's New 'Breakthrough Therapy' Designation. *New England Journal of Medicine* 369(20), pp. 1877–1880. doi: 10.1056/NEJMp1311439.

Simaria, A.S. et al. 2014. Allogeneic cell therapy bioprocess economics and optimization: Single-use cell expansion technologies. *Biotechnology and Bioengineering* 111(1), pp. 69–83. doi: 10.1002/bit.25008.

Singh, H. et al. 2013. Manufacture of Clinical-Grade CD19-Specific T Cells Stably Expressing Chimeric Antigen Receptor Using Sleeping Beauty System and Artificial Antigen Presenting Cells. *PLoS ONE* 8(5), pp. 1–11. doi: 10.1371/journal.pone.0064138.

Singh, N. et al. 2010. Potential toxicity of superparamagnetic iron oxide nanoparticles (SPION). *Nano Reviews* 1(0), pp. 1–15. doi: 10.3402/nano.v1i0.5358.

Sivertsson, L. et al. 2012. Hepatic Differentiation and Maturation of Human Embryonic Stem Cells Cultured in a Perfused Three-Dimensional Bioreactor. *Stem Cells and Development* 22(4), p. 121102064642003. doi: 10.1089/scd.2012.0202.

Smith, C. et al. 2015. Ex vivo expansion of human T cells for adoptive immunotherapy using the novel Xeno-free CTS Immune Cell Serum Replacement. *Clinical & translational immunology* 4(1), p. e31. doi: 10.1038/cti.2014.31.

Smith, D.M. 2012. Assessing commercial opportunities for autologous and allogeneic cell-based products. *Regenerative Medicine* 7(5), pp. 721–732. doi: 10.2217/rme.12.40.

Soldner, F. et al. 2009. Parkinson's Disease Patient-Derived Induced Pluripotent Stem Cells Free of Viral Reprogramming Factors. *Cell* 136(5), pp. 964–977. doi: 10.1016/j.cell.2009.02.013.

Somerville, R.P. et al. 2012. Clinical scale rapid expansion of lymphocytes for adoptive cell transfer therapy in the WAVE(R) bioreactor. *Journal of Translational Medicine* 10, p. 69. doi: 10.1186/1479-5876-10-69.

Somerville, R.P.T. and Dudley, M.E. 2012. Bioreactors get personal. *Oncoimmunology* 1(8), pp. 1435–1437. doi: 10.4161/onci.21206.

Spees, J.L. et al. 2004. Internalized antigens must be removed to prepare hypoimmunogenic mesenchymal stem cells for cell and gene therapy. *Molecular Therapy* 9(5), pp. 747–756. doi: 10.1016/j.ymthe.2004.02.012.

Stadtfeld, M. et al. 2008. Reprogramming of Pancreatic β Cells into Induced Pluripotent Stem Cells. *Current Biology* 18(12), pp. 890–894. doi: http://dx.doi.org/10.1016/j.cub.2008.05.010.

Stonier, A. et al. 2012. Decisional tool to assess current and future process robustness in an antibody purification facility. *Biotechnology Progress* 28(4), pp. 1019–1028. doi: 10.1002/btpr.1569.

Stonier, A. 2013. *A Dynamic Decision Support Tool For Use in The Design of Bio-manufacturing Facilities and Processes*. University College London.

Sullivan, G.J. et al. 2010. Generation of functional human hepatic endoderm from human induced pluripotent stem cells. *Hepatology* 51(1), pp. 329–35. doi: 10.1002/hep.23335.

Lo Surdo, J. and Bauer, S.R. 2012. Quantitative Approaches to Detect Donor and Passage Differences in Adipogenic Potential and Clonogenicity in Human Bone Marrow-Derived Mesenchymal Stem Cells. *Tissue Engineering. Part C, Methods* 18(11), pp. 877–889. doi: 10.1089/ten.tec.2011.0736.

Surmacz, B. et al. 2012. Directing differentiation of human embryonic stem cells toward anterior neural ectoderm using small molecules. *Stem Cells* 30(9), pp. 1875–1884. doi: 10.1002/stem.1166.

Takahashi, K. et al. 2007. Induction of Pluripotent Stem Cells from Adult Human Fibroblasts by Defined Factors. *Cell* 131(5), pp. 861–872. doi: 10.1016/j.cell.2007.11.019.

Tamura, A. et al. 2012. Temperature-responsive poly(N-isopropylacrylamide)-grafted microcarriers for large-scale non-invasive harvest of anchorage-dependent cells. *Biomaterials* 33(15), pp. 3803–3812. doi: 10.1016/j.biomaterials.2012.01.060.

Táncos, Z. et al. 2016. Establishment of induced pluripotent stem cell (iPSC) line from a 75-year old patient with late onset Alzheimer's disease (LOAD). *Stem Cell Research* 17(1), pp. 81–83. doi: http://dx.doi.org/10.1016/j.scr.2016.05.013.

Tey, S.-K. 2014. Adoptive T-cell therapy: adverse events and safety switches. *Clinical & translational immunology* 3(6), p. e17. doi: 10.1038/cti.2014.11.

Thomas, R.J. et al. 2009. Automated, scalable culture of human embryonic stem cells in feeder-free conditions. *Biotechnology and Bioengineering* 102(6), pp. 1636–1644. doi: 10.1002/bit.22187.

Trainor, N. et al. 2014. c o m m e n ta r y Rethinking clinical delivery of adult stem cell therapies. *Nature Publishing Group* 32(8), pp. 729–735. doi: 10.1038/nbt.2970.

Tumaini, B. et al. 2013. Simplified process for the production of anti–CD19-CAR–engineered T cells. *Cytotherapy* 15(11), pp. 1406–1415. doi:

10.1016/j.jcyt.2013.06.003.

Tzatzalos, E. et al. 2016. Engineered heart tissues and induced pluripotent stem cells: Macro- and microstructures for disease modeling, drug screening, and translational studies. *Advanced Drug Delivery Reviews* 96, pp. 234–244. doi: 10.1016/j.addr.2015.09.010.

Ungrin, M.D. et al. 2012. Rational bioprocess design for human pluripotent stem cell expansion and endoderm differentiation based on cellular dynamics. *Biotechnology and Bioengineering* 109(4), pp. 853–866. doi: 10.1002/bit.24375.

Uosaki, H. et al. 2011. Efficient and scalable purification of cardiomyocytes from human embryonic and induced pluripotent stem cells by VCAM1 surface expression. *PLoS ONE* 6(8). doi: 10.1371/journal.pone.0023657.

Valton, J. et al. 2015. A Multidrug-resistant Engineered CAR T Cell for Allogeneic Combination Immunotherapy. *Molecular therapy : the journal of the American Society of Gene Therapy* 23(9), pp. 1507–18. doi: 10.1038/mt.2015.104.

Vannucci, L. et al. 2013. Viral vectors: a look back and ahead on gene transfer technology. *The new microbiologica* 36(1), pp. 1–22.

Vera, J.F. et al. 2010. Accelerated production of antigen-specific T cells for preclinical and clinical applications using gas-permeable rapid expansion cultureware (G-Rex). *Journal of immunotherapy (Hagerstown, Md. : 1997)* 33(3), pp. 305–15. doi: 10.1097/CJI.0b013e3181c0c3cb.

Veraitch, F.S. et al. 2008. The impact of manual processing on the expansion and directed differentiation of embryonic stem cells. *Biotechnology and Bioengineering* 99(5), pp. 1216–1229. doi: 10.1002/bit.21673.

Villa-Diaz, L.G. et al. 2010. Synthetic polymer coatings for long-term growth of human embryonic stem cells. *Nature Biotechnology* 28(6), pp. 581–583. doi:

10.1038/nbt.1631.

Villa-Diaz, L.G. et al. 2013. Concise review: The evolution of human pluripotent stem cell culture: From feeder cells to synthetic coatings. *Stem Cells* 31(1), pp. 1–7. doi: 10.1002/stem.1260.

Vosough, M. et al. 2013. Generation of functional hepatocyte-like cells from human pluripotent stem cells in a scalable suspension culture. *Stem cells and development* 22(20), pp. 2693–705. doi: 10.1089/scd.2013.0088.

Walker, A. and Johnson, R. 2016. Commercialization of cellular immunotherapies for cancer. *Biochemical Society Transactions* 44(2), p. 329 LP-332.

Wang, D. and Bodovitz, S. 2010. Single cell analysis: The new frontier in 'omics'. *Trends in Biotechnology* 28(6), pp. 281–290. doi: 10.1016/j.tibtech.2010.03.002.

Wang, Y. et al. 2013. Scalable expansion of human induced pluripotent stem cells in the defined xeno-free E8 medium under adherent and suspension culture conditions. *Stem Cell Research* 11(3), pp. 1103–1116. doi: 10.1016/j.scr.2013.07.011.

Want, A.J. et al. 2012. Large-scale expansion and exploitation of pluripotent stem cells for regenerative medicine purposes: beyond the T flask. *Regenerative medicine* 7(1), pp. 71–84. doi: 10.2217/rme.11.101.

Warren, L. et al. 2010. Highly Efficient Reprogramming to Pluripotency and Directed Differentiation of Human Cells with Synthetic Modified mRNA. *Cell Stem Cell* 7(5), pp. 618–630. doi: 10.1016/j.stem.2010.08.012.

Watanabe, K. et al. 2007. A ROCK inhibitor permits survival of dissociated human embryonic stem cells. *Nature biotechnology* 25(6), pp. 681–686. doi: 10.1038/nbt1310.

Weber, C. et al. 2007. Expansion and Harvesting of hMSC-TERT. *The Open*

Biomedical Engineering Journal 1(1), pp. 38–46. doi: 10.2174/1874120700701010038.

Wegener, C. 2014. Cell washing with the LOVO cell processing system. *BioProcess International* August(Industry Yearbook 2014-2015), p. 78.

Weil, B.D. et al. 2017. An integrated experimental and economic evaluation of cell therapy affinity purification technologies. *Regenerative Medicine* 12(4), pp. 397–417. doi: 10.2217/rme-2016-0156.

Weil, B.D. and Veraitch, F.S. 2013. Bioprocessing challenges associated with the purificaiton of cellular therapies. In: *Stem Cells and Cell Therapy*., pp. 293–326. doi: 10.1007/978-3-319-02904-7.

Weng, Z. et al. 2014. A Simple, Cost-Effective but Highly Efficient System for Deriving Ventricular Cardiomyocytes from Human Pluripotent Stem Cells. *Stem cells and development* 0(0), pp. 1–13. doi: 10.1089/scd.2013.0509.

Wolfe, R.P. et al. 2012. Effects of shear stress on germ lineage specification of embryonic stem cells. *Integrative Biology* 4(10), p. 1263. doi: 10.1039/c2ib20040f.

Wolfe, R.P. and Ahsan, T. 2013. Shear stress during early embryonic stem cell differentiation promotes hematopoietic and endothelial phenotypes. *Biotechnology and Bioengineering* 110(4), pp. 1231–1242. doi: 10.1002/bit.24782.

Wu, S.M. and Hochedlinger, K. 2011. Harnessing the potential of induced pluripotent stem cells for regenerative medicine. *Nat Cell Biol* 13(5), pp. 497–505.

Yajuan, X. et al. 2012. A Comparison of the Performance and Application Differences Between Manual and Automated Patch-Clamp Techniques. *Current Chemical Genomics* 6, pp. 87–92.

Yang, H.S. et al. 2010. Suspension culture of mammalian cells using thermosensitive microcarrier that allows cell detachment without proteolytic enzyme

treatment. *Cell Transplantation* 19(9), pp. 1123–1132. doi: 10.3727/096368910X516664.

Yang, S. et al. 2008. Clinical-scale lentiviral vector transduction of PBL for TCR gene therapy and potential for expression in less differentiated cells. *J Immunother.* 31(9), pp. 830–839. doi: 10.1097/CJI.0b013e31818817c5.Clinical-scale.

Yang, Y. et al. 2015. Challenges and opportunities of allogeneic donor-derived CAR T cells. *Current opinion in hematology* 22(6), pp. 509–15. doi: 10.1097/MOH.0000000000000181.

Yla-Herttuala, S. 2015. Glybera/'s Second Act: The Curtain Rises on the High Cost of Therapy. *Mol Ther* 23(2), pp. 217–218.

Yoon, K.P. and Hwang, C. 1995. Multiple Attribute Decision Making. Hwang, C.-L. ed. doi: 10.4135/9781412985161.

Yu, J. et al. 2009. Human Induced Pluripotent Stem Cells Free of Vector and Transgene Sequences. *Science (New York, N.Y.)* 324(5928), pp. 797–801. doi: 10.1126/science.1172482.

Zeevi-Levin, N. et al. 2012. Cardiomyocytes derived from human pluripotent stem cells for drug screening. *Pharmacology and Therapeutics* 134(2), pp. 180–188. doi: 10.1016/j.pharmthera.2012.01.005.

Zhang, J. et al. 2009. Functional cardiomyocytes derived from human induced pluripotent stem cells. *Circulation Research* 104(4). doi: 10.1161/CIRCRESAHA.108.192237.

Zhou, W. and Freed, C.R. 2009. Adenoviral gene delivery can reprogram human fibroblasts to induced pluripotent stem cells. *Stem Cells* 27(11), pp. 2667–2674. doi: 10.1002/stem.201.

Zhou, X. et al. 2003. Lentivirus-Mediated Gene Transfer and Expression in

Established Human Tumor Antigen-Specific Cytotoxic T Cells and Primary Unstimulated T Cells. *Human Gene Therapy* 14(11), pp. 1089–1105. doi: 10.1089/104303403322124800.

Zhu, S. et al. 2011. Chemical strategies for stem cell biology and regenerative medicine. *Annual review of biomedical engineering* 13, pp. 73–90. doi: 10.1146/annurev-bioeng-071910-124715.

Zweigerdt, R. 2007. The art of cobbling a running pump—Will human embryonic stem cells mend broken hearts? *Seminars in Cell & Developmental Biology* 18(6), pp. 794–804. doi: http://dx.doi.org/10.1016/j.semcdb.2007.09.014.

Zweigerdt, R. et al. 2011. Scalable expansion of human pluripotent stem cells in suspension culture. *Nature protocols* 6(5), pp. 689–700. doi: 10.1038/nprot.2011.318.

Zwi-Dantsis, L. et al. 2011. Scalable production of cardiomyocytes derived from c-Myc free induced pluripotent stem cells. *Tissue engineering. Part A* 17, pp. 1027–1037. doi: 10.1089/ten.tea.2010.0235.

Appendix A: An integrated experimental and economic evaluation of cell therapy affinity purification technologies

A1. Foreword

This section of the appendix contains the manuscript for a paper submitted to *Regenerative Medicine*. The work presented in the manuscript was carried out jointly the manuscript's first author, Dr Ben Weil, and the author of this thesis. I, Michael Jenkins, carried out the bioprocess economic modelling methods described in Section 2.2 of the manuscript. Dr Weil was responsible for the experimental work and results described in Sections 2.1. The manuscript was drafted as a joint effort between Dr. Ben Weil and I, with additional input from other listed authors within the manuscript.

Appendix B: Papers published, or submitted for publication as part of this thesis

The following papers, published during the course of this thesis are included in the appendix below:

Jenkins, M.J. & Farid, S.S., 2015. Human pluripotent stem cell-derived products: Advances towards robust, scalable and cost-effective manufacturing strategies. *Biotechnology Journal*, 10(1), pp.83–95.

Jenkins, M.J. et al., 2016. Patient-specific hiPSC bioprocessing for drug screening: Bioprocess economics and optimisation. *Biochemical Engineering Journal*, 108, pp.84–97.

The following paper and book chapter have also been produced as part of the work carried out in preparation of this thesis. Weil et al. (2017) can be found in Appendix A and the book chapter has not been included to its length, however the content is largely based upon Chapters 1 & 2 of this thesis.

Weil, B.D. et al., 2017. An integrated experimental and economic evaluation of cell therapy affinity purification technologies. *Regen Med*, 12(4), pp.397-417

Jenkins, M.J. & Farid, S.S., 2017. Bioprocesses for Cell Therapies. In G. Jagschies et al., eds. Handbook of Bioprocessing. Elsevier, p. In press.

A final paper has also been drafted, based on Chapter 6 of this thesis. This will be submitted to *Biochemcial Engineering Journal* in Q4 2017.

Biotechnology Journal
www.biotechnology-journal.com

Biotechnol. J. 2015, 10, 83–95

DOI 10.1002/biot.201400348

Review

Human pluripotent stem cell-derived products: Advances towards robust, scalable and cost-effective manufacturing strategies

Michael J. Jenkins and Suzanne S. Farid

Department of Biochemical Engineering, University College London, London, UK

The ability to develop cost-effective, scalable and robust bioprocesses for human pluripotent stem cells (hPSCs) will be key to their commercial success as cell therapies and tools for use in drug screening and disease modelling studies. This review outlines key process economic drivers for hPSCs and progress made on improving the economic and operational feasibility of hPSC bioprocesses. Factors influencing key cost metrics, namely capital investment and cost of goods, for hPSCs are discussed. Step efficiencies particularly for differentiation, media requirements and technology choice are amongst the key process economic drivers identified for hPSCs. Progress made to address these cost drivers in hPSC bioprocessing strategies is discussed. These include improving expansion and differentiation yields in planar and bioreactor technologies, the development of xeno-free media and microcarrier coatings, identification of optimal bioprocess operating conditions to control cell fate and the development of directed differentiation protocols that reduce reliance on expensive morphogens such as growth factors and small molecules. These approaches offer methods to further optimise hPSC bioprocessing in terms of its commercial feasibility.

Received 07 JUL 2014
Revised 18 SEP 2014
Accepted 13 OCT 2014

Keywords: Bioprocess economics · Cell therapy · Regenerative medicine · Scale-up · Pluripotent stem cells

1 Introduction

Human pluripotent stem cells (hPSCs) have opened fresh avenues in modern medicine that have the potential to revolutionise healthcare, particularly since the first derivation of induced pluripotent stem cells (iPSCs) [1, 2]. Human embryonic stem cells (hESCs) and human-induced pluripotent stem cells (hiPSCs) have the capacity to differentiate into all mature cell types, making them attractive candidates for use as cell therapies [3]. Moreover, hPSCs also offer a unique, novel platform by which to augment, and even redefine, current drug discovery and drug screening programmes by the provision of a human in vitro tool on which to perform efficacy and toxicity screens for novel chemical entities (NCEs) [4, 5]. hiPSCs could also pave the way for personalised medicine through the medium of responders versus non-responder 'trial in a dish' models [6].

hPSCs can provide a cornerstone of the regenerative medicine industry via the provision of cell therapies for diseases with unmet clinical needs. hiPSCs in particular might provide a diagnostic tool capable of assuaging the high late-phase failure rate of NCEs in clinical trials [7, 8]. The market for stem cell research products exceeded $3bn at the end of 2013 (http://tinyurl.com/n26fe4z). hPSCs for use as research tools are currently marketed at $2000–$3000/vial [9]. However, the value of this market is likely to be incremental when considered against hPSC-derived cell therapies [10], which has the potential to tap into a multi-billion dollar global market [11]. If hPSCs are

Correspondence: Dr. Suzanne S. Farid, Department of Biochemical Engineering, University College London, Bernard Katz Building, Gordon Street, London WC1H 0AH, UK
E-mail: s.farid@ucl.ac.uk

Abbreviations: COG, cost of goods; **cGMP,** current good manufacturing practice; **cGTP,** current good tissue practice; **FCI,** fixed capital investment; **hPSC,** human pluripotent stem cell; **QbD,** quality by design; **SUB,** single-use bioreactor

Table 1. Bioprocess development considerations for hPSC-derived products

Consideration	Example Criteria
Operational performance	Expansion yields (harvest densities) Expansion folds Differentiation efficiencies DSP yields Purity Resource utilisation Scalability Lot processing time
Economic	Capital investment Cost of goods (materials, labour, quality control and indirect) Economies of scale – scale-up versus scale-out Fresh versus frozen product transportation and storage Process development costs Supply chain replenishment Product shelf-life Reimbursement value
Quality control and regulatory compliance	cGMP and cGTP standards Process robustness and reproducibility Process validation, acceptable ranges of operation Product characterisation Quality, consistency and source of raw materials Automated versus manual processing
Safety	Contamination and containment Live human tissue handling Patient safety – side-effects, risk of tumour formation
Flexibility	Process changes Manufacturing demand changes Process bottlenecks Process scalability

to achieve their full clinical and commercial potential, significant challenges must be overcome with regards to current abilities to produce hPSC-derived cells at commercially relevant scales.

At the forefront of current challenges to hPSC-derived therapies is the production of cells at a relevant quantity and quality to support their function. Details on the bioprocess techniques for hPSC therapies currently being manufactured for preclinical and clinical trials or for use as research tools are provided in Table 1. To date, hPSC-derived products in development have mainly consisted of retinal progenitor cells and pancreatic β-cells derived from hESCs [12–15], or a variety of cell lineages such as neurons, cardiomyocytes and hepatocytes derived from hPSCs for use as research tools [16]. Promising results have also been observed for cell therapies derived from hiPSCs, such as retinal pigment epithelial cells [17]. Table 2 indicates that most products in clinical development still depend on planar technologies. Traditional, planar technologies that offer reliable tools for laboratory-based protocols are labour-intensive and do not lend themselves to large scale, allogeneic processes [18]. Dose sizes reported for hPSC-derived cell therapy products currently range from 5×10^4 cells for indications such as macular degeneration to 10^8 cells for diseases such as diabetes (Table 2). Furthermore, it has been estimated that large doses, of around 10^9 cells, will be needed to treat conditions such as myocardial infarction and liver disease [19, 20]. Whilst this review focuses on process techniques for the production of single-cell type populations, therapies for certain disease types will necessitate transplantation of a functional tissue-like structure. Novel, organoid development techniques may therefore provide a method of production of tissue-like structure representing a variety of different organs from small seed populations of hPSCs. These have potential applications as either transplantable therapies or research tools [21–24].

Planar technologies may struggle to satisfy the global demand for hPSC-derived cell therapies requiring high dose sizes [20, 25]. Furthermore, there is widespread use of xenogeneic materials associated with traditional hPSC technologies, preventing their use in the production of clinical grade hPSC-derived cells. Differentiation strategies have often represented idiosyncratic protocols that have proven difficult to translate to robust bioprocess unit operations [26]. Media costs associated with hPSC processes are of further concern; many media supplements render the products of current hPSC processes prohibitively expensive for purpose. Additionally, studies into the poorly understood interactions between hPSCs and the microenvironment provided by media components and cell anchorage materials are only now beginning to take place; significant gaps exist in our knowledge of how the design of such materials affects hPSC activity [27].

Previous reviews in this field have discussed advances in the large-scale expansion and bioreactor-based culture of hPSCs (e.g. [25, 28–30]). Other studies have focused upon the impact of the design of microcarriers and anchorage materials on hPSC bioprocessing (e.g. [27, 31–33]). Herein, we aim to summarise key considerations and methods that might be employed in order to achieve cost-effective bioprocess design across a range of manufacturing scales. Key process economic metrics and drivers are outlined. A discussion of advancements in robust, GMP-based expansion and directed differentiation strategies is provided. Finally, a review of recent innovations in integrated bioprocess design is presented.

Table 2. Technologies used for expansion and differentiation of hPSC-derived cell products used in clinical trials or as research tools

Company	Indication	Target cell type	Dose size	Cell expansion[a] details	Differentiation details[a]	Source
Cellectis	Diabetes mellitus (type I)	Insulin producing β-cells	ND	SUB: hollow fiber, multicompartment perfusion bioreactor	SUB: hollow fiber, multicompartment perfusion bioreactor	[12]
Advanced Cell Technology	Macular degeneration	Retinal pigment epithelial (RPE) cells	5×10^4	Planar: well-plates, MEF feeder layer, three passages	Planar: well-plates EB formation	[13]
CellCure	Macular degeneration	RPE cells	2×10^4	Planar: well-plates xeno-free media	Planar: well-plates, 8-wk process, serum-free conditions	[14]
Healios	Macular degeneration	RPE cells	5×10^4	Planar: plate-based custom designed automated process platform	Planar: plate-based custom designed automated process platform	[17]
ViaCyte	Diabetes mellitus (types I and II)	Pancreatic β-cell precursors	10^8	Planar: multi-layer cell factories, 2-wk process, xeno-free media	Planar: plate-based aggregate differentiation, 2-wk process, Xeno-free media	[15]
Geron[b]	Spinal cord injuries	Oligodendrocyte progenitor cells	2×10^6	Planar: matrigel coated T-flasks, 3- to 5-wk process	Planar: T-flasks, 6-wk process, growth factor-based protocol	[111]
Cellular Dynamics International	hiPSC-derived cells for use as research tools	Cardiomyocytes, neurons, hepatocytes, endothelial cells	N/A	SUB: litre-scale, five passages, Xeno-free media	SUB: litre-scale, chemically defined conditions	[16]

a) Technologies for expansion and differentiation operations are detailed alongside process durations and media where this information is available.
b) Geron's GRNOPC1 therapy was withdrawn from trials but has been included in this table for comparison.

2 Cell therapy bioprocess economics

When examining process options for hPSC manufacture, it is important to consider not only the operational performance but also the consequences on the economics, quality, regulatory compliance, safety and flexibility. These key considerations are summarised in Table 1. This review pays particular attention to progress made on improving the economic and operational feasibility of hPSC bioprocessing.

Reimbursement pressures have resulted in an increased awareness of the importance of estimating and improving manufacturing costs for stem cell products. This section discusses factors that influence two key cost metrics: fixed capital investment (FCI) and cost of goods (COG).

2.1 Capital investment

The FCI represents the cost to build a manufacturing facility ready for start-up. It includes the cost of the building with the fixed (non-disposable) equipment, piping, instrumentation and utilities installed. Estimates of facility costs are often made using factorial estimates. These are well established for traditional stainless steel biopharmaceutical facilities using the Lang Factor method [34], which involves multiplying the total equipment purchase cost by the 'Lang factor'. At present, there are no published studies that have determined an appropriate factorial method for stem cell manufacturing facilities. The Lang factor is usually derived based on the analysis of costs of previous projects; as yet very few FCI benchmarks have been published for stem cell manufacturing facilities. Investment costs for stem cell facilities will also be influenced by the degree of open versus closed processing and the consequences on the cleanroom classification required and whether automated or manual process techniques are employed. Stem cell bioprocessing is also dependent on disposable or single-use process platforms such as T-flasks, CellStacks and single-use bioreactors (SUBs). To this end, a Lang factor method adapted for disposable-based biopharmaceutical facilities is currently the best method available by which to approximate the FCI associated with stem cell manufacturing [35]. Ongoing work at University College London is focused upon developing a method for estimating FCI that is specific to stem cell manufacturing facilities.

2.2 Cost of goods

The COG represents the cost to manufacture a stem cell product and comprises direct (e.g. materials) and indirect (e.g. maintenance) costs. Simaria et al. [20] summarise key factors that influence COG values for stem cell products; these include process efficiencies (e.g. harvest den-

sities post-expansion, differentiation yields), technology choices (e.g. planar vs. microcarrier-based SUBs), and resources required and their unit costs (e.g. media, single-use vessels and labour). Economies of scale are a relevant factor as demand and lot size are varied as well as dose for cell therapies and required cell population sizes for cells as drug screening tools. Outputs are usually expressed as COG per cell population for screening tools or COG per dose for therapeutic applications.

Decision-support software can aid the design of cost-effective bioprocesses. However, to date, few published cost studies exist for stem cell bioprocessing. Commercially available flowsheeting software packages have been employed to cost stem cell process designs at fixed scales [36]. Simaria et al. [20] and Hassan et al. [37] present the development and application of decisional tools that integrate models for mass balancing, equipment sizing and bioprocess economics with optimisation algorithms for allogeneic mesenchymal stem cell (MSC) production. The tools were used to predict the most cost-effective upstream and downstream technologies for commercial MSC manufacture across a range of different scales and doses. The analyses presented in these works illustrate how such tools can be used to determine the scale at which planar technologies cease to be cost-effective in contrast to microcarrier-based SUBs, when downstream processing bottlenecks occur, as well as future required performance capabilities of promising technologies to close existing technology gaps and meet COG targets. This approach is being extended [38] to hPSC processes, which typically have additional process steps such as differentiation, so as to identify key economic drivers for drug screening and therapeutic applications, and predict technical innovations required to bridge the gaps constraining widespread application of hPSCs.

In addition to considering the costs of stem cell bioprocessing alternatives, it is also useful to capture the impact of uncertainties such as lot-to-lot variability and contamination risks, particularly when manual processing techniques are employed [39]. Stochastic modelling techniques, such as the Monte Carlo simulation method, have been used to evaluate process robustness under uncertainty in the biopharmaceutical sector [35, 40, 41]. Stochastic modelling has yet to be applied to iPSC processing, but will form an important part of future work in order to develop robust and cost-effective hPSC bioprocesses.

2.3 Process economic drivers

In order to achieve cost-effective bioprocesses for hPSCs, efforts need to focus on increasing the overall productivity and/or decreasing the overall production costs. Hence, critical process economic drivers for hPSC processes include expansion and differentiation yields as well as the cost of materials and labour. The remainder of this paper therefore focuses on progress made on the expansion and differentiation yields in planar and bioreactor technologies as well as the development of media and cell-anchorage materials for these unit operations.

3 hPSC bioprocessing strategies: Expansion

3.1 Planar culture systems for hPSC expansion

Until recently, planar hPSC culture platforms relied heavily on the use of xenogeneic growth substrates and non-human feeder layers, which risk contamination of hPSC-derived products. Furthermore, feeder layers differentially secrete signalling factors, resulting in poorly defined culture conditions that are unsuitable for empirical study of hPSC expansion [42]. The development of anchorage materials comprising of a mixture of synthetic and/or recombinant biological motifs have allowed hPSC culture to progress away from the use of feeder layers [31].

The labour-intensive nature of T-flasks limits their throughput and applicability to larger-scale processes [18, 25]. Systems that stack multiple culture chambers above one another vertically have enabled greater cell yields than traditional 2D culture methods at lower factory floor footprints [43]. The Cell Factory (ThermoFisher Scientific, Waltham, MA, USA), CellStack/ HyperStack (Corning, New York, NY, USA) and Xpansion (Pall Life Sciences, Port Washington, NY, USA) systems are examples of this. Inflated facility size requirements and subsequent capital investment costs associated with 2D culture scale-up are challenges facing companies hoping to produce hPSCs on a commercial scale [44, 45].

Automated, closed-process systems such as the CompacT SelecT (Sartorius AG, Gottingen, Germany), capable of handling 90 × T175 flasks simultaneously, and the Nunc Automatic Cell Factory Manipulator (ThermoFisher Scientific), capable of manipulating 4 × 40 layer vessels, may help increase the throughput of 2D hPSC bioprocess strategies [46] during expansion and differentiation. Automated systems allow processing to take place in smaller, lower clean rooms compared to manual processing. The closed processing offered by automation systems provides greater process control and reproducibility compared to manual processes [39].

Planar processing platforms will continue to have a place in commercial hPSC bioprocesses. This is particularly likely for the production of autologous cell therapies and patient-specific hPSC-derived cells for personalised medicine drug screening that necessitate a scale-out, rather than a scale-up approach to bioprocess design [43].

3.2 Three-dimensional culture systems for hPSC expansion

There are two main methods of 3D hPSC culture; the use of suspended microcarriers as adherent surfaces for stem

cell growth [47], or growth of hPSCs as suspended aggregates in SUBs [48]. 3D hPSC culture systems allow online process monitoring, provide greater scalability potential and reduce facility size requirements when compared to planar technologies. Bioreactor systems also permit strict control of conditions during bioprocesses [49]. A challenge to implementation of 3D culture of hPSCs is exposure of cells to shear forces, which must be tightly controlled as they can impact upon hPSC fate determination [50, 51]. Development of xeno-free, defined media [52] is crucial to the robust bioprocessing of hPSCs. The simplicity of such media may reduce costs associated with hPSC expansion materials by 30–60% [53].

3.2.1 *Microcarrier-based systems for hPSC expansion*

Microcarriers are small beads or discs, which permit propagation or directed differentiation of hPSCs within a 3D bioreactor. hPSC studies investigating microcarriers have recently achieved expansion folds as high as 28-fold over 6 days [54]. Microcarrier-based expansion folds are often higher than those in 2D expansion studies across similar timescales [46, 47, 55–57]. Several recently published reviews include summary tables for SUB-based hPSC expansion studies (using both microcarrier and aggregate culture strategies [25, 28, 29].

A critical property of microcarriers is their high surface area to volume ratio, on which large populations of hPSC cells may be cultured in a relatively small vessel, alleviating the costs associated with expensive media and supplements necessary for hPSC bioprocessing [28, 56]. Microcarriers are able to support expansion and long-term self-renewal of hPSCs over multiple passages, proving the platform's capability to support production of clinically relevant cell numbers [47]. Microcarrier culture of hPSCs also results in cell colonies that generally have less than 10 layers [58]; thus concentration profiles of nutrients and signalling molecules are less likely to occur than in aggregate-based cultures.

The common use of microcarrier coatings that contain animal-derived components, which are unsuitable for use in the manufacture of cell therapies, is a significant challenge to culture of hPSCs on microcarriers. Serum-free and feeder-free microcarrier platforms are available for hPSC-based processing, although many of these utilise the microcarrier coating, Matrigel, which is derived from murine origins [25]. Recombinant human proteins can now be used as a substitute for animal-derived microcarrier coatings in planar and 3D microcarrier cultures [59, 60]. However, such proteins can be difficult to isolate, expensive to produce, and prone to lot-to-lot variation. Synthetic substrates, which circumvent consistency issues associated with recombinant substrates, have been developed in planar conditions and successfully applied to microcarrier-based hPSC culture [61–63].

Xeno-free microcarrier coatings utilise polymers to mimic Matrigel and feeder layer properties in order to encourage attachment and self-renewal of hPSCs on microcarriers. Expansion folds on xeno-free microcarriers comparable to those coated with Matrigel have been reported [60, 63]. It has been proposed that positively charged microcarriers can be used to successfully support hPSC expansion at clinically relevant scales and similar cell concentrations and expansion folds to coated microcarriers were achieved [58]. Methods of xeno-free hPSC culture represent a regulatory compliant approach to the production of hPSCs for clinical applications; they also reduce additional expenses incurred by the use of supplementary serums. Development of xeno-free microcarrier coatings is one area where a quality-by-design (QbD) approach to product development has allowed elucidation of specific properties of microcarriers that affect hPSC self-renewal.

Harvesting of cells from microcarriers is usually carried out using enzymatic separation, which can add to material costs associated with microcarrier-based culture of hPSCs. Microcarriers coated in thermo-sensitive polymers that allow detachment of seeded cells obviate the need for dissociation enzymes, although studies in this area are still in their preliminary phases in this area [64].

Parallel to developing GMP-based hPSC expansion protocols, research has focused on optimising bioreactor conditions for dynamic hPSC expansion processes so as to increase achievable expansion folds and cell concentrations. This will help reduce COG associated with manufacture of hPSCs. Controlling the dissolved oxygen levels has been found to be critical during hPSC culture on microcarriers in SUBs; 2.5 higher expansion folds and ~85% improvements in maximum cell concentrations were reported in a hypoxic environment when compared to uncontrolled conditions [57]. Furthermore, attachment of hPSCs to microcarriers as single cells can improve seeding efficiency from 30 to over 80% and reduce durations associated with microcarrier loading compared to clump seeding [63].

3.2.2 *Aggregate suspension culture of hPSCs*

hPSCs can be cultured as suspended aggregates in bioreactors. When hPSCs are grown as aggregates the rho-associated protein kinase inhibitor (ROCKi), Y-27632, is used to protect single cells from dissociation-induced apoptosis [65]. Each cell aggregate is treated as a de facto colony. Aggregate sizes must be controlled in suspension bioreactors to prevent differentiation of cells in larger colonies [66–68]. It has been reported that aggregate culture of stem cells increases the therapeutic potential and the differentiation efficiency of hPSCs via the sustainment of endogenous signalling within cell colonies [32]. Aggregate expansion of hPSCs also negates the need for expensive (and sometimes undefined) components of substrates upon which hPSCs are cultivated in adherent cultures [67]. Aggregate culture of hPSCs rely more heavily on the expensive media supplements (such as GFs)

compared to microcarrier culture [54]. Several groups have proposed methods of hPSC culture through the use of cell aggregates with the potential to be scaled up in order to produce clinically relevant cell numbers [67–69]. Twenty-fivefold expansion has been achieved over 14 days during aggregate-based hPSC culture [49] and studies into expansion of hPSCs as aggregates yield similar expansion-folds when compared to microcarrier systems [70–72]. Long-term maintenance of hPSCs in aggregates in dynamic bioreactor conditions over several passages has also been proven to be feasible [49, 68]. Aggregate-based hPSC cultivation necessitates frequent manual interactions in order to control aggregate sizes [28, 71, 73], which will adversely affect labour costs and the robustness of aggregate-based hPSC bioprocesses.

Agitation rates can be used to successfully modulate uniform aggregate size in order to improve expansion of hPSCs as aggregates and reduce cell loss due to shear forces [53, 68]. This is also the case with microcarrier cultures, where impeller speeds of between 45 and 60 rpm were found to promote optimal cell population doubling times [74]. The effects of shear on hPSC self-renewal and lineage determination is an area of intensifying research, although currently this is a poorly understood area in terms of the effect of mechanical strain on hPSC fate determination [29, 75].

The importance of cell inoculation concentration has been demonstrated during aggregate culture of hPSCs in dynamic bioreactor conditions; seeding concentrations of 2–3 × 10^5 cells/mL were found to maximise viability of hPSCs [68, 76]. Single cell inoculation has also been estimated to reduce cell losses by up to 60% [68]. Cell concentrations of up to 3.4 × 10^6 hPSCs/mL have been achieved using dynamic, aggregate-based culture techniques [76]. This represents 1.9-fold improvement over maximum cell concentrations achieved in planar systems, although it is significantly lower than the maximum cell concentrations achieved in xeno-free hPSC cultures performed in microcarrier-based systems (6 × 10^6 cells/mL) [77].

A few aggregate hPSC expansion processes combine xeno-free conditions with defined media [53, 69, 71]. These investigations represent a valuable effort to remove media supplements that either introduce the risk of xenogeneic material to hPSCs or expose media to lot-to-lot variability, although early attempts resulted in relatively modest expansion folds [69].

4 hPSC bioprocessing strategies: Differentiation

4.1 Planar strategies for hPSC differentiation

Traditional stem cell differentiation protocols were designed around bench-scale research paradigms and little effort was made to incorporate reproducibility and process robustness into these experiments [78]. Directed differentiation strategies often involve exposing hPSCs to a cocktail of morphogens, at specific time-points throughout the differentiation process [79–82]. Similar to hPSC expansion, traditional differentiation strategies rely heavily upon the use of xenogeneic materials [83]. Planar differentiation protocols, that are free of xenogeneic material, have been reported [84]. Despite such progress, many differentiation protocols are inherently variable owing to the laboratory idiosyncrasies of individual technicians, thus reliable and robust differentiation processes are still in their infancy. Timescales and efficiencies also vary significantly between experiments even when the same cell type is targeted for production (Table 3).

The use of small molecules within differentiation protocols has helped to improve their reproducibility via reduced use of recombinant growth factors [85, 86]. Several groups have created highly simplified protocols, whilst still improving the efficiency and processing times of 2D differentiation processes, by replacing growth factors with small molecules in the preliminary stages of differentiation protocols [84, 87, 88]. A protocol with the specified aim of creating a differentiation process capable of creating dopaminergic neurons for transplantation in T-flasks has been developed [89]. This strategy enabled the production of cryopreservable dopaminergic neurons with a high level of efficiency, allowing better control of time management in within the differentiation process. This approach is well served to reduce bottlenecks in the downstream phases of autologous hPSC processes. Further advances have proven it is possible to derive progenitor cells, suitable for transplantation as cell therapies at high efficiencies [90] and in xeno-free and small-molecule free, defined conditions [91]. Negation of the need for small molecules and growth factors also has the potential to drastically reduce the cost of differentiation procedures.

4.2 Bioreactor-based systems for hPSC differentiation

Concentrated research into bioreactor-based differentiation strategies has stemmed from the need to translate differentiation from a lab-scale area of research into processes capable of producing industrially relevant cell numbers in a reproducible manner. A number of studies in which hPSCs have been successfully differentiated in bioreactor conditions have been carried out, either attached to microcarriers [92] or in the form of cell aggregates [93, 94]. Differentiation strategies developed in 3D bioreactors, particularly stirred-tank vessels, lend themselves to large-scale processes far better than their planar counterparts as labour-intensive tasks, such as media exchanges, can be fully automated in such vessels, which also offer processing advantages such as online environmental monitoring and control. Research carried out on

compared to microcarrier culture [54]. Several groups have proposed methods of hPSC culture through the use of cell aggregates with the potential to be scaled up in order to produce clinically relevant cell numbers [67–69]. Twenty-fivefold expansion has been achieved over 14 days during aggregate-based hPSC culture [49] and studies into expansion of hPSCs as aggregates yield similar expansion-folds when compared to microcarrier systems [70–72]. Long-term maintenance of hPSCs in aggregates in dynamic bioreactor conditions over several passages has also been proven to be feasible [49, 68]. Aggregate-based hPSC cultivation necessitates frequent manual interactions in order to control aggregate sizes [28, 71, 73], which will adversely affect labour costs and the robustness of aggregate-based hPSC bioprocesses.

Agitation rates can be used to successfully modulate uniform aggregate size in order to improve expansion of hPSCs as aggregates and reduce cell loss due to shear forces [53, 68]. This is also the case with microcarrier cultures, where impeller speeds of between 45 and 60 rpm were found to promote optimal cell population doubling times [74]. The effects of shear on hPSC self-renewal and lineage determination is an area of intensifying research, although currently this is a poorly understood area in terms of the effect of mechanical strain on hPSC fate determination [29, 75].

The importance of cell inoculation concentration has been demonstrated during aggregate culture of hPSCs in dynamic bioreactor conditions; seeding concentrations of 2–3 × 10^5 cells/mL were found to maximise viability of hPSCs [68, 76]. Single cell inoculation has also been estimated to reduce cell losses by up to 60% [68]. Cell concentrations of up to 3.4 × 10^6 hPSCs/mL have been achieved using dynamic, aggregate-based culture techniques [76]. This represents 1.9-fold improvement over maximum cell concentrations achieved in planar systems, although it is significantly lower than the maximum cell concentrations achieved in xeno-free hPSC cultures performed in microcarrier-based systems (6 × 10^6 cells/mL) [77].

A few aggregate hPSC expansion processes combine xeno-free conditions with defined media [53, 69, 71]. These investigations represent a valuable effort to remove media supplements that either introduce the risk of xenogeneic material to hPSCs or expose media to lot-to-lot variability, although early attempts resulted in relatively modest expansion folds [69].

4 hPSC bioprocessing strategies: Differentiation

4.1 Planar strategies for hPSC differentiation

Traditional stem cell differentiation protocols were designed around bench-scale research paradigms and little effort was made to incorporate reproducibility and process robustness into these experiments [78]. Directed differentiation strategies often involve exposing hPSCs to a cocktail of morphogens, at specific time-points throughout the differentiation process [79–82]. Similar to hPSC expansion, traditional differentiation strategies rely heavily upon the use of xenogeneic materials [83]. Planar differentiation protocols, that are free of xenogeneic material, have been reported [84]. Despite such progress, many differentiation protocols are inherently variable owing to the laboratory idiosyncrasies of individual technicians, thus reliable and robust differentiation processes are still in their infancy. Timescales and efficiencies also vary significantly between experiments even when the same cell type is targeted for production (Table 3).

The use of small molecules within differentiation protocols has helped to improve their reproducibility via reduced use of recombinant growth factors [85, 86]. Several groups have created highly simplified protocols, whilst still improving the efficiency and processing times of 2D differentiation processes, by replacing growth factors with small molecules in the preliminary stages of differentiation protocols [84, 87, 88]. A protocol with the specified aim of creating a differentiation process capable of creating dopaminergic neurons for transplantation in T-flasks has been developed [89]. This strategy enabled the production of cryopreservable dopaminergic neurons with a high level of efficiency, allowing better control of time management in within the differentiation process. This approach is well served to reduce bottlenecks in the downstream phases of autologous hPSC processes. Further advances have proven it is possible to derive progenitor cells, suitable for transplantation as cell therapies at high efficiencies [90] and in xeno-free and small-molecule free, defined conditions [91]. Negation of the need for small molecules and growth factors also has the potential to drastically reduce the cost of differentiation procedures.

4.2 Bioreactor-based systems for hPSC differentiation

Concentrated research into bioreactor-based differentiation strategies has stemmed from the need to translate differentiation from a lab-scale area of research into processes capable of producing industrially relevant cell numbers in a reproducible manner. A number of studies in which hPSCs have been successfully differentiated in bioreactor conditions have been carried out, either attached to microcarriers [92] or in the form of cell aggregates [93, 94]. Differentiation strategies developed in 3D bioreactors, particularly stirred-tank vessels, lend themselves to large-scale processes far better than their planar counterparts as labour-intensive tasks, such as media exchanges, can be fully automated in such vessels, which also offer processing advantages such as online environmental monitoring and control. Research carried out on

Table 3. Key performance characteristics of planar and bioreactor-based differentiation protocols

Derived cell-type	Method	Time (days)	Number of target cells per input hPSC (ratio)	Reported efficiency (%)	Max. cell concentration (cells/mL)[a]	Refs.
Cardiomyocyte	2D monolayer	9	ND	64.8 ± 3.3	$2.5–5 \times 10^4$	[87]
Cardiomyocyte	2D EB formation	60	0.81	10 ± 2 – 22 ± 4	ND	[80]
Hepatocytes	2D EB formation	ND	ND	50 ± 2	$1–5 \times 10^4$	[81]
Hepatocytes	2D monolayer	14	ND	73 ± 18	ND	[82]
Motor neurons	2D monolayer	14	ND	33.6 ± 12	ND	[79]
Neural nociceptors	2D monolayer	15	ND	61 ± 2	1×10^4	[88]
Neurons	2D monolayer	~7	ND	ND	4.5×10^4	[84]
Dopaminergic neurons	2D monolayer	~28	ND	30 ± 2	ND	[89]
Neural progenitor cells	2D monolayer	6	ND	90 ± 1	5×10^4	[91]
Endoderm progenitors	2D monolayer	4	ND	73.2 ± 1.6	1.3×10^5	[90]
Cardiomyocytes	2D EB formation	16–18	70	87 ± 3.4	$4.5\text{-}6 \times 10^4$	[97]
Cardiomyocytes	SUB microcarriers	16	0.33	15.7 ± 3.3	1.36×10^6	[93]
Haematopoietic cells	SUB microcarriers	7	4.41	ND	ND	[92]
Cardiomyocytes	SUB cell aggregates	18	23	100% beating aggregates	$4.3 \times 10^5–5.2 \times 10^5$	[96]
Hepatocyte-like cells (HLCs)	SUB cell aggregates	21	ND	18 ± 7	$3–5 \times 10^5$	[94]

ND, no data.
a) In planar studies cell concentrations per mL have been estimated based on cell densities and recommended working volume for vessels used in these studies as no cell concentrations are provided in studies of this type.

SUB-based differentiation of mPSCs suggests that the use of spinner flasks resulted in a 12-fold reduction of the man hours spent in the laboratory when compared to planar techniques [95].

hPSCs can be differentiated towards a number of clinically relevant lineages in SUBs including cardiac [96], haematopoietic [92], neuronal [77] and hepatocyte-like [94] (see Table 3 for summary). Bioreactor-based differentiation will be necessary in order to produce certain hPSC-derived cell products at commercially relevant scales, however it must be considered that such processes will only be made more cost-effective by making concurrent improvements in differentiation efficiencies and through the reduction of expensive media supplements in such protocols. Bioreactor-based differentiation would benefit from the translation of highly efficient protocols demonstrated in planar systems [88, 91, 97] to SUB systems. Such protocols have the potential to result in differentiation efficiencies that are higher than those achieved with SUB-based bioreactors alone. A novel, microparticle-based approach to morphogen delivery to PSC aggregates was reported as a method to achieve up to a 12-fold reduction in morphogen use during bioreactor-based differentiation protocols [98]. Such systems provide a valuable method by which to reduce material costs associated with SUB-based hPSC culture.

One question arising from the birth of SUB-based hPSC differentiation is how a dynamic, controlled environment might be harnessed to augment processing strategies in this area [51]. One of the reasons for the lack of characterisation with regards to the effects of shear on hPSCs, is that different dynamic culture systems result in different shear profiles. Thus, drawing comparisons across separate studies is difficult [75]. However, scale-down studies suggest that shear stress during early hPSC differentiation promotes mesodermal, endothelial and haematopoietic phenotypes even when the presence of morphogens promoting these lineages were absent [99–101]. Interestingly, in early stages of differentiation, hPSCs lineage determination seems to be insensitive to the magnitude of shear stress; however in later stages, progenitor cell activity appears to be more magnitude-sensitive [100, 102]. Shear forces have been shown to partially negate the need for costly media supplements in published studies [99, 100]; broadening our knowledge of the way that shear stress impacts upon hPSC culture must be seen as an important factor in bioprocess optimisation. Hypoxic environments, which can be tightly controlled within SUBs, have also been shown to enhance differentiation of hPSCs towards both ectoderm and mesoderm cell lineages [96, 103].

Novel, microfluidic systems could be a key tool in elucidating the effects of specific environmental parameters on hPSC propagation and differentiation. Microfluidic bioreactors provide an ultra-scale down, high throughput platform by which to study single cells or colonies in strictly defined conditions [104–107]. The cellular processes governing hPSC fate are complex and cannot be attributed to a single given parameter. Microfluidic devices are well placed, as a low cost development plat-

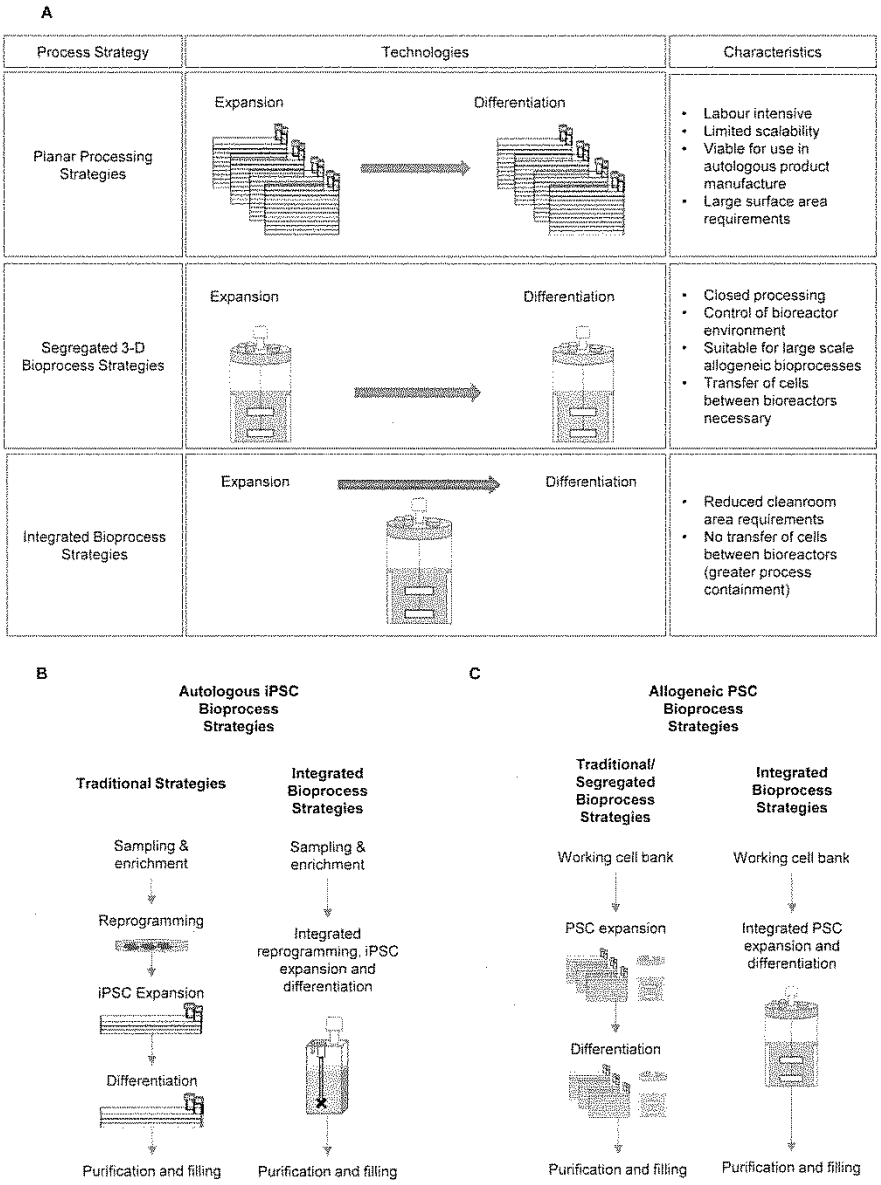

Figure 1. hPSC bioprocess strategies and their characteristics: **(A)** Planar processing strategies (top panels) rely on multi-layer vessels. Development of SUBs for PSC culture and differentiation has allowed development of 3D strategies, which are suitable for large-scale allogeneic bioprocesses (middle panels). Integrated bioprocesses allow hPSC expansion and differentiation to be carried out as a single unit operation in the same bioreactor (bottom panels). **(B)** Traditional and integrated autologous iPSC bioprocess strategies: Tradtional planar strategies neccessitate the need for use of well-plates and T-Flasks. Novel, automated bioreactor systems such as the Ambr system (Sartorius AG) may allow implementation of bioprocess strategies whereby reprogramming, iPSC expansion and differentiation are carried out within a single bioreactor. **(C)** Segregated and integrated allogeneic bioprocess strategies: Traditional allogneic bioprocess strategies utilise multi-layer, planar technologies. Segregated bioprocessing stratagies make use of separate SUBs for hPSC expansion and differentiation. Integrated bioprocessing allows hPSC expansion and differentiation to be carried out within a single bioreactor as a single unit opearation.

form, to enhance our understanding of how defined microenvironmental conditions can affect hPSC activity [108].

The effect of the biochemical properties of microcarriers on hPSC fate determination is poorly understood. It has also been suggested that the mechanical properties of microcarriers, such as their stiffness and size can also be investigated and optimised for specific purposes [27]. Rational design of microcarriers could provide an optimized bioprocess platform with which to manufacture specific hPSC-derived cell lineages. This would enable better control of cells' microenvironment and thus allow more efficient differentiation processes that do not rely as heavily on expensive media supplements as current platforms do.

5 Integrated bioprocess design strategies for hPSCs

Novel, integrated hPSC bioprocesses, whereby multiple unit operations are carried out using continuous culture strategies, are being explored as an alternative to segregated bioprocess strategies. Integrated bioprocesses negate the need for labour-intensive processes that usually take place following hPSC expansion such as harvest and transfer of cells prior to differentiation. Processing hPSCs in this manner can help to avoid process bottlenecks and increase throughputs of hPSC product manufacture. Additionally, integrated iPSC bioprocess protocols offer greater containment capabilities, reducing the potential for contamination within the bioprocess. Several studies in which hPSC expansion and differentiation are carried out as a single unit operation using continuous culture strategies exist [67, 74, 77]. Figure 1A illustrates how these strategies differ from segregated culture and differentiation of hPSCs. Only a handful of investigations into this relatively new area of hPSC bioprocess research have been published and these are summarised in Table 4.

Early investigations incorporating expansion and differentiation focused on overcoming the technical hurdles of carrying out two different operations in one integrated process step; as such only modest yields of target cells were achieved [74]. Recent studies have sought to optimise integrated iPSC bioprocesses via strategies such as the determination of optimal aggregate size during hPSC culture and differentiation [67]. Switching feeding regimes from once to twice per day was found to double the achievable cell density during the expansion phase of an integrated bioprocess, although process economic analysis comparing the two approaches was not offered [77]. The reported expansion folds and differentiation efficiencies for integrated bioprocesses compare well with separated systems of a similar nature (Table 4).

To date, no studies have produced an integrated process for hPSCs from derivation all the way through to differentiation. This has been achieved with mouse

Table 4. Key performance characteristics of studies investigating the integrated expansion and differentiation of hPSCs

Culture conditions	Cell type (iPSC/ESC)	Target cell type	Expansion max. cell density (cells/mL) (fold expansion)	Differentiation max. cell density (cells/mL) (fold expansion)	Reported differentiation efficiency (%)	Process time (days)	Target cells produced per input hPSC	Xeno-free (Y/N)	Refs.
Microcarrier (DE53 Whatman)	hiPSC	Neural progenitor cells (NPCs)	6.1×10^6 (20)	1.1×10^6 (16.6)	78 ± 4.7	25	333	N	[77]
Microcarrier (DE53 Whatman)	hESC	NPCs	4.3×10^6 (21.3)	1×10^6 (17.7)	83 ± 8.5	23	371	N	[77]
Aggregate culture	hESC	Definitive endoderm progenitors (DEPs)	ND (5000)[a]	ND (23.5)	> 80%	22	65,000[a]	N	[67]
Microcarrier (collagen-coated hyclone)	hESC	DEPs	1×10^6 (34–45)	4×10^5 (ND)	$84.2 \pm 2.3\%$	12	4	N	[74]

Parameters given for both expansion and differentiation where available. ND = No data given.
a) hESCs underwent four rounds of expansion during this study, as opposed to one round of expansion in other studies shown here. This may contribute to the disparity in performance parameters between this study and others shown here. {(Please start this sentence as a new line)}

iPSCs (miPSCs) in a SUB [109]. To our knowledge, there are only two studies exhibiting 'suspension culture reprogrammed iPSCs', both of which deal with miPSCs [109, 110]. Translation of integrated miPSC production techniques described by Baptista et al. [110] to hiPSC processing may be particularly useful in the production of autologous stem cell therapies, where continuous derivation of large numbers hiPSCs would help reduce the bottlenecks bought about by cellular reprogramming. Moreover, it may provide a 'black box' platform to derive, expand and differentiate a patient's cells in a single, contained unit that could be installed at point-of-care centres for relevant disease types. Novel, controlled miniature bioreactor systems, such as the ambr15 (Sartorius AG), might offer a suitable platform for autologous hiPSC product manufacture, where limited cell numbers are required and scale-out strategies necessitate alternatives to large-scale bioreactors (Fig. 1B and 1C).

6 Concluding remarks

The fulfilment of the clinical potential of hPSCs depends on the development of scalable, robust, GMP-compliant bioprocesses. Concentrated efforts to develop rigorously designed bioprocesses with a greater emphasis placed on QbD will continue to enhance process understanding with respects to defining critical quality attributes and identifying key process variables that must be controlled. hPSC-derived products are subject to strict economic boundaries owing to the nature of global healthcare systems. Future work must build upon the promise of works reviewed in this paper in order to make delivering such products on budget an achievable goal. Novel approaches discussed in this review offer methods to further optimise hPSC bioprocessing platforms.

Financial support from the UK Engineering and Physical Sciences Research Council (EPSRC) (grant reference number: EP/G034656/1) and Neusentis Ltd. is gratefully acknowledged. UCL hosts the EPSRC Centre for Innovative Manufacturing in Emergent Macromolecular Therapies with Imperial College London and a consortium of industrial and government partners. The authors are very grateful to Sally Hassan in the Department of Biochemical Engineering at UCL for her contributions towards Table 1.

The authors declare no financial or commercial conflict of interest.

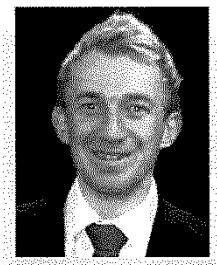

Michael J. Jenkins is a doctoral research student in Biochemical Engineering at University College London (UCL) in the UK. Michael's project, in collaboration with Neusentis Ltd., focuses on cost-effective bioprocess design for hPSC-derived cell products including cell therapies and drug screening tools. His research involves the creation of novel decisional tools that combine process economics analysis, bioprocess optimisation and uncertainty analyses of hPSC bioprocesses. He obtained his Master's degree in Biochemical Engineering at UCL, with a year as an exchange student within the Biotechnology Department at Lund University, Sweden.

Suzanne S. Farid is Professor in Bioprocess Systems Engineering at the Advanced Centre for Biochemical Engineering at University College London (UCL) in the UK and Co-Director of the EPSRC Centre for Innovative Manufacturing in Emergent Macromolecular Therapies. She leads research on 'Bioprocess Decisional Tools' that has pioneered the development of algorithms at the process–business interface to facilitate cost-effective bioprocess design, capacity planning and R&D portfolio management. She sits on the UK BioIndustry Association Manufacturing Advisory Committee and is a Fellow of the IChemE. She obtained her Bachelor's and Ph.D. degrees in Biochemical Engineering with UCL and Lonza Biologics.

7 References

[1] Takahashi, K., Yamanaka, S., Induction of pluripotent stem cells from mouse embryonic and adult fibroblast cultures by defined factors. *Cell* 2006, *126*, 663–676.
[2] Takahashi, K., Tanabe, K., Ohnuki, M., Narita, M. et al., Induction of pluripotent stem cells from adult human fibroblasts by defined factors. *Cell* 2007, *131*, 861–872.
[3] Robinton, D. A., Daley, G. Q., The promise of induced pluripotent stem cells in research and therapy. *Nature* 2012, *481*, 295–305.
[4] Ebert, A. D., Svendsen, C. N., Human stem cells and drug screening: Opportunities and challenges. *Nat. Rev. Drug Discov.* 2010, *9*, 367–372.
[5] Grskovic, M., Javaherian, A., Strulovici, B., Daley, G. Q., Induced pluripotent stem cells –Opportunities for disease modelling and drug discovery. *Nat. Rev. Drug Discov.* 2011, *10*, 915–929.
[6] Kiskinis, E., Eggan, K., Progress toward the clinical application of patient-specific pluripotent stem cells. *J. Clin. Invest.* 2010, *120*, 51–59.
[7] Wu, S. M., Hochedlinger, K., Harnessing the potential of induced pluripotent stem cells for regenerative medicine. *Nat. Cell Biol.* 2011, *13*, 497–505.

[8] Zeevi-Levin, N., Itskovitz-Eldor, J., Binah, O., Cardiomyocytes derived from human pluripotent stem cells for drug screening. *Pharmacol. Ther.* 2012, *134*, 180–188.
[9] Rajamohan, D., Matsa, E., Kalra, S., Crutchley, J. et al., Current status of drug screening and disease modelling in human pluripotent stem cells. *Bioessays* 2013, *35*, 281–298.
[10] McKernan, R., McNeish, J., Smith, D., Pharma's developing interest in stem cells. *Cell Stem Cell* 2010, *6*, 517–520.
[11] Smith, D. M., Assessing commercial opportunities for autologous and allogeneic cell-based products. *Regen. Med.* 2012, *7*, 721–732.
[12] Sivertsson, L., Synnergren, J., Jensen, J., Bjorquist, P., Ingelman-Sundberg, M., Hepatic differentiation and maturation of human embryonic stem cells cultured in a perfused three-dimensional bioreactor. *Stem Cells Dev.* 2013, *22*, 581–594.
[13] Schwartz, S. D., Hubschman, J. P., Heilwell, G., Franco-Cardenas, V. et al., Embryonic stem cell trials for macular degeneration: A preliminary report. *Lancet* 2012, *379*, 713–720.
[14] Idelson, M., Alper, R., Obolensky, A., Ben-Shushan, E. et al., Directed differentiation of human embryonic stem cells into functional retinal pigment epithelium cells. *Cell Stem Cell* 2009, *5*, 396–408.
[15] Schulz, T. C., Young, H. Y., Agulnick, A. D., Babin, M. J. et al., A scalable system for production of functional pancreatic progenitors from human embryonic stem cells. *PLoS ONE* 2012, *7*, e37004.
[16] Parker, C., Novel application and requirements for the broad adoption of iPSC-derived cellular materials. *World Stem Cells Regenerative Medicine Congress 2014*, London, UK, 2014.
[17] Kagimoto, H. T. S., Debating the first iPS cell-derived therapy human trial for AMD. *World Stem Cells Regenerative Medicine Congress 2014*, London, UK, 2014.
[18] Placzek, M. R., Chung, I. M., Macedo, H. M., Ismail, S. et al., Stem cell bioprocessing: Fundamentals and principles. *J. R. Soc. Interface* 2009, *6*, 209–232.
[19] Mason, C., Dunnill, P., Quantities of cells used for regenerative medicine and some implications for clinicians and bioprocessors. *Regen. Med.* 2009, *4*, 153–157.
[20] Simaria, A. S., Hassan, S., Varadaraju, H., Rowley, J. et al., Allogeneic cell therapy bioprocess economics and optimization: Single-use cell expansion technologies. *Biotechnol. Bioeng.* 2014, *111*, 69–83.
[21] Lancaster, M. A., Knoblich, J. A., Organogenesis in a dish: Modeling development and disease using organoid technologies. *Science* 2014, *345*, 283.
[22] Lancaster, M. A., Renner, M., Martin, C. A., Wenzel, D. et al., Cerebral organoids model human brain development and microcephaly. *Nature* 2013, *501*, 373–379.
[23] Takasato, M., Er, P. X., Becroft, M., Vanslambrouck, J. M. et al., Directing human embryonic stem cell differentiation towards a renal lineage generates a self-organizing kidney. *Nat. Cell Biol.* 2014, *16*, 118–126.
[24] Nakano, T., Ando, S., Takata, N., Kawada, M. et al., Self-formation of optic cups and storable stratified neural retina from human ESCs. *Cell Stem Cell* 2012, *10*, 771–785.
[25] Want, A. J., Nienow, A. W., Hewitt, C. J., Coopman, K., Large-scale expansion and exploitation of pluripotent stem cells for regenerative medicine purposes: Beyond the T flask. *Regen. Med.* 2012, *7*, 71–84.
[26] Klimanskaya, I., Rosenthal, N., Lanza, R., Derive and conquer: Sourcing and differentiating stem cells for therapeutic applications. *Nat. Rev. Drug Discov.* 2008, *7*, 131–142.
[27] Sart, S., Agathos, S. N., Li, Y., Engineering stem cell fate with biochemical and biomechanical properties of microcarriers. *Biotechnol. Prog.* 2013, *29*, 1354–1366.
[28] Serra, M., Brito, C., Correia, C., Alves, P. M., Process engineering of human pluripotent stem cells for clinical application. *Trends Biotechnol.* 2012, *30*, 350–359.
[29] Abbasalizadeh, S., Baharvand, H., Technological progress and challenges towards cGMP manufacturing of human pluripotent stem cells based therapeutic products for allogeneic and autologous cell therapies. *Biotechnol. Adv.* 2013, *31*, 1600–1623.
[30] Chen, A. K., Reuveny, S., Oh, S. K., Application of human mesenchymal and pluripotent stem cell microcarrier cultures in cellular therapy: Achievements and future direction. *Biotechnol. Adv.* 2013, *31*, 1032–1046.
[31] Villa-Diaz, L. G., Ross, A. M., Lahann, J., Krebsbach, P. H., Concise review: The evolution of human pluripotent stem cell culture: From feeder cells to synthetic coatings. *Stem Cells* 2013, *31*, 1–7.
[32] Sart, S., Schneider, Y. J., Li, Y., Agathos, S. N., Stem cell bioprocess engineering towards cGMP production and clinical applications. *Cytotechnology* 2014, *66*, 709–722.
[33] Lund, A. W., Yener, B., Stegemann, J. P., Plopper, G. E., The natural and engineered 3D microenvironment as a regulatory cue during stem cell fate determination. *Tissue Eng. B Rev.* 2009, *15*, 371–380.
[34] Lang, H. J., Simplified approach to preliminary cost estimates. *Chem. Eng.* 1948, *55*, 112–113.
[35] Pollock, J., Ho, S. V., Farid, S. S., Fed-batch and perfusion culture processes: Economic, environmental, and operational feasibility under uncertainty. *Biotechnol. Bioeng.* 2013, *110*, 206–219.
[36] Darkins, C. L., Mandenius, C.-F., Design of large-scale manufacturing of induced pluripotent stem cell derived cardiomyocytes. *Chem. Eng. Res. Des.* 2014, *92*, 1142–1152.
[37] Hassan, S., Simaria, A. S., Varadaraju, H., Rowley, J., Farid, S. S., A tool to predict the economic benefit of alternative technologies for allogeneic cell therapy manufacture at commercial scale. *245th American Chemical Society (ACS) National Meeting*, New Orleans, Louisiana, USA, 2013.
[38] Farid, S. S., Hassan, S., Simaria, A. S., Varadaraju, H., Warren, K., Can the cell therapy sector achieve acceptable cost of goods at the commercial scale? *20th ISCT Annual Meeting*, Paris, France, 2014.
[39] Veraitch, F. S., Scott, R., Wong, J. W., Lye, G. J., Mason, C., The impact of manual processing on the expansion and directed differentiation of embryonic stem cells. *Biotechnol. Bioeng.* 2008, *99*, 1216–1229.
[40] Farid, S. S., Washbrook, J., Titchener-Hooker, N. J., Decision-support tool for assessing biomanufacturing strategies under uncertainty: Stainless steel versus disposable equipment for clinical trial material preparation. *Biotechnol. Prog.* 2005, *21*, 486–497.
[41] Lim, A. C., Washbrook, J., Titchener-Hooker, N. J., Farid, S. S., A computer-aided approach to compare the production economics of fed-batch and perfusion culture under uncertainty. *Biotechnol. Bioeng.* 2006, *93*, 687–697.
[42] Eiselleova, L., Peterkova, I., Neradil, J., Slaninova, I. et al., Comparative study of mouse and human feeder cells for human embryonic stem cells. *Int. J. Dev. Biol.* 2008, *52*, 353–363.
[43] Rowley, J., Abraham, E., Campbell, A., Brandwein, H., Oh, S., Meeting lot-size challenges of manufacturing adherent cells for therapy. *BioProcess Int.* 2012, *10*, 16–22.
[44] Rodrigues, C. A. V., Fernandes, T. G., Diogo, M. M., da Silva, C. L., Cabral, J. M. S., Stem cell cultivation in bioreactors. *Biotechnol. Adv.* 2011, *29*, 815–829.
[45] Brandenburger, R., Burger, S., Campbell, A., Fong, T. et al., Cell therapy bioprocessing. *BioProcess Int.* 2011, *9*, 30–37.
[46] Thomas, R. J., Anderson, D., Chandra, A., Smith, N. M. et al., Automated, scalable culture of human embryonic stem cells in feeder-free conditions. *Biotechnol. Bioeng.* 2009, *102*, 1636–1644.
[47] Oh, S. K. W., Chen, A. K., Mok, Y., Chen, X. et al., Long-term microcarrier suspension cultures of human embryonic stem cells. *Stem Cell Res.* 2009, *2*, 219–230.
[48] Gerecht-Nir, S., Cohen, S., Itskovitz-Eldor, J., Bioreactor cultivation enhances the efficiency of human embryoid body (hEB) formation and differentiation. *Biotechnol. Bioeng.* 2004, *86*, 493–502.

[49] Olmer, R., Lange, A., Selzer, S., Kasper, C. et al., Suspension culture of human pluripotent stem cells in controlled, stirred bioreactors. *Tissue Eng. C Methods* 2012, *18*, 772–784.
[50] Chisti, Y., Hydrodynamic damage to animal cells. *Crit. Rev. Biotechnol.* 2001, *21*, 67–110.
[51] Leung, H. W., Chen, A., Choo, A. B., Reuveny, S., Oh, S. K., Agitation can induce differentiation of human pluripotent stem cells in microcarrier cultures. *Tissue Eng. C Methods* 2011, *17*, 165–172.
[52] Chen, G., Gulbranson, D. R., Hou, Z., Bolin, J. M. et al., Chemically defined conditions for human iPSC derivation and culture. *Nat. Methods* 2011, *8*, 424–429.
[53] Wang, Y., Chou, B. K., Dowey, S., He, C. et al., Scalable expansion of human induced pluripotent stem cells in the defined xeno-free E8 medium under adherent and suspension culture conditions. *Stem Cell Res.* 2013, *11*, 1103–1116.
[54] Marinho, P. A., Vareschini, D. T., Gomes, I. C., Paulsen Bda, S. et al., Xeno-free production of human embryonic stem cells in stirred microcarrier systems using a novel animal/human-component-free medium. *Tissue Eng. C Methods* 2013, *19*, 146–155.
[55] Phillips, B. W., Horne, R., Lay, T. S., Rust, W. L. et al., Attachment and growth of human embryonic stem cells on microcarriers. *J. Biotechnol.* 2008, *138*, 24–32.
[56] Fernandes, A. M., Marinho, P. A., Sartore, R. C., Paulsen, B. S. et al., Successful scale-up of human embryonic stem cell production in a stirred microcarrier culture system. *Braz. J. Med. Biol. Res.* 2009, *42*, 515–522.
[57] Serra, M., Brito, C., Sousa, M. F., Jensen, J. et al., Improving expansion of pluripotent human embryonic stem cells in perfused bioreactors through oxygen control. *J. Biotechnol.* 2010, *148*, 208–215.
[58] Chen, A. K., Chen, X., Lim, Y. M., Reuveny, S., Oh, S. K., Inhibition of ROCK-myosin II signaling pathway enables culturing of human pluripotent stem cells on microcarriers without extracellular matrix coating. *Tissue Eng. C Methods* 2014, *20*, 227–238.
[59] Rodin, S., Domogatskaya, A., Strom, S., Hansson, E. M. et al., Long-term self-renewal of human pluripotent stem cells on human recombinant laminin-511. *Nat. Biotechnol.* 2010, *28*, 611–615.
[60] Chen, A. K., Chen, X., Choo, A. B., Reuveny, S., Oh, S. K., Critical microcarrier properties affecting the expansion of undifferentiated human embryonic stem cells. *Stem Cell Res.* 2011, *7*, 97–111.
[61] Melkoumian, Z., Weber, J. L., Weber, D. M., Fadeev, A. G. et al., Synthetic peptide-acrylate surfaces for long-term self-renewal and cardiomyocyte differentiation of human embryonic stem cells. *Nat. Biotechnol.* 2010, *28*, 606–610.
[62] Villa-Diaz, L. G., Nandivada, H., Ding, J., Nogueira-de-Souza, N. C. et al., Synthetic polymer coatings for long-term growth of human embryonic stem cells. *Nat. Biotechnol.* 2010, *28*, 581–583.
[63] Fan, Y., Hsiung, M., Cheng, C., Tzanakakis, E. S., Facile engineering of xeno-free microcarriers for the scalable cultivation of human pluripotent stem cells in stirred suspension. *Tissue Eng. A* 2014, *20*, 588–599.
[64] Tamura, A., Kobayashi, J., Yamato, M., Okano, T., Temperature-responsive poly(N-isopropylacrylamide)-grafted microcarriers for large-scale non-invasive harvest of anchorage-dependent cells. *Biomaterials* 2012, *33*, 3803–3812.
[65] Watanabe, K., Ueno, M., Kamiya, D., Nishiyama, A. et al., A ROCK inhibitor permits survival of dissociated human embryonic stem cells. *Nat. Biotechnol.* 2007, *25*, 681–686.
[66] Krawetz, R., Taiani, J. T., Liu, S., Meng, G. et al., Large-scale expansion of pluripotent human embryonic stem cells in stirred-suspension bioreactors. *Tissue Eng. C Methods* 2010, *16*, 573–582.
[67] Ungrin, M. D., Clarke, C., Yin, T., Niebrugge, S. et al., Rational bioprocess design for human pluripotent stem cell expansion and endoderm differentiation based on cellular dynamics. *Biotechnol. Bioeng.* 2012, *109*, 853–866.
[68] Abbasalizadeh, S., Larijani, M. R., Samadian, A., Baharvand, H., Bioprocess development for mass production of size-controlled human pluripotent stem cell aggregates in stirred suspension bioreactor. *Tissue Eng. C Methods* 2012, *18*, 831–851.
[69] Chen, V. C., Couture, S. M., Ye, J., Lin, Z. et al., Scalable GMP compliant suspension culture system for human ES cells. *Stem Cell Res.* 2012, *8*, 388–402.
[70] Zweigerdt, R., Olmer, R., Singh, H., Haverich, A., Martin, U., Scalable expansion of human pluripotent stem cells in suspension culture. *Nat. Protoc.* 2011, *6*, 689–700.
[71] Amit, M., Laevsky, I., Miropolsky, Y., Shariki, K. et al., Dynamic suspension culture for scalable expansion of undifferentiated human pluripotent stem cells. *Nat. Protoc.* 2011, *6*, 572–579.
[72] Olmer, R., Haase, A., Merkert, S., Cui, W. et al., Long term expansion of undifferentiated human iPS and ES cells in suspension culture using a defined medium. *Stem Cell Res.* 2010, *5*, 51–64.
[73] Singh, H., Mok, P., Balakrishnan, T., Rahmat, S. N., Zweigerdt, R., Up-scaling single cell-inoculated suspension culture of human embryonic stem cells. *Stem Cell Res.* 2010, *4*, 165–179.
[74] Lock, L. T., Tzanakakis, E. S., Expansion and differentiation of human embryonic stem cells to endoderm progeny in a microcarrier stirred-suspension culture. *Tissue Eng. A* 2009, *15*, 2051–2063.
[75] Fridley, K. M., Kinney, M. A., McDevitt, T. C., Hydrodynamic modulation of pluripotent stem cells. *Stem Cell Res. Ther.* 2012, *3*, 45.
[76] Kehoe, D. E., Jing, D. H., Lock, L. T., Tzanakakis, E. S., Scalable stirred-suspension bioreactor culture of human pluripotent stem cells. *Tissue Eng. A* 2010, *16*, 405–421.
[77] Bardy, J., Chen, A. K., Lim, Y. M., Wu, S. et al., Microcarrier suspension cultures for high-density expansion and differentiation of human pluripotent stem cells to neural progenitor cells. *Tissue Eng. C Methods* 2013, *19*, 166–180.
[78] Mordwinkin, N., Burridge, P., Wu, J., A review of human pluripotent stem cell-derived cardiomyocytes for high-throughput drug discovery, cardiotoxicity screening, and publication standards. *J. Cardiovasc. Transl. Res.* 2013, *6*, 22–30.
[79] Karumbayaram, S., Novitch, B. G., Patterson, M., Umbach, J. A. et al., Directed differentiation of human-induced pluripotent stem cells generates active motor neurons. *Stem Cells* 2009, *27*, 806–811.
[80] Zhang, J., Wilson, G. F., Soerens, A. G., Koonce, C. H. et al., Functional cardiomyocytes derived from human induced pluripotent stem cells. *Circ. Res.* 2009, *104*, e30–e41.
[81] Ghodsizadeh, A., Taei, A., Totonchi, M., Seifinejad, A. et al., Generation of liver disease-specific induced pluripotent stem cells along with efficient differentiation to functional hepatocyte-like cells. *Stem Cell Rev.* 2010, *6*, 622–632.
[82] Sullivan, G. J., Hay, D. C., Park, I. H., Fletcher, J. et al., Generation of functional human hepatic endoderm from human induced pluripotent stem cells. *Hepatology* 2010, *51*, 329–335.
[83] Martinez, Y., Dubois-Dauphin, M., Krause, K. H., Generation and applications of human pluripotent stem cells induced into neural lineages and neural tissues. *Front. Physiol.* 2012, *3*, 47.
[84] Surmacz, B., Fox, H., Gutteridge, A., Lubitz, S., Whiting, P., Directing differentiation of human embryonic stem cells toward anterior neural ectoderm using small molecules. *Stem Cells* 2012, *30*, 1875–1884.
[85] Zhu, S., Wei, W., Ding, S., Chemical strategies for stem cell biology and regenerative medicine. *Annu. Rev. Biomed. Eng.* 2011, *13*, 73–90.
[86] Li, W., Jiang, K., Ding, S., Concise review: A chemical approach to control cell fate and function. *Stem Cells* 2012, *30*, 61–68.
[87] Burridge, P. W., Thompson, S., Millrod, M. A., Weinberg, S. et al., A universal system for highly efficient cardiac differentiation of human induced pluripotent stem cells that eliminates interline variability. *PLoS ONE* 2011, *6*, e18293.

[88] Chambers, S. M., Qi, Y., Mica, Y., Lee, G. et al., Combined small-molecule inhibition accelerates developmental timing and converts human pluripotent stem cells into nociceptors. *Nat. Biotechnol.* 2012, *30*, 715–720.
[89] Liu, Q., Pedersen, O. Z., Peng, J., Couture, L. A. et al., Optimizing dopaminergic differentiation of pluripotent stem cells for the manufacture of dopaminergic neurons for transplantation. *Cytotherapy* 2013, *15*, 999–1010.
[90] Diekmann, U., Lenzen, S., Naujok, O., A reliable and efficient protocol for human pluripotent stem cell differentiation into the definitive endoderm based on dispersed single cells. *Stem Cells Dev.* 2014, DOI:10.1089/scd.2014.0143.
[91] Lippmann, E. S., Estevez-Silva, M. C., Ashton, R. S., Defined human pluripotent stem cell culture enables highly efficient neuroepithelium derivation without small molecule inhibitors. *Stem Cells* 2014, *32*, 1032–1042.
[92] Lu, S. J., Kelley, T., Feng, Q., Chen, A. et al., 3D microcarrier system for efficient differentiation of human pluripotent stem cells into hematopoietic cells without feeders and serum (corrected). *Regen. Med.* 2013, *8*, 413–424.
[93] Lecina, M., Ting, S., Choo, A., Reuveny, S., Oh, S., Scalable platform for human embryonic stem cell differentiation to cardiomyocytes in suspended microcarrier cultures. *Tissue Eng. C Methods* 2010, *16*, 1609–1619.
[94] Vosough, M., Omidinia, E., Kadivar, M., Shokrgozar, M. A. et al., Generation of functional hepatocyte-like cells from human pluripotent stem cells in a scalable suspension culture. *Stem Cells Dev.* 2013, *22*, 2693–2705.
[95] Zwi-Dantsis, L., Mizrahi, I., Arbel, G., Gepstein, A., Gepstein, L., Scalable production of cardiomyocytes derived from c-Myc free induced pluripotent stem cells. *Tissue Eng. A* 2011, *17*, 1027–1037.
[96] Niebruegge, S., Nehring, A., Bar, H., Schroeder, M. et al., Cardiomyocyte production in mass suspension culture: Embryonic stem cells as a source for great amounts of functional cardiomyocytes. *Tissue Eng. A* 2008, *14*, 1591–1601.
[97] Weng, Z., Kong, C. W., Ren, L., Karakikes, I. et al., A simple, cost-effective but highly efficient system for deriving ventricular cardiomyocytes from human pluripotent stem cells. *Stem Cells Dev.* 2014, *23*, 1704–1716.
[98] Bratt-Leal, A. M., Nguyen, A. H., Hammersmith, K. A., Singh, A., McDevitt, T. C., A microparticle approach to morphogen delivery within pluripotent stem cell aggregates. *Biomaterials* 2013, *34*, 7227–7236.
[99] Wolfe, R. P., Leleux, J., Nerem, R. M., Ahsan, T., Effects of shear stress on germ lineage specification of embryonic stem cells. *Integr. Biol. (Camb.)* 2012, *4*, 1263–1273.
[100] Wolfe, R. P., Ahsan, T., Shear stress during early embryonic stem cell differentiation promotes hematopoietic and endothelial phenotypes. *Biotechnol. Bioeng.* 2013, *110*, 1231–1242.
[101] Ahsan, T., Nerem, R. M., Fluid shear stress promotes an endothelial-like phenotype during the early differentiation of embryonic stem cells. *Tissue Eng. A* 2010, *16*, 3547–3553.
[102] Adamo, L., Naveiras, O., Wenzel, P. L., McKinney-Freeman, S. et al., Biomechanical forces promote embryonic haematopoiesis. *Nature* 2009, *459*, 1131–1135.
[103] Bae, D., Mondragon-Teran, P., Hernandez, D., Ruban, L. et al., Hypoxia enhances the generation of retinal progenitor cells from human induced pluripotent and embryonic stem cells. *Stem Cells Dev.* 2012, *21*, 1344–1355.
[104] Cimetta, E., Figallo, E., Cannizzaro, C., Elvassore, N., Vunjak-Novakovic, G., Micro-bioreactor arrays for controlling cellular environments: Design principles for human embryonic stem cell applications. *Methods* 2009, *47*, 81–89.
[105] Wang, D., Bodovitz, S., Single cell analysis: The new frontier in 'omics'. *Trends Biotechnol.* 2010, *28*, 281–290.
[106] Prabhakarpandian, B., Shen, M. C., Pant, K., Kiani, M. F., Microfluidic devices for modeling cell–cell and particle–cell interactions in the microvasculature. *Microvasc. Res.* 2011, *82*, 210–220.
[107] Reichen, M., Macown, R. J., Jaccard, N., Super, A. et al., Microfabricated modular scale-down device for regenerative medicine process development. *PLoS ONE* 2012, *7*, e52246.
[108] Macown, R. J., Veraitch, F. S., Szita, N., Robust, microfabricated culture devices with improved control over the soluble microenvironment for the culture of embryonic stem cells. *Biotechnol. J.* 2014, *9*, 805–813.
[109] Fluri, D. A., Tonge, P. D., Song, H., Baptista, R. P. et al., Derivation, expansion and differentiation of induced pluripotent stem cells in continuous suspension cultures. *Nat. Methods* 2012, *9*, 509–516.
[110] Baptista, R. P., Fluri, D. A., Zandstra, P. W., High density continuous production of murine pluripotent cells in an acoustic perfused bioreactor at different oxygen concentrations. *Biotechnol. Bioeng.* 2013, *110*, 648–655.
[111] Nistor, G. I., Totoiu, M. O., Haque, N., Carpenter, M. K., Keirstead, H. S., Human embryonic stem cells differentiate into oligodendrocytes in high purity and myelinate after spinal cord transplantation. *Glia* 2005, *49*, 385–396.

Biochemical Engineering Journal 108 (2016) 84–97

Contents lists available at ScienceDirect

Biochemical Engineering Journal

journal homepage: www.elsevier.com/locate/bej

Regular article

Patient-specific hiPSC bioprocessing for drug screening: Bioprocess economics and optimisation

Michael Jenkins[a], James Bilsland[b], Timothy E. Allsopp[b], Sa V. Ho[c], Suzanne S. Farid[a,*]

[a] Department of Biochemical Engineering, University College London, Gordon Street, London WC1H 0AH, United Kingdom
[b] Neurosciences & Pain Research Unit, Pfizer, The Portway Building, Granta Park, Great Abington, Cambridge CB21 6GS, United Kingdom
[c] Biotherapeutic Pharmaceutical Sciences, Pfizer, 1 Burtt Road, Andover, MA, USA

ARTICLE INFO

Article history:
Received 13 April 2015
Received in revised form
15 September 2015
Accepted 26 September 2015
Available online 1 October 2015

Keywords:
Human induced pluripotent stem cells
Drug screening
Modelling
Optimisation
Bioprocess design
Scale up

ABSTRACT

This paper describes a decisional tool that is designed to identify cost-effective process designs for drug screening products derived from human induced pluripotent stem cells (hiPSC). The decisional tool comprises a bioprocess economics model linked to a search algorithm to assess the financial impact of manual and automated bioprocessing strategies that use 2D-planar tissue culture technologies. The tool was applied to a case study that examines the production of patient-specific iPSC-derived neurons for drug screening. The production strategies were compared across three analytical drug screening methods, each requiring cell production at a distinct scale (manual patch-clamp analysis, high throughput screening and plate-based pharmacology), as well as different annual cell line utilization requirements ('throughputs') (between 10 and 100 lines) so as to represent different industry scenarios. The tool determined the critical cell line throughput where the most cost-effective production strategy switched from the manual to automated workflow. The key process economics driver was the number of iPSC expansion stages required. Stochastic modelling of the bioprocess illustrated that the automated was more robust than the manual workflow in the scenarios investigated. The tool predicted the level of performance improvements required in iPSC expansion and differentiation as well as reductions in indirect costs and media costs so as to achieve an acceptable cost of goods (COG).

1. Introduction

The advent of hiPSC technology [1] has provided an opportunity to revolutionise modern medicine. Aside from their potential use in the cell therapy sector as clinical grade raw material to produce treatments for a variety of disorders with unmet clinical needs, hiPSCs also offer a more near term application as a tool with which current drug discovery, phenotypic screens, and safety testing programmes might be qualitatively improved [2–5]. This article investigates the production of patient-specific hiPS-cell lines, namely a cell line which is derived from a single patient in order to capture their individual genotype and phenotype. Manufacture of patient-specific cell lines will require scale-out of the process, whereby the manufacturing scale or lot size is kept constant and replicated for each cell line. In contrast, manufacture of non patient-specific cell lines can benefit from scale-up, whereby the manufacturing scale or lot size is increased when larger demands of a cell line are required (see Fig. 1a). Non patient-specific cell lines are more likely to be used for purposes that are independent of the specific genotype or phenotype of a cell.

In drug development, many pre-clinical testing platforms based on animal species prove to be of limited predictive value due to fundamental biochemical, physiological and genomic variations from humans [6–8]. hiPSC-differentiated somatic cells offer an alternative, humanised platform for pre-clinical efficacy and toxicity studies for novel therapeutics in development [9]. They also afford a predictive platform at the preclinical to clinical interface in, for example, safety vigilance of novel therapeutics in development, pinpointing drug responders from non-responders and stratifying patients into treatment groups in patient cohorts. Furthermore, the ability of patient-specific hiPSC-derived cells to model genetic and epigenetic variations of a broad spectrum population may also augment phase I/II clinical trials via the demonstration of a drug's safety

Abbreviations: COG, cost of goods; CTS, CompacT SelecT™ automated cell culture machine; FCI, fixed capital investment; hPSC, human pluripotent stem cell; HTS, high throughput screening; iPSC, induced pluripotent stem cell; PCA, patch-clamp analysis; NCE, novel chemical entity; PBP, plate-based pharmacological analysis; PSC, pluripotent stem cell.

* Corresponding author.
E-mail address: s.farid@ucl.ac.uk (S.S. Farid).

http://dx.doi.org/10.1016/j.bej.2015.09.024

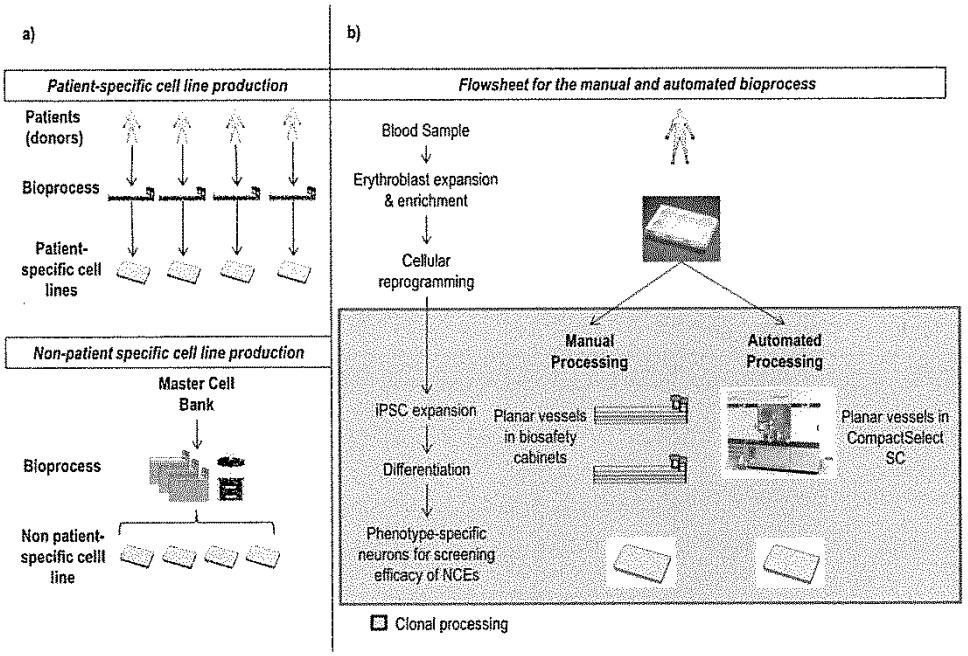

Fig. 1. (a) Outline of process techniques for patient-specific cell lines and non-specific cell lines. The bioprocess for a single patient-specific cell line is scaled-out to achieve a higher throughput. Non-specific bioprocesses are scaled-up to achieve a higher throughput. (b) An overview of the bioprocess strategies considered within this case study. Clonal processing is employed following cellular reprogramming, therefore the technology used to process each donor sample remains constant until this point, regardless of the scale of the bioprocess.

and efficacy within a target population in vitro. Patient-specific hiPSC-derived cells may be of particular use in the assessment of NCEs where the degree of efficacy observed within a cohort may depend upon a specific geno- or phenotype [10]. In this manner they have the potential to lower the time, costs, and risks associated with committing a drug to clinical trials. The cost of bringing a new drug to market is currently estimated to be US$1.2bn–US$1.7bn. When juxtaposed with a clinical attrition rate that can be close to 90% (phase I to approval) [11], such an expensive and complex development cycle has caused drug developers to display caution when committing candidate therapies to clinical trials [12,13].

hiPSC-derived cell types have faced challenges in their implementation owing partly to key issues associated with their production at large scale. Many current iPSC manufacturing protocols are based upon planar, 2-D culture vessels due to their affordability and simplicity [14]. However, lack of scalability owing to limitations in surface area to volume ratio and the inability to conduct online process monitoring are major drawbacks to many 2-D culture systems, as is their labour-intensive nature, which limits their throughput and applicability to larger scale processes [15,16]. Non patient-specific cell processing may benefit from recent iPSC bioprocessing advances, such as single-use bioreactors (SUBs) and microcarriers, which offer both greater potential for scale-up and an enhanced degree of containment in comparison to planar vessels [17–22]. However, patient-specific bioprocesses are not amenable to scale-up and will likely depend upon planar culture technologies, which may be useful when producing cell populations numbering in the low millions [23,24]. Automation systems designed to accommodate planar culture vessels, such as the CompacT SelecT™ (CTS) (Sartorius, Royston, UK), have the potential to reduce the labour requirements, possible points of contamination, and to improve the reliability associated with autologous hiPSC bioprocessing [25–27]. Such systems could be implemented to help achieve large-scale manufacture of patient-specific stem cell products.

The biopharmaceutical sector has benefitted from the use of decisional tools that are able to evaluate alternative process designs in silico in order to achieve cost-effective process design and equipment selection [28–32]. As a nascent field, hiPSC processing is faced with a lack of consensus as to optimal process designs and scale-up/out strategies. Decisional tools similar to those applied to the biopharmaceutical sector can therefore prove useful for identifying key economic drivers and technical innovations required to bridge the gaps constraining widespread application of hiPSC-derived cells. There are only a limited number of studies investigating the impact of process design on manufacturing COG within the stem cell sector. Previous analyses have provided estimates of the current limitations [15,33] and relative cost of PSC processing technologies, including the use of commercially available flow-sheeting software (SuperPro Designer, Intelligen Inc., NJ, USA) to evaluate the economic potential of large-scale iPSC-derived cell bioprocess designs [34]. For other cell types, for example mesenchymal stromal cells for therapy, others have illustrated how a decisional tool can be developed to determine the scales at which microcarriers in SUBs becomes preferable to planar processing platforms during the expansion phase [16].

In this paper, an integrated decisional tool that combines both bioprocess economic modelling and optimisation of the manufacture of patient-specific iPSC-derived neurons for use as a tool in the screening of NCEs is described. The bioprocess economics model and integrated brute-force search algorithm are designed to iden-

tify the process design that minimises the COG. The use of specified automation equipment such as the CTS for iPSC cell bioprocessing and its impact upon the overall COG is also evaluated as an alternative to existing, manual bioprocessing options (Fig. 1b).

2. Tool description

A decisional tool was developed to evaluate the COG associated with different bioprocess strategies and equipment sizing of technologies to be used during the manufacture of patient-specific iPSC-derived cell lines. It comprises a bioprocess economics model, an information database, and an integrated brute-force search algorithm. The tool was constructed in and is implemented via Microsoft Excel (Microsoft Corporation, WA, USA) and the Visual Basic for Applications tool (VBA) (Microsoft Corporation). A brute-force search algorithm generates possible process configurations, from a database of specified process technologies, to be evaluated by the bioprocess economics model. Microsoft Excel was used because of its dual functionality in being able to act as a database for model inputs and outputs in addition to a tool by which to construct a bioprocess economics model. VBA's simple integration with MS Excel makes it ideal for efficiently linking the database and bioprocess economics model to the optimisation algorithm.

2.1. Deterministic bioprocess economics model

The bioprocess economics model evaluates the COG per cell line for different bioprocess configurations. A critical feature of patient-specific cell bioprocesses is that they dictate the adoption of a scale-out, rather than scale-up, approach to process design and development as throughput increases. Therefore, separate processing of individual donor products is assumed throughout the model, i.e. separate culture vessels are used for cells from separate donors.

A key parameter when evaluating equipment sizing strategies is the type of technology to be used within each unit operation and the number of units required to process the required number of cells from each donor sample. For a given cell output, P (cells per cell line), the number of units ($u_{con,i,j}$) required of a particular technology, j, for a given unit operation, i, is calculated as;

$$u_{con,i,j} = \frac{P_i}{d_{h,i} \times a_j} \quad (1)$$

where a_j is the available surface area per unit for each technology and $d_{h,i}$ represents the harvest density (cells/cm^2) for a given unit operation.

Determining the number of units for a given technology allows the bioprocess economics model to draw on information stored in the database so as to evaluate the COG/cell line via a cascade of equations. Thus, the bioprocess economics model is able to calculate the total COG/cell line:

$$\frac{COG}{\text{Cell line}} = \left(\sum_i \left[C^{ann}_{mat,i} + C^{ann}_{lab,i} \right] \right) + \frac{C^{ann}_{indirect,}}{D_{ann}} \quad (2)$$

where $C_{mat,i}$ and $C_{lab,i}$ are the costs of raw materials and labour, or the direct costs, associated with each individual unit operation within the bioprocess. D_{ann} is the annual throughput (cell lines produced per year). Direct costs attributed to a specific unit operation are calculated separately for each individual unit operation, whereas indirect costs are calculated on a whole bioprocess basis because fixed equipment may be shared between multiple unit operations.

Table 1
Methods and feeding regimes for bioprocess unit operations.

Unit operation	Method	Feeding regime
Erythroblast expansion & enrichment	Culture-based expansion and purification of erythroblasts	Daily media replacement
Cellular reprogramming	Sendai virus transduction of Yamanaka factors	Media replacement every two days during transduction Daily media replacement during iPSC generation period
iPSC expansion	Monolayer 10% of viable cells banked to safeguard against process failure during differentiation	Daily media replacement
Differentiation	Monolayer, small molecule based	Twice weekly media replacement

Table 2
Labour tasks and their duration.

Labour task	Time required (h) (t_i)
Media preparation	1
Cell harvest	0.75
Cell seeding	0.5
Media replacement	0.5
Viral transduction	1.5
CompacT SelecT setup	2
CompacT SelecT termination	2
Culture check (manual)	0.5
Culture check (automated)	0.25

Material costs per unit operation, $C^{ann}_{mat,i}$, are calculated as a function of the utilisation of chemicals (e.g. media) and consumables (e.g. plastic culture vessels):

$$C^{ann}_{mat,i} = u_{i,j} \left[V_{med,j} \times a_{i,j} \times C_{med,i} \right] + C_j \quad (3)$$

where $V_{med,j}$ is the media utilisation (mL/cm^2), $C_{med,i}$ the cost of media used within a particular unit operation i and C_j the price per unit associated with a given technology j.

Assumptions regarding media replacement regimes, which are taken into account by the deterministic model, can be found in Table 1.

Labour costs are calculated as a function of the time required to carry out tasks specific to each unit operation of the iPSC bioprocess (t_i). It is assumed that for each technology type an operator could handle a given number of units, ω_j, within this time period. Therefore:

$$C^{ann}_{lab,i} = \left(\frac{u_{ij}}{\omega_j} \right) \times t_i \times w \quad (4)$$

where w represents the hourly cost of labour. Individual labour tasks and their durations can be found in Table 2.

2.1.1. Indirect costs

Fixed capital investment costs are calculated using an adjusted Lang factor developed at UCL for estimating capital investment costs associated with disposable facilities [32]. The Lang factor method assigns a proportionality constant to the total equipment purchase cost in order to provide a facility capital investment (FCI) estimate [35]. The Lang factor accounts for items that contribute to the cost to build the facility such as pipework, instrumentation, building works, construction, commissioning and validation.

$$FCI = F_{lang} \times C_{fixed} \quad (5)$$

where C_{fixed} represents the cost of any fixed equipment within the bioprocess facility. The fixed equipment costs are calculated thus:

$$C_{fixed} = \sum_{i=1}^{n} \left(\lceil \frac{u_{i,x}}{\alpha_{inc,i}} \rceil \times C_{inc} + \lceil \frac{u_{i,x}}{\alpha_{bsc,i}} \rceil \times C_{bsc} + \lceil \frac{u_{i,x}}{\alpha_{CTS,i}} \rceil \times C_{CTS} \right) \quad (6)$$

where α_{inc}, α_{bsc} and α_{CTS} are the capacities of incubators, biosafety cabinets and CTS (when automated processing is employed), respectively, with regards to a particular technology, i, during the bioprocess. C_{inc}, C_{bsc} and C_{CTSt} refer to the cost of individual units of fixed equipment used within the bioprocess. It was assumed that biosafety cabinets could only be used by one operator at a time.

In this study the main annual indirect cost considered was the depreciation, calculated by dividing fixed capital investment costs by the depreciation period, t_{dep}, representing the lifespan of fixed equipment:

$$C_{indirect}^{ann} = \frac{C_{fixed}}{t_{dep}} \quad (7)$$

Within unit operations such as iPSC expansion, where multiple expansion stages are required, different technologies may be preferable for each subsequent stage. Therefore, each expansion stage was treated as a de facto unit operation and logic constraints were put in place such that technologies in preliminary expansion stages were smaller, or equal in size to candidate technologies in subsequent ones (i.e. $a_{i,j-1} \leq a_{i,j}$). This is in order to abide by standard processing protocols, whereby the size of the equipment used in the expansion stages of stem cell culture is traditionally scaled up as cell populations continue to grow.

Additionally, process designs returning fixed equipment utilisation values of greater than 95% were discarded from results. This is to avoid utilisation of such equipment exceeding capacity in the event where additional vessels might be required owing to variations in processing parameters.

2.2. Brute-force search algorithm

The brute-force algorithm has been designed to determine optimal equipment sizing for each unit operation within the process via a procedure which examines all possible bioprocess designs according to process technologies housed in the database.

The bioprocess economics model described above is able to calculate the COG per cell line for a specified process configuration using technologies of a given size. A brute-force search algorithm develops all of the available process designs for the bioprocess economics model to quantify on the basis of COG per cell line. This bioprocess economics model then generates COG data for the array of alternative process designs. The output data is then screened in order to identify the bioprocess design that minimises COG. Fig. 2 illustrates how the optimisation algorithm works alongside the bioprocess economics model to achieve cost-effective process design.

2.3. Stochastic modelling

The deterministic COG provided by the tool described in the previous section allowed identification of the optimal bioprocess design and equipment sizing within each unit operation of the bioprocess. However, deterministic analyses cannot offer an evaluation of the robustness of iPSC bioprocessing strategies. Achieving process reproducibility is a significant challenge within stem cell bioprocessing, particularly when manual processing strategies are employed [14,25,26]. Furthermore, accounting for donor-to-donor variability also presents a unique challenge. The Monte Carlo simulation method was applied to the decisional tool to provide stochastic modelling of the iPSC bioprocess in order to quantify the robustness and reproducibility of automated and manual iPSC bioprocess strategies. Adjusting input parameters also allowed the model to capture variations in COG that arise as a result of donor-to-donor variability within key process parameters.

Previously published reports have suggested that manual bioprocesses result in greater variability than those which are automated [26,37]. Hence, narrower distributions have been assigned for the automated iPSC bioprocess to reflect this (input probability distributions are shown in Table 6). Probability ranges have been corroborated with industry experts to ensure they are representative.

The Monte Carlo simulation method was used to carry out probability-based economic assessment of the manual and automated bioprocess. During the Monte Carlo simulation, the process flow-sheet was held constant. The culture vessels tested within the Monte Carlo analysis were those selected as the most cost-effective by the brute-force search algorithm. In order to ensure that the target cell population size was achieved for each donor cell-line, the direct resources and fixed equipment required were re-calculated during each Monte Carlo simulation to account for the variations in process parameters as a result of the assigned input distributions. Future improvements to screening methods may allow one to identify single-nuclear polymorphisms (SNPs) in the original donor sample that correlate with bioprocess performance. In future, this method could allow the likely performance of a donor's iPSCs to be ascertained prior to the bioprocess. Thus, prospective re-sizing of the bioprocess may be a feasible option; therefore, the number of culture vessels has been left as a variable in the Monte Carlo analysis.

3. Case study setup

3.1. Tool application

A representative case study was developed in partnership with Pfizer's Neuroscience and Pain Research Unit (Great Abington, Cambridge, UK) that focused on optimising the production of patient-specific iPSC-derived cells for drug screening. Specifically, it addressed the generation of iPSC-derived neurons to supply patient drug responder versus non-responder, "trial in a dish" screening platforms with which to augment clinical trials for NCEs. It is estimated that cell lines from 50 separate donors could be required to run such a screening programme. To investigate the effect of scale-out on the COG associated with the bioprocess, throughputs of 10, 50 & 100 cell lines per year were investigated by this study.

There are a variety of analytical methods by which to carry out drug screening. Currently, the resting or active status of the membrane potential in functional iPSC-derived neurons are analysed by patch-clamp analysis (PCA), a manual technique which requires a small sample population of iPSC-derived neurons (10^5). Whilst this is a data-rich analytical method, it samples only a small number of cells and is therefore a poor representation of whole cell populations [36]. Powerful, automated analytical techniques such as high throughput screening (HTS) and plate-based pharmacological analysis (PBP) are also available methods by which to screen cells' reactions to NCEs. These techniques require larger sized cell populations (2×10^6 and 10^7 cell, respectively), but offer high throughput analytical platforms. The level of scale-up required of the bioprocess required to manufacture each individual cell line is dependent on the analytical technique used for drug screening, along with characteristics of different analytical techniques (Fig. 3).

Two different manufacturing strategies were considered during this case study; manual bioprocess techniques were evaluated alongside an automated iPSC bioprocess, whereby iPSC expansion and differentiation were carried out using the CompacT SelecT SC

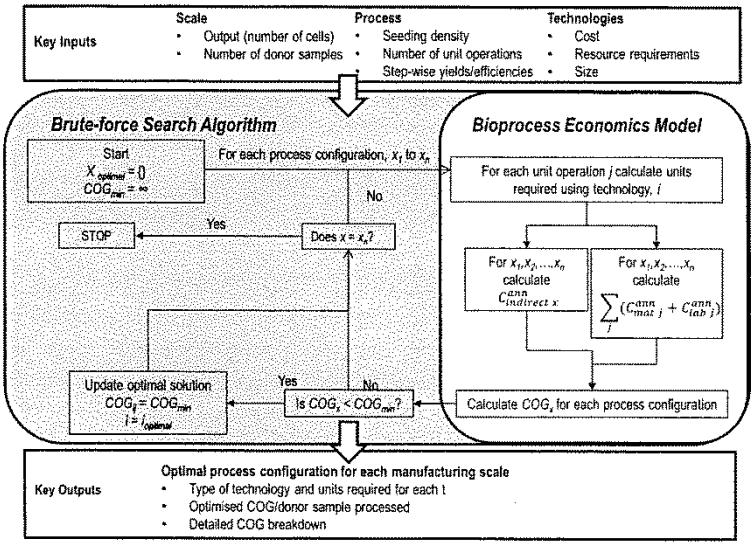

Fig. 2. Tool schematic showing evaluative network used to identify the optimal bioprocess design, $x_{optimal}$.

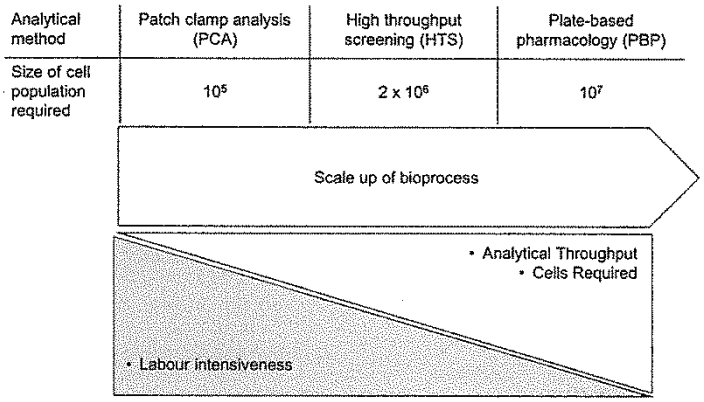

Fig. 3. Cell population sizes of iPSC-derived neurons required to satisfy the demands of different analytical drug screening techniques. The required population size dictates the scale of the bioprocess required to produce cells for each analytical method. The lower panels illustrate graphically key characteristics of each analytical technique.

(Sartorius, Royston, UK). The decisional tool was applied primarily in order to select the most cost-effective process design in both instances. However, process reproducibility in stem cell bioprocessing is a significant challenge. As such, stochastic modelling was also employed to ascertain the robustness of both manufacturing strategies using the Monte Carlo simulation method.

3.2. Process overview

The process flowsheet used for the case study (Fig. 1) employs processing of individual clones following the reprogramming stage; as such, the preliminary unit operations are of a constant scale regardless of the final number of iPSC-derived neurons produced from each cell line. Therefore, the main focus of this case study comprises the iPSC expansion and differentiation unit operations. Further details regarding the methods used and feeding regimes assumed for each unit operation can be found in Table 1. Media changes are assumed to involve a full exchange of media within a process vessel.

The planar technologies considered within the case study included well plates (WP) as well as standard and compact multi-layer versions of T-flasks (T, cT, 3-F, 5-F) and stacked vessels (L-2, L-5, cL-12). Their key input parameters are stored within the tool's database (Table 3). This data was compiled using vendor websites and consultation with industry experts so as to properly capture the characteristics of each candidate technology. Key process and cost assumptions are summarised (Tables 4 and 5) and where possible, these values have been compiled via a thorough review of available literature on planar bioprocessing of iPSCs and their derivatives. All assumptions listed in Tables 4 and 5 were then corroborated with

Table 3
Process technologies tested by the tool and their key performance parameters.

Technology type (i)	Surface area (cm²/unit) (a_i)	Cost (£/unit) ($C_{con\ i}$)	Media requirements (mL/unit) ($V_{req\ i}$)	Max units per operator ($\omega_{op\ i}$)	Incubator capacity (double stack) ($\delta_{inc\ i}$)	Requires BSC cabinet (Y/N)	CompacT SelecT capacity
T-25	25	£1.54	7	4	100	Y	–
T-75	75	£2.21	18.75	4	100	Y	90
T-175	175	£4.95	50	4	100	Y	90
T-225	225	£5.27	56.25	4	100	Y	–
6-WP[a]	9.5	£2.10	2	24	600	Y	–
24-WP[a]	1.9	£2.66	0.5	48	2400	Y	–
L-2[b]	1272	£55.08	315	2	60	Y	–
L-5[b]	3180	£180.49	787.5	2	24	Y	–
cL-12[c]	6000	£287.69	1300	2	24	Y	–
3-F[d]	525	£10.20	150	–	–	N	90
5-F[e]	875	£17.00	250	–	–	N	90
cT[f]	1720	£63.58	500	–	–	N	90

[a] Well plate.
[b] Multilayer planar vessels e.g. CellSTACK (Corning).
[c] Compact multilayer vessel e.g. 12-layer HYPERStack (Corning).
[d] 3-layer T-flasks e.g. Triple Flask (Nunc) or Falcon Multi-Flask (Corning).
[e] 5-layer T-flasks e.g. Falcon Multi-Flask (Corning).
[f] Compact multilayer flask e.g. 10-layer HYPERFlask (Corning).

Table 4
Key process assumptions.

Unit operation (j)	Seeding density (cells/cm²)	Harvest density (cells/cm²) ($d_{h,i}$)	Yield/harvest yield/efficiency (%)	Fold expansion
Erythroblast enrichment	1.5×10^5	3.2×10^5	25 (Yield)	N/A
Erythroblast expansion	1.5×10^5	3.2×10^5	95 (harvest yield)	2
Reprogramming (transduction)	2.6×10^5	2.6×10^5	95 (harvest yield)	N/A
Reprogramming (generation)	10^4	10^4	0.5 (efficiency)	N/A
iPSC expansion	4.2×10^4	3×10^5	90 (per passage)	7
Differentiation	3×10^5	3×10^5	35 (efficiency)	N/A

Table 5
Key process cost parameters.

Cost Parameter		Value[a]
Media		
	Differentiation media	£0.55–£0.67/mL
	Expansion medium	£0.43/mL
	Reprogramming vector	£664/donor
Labour		£60/h
Fixed equipment		
	Incubator (Large)	£11,890
	Incubator (Small)	£5,175
	CompacT SelecT	£550,000
	Biosafety cabinet	£11,390
Depreciation period		10 Years
Lang factor (manual bioprocess strategy)		23.7
Lang factor (automated bioprocess strategy)		16

[a] Price ranges are provided where more than one type of media is used within a unit operation.

industry experts to ensure they were representative. While sensible inputs and assumptions were sought, the primary aim of the paper was to demonstrate the application of the proposed methodology to provide visibility of the cost structure and the most significant process economics drivers for iPSC generation for drug screening applications. Hence, the actual inputs and answers should not be seen as definitive but an illustration of how to approach such an assessment. The risk of batch failure was also considered. The manual bioprocess strategy was assumed to exhibit a higher probability of batch failure (4%) compared to the automated strategy (2%) given the greater human intervention and degree of open processing in the manual strategy. Failure rates were assumed to capture the worst-case scenario, i.e. failure occurs during the final stages of differentiation. Therefore, the direct costs of iPSC expansion and differentiation for additional donor samples required due to process failure were added to the final COG figure within the deterministic model to account for additional processing as a result of the batch failure rate. Only iPSC expansion and differentiation were assumed to be repeated following a failed lot because of the cell banking procedure in place.

4. Results and discussion

The decisional tool was used to assess the cost-effectiveness of alternative bioprocess designs across a range of different scales of production. A deterministic model was developed in order to carry out COG comparisons between different process designs and sensitivity analyses were used to further investigate economic drivers associated with the iPSC bioprocess. The tool was then adapted for stochastic modelling in order to evaluate the robustness under uncertainty of automated and manual bioprocessing strategies using the Monte Carlo simulation method.

4.1. Deterministic cost modelling

4.1.1. Optimal bioprocess designs across different scales and throughputs

The optimal combination of process technologies for the final iPSC expansion stages and differentiation operation, for both the manual and automated bioprocess are depicted in Fig. 4. The number of iPSC-derived neurons produced per cell line is representative of the size of cell populations needed to satisfy the demands of PCA, HTS and PBP analysis (moving vertically from the top to the bottom

a)

		Cell lines produced per year	
Analytical Method [required output (iPSC-neurons/cell line)]	Unit Operation	50	100
Patch Clamp Analysis [10^5]	Expansion (final stage)	6-WP [4]	6-WP [4]
	Differentiation	T-25 [1]	T-25 [1]
High Throughput Screening [2 x 10^6]	Expansion (final stage)	T-75 [4]	T-75 [4]
	Differentiation	T-175 [1]	T-175 [1]
Plate-Based Pharmacological Assay [10^7]	Expansion (final stage)	L-2 [2]	L-2 [2]
	Differentiation	T-225 [4]	T-225 [4]

b)

		Cell lines produced per year	
Analytical Method [required output (iPSC-neurons/cell line)]	Unit Operation	50	100
Patch Clamp Analysis [10^5]	Expansion (final stage)	T-75 [4]	T-75 [4]
	Differentiation	T-75 [1]	T-75 [1]
High Throughput Screening [2 x 10^6]	Expansion (final stage)	T-75 [4]	T-75 [4]
	Differentiation	T-175 [1]	T-175 [1]
Plate-Based Pharmacological Assay [10^7]	Expansion (final stage)	T-175 [25]	3-F [11]
	Differentiation	5-F [1]	5-F [1]

Fig. 4. Matrices showing the optimal bioprocess configuration for the final stage of expansion and differentiation for (a) manual bioprocess strategies and (b) automated bioprocess strategies across the range of scale investigated in this study. Lighter shaded cells indicate cheaper COG per cell line relative to other bioprocess designs shown in the matrices, where the lightest shade indicates the cheapest COG per cell line output value.

of the matrices). The cell population outputs per cell line required for each of these analytical methods are shown in Fig. 3, and also in Fig. 4. Annual throughputs of 10, 50 and 100 cell populations have been shown to depict the effects of scale-out on optimal bioprocess design. The bioprocess throughput, in terms of cell lines produced per year, increases horizontally from left to right across each matrix. The matrices show the optimal technology size and the number of units required (in square brackets) per cell line for each scale tested.

Depicting optimal technology sizing for manual bioprocessing shows that as the size of cell populations produced increases, there is a trend towards technologies with a larger surface area (Fig. 4a). Larger technologies, which require fewer vessels, are selected as the optimal bioprocess design. For example 2 × 2-layer CellSTACK vessels (L-2) are preferred for the final expansion stage when producing 10^7 cells per cell line (for PBP), as opposed to 4 × T-75 flasks if 2×10^6 cells per cell line were to be produced (for HTS analysis). Larger vessels are preferred when larger cell populations are produced when a manual bioprocess strategy is employed as depicted by the direct cost breakdown for optimal technologies for the manual bioprocess at different production scales at a throughput of 50 donor samples per year for the final expansion stage and differentiation (Fig. 5). The utilisation of available surface area in smaller technologies is higher, thus they make more efficient use of media. Material expenditures can be reduced if smaller cell populations are produced (such as those required for PCA and HTS analysis) if smaller technologies are used. This is exhibited by a 39% reduction in direct costs if T-75 flasks are used as opposed to L-2 vessels for the final iPSC expansion stage at the HTS scale (Fig. 5a). However, when satisfying the demands of PBP, the additional labour costs incurred by the use of large numbers of units of smaller vessels far outweigh the incremental reduction in material costs that such technologies offer within the manual bioprocess. The COG per cell line for the differentiation can be reduced by 76% if T-225 flasks are employed rather than T-25 flasks (Fig. 5b). This is due to the reduction in the resultant labour costs associated with the use of T-225s. Darker shades within each area of the matrices (Fig. 4) are illustrative of higher COG/cell line. Thus, the matrix also demonstrates the economies of scale that can be achieved when the number of cell lines produced per year increases. This is particularly true with regards to automated processing (Fig. 4b), where a greater range in the COG between different annual donor sample throughputs can be observed than for the manual bioprocessing strategy.

A COG breakdown for the different equipment sizing configurations available for use in the final stage of expansion and differentiation for the automated bioprocess strategy, whereby 10^7 iPSC-derived neurons are produced per cell line at a throughput of

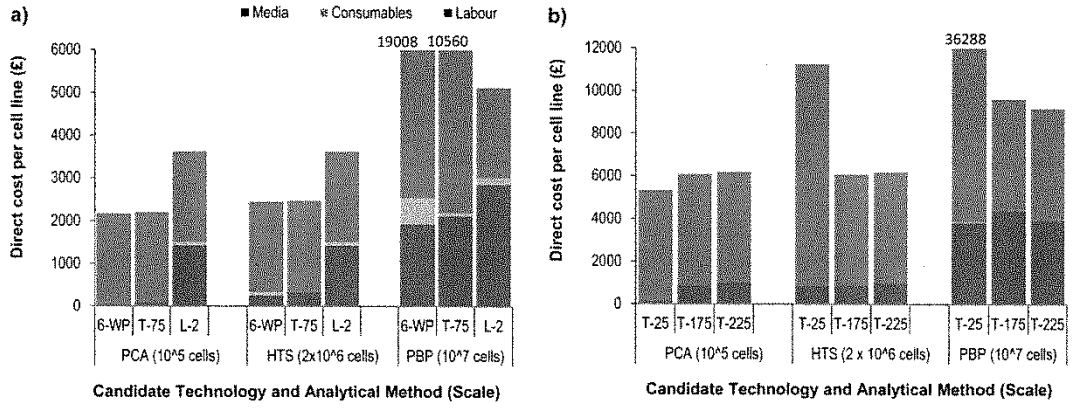

Fig. 5. Direct cost breakdown for the optimal technologies at scales satisfying the demands of the three analytical drug screening techniques (PCA, HTS & PBP) at a throughput of 50 cell lines/yr for (a) the final stage of expansion and (b) differentiation. Required iPSC-derived neuron outputs per donor are shown in brackets on the *x*-axis. Maximum values on the *y*-axis have been assigned to maintain scales whereby data can be clearly seen. Therefore for scales satisfying demands of PBP, direct costs beyond these values are labelled above the relevant columns.

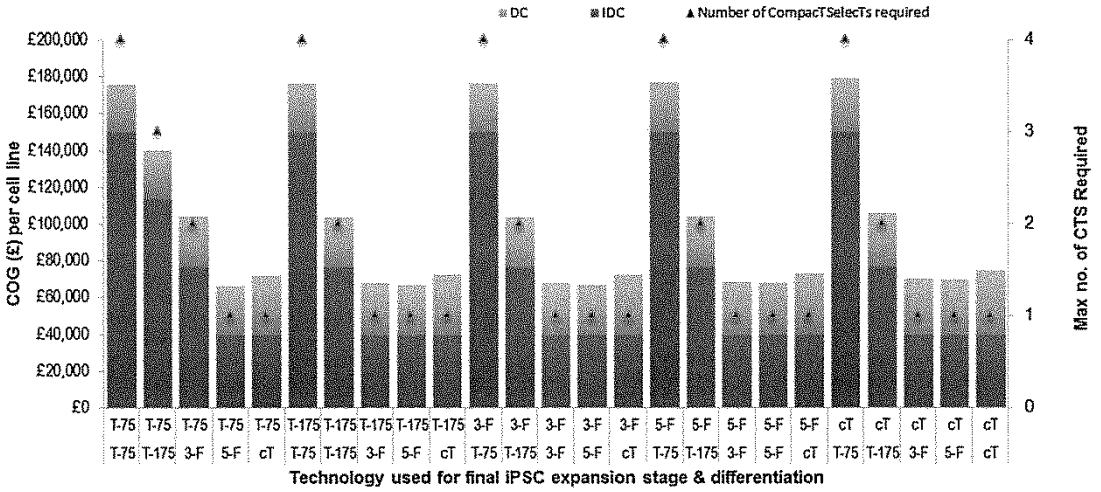

Fig. 6. COG breakdown for possible equipment sizing configurations for an automated process strategy for the final iPSC expansion stage and differentiation unit operations at a throughput of 50 cell lines/yr, whereby populations of 10^7 cells are produced to satisfy the demands of PBP analysis. CTS utilisation refers to percentage utilisation of CompacT SelecT automated processing equipment, i.e. 367% will require 4 CompacT SelecT units. DC = direct costs. IDC = indirect costs.

50 cell lines per year is shown in Fig. 6. The use of smaller vessels, such as T-75s, necessitates the use of multiple CTS machines due to the number of vessels required for such technologies, which corroborates results described earlier (Fig. 4b), in that larger technologies are preferred for this throughput in the optimal technology matrix. This is particularly true of vessels used during differentiation, a lengthy process that occupies equipment capacity for long periods of time. The optimal process configuration, where the technologies selected were 11 × T-75 flasks for the final iPSC expansion stage and 1 × 5-F (5-layer T-flask) for differentiation, results in a maximum requirement of 1CTS machine. However, were T-75s and T-175s to be used for the respective process steps above (as is optimal for producing cells for HTS analysis), then 4CTS machines would be required to produce cell populations satisfying the demands of PBP analysis. The latter of these options results in only an incremental direct costs reduction (~1%), whereas the resultant indirect costs are 375% higher than the optimal process design. Larger technologies, which can house cell populations in a smaller number of vessels, are preferred as they do not have as significant an impact on automated processing equipment utilisation. Owing to the automated nature of this processing strategy, the use of multiple vessels does not impact significantly upon labour costs, unlike manual processing, where it is important to minimise the number of units required in order to drive down labour costs.

Analysis of COG breakdowns for manual and automated bioprocesses when the demands of HTS and PBP analysis at throughputs of 50 and 100 cell lines per year are satisfied shows that automated processing can significantly reduce labour costs associated with stem cell bioprocesses (Fig. 7). This is particularly due to additional ancillary tasks associated with manual bioprocess strategies, such as media changes and cell seeding and harvesting. Material costs do not fluctuate greatly between manual and automated processing. However, savings on the cost of labour are outweighed by the additional indirect costs (a function of fixed capital investment required) for the automated bioprocess when 50 cell lines are produced. A 10% COG per cell line reduction is offered by manual processing when cells are produced for PBP analysis. At a throughput of 100 cell lines per year, the additional indirect costs associated with automated bioprocess strategies are spread across enough cell lines to provide significant COG reductions (19% at PBP scale) against the manual bioprocess - the cost of which is heavily weighted by labour costs. This is supported further by percentage COG breakdowns for the manual and automated bioprocesses when cell lines are produced to satisfy the demands of PBP analysis. At higher annual throughputs, direct costs make up a higher percentage of the COG breakdown. For the automated bioprocess, direct costs account for 41% of COG (70% for manual processing) when 50 cell lines are produced per year, compared to 58% (72% for manual processing) if 100 cell lines are produced annually. This analysis provides evidence that automation of patient-specific iPSC bioprocesses can provide significant COG reductions at scales sufficient to warrant the additional capital expenditure. Indirect costs dominate the COG breakdown for the automated bioprocess (Fig. 6) hence minimisation of the number of pieces of automation equipment must be achieved in order to curtail COGs.

There is no significant reduction in either the labour costs or material costs for both the manual and the automated bioprocess at throughputs of 50 and 100 cell lines per year (Fig. 7). However, when the process is scaled out, smaller COG figures are realised as a result of reductions in the indirect costs per cell line. This suggests that economies of scale can only be achieved for patient-specific hiPSC bioprocesses requiring scale-out through shared use of fixed equipment. Bioprocess scheduling and equipment sizing in order to maximise use of fixed equipment and minimise the required size of cleanrooms must therefore be considered during process design in this area.

It can be concluded that a threshold throughput exists where automated bioprocesses offer a COG reduction compared to a manual bioprocesses. This is in accordance with previous studies in stem cell bioprocess design [16]. When assessing the COG per cell line for both the automated and manual bioprocess at throughputs ranging from 50 to 200 cell lines, the point at which the automated bioprocess becomes more cost-effective than the manual bioprocess is at a throughput of 65 cell lines (Fig. 8). The spike on the line representing COG per cell line for automated bioprocesses also depicts the throughput at which it is necessary to purchase additional automated processing equipment (a throughput of 110 cell lines). The switchpoint identified between automated and manual processing

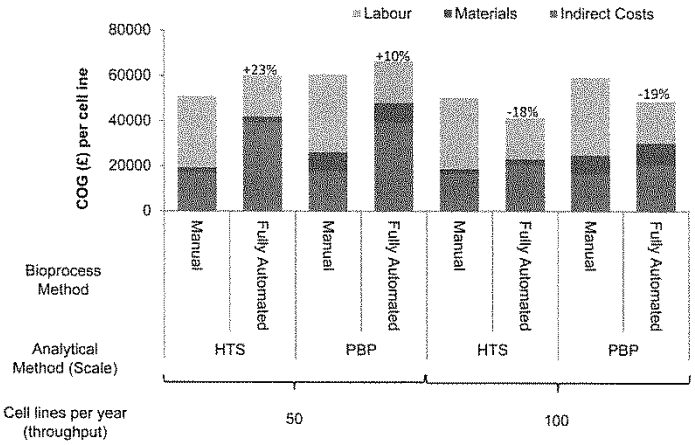

Fig. 7. COG breakdown for manual and automated bioprocess strategies at throughputs of 50 and 100 cell lines, whereby populations of 10^7 cells are produced in order to satisfy the demands of PBP. Percentage changes in COG/cell line caused by implementing an automated bioprocess strategy are shown above columns representing automated bioprocess COG breakdowns.

Table 6
Probability distributions assigned to key bioprocess performance parameters in the stochastic Monte Carlo analysis of the manual and automated bioprocess strategies.

Parameter	Probability distribution type	Manual bioprocess probability distribution profile (min, most likely, max)	Automated bioprocess probability distribution profile (min, most Likely, max)
iPSC expansion harvest yield	Triangular	75%, 90%, 95%	85%, 90%, 95%
iPSC expansion harvest density	Triangular	2.5×10^5, 3×10^5, 3.5×10^5	2.7×10^5, 3×10^5, 3.3×10^5
iPSC expansion fold	Triangular	6.3, 7, 7.7	6.6, 7, 7.4
Differentiation efficiency	Triangular	20%, 35%, 45%	30%, 35%, 40%
Differentiation harvest yield	Triangular	80%, 90%, 95%	85%, 90%, 95%
Differentiation seeding density	Triangular	0.8×10^4, 1×10^5, 1.1×10^5	0.9×10^5, 1×10^5, 1.1×10^5

Note: most likely values in the distribution profiles are taken from the base case scenario from the deterministic bioprocess economics model.

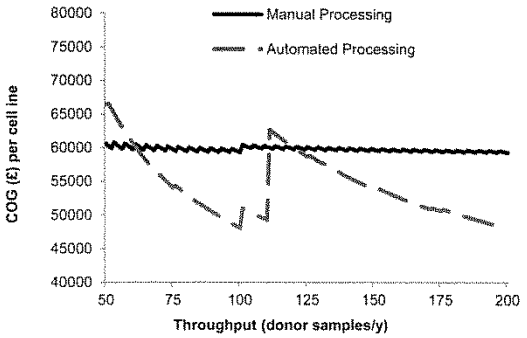

Fig. 8. COG per cell line at annual throughputs ranging from 50 to 200 cell lines of 107 iPSC-derived neurons for manual and automated processing.

are specific to the modelling assumptions made in this particular case study.

The assumed cost of automation equipment is based upon the current purchase cost for a functional CTS machine. At the time of writing, this was the only piece of automation equipment that could fully support this bioprocess. In the future, other pieces of equipment may become available and competition may drive down the cost of automation equipment. The effect of the price of automation equipment price on bioprocess COG can be seen in the Supplementary information accompanying this paper (Fig. S1).

4.1.2. Sensitivity analysis

In order to further identify key economic drivers associated with the iPSC-derived bioprocess, and to provide further understanding of where process development and optimisation resources might be best focused, a sensitivity analysis was carried out. Several process and cost parameters were varied to reflect their best and worst case values. The tool was used to test the resultant change upon the COG per cell line values that these variations. The Tornado charts (Fig. 9) illustrate the effect on COG that variations in key parameters caused for (a) the manual bioprocess and (b) the automated bioprocess at a throughput of 50 cell lines per year (where cell populations that satisfy the demands of PBP are produced). The number of iPSC expansion stages required was the greatest economic driver for both the manual and automated bioprocess strategies (Fig. 9). Variations in the number of iPSC expansion stages can occur due to fluctuations in key performance parameters. The impact of this parameter upon COG can be significant, as each additional iPSC expansion stage necessitates additional direct resources and fixed

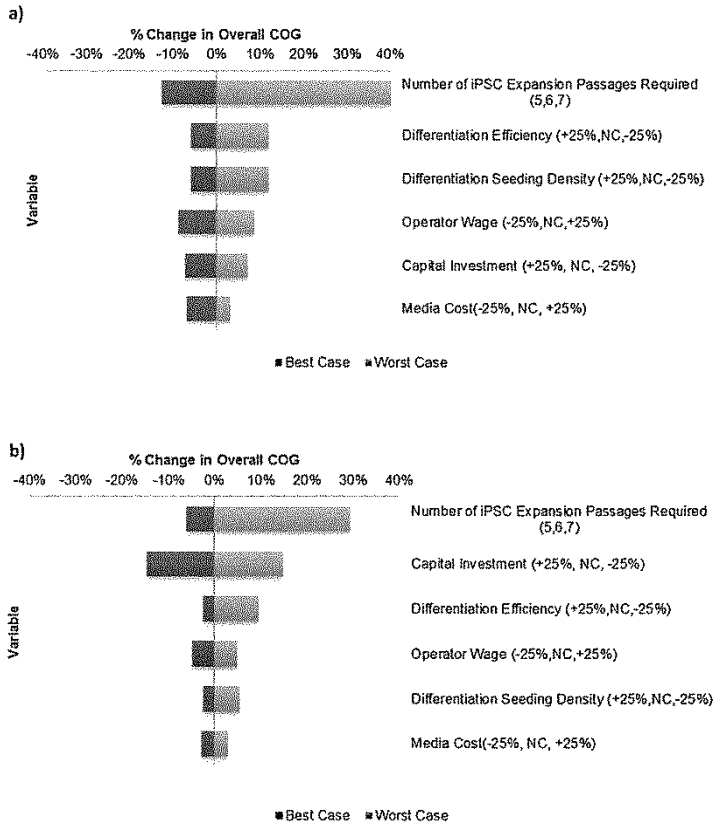

Fig. 9. Tornado plots showing the effect of variations in key parameters on COG for (a) the manual bioprocess strategy and (b) the automated bioprocess strategy at a throughput of 50 cell lines/ year. Best case and Worst case values are shown in brackets on the *y*-axis labels.

Table 7
Key statistical parameters of the COG per cell line values for the manual and automated bioprocess strategies from the stochastic Monte Carlo analysis.

	50 cell lines per year		100 cell lines per year	
	Manual bioprocess	Automated bioprocess	Manual bioprocess	Automated bioprocess
Mean (μ)	£64,841	£66,655	£65,405	£48,601
Standard deviation	£8481	£3025	£9493	£3221
$P(COG < \mu_{automated})$	0.81	0.93	0	0.89

equipment capacity. Thus, a change in the number of iPSC expansion stages required within a bioprocess will significantly affect COG per cell line.

Labour costs are also a significant cost driver for the manual bioprocess, resulting in an 18% difference in COG between the best and worst case scenarios. The fact that labour costs have been identified as a key process economic driver is perhaps unsurprising; this parameter dominates the COG breakdown at high cell line throughputs (see Fig. 7a). Similarly, the secondary cost driver for the automated bioprocess is FCI costs, which are the largest contributor to the COG breakdown for this process strategy (Fig. 7b).

4.2. Stochastic modelling

The mean COG/cell line value for the automated bioprocess is higher than that of the manual bioprocess when producing 50 cell lines per year, whereas at 100 cell lines per year, this value is higher for the manual bioprocess, as described by the stochastic analysis (Table 7). These figures are consistent with the deterministic model results, which also show the same trend (Fig. 7).

The results of the Monte Carlo analysis (Table 7 and Fig. 10a and b) show that the standard deviation and range of COG values for the automated bioprocess strategy at throughputs of both 50 and 100 cell lines per year (£3,025 (GBP) and £3,221 respectively) are significantly lower than those of the manual bioprocess strategy

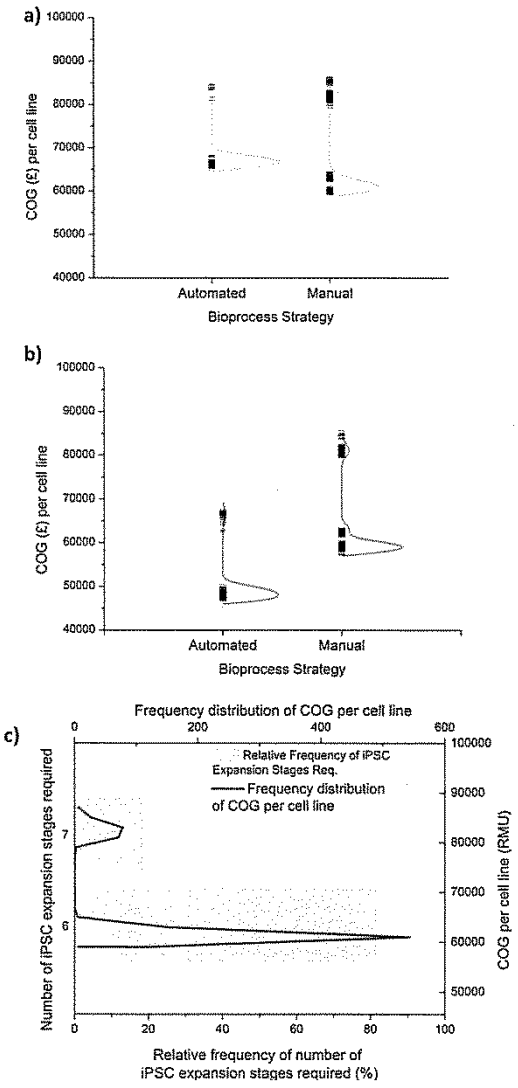

Fig. 10. Frequency distributions for the COG per cell line outputs for the automated and manual bioprocess strategies under uncertainty when producing (a) 50 cell lines per year and (b) 100 cell lines per year. (c) Relative frequency of the different number of iPSC expansion stages for the manual bioprocess strategy for 50 cell lines per year superimposed onto the COG per cell line frequency distribution. Dashed lines depict individual COG per cell line outputs and continuous curves represent the frequency distributions of the COG per cell line outputs.

(£8,481 and £9,493 at 50 and 100 cell lines per year, respectively). This suggests that the automated bioprocess is more robust from a bioprocess economics standpoint than the manual bioprocess. The frequency density curves and COG distributions (Fig. 10a and b) follow a distinct pattern. They are bimodal with a positive skew and hence the majority of COG values are concentrated at the lower end of the distribution and are followed by a long tail with a smaller peak at the upper end of the distribution with higher COG values. This is particularly true of the frequency distribution curves of the manual bioprocess, where the peaks at the upper end of the distribution where high COG values occur are larger compared to those for the automated bioprocess. One explanation of the shape of the frequency distributions can be illustrated in Fig. 10c, which shows the relative frequency at which the number of iPSC expansion passages required for the manual bioprocess (at a throughput of 50 cell lines per year) rises from six (as in the base case) to seven based on process variability modelled in Monte Carlo analysis. The frequency distribution of the COG per cell line for the manual bioprocess from Fig. 10a is also displayed on Fig. 10c. This shows that the minor peak with high COG values that appears in Fig. 10a and b is due to the requirement of an additional stage of iPSC expansion owing to process variations modelled during the Monte Carlo simulation. Fig. 10c also emphasises the importance of minimising the number of iPSC expansion stages as a strategy for minimisation of COG.

4.3. *Can an acceptable COG for in-house manufacture of patient-specific hiPSC derived cell lines be achieved?*

List prices from vendors for a vial containing 10^6 non patient-specific hPSC-derived cells currently lie in the region of US$ 1000–2000. This study shows that, unlike non patient-specific stem cell bioprocesses, where both direct and indirect cost savings can be achieved on a per million cells basis via appropriate scale-up strategies [16] economies of scale can only be achieved in patient-specific cell lines through shared use of fixed equipment. Direct costs per cell line do not fluctuate significantly, regardless of throughput (Fig. 7). The market price of patient-specific cell lines may therefore be assumed to be higher than their non-specific counterparts; not only because of the added expenditure as a result of scale-out processing, but also the added analytical value provided by such products in responder versus non-responder studies and potential personalised medicine regimes (see Section 1). This is reflected in the fact that patient-specific hPSC-derived cell lines are marketed for ~US$50k (~£35k) for 10^7 cells, including the additional costs of iPSC derivation and genetic engineering.

This case study reflects an in-house hiPSC-derived cell line manufacturing regime. According to the stochastic modelling above, the minimum COG per cell line that can be achieved is ~£45,000. This is significantly higher than current market prices for such products. In order for in-house production of cell lines for drug screening to be worthwhile, an acceptable COG per cell line must be below current market prices. A scenario analysis was designed to identify the process improvements required to reduce COG per cell line to below £35,000. Within the scenario analysis, reductions in the indirect costs and media costs have been assumed. A one-off new-build facility has been assumed for this case study in order to capture the fixed equipment costs associated with manufacturing patient-specific cell lines. In reality, such an in-house facility would likely be used for multiple research activities. To reflect this, indirect costs of 60% and 75% of the base case value have been investigated in this analysis. Established Big Pharma companies might also make use of existing experience in pharmaceutical reagent manufacturing in order to produce media components and small molecules required for certain unit operations in-house. This would allow some media components to be produced at cost price, rather than purchasing them at vendor list prices (as assumed in base case results). COG per cell line at both base case media costs and a 25% reduction in media costs have been modelled in this analysis. The process parameters varied in this analysis were the differentiation efficiency and iPSC expansion fold per stage. These parameters were chosen for two reasons; primarily they both impact upon the number of iPSC expansion stages required. This was identified as a key process economics driver in the sensitivity analysis (Fig. 9). Secondly, advances

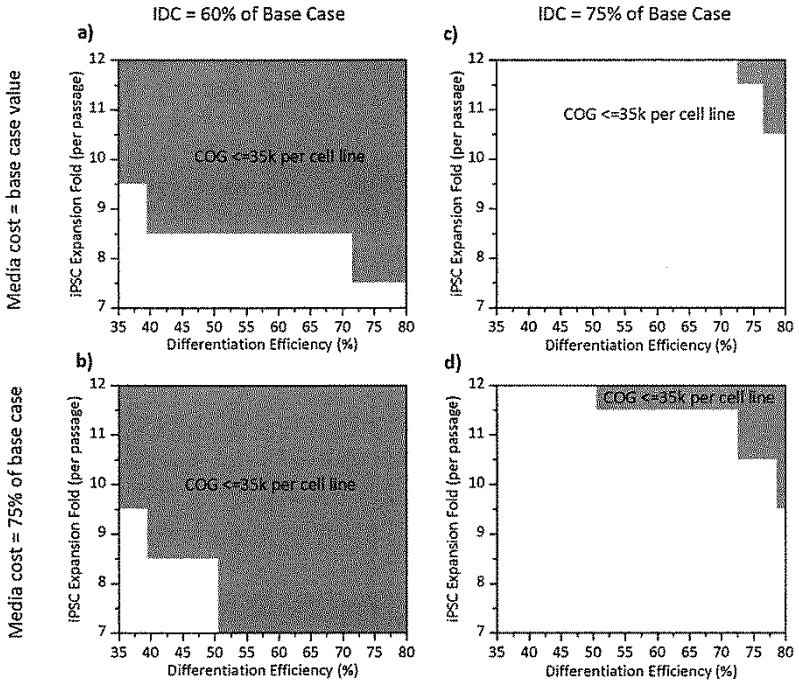

Fig. 11. Contour plots showing windows of operation where COG ≦ £35k/ cell line when (a) media cost = base scenario and IDC = 60% of base case values (b) media cost = 75% of the base scenario and IDC = 60% of base case values (c) media costs = base case value and IDC = 75% of base case values (d) media costs = 75% of base case value and IDC = 75% of base case. Shaded areas on the plots show windows of operation whereby COG ≦ £35,000/cell line, white areas of the plots represent windows of operation whereby COG > £35 k/ cell line. IDC = indirect costs.

in media composition and morphogen delivery systems during iPSC expansion and differentiation are areas of concentrated research. Innovations in these areas have proven that improvements in these parameters are achievable on the base case values assumed in this case study [21,22,38–41].

The in-house scenario considered in this project was for a single drug screening project application and hence the indirect costs were only spread across this activity. In future it is possible to envisage several drug screening applications where the investment is offset across several projects similar to how a vendor may achieve economies of scale. Hence the impact of lowering the indirect costs was explored. If indirect costs are 60% of base case value, there is a large window of operation whereby a COG ≦ £35k per cell line, even when media costs remain at the base case value (Fig. 11a). Indeed, if the achievable iPSC expansion fold can be increased from 7 to 10, then it would be acceptable for differentiation efficiency to remain at 35%. If media costs could be reduced by 25%, then a differentiation efficiency of 50% (up from 35% in the base case scenario) would be required for COG ≦ £35k per cell line, even if the iPSC expansion fold could not be improved. The windows of operation shrink significantly at both base case and reduced media cost values when indirect costs increase from 60% to 75% of the base case values (Fig. 11c and d). In this instance, improvements in both differentiation efficiency and iPSC expansion to 76% and 11%, respectively, would be required. Less dramatic improvements would be necessary if media costs could be reduced by 25%. In this instance differentiation efficiencies as low as 52% and iPSC expansion folds of 10 could allow COG ≦ £35k per cell line to be achieved. The maximum indirect cost (% base case) whilst media costs remain at base case value whereby a COG ≦ £35k per cell line is still feasible was found to be 77%. When media costs are 75% of the base case values, this value increases to 81%. Both of these instances would require improvements to produce a 12-fold expansion during iPSC culture and a differentiation efficiency of 79%. Conversion of hiPSCs to neurons at efficiencies beyond 80% have been reported [41] as have iPSC expansion folds of up to 11.3 over 7 days in planar conditions, or up to 28 in bioreactor conditions [22,42] Therefore, realising the windows of operation discussed above is not infeasible. In the event that fixed capital investment (or indirect costs) can be reduced by 25% or more there are realistic scenarios whereby in-house manufacture of patient-specific, iPSC-derived cell lines could be worthwhile for companies wishing to carry out responder versus non-responder studies as part of drug development regimes. Lower indirect cost values could be achieved by either retrospective fitting of an existing research facility, or by diversifying the functionality of a new-build facility. The scenarios analysed above also illustrate how changes to the bioprocess in terms of the key process parameters might impact upon COG and shows how the findings of this study might be applied to bioprocesses other than the one that is the focus of this work.

The scenarios examined here determine an acceptable COG to be less than current market prices for patient-specific, hiPSC-derived cell lines. This is because this case study examines production of such cell lines for use in in-house studies. Were the cell lines discussed in this case study to be manufactured for sale, the acceptable COG figure would be far lower in order to take into account COG as

a percentage of sales. Smith (2010) determines this value to be in the range of 40–60% for autologous products. It is possible to conclude that acceptable COG for patient-specific hiPSC-derived cell lines designed for sale is in the region of £14,000–£21,000 per cell line (whereby 10^7 cells are produced for each line). It is assumed that a process producing cell lines for commercial sale would be of a far greater scale than the bioprocess examined in this study (i.e. 100 cell lines per year). Identification of process improvements required to reduce the COG derived in this study to such values is therefore beyond the scope of this paper. However, future work will focus upon large-scale bioprocess design strategies in order to maintain a supply chain of hPSC-derived cell lines to a number of clients.

5. Conclusion

A decisional tool is presented that consists of a bioprocess economics model with an integrated brute-force search algorithm. The tool has been applied to an industrial case study, in which patient-specific iPSC-derived neurons are produced for use in responder versus non-responder studies as part of the development of NCEs to be used in personalised medicine regimes. Via the use of this tool, optimal equipment sizing regimes were identified for both a manual and an automated hPSC bioprocess. Furthermore, it can be concluded that whilst the most cost-effective option of the two process strategies tested is dependent on the throughput of the process, the use of automation equipment was found to result in a more robust bioprocess in terms of COG values when tested under uncertainty. Indirect cost reductions are required in order to achieve acceptable manufacturing COG. This might be done by retrospectively fitting existing facilities, or diversifying functionality of a new-build facility in order to offset some of the required fixed capital investment to other projects. Were an existing full-scale process to be adapted from a manual to an automated bioprocess it would be wise to take into account the cost and time required to train staff to use automated equipment. Furthermore, the logistics and costs of updating facility infrastructure to cope with automated processing should be considered in the case of retro-fitting an existing facility. This work modelled a relatively small scale bioprocess in commercial terms. However, the outputs can be of use in aiding decision making early on in bioprocess design for patient-specific cell line production at a variety of scales. Expanding the decisional tool presented here to account for larger scale bioprocesses, including the production of cells for autologous and allogeneic cell therapies will be the focus of future work.

Acknowledgments

Financial support from the UK Engineering and Physical Sciences Research Council (EPSRC) (grant reference number: EP/G034656/1) and Neurosciences & Pain research unit, Pfizer, is gratefully acknowledged. UCL hosts the EPSRC centre for Innovative Manufacturing in Emergent Macromolecular Therapies with Imperial College London and a consortium of industrial and government users.

Appendix A. Supplementary data

Supplementary data associated with this article can be found, in the online version, at http://dx.doi.org/10.1016/j.bej.2015.09.024.

References

[1] K. Takahashi, K. Tanabe, M. Ohnuki, M. Narita, T. Ichisaka, K. Tomoda, S. Yamanaka, Induction of pluripotent stem cells from adult human fibroblasts by defined factors, Cell 131 (2007) 861–872.
[2] L.L. Rubin, Stem cells and drug discovery: the beginning of a new era? Cell 132 (2008) 549–552.
[3] C. Mason, P. Dunnill, Quantities of cells used for regenerative medicine and some implications for clinicians and bioprocessors, Regen. Med. 4 (2009) 153–157.
[4] S.M. Wu, K. Hochedlinger, Harnessing the potential of induced pluripotent stem cells for regenerative medicine, Nat. Cell Biol. 13 (2011) 497–505.
[5] D.A. Robinton, G.Q. Daley, The promise of induced pluripotent stem cells in research and therapy, Nature 481 (2012) 295–305.
[6] H. Pearson, The bitterest pill, Nature 444 (2006) 532–533.
[7] E. Kiskinis, K. Eggan, Progress toward the clinical application of patient-specific pluripotent stem cells, J. Clin. Invest. 120 (2010) 51–59.
[8] C.W. Scott, M.F. Peters, Y.P. Dragan, Human induced pluripotent stem cells and their use in drug discovery for toxicity testing, Toxicol. Lett. 219 (2013) 49–58.
[9] A.D. Ebert, C.N. Svendsen, Human stem cells and drug screening: opportunities and challenges, Nat. Rev. Drug Discov. 9 (2010) 367–372.
[10] S.J. Engle, F. Vincent, Small molecule screening in human induced pluripotent stem cell-derived terminal cell types, J. Biol. Chem. 289 (2014) 4562–4570.
[11] M. Hay, D.W. Thomas, J.L. Craighead, C. Economides, J. Rosenthal, Clinical development success rates for investigational drugs, Nat. Biotechnol. 32 (2014) 40–51.
[12] N. Zeevi-Levin, J. Itskovitz-Eldor, O. Binah, Cardiomyocytes derived from human pluripotent stem cells for drug screening, Pharmacol. Ther. 134 (2012) 180–188.
[13] C.K. Huaising, D.G. Bruce, Concise review: drug discovery in the age of the induced pluripotent stem cell, Stem Cells Trans. Med. 3 (2014) 500–509.
[14] M.R. Placzek, I.M. Chung, H.M. Macedo, S. Ismail, T. Mortera Blanco, M. Lim, J.M. Cha, I. Fauzi, Y. Kang, D.C. Yeo, C.Y. Ma, J.M. Polak, N. Panoskaltsis, A. Mantalaris, Stem cell bioprocessing: fundamentals and principles, J. R. Soc. Interface 6 (2009) 209–232.
[15] A.J. Want, A.W. Nienow, C.J. Hewitt, K. Coopman, Large-scale expansion and exploitation of pluripotent stem cells for regenerative medicine purposes: beyond the T flask, Regen. Med. 7 (2012) 71–84.
[16] A.S. Simaria, S. Hassan, H. Varadaraju, J. Rowley, K. Warren, P. Vanek, S.S. Farid, Allogeneic cell therapy bioprocess economics and optimization: single-use cell expansion technologies, Biotechnol. Bioeng. 111 (2014) 69–83.
[17] D.E. Kehoe, D.H. Jing, L.T. Lock, E.S. Tzanakakis, Scalable stirred-suspension bioreactor culture of human pluripotent stem cells, Tissue Eng. A 16 (2010) 405–421.
[18] S. Abbasalizadeh, M.R. Larijani, A. Samadian, H. Baharvand, Bioprocess development for mass production of size-controlled human pluripotent stem cell aggregates in stirred suspension bioreactor, Tissue Eng. C Methods 18 (2012) 831–851.
[19] D.A. Fluri, P.D. Tonge, H. Song, R.P. Baptista, N. Shakiba, S. Shukla, G. Clarke, A. Nagy, P.W. Zandstra, Derivation, expansion and differentiation of induced pluripotent stem cells in continuous suspension cultures, Nat. Methods 9 (2012) 509–516.
[20] M. Shafa, K. Sjonnesen, A. Yamashita, S. Liu, M. Michalak, M.S. Kallos, D.E. Rancourt, Expansion and long-term maintenance of induced pluripotent stem cells in stirred suspension bioreactors, J. Tissue Eng. Regen. Med. 6 (2012) 462–472.
[21] M.D. Ungrin, G. Clarke, T. Yin, S. Niebrugge, M.C. Nostro, F. Sarangi, G. Wood, G. Keller, P.W. Zandstra, Rational bioprocess design for human pluripotent stem cell expansion and endoderm differentiation based on cellular dynamics, Biotechnol. Bioeng. 109 (2012) 853–866.
[22] J. Bardy, A.K. Chen, Y.M. Lim, S. Wu, S. Wei, H. Weiping, K. Chan, S. Reuveny, S.K. Oh, Microcarrier suspension cultures for high-density expansion and differentiation of human pluripotent stem cells to neural progenitor cells, Tissue Eng. C: Methods 19 (2013) 166–180.
[23] R. Shaw, Stem-cell-based therapies, Bioproc. Int. 9 (2011) 20–25.
[24] M.J. Jenkins, S.S. Farid, Human pluripotent stem cell-derived products: advances towards robust, scalable and cost-effective manufacturing strategies, Biotechnol. J 10 (2015) 83–95.
[25] F.S. Veraitch, R. Scott, J.W. Wong, G.J. Lye, C. Mason, The impact of manual processing on the expansion and directed differentiation of embryonic stem cells, Biotechnol. Bioeng. 99 (2008) 1216–1229.
[26] R.J. Thomas, D. Anderson, A. Chandra, N.M. Smith, L.E. Young, D. Williams, C. Denning, Automated, scalable culture of human embryonic stem cells in feeder-free conditions, Biotechnol. Bioeng. 102 (2009) 1636–1644.
[27] J. Hambor, Bioreactor design and bioprocess controls for industrialised cell processing, Bioproc. Int. 10 (2012) 22–33.
[28] S.S. Farid, J.L. Novais, S. Karri, J. Washbrook, N.J. Titchener-Hooker, A tool for modeling strategic decisions in cell culture manufacturing, Biotechnol. Prog. 16 (2000) 829–836.
[29] S.S. Farid, J. Washbrook, N.J. Titchener-Hooker, Decision-support tool for assessing biomanufacturing strategies under uncertainty: stainless steel versus disposable equipment for clinical trial material preparation, Biotechnol. Prog. 21 (2005) 486–497.
[30] S. Chhatre, R. Francis, K. O'Donovan, N.J. Titchener-Hooker, A.R. Newcombe, E. Keshavarz-Moore, A prototype software methodology for the rapid evaluation of biomanufacturing process options, Biotechnol. Appl. Biochem. 48 (2007) 65–78.
[31] A. Stonier, A.S. Simaria, M. Smith, S.S. Farid, Decisional tool to assess current and future process robustness in an antibody purification facility, Biotechnol. Prog. 28 (2012) 1019–1028.

[32] S.V. J. Pollock, S.S. Farid Ho, Fed-batch and perfusion culture processes: economic, environmental, and operational feasibility under uncertainty, Biotechnol. Bioeng. 110 (2013) 206–219.
[33] J. Rowley, E. Abraham, A. Campbell, H. Brandwein, S. Oh, Meeting lot-size challenges of manufacturing adherent cells for therapy, Bioproc. Int. 10 (2012) 16–22.
[34] C.L. Darkins, C.-F. Mandenius, Design of large-scale manufacturing of induced pluripotent stem cell derived cardiomyocytes, Chem. Eng. Res. Des. 92 (2013) 1142–1152.
[35] H.J. Lang, Simplified approach to preliminary cost estimates, Chem. Eng. 55 (1948) 112–113.
[36] X. Yajuan, L. Xin, L. Zhiyuan, A comparison of the performance and application differences between manual and automated patch-clamp techniques, Curr. Chem. Genom. 6 (2012) 87–92.
[37] R.L. Dutton, J.S. Fox, Robotic processing in barrier-isolator environments: a life cycle cost approach, Pharm. Eng. 26 (2006).
[38] S.M. Chambers, C.A. Fasano, E.P. Papapetrou, M. Tomishima, M. Sadelain, L. Studer, Highly efficient neural conversion of human ES and iPS cells by dual inhibition of SMAD signaling, Nat. Biotechnol. 27 (2009) 275–280.
[39] G. Chen, J.A. Thomson, Simplified basic media for human pluripotent cell culture, in Google Patents, 2012.
[40] B. Surmacz, H. Fox, A. Gutteridge, S. Lubitz, P. Whiting, Directing differentiation of human embryonic stem cells toward anterior neural ectoderm using small molecules, Stem Cells 30 (2012) 1875–1884.
[41] E.S. Lippmann, M.C. Estevez-Silva, R.S. Ashton, Defined human pluripotent stem cell culture enables highly efficient neuroepithelium derivation without small molecule inhibitors, Stem Cells 32 (2014) 1032–1042.
[42] P.A. Marinho, D.T. Vareschini, I.C. Gomes, S. Paulsen Bda, D.R. Furtado, R. Castilho Ldos, S.K. Rehen, Xeno-free production of human embryonic stem cells in stirred microcarrier systems using a novel animal/human-component-free medium, Tissue Eng. C: Methods 19 (2013) 146–155.

Appendix C: Validation

C1: Introduction

This section of the appendix was produced as part of the Bioprocess Validation MBI Course undertaken as a mandatory component of the EngD in February 2014. The section represents an overview of the validation challenges associated with the production of patient-specific cell lines for drug screening. However, broader regulatory and validation issues affecting the scale-up of cell therapy bioprocesses are also considered.

C2: Key Validation Issues

C2.1 Final Product Functionality

iPSC-derived cells can be used to assess efficacy and toxicity of NCEs. In order for the cells to be used as a viable screening tool they must be homogeneous between patients in terms of the functionality of the cells. Currently, iPSC-derived neurons are produced for in-house use at Pfizer using planar platforms. Variations in product quality could occur due to differences in holding times used during cell harvest steps. Thus, appropriate holding times must be defined so that cell functionality and potency is not affected during processing. Critical quality attributes (CQAs) must be defined in order to ensure proper product characterisation. In stem cell processing this can include measuring biomarker expression, analysis of cell morphology to determine the type of cell and its potency. Functionality assays such as ion-channel assays can be used to carry out QC and QA tests on samples from iPSC-derived neuron populations. Acceptable ranges for each of these parameters should be defined in order to allow process validation to take place and prove the robustness of the product

C2.2 Choice of Media

Advances in stem cell bioprocessing were hindered for a long period by the widespread use of complex media containing animal derived components. This is especially true of differentiation processes, which often rely on exogenous growth factors to direct pluripotent stem cells to a specific fate. A directed differentiation protocol to induce neuronal differentiation through the use of small molecules has been developed (Surmacz et al. 2012), thus reducing the reliance on growth factors. From a validation this is an important step as it allows a QbD approach to designing differentiation processes because there is an understanding of why components drive differentiation to a specific lineage, rather than simply knowing what happens when cells are exposed to certain growth factors. This is also the case for cell culture media, where rational design of new, defined media has sought to analyse and understand the key functions of complex components of media and simplify such media by only including the necessary compounds. This will allow a QbD approach to process design to be adopted with regards to developing windows of operation to be created with respect to the concentrations of molecules added to the media, as well as the timepoints at which such molecules are added to the media (this is particularly important in directed differentiation protocols).

C2.3 Reproducibility of Process

Process automation is a growing trend within cell therapy bioprocessing. It is thought that automation will improve process reproducibility by negating some of the variability introduced by manual processing of stem cells such as:

- creation of possible points of contamination throughout the bioprocess
- idiosyncrasies of lab technicians

Automated processing will thus help define and understand the design space of cell therapy bioprocess as it will allow cause and effect relationships to be identified between CPPs and CQAs, whereas manual processing can skew these relationships

due to the inherent variability associated with this method. Automated processing is also far more reliable than manual processing and thus can help de-risk a validated process

C3. Validation and regulatory issues affecting process scale-up

Scale-up of stem cell therapies is a crucial stage of bioprocess development. This will involve creating larger populations of cells in order to create processes with a higher throughput; in cases where patient-specific cells are being produced this is likely to be a scale-out process. For allogeneic, or universal products, a scale-up operation is more appropriate. There are variety of validation issues that come with implementing the scale-up strategies investigated in this thesis. It is clearly important to assess what are the critical process parameters when seeking to adapt a process and justify an acceptable operating space so as not to adversely affect CQAs of the final product.

C3.1 Conversion from Static, Planar Culture Vessels to Dynamic, 3-D Bioreactors

Trends in stem cell bioprocessing suggest that 3-D bioreactors may need to be employed in order to meet demand in terms of cell numbers and to reduce facility size requirements. Shifting to dynamic, bioreactor based bioprocessing presents a number of issues from a validation perspective. The effect of shear stress on cells is not fully understood. It may be possible to harness shear forces within bioreactors to modulate cell fate, however, before this is done process development studies must successfully define the effect of shear forces on cell colonies. Novel process analytical tools (PATs) should be applied in order to quantify the effect of shear of CQAs associated product quality. Microfluidic tools and other USD devices are well-placed to serve such a purpose. This will enable a well-defined operating space that should be independent of scale for dynamic culture of hiPSCs and their derivatives.

C3.2 Adaptation from Monolayer to Microcarrier Culture

Whilst monolayers and microcarriers both offer culture platforms for adherent cells, it is important for microcarrier properties to be fully characterised in terms of their effect on cells' microenvironment and activity (self-renewal vs differentiation). It is important to consider the mechanical properties of microcarriers as well as their exterior biochemical properties when validating their use for hiPSC processes (Sart et al. 2013). The effects of mechanical properties, such as stiffness and size, of mircocarriers on hiPSC colony size and spreading should also be factored into any process design decisions. It will also be important to use microcarrier coatings which are fully defined and free of xenogeneic products. Synthetic coatings are preferable due to lot-lot variatbility that can occur with recombinant proteins. The integrity of both cells for diagnostic purposes and those that are intended for use as cell therapies must be ensured by the removal of animal-derived components from the process stream. Defined microcarrier coatings will also allow the effects of each component of the coating to be quantified in terms of its effect on stem cell activity. Full characterisation of the effcts of different polymers on the coatings of microcarriers will allow and QbD approach to rational design of microcarriers for stem cell bioprocesses. It is likely that microcarriers may be produced by a CMO, but an understanding of their properties is still crucial in order to develop large scale, robust processes.

C3.3 Large-Scale Harvest Strategies

Dynamic culture also presents issues with regards to harvesting cultured/ differentiated cells. Process development studies must identify whether or not the dynamic nature of 3-D bioreactors has any impact upon a) the concentration of harvest enzyme required b) the holding time required for harvest using enzymatic dissociation and the effects of these parameters on CQAs such as cell functionality/ viability. Additionally, it might be that changes to the process to reduce COGs might occur, one such modification could be the use of thermo-sensitive microcarriers that

degrade at specific temperature to obviate the need for enzyme-based harvest strategies (which will reduce material costs associated with hiPSC bioprocesses). Again, it is important to adopt a QbD approach to carry out rigorous experimentation in order to understand the effects such a modification might have on CQAs determined by Pfizer to define the quality of their product.